Advances in High Energy Physics

Joint Topics on Exotic Hadron States and Heavy Flavor Hadronic Decay

Lead Guest Editor: Xian-Wei Kang
Guest Editors: Jose A. Oller, Ling-Yun Dai, and Tao Luo

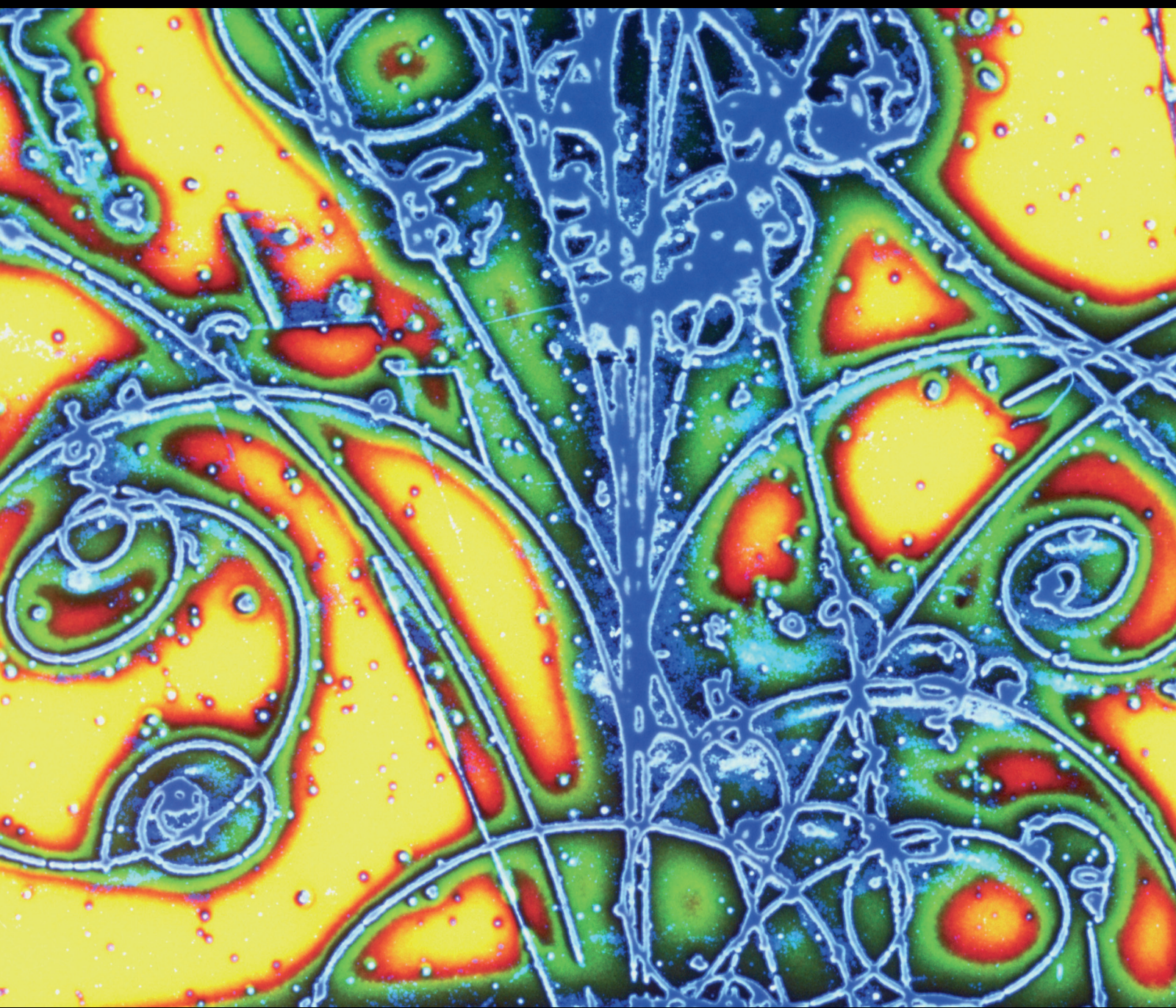

Joint Topics on Exotic Hadron States and Heavy Flavor Hadronic Decay

Advances in High Energy Physics

Joint Topics on Exotic Hadron States and Heavy Flavor Hadronic Decay

Lead Guest Editor: Xian-Wei Kang
Guest Editors: Jose A. Oller, Ling-Yun Dai, and Tao Luo

Editorial Board

Contents

Hindawi
Advances in High Energy Physics
Volume 2019, Article ID 3765306, 2 pages
https://doi.org/10.1155/2019/3765306

Editorial

Joint Topics on Exotic Hadron States and Heavy Flavor Hadronic Decay

Xian-Wei Kang,[1] **J. A. Oller**,[2] **Ling-Yun Dai**,[3] **and Tao Luo**[4]

[1] *College of Nuclear Science and Technology, Beijing Normal University, Beijing 100875, China*
[2] *Departamento de Física, Universidad de Murcia, 30071 Murcia, Spain*
[3] *School of Physics and Electronics, Hunan University, Changsha 410082, China*
[4] *Key Laboratory of Nuclear Physics and Ion-Beam Application (MOE) and Institute of Modern Physics, Fudan University, Shanghai 200443, China*

Correspondence should be addressed to Xian-Wei Kang; kxw198710@126.com and Tao Luo; luot@fudan.edu.cn

Received 28 May 2019; Accepted 28 May 2019; Published 16 July 2019

The internal structure of a hadron, as a key topic in the nuclear and particle physics, can be accessed by hadronic scattering, production, and/or its decay. As it is known Quantum Chromodynamics (QCD) is a nonperturbative quantum field theory at the low-energy region, and many approaches have been proposed for studying different aspects of this rich dynamics, e.g., the various quark models, Bethe-Salpeter (BS) equation approach, QCD sum rules, and low-energy effective field theories. Flavor physics is a research field which allows us to probe the charm and beauty quark decays. On the other hand, the exotic heavy-quark hadron physics becomes very fashionable since the discovery of the X(3872). As we know QCD does not exclude the existence of exotic hadrons (with quantum numbers that do not fit for $q\overline{q}$ in the case of mesons and qqq for baryons), but we still have no way to predict all the exotic hadrons from first-principle calculations (despite the advances in lattice QCD). Studies on the $XY\,Z$ states certainly help our understanding on the underlying dynamics of QCD. Based on such circumstance, we propose a current special issue, where both theoretical and experimental papers have been attracted.

In the paper by F. Yan and B. Zheng, a tag method is proposed that allows a direct absolute measurement of the decay branching fractions of the J/ψ with the data set at the $\psi(3686)$; namely, the J/ψ is produced from the decay $\psi(3686) \longrightarrow J/\psi\pi^+\pi^-$. The next paper by P. G. Ortega *et al.* develops the unquenching of the quark model, where the quark-antiquark pair creation (or continuum coupling effect) is incorporated, and especially, the coupling between quark-antiquark states and meson-meson channels is treated nonperturbatively, an improvement compared to the Cornell Model. In the paper by J. Zhang *et al.*, they make a combined fit to the measured cross sections of $e^+e^- \longrightarrow \omega\chi_{c0}, \pi^+\pi^- h_c, \pi^+\pi^- J/\psi, \pi^+\pi^-\psi(3686)$ and $\pi^+ D^0 D^{*-}$ + *c.c.*, with the aim of better understanding the nature of the $Y(4220), Y(4390)$, and $Y(4660)$. They find that the two resonances $Y(4220)$ and $Y(4390)$ are sufficient to explain these cross sections below 4.6 GeV, and also the lower limits of their leptonic decay widths are determined. H. Mutuk in the following paper revisits the potential model by using either the power potential or the logarithmic potential and obtains many physical quantities, including the spin averaged masses, hyperfine splittings, Regge trajectories of pseudoscalar and vector mesons, decay constants, leptonic decay widths, two-photon and two-gluon decay widths, and some allowed M1 transitions. He finds a good agreement with experimental data and other theoretical studies. In another paper by the same author, the mass spectra and decay constants of pseudoscalar and vector heavy-light mesons (B, B_s, D, D_s) are investigated by applying QCD sum rules with a simple interpolating current, as well as within the quark model using the harmonic oscillator wave functions. Again, a good agreement with experiment is achieved. In the paper by Z.-Y. Wang *et al.*, the authors conclude that the $X(5568)$ cannot be a $B\overline{K}$ molecular state by applying a method based on the BS equation, which is in line with

many other theoretical points of view. More specifically, the BS equation is solved numerically in the covariant instantaneous approximation, with the interaction potential containing one-particle exchange diagrams and introducing two different form factors (monopole and dipole form factor) in the vertices.

In the next paper H. Zhou *et al.* study the possibly enhanced CP violation in the singly Cabibbo-suppressed decay $D^0 \longrightarrow K^+K^-\pi^0$. The authors consider the interference between the two intermediate resonances $K^*(892)^+$ and $K^*(892)^-$ and the amplitude is calculated in the factorization-assisted topological approach. Results show that the regional CP asymmetry in the overlapped region of the phase space can be an order of magnitude as large as 10^{-3}, which may be accessed in the future high-statistic charm factories. In the paper by Y.-H. Chen, the author calculates the chromopolarizability of a quarkonium, which is a quantity describing the interaction between the quarkonium and soft gluonic fields. In the transition $\psi(3686) \longrightarrow J/\psi\pi\pi$, the nonperturbative $\pi\pi$ final state interaction (FSI) is treated model-independently with the use of the dispersion theory. The values of chromopolarizability are obtained, and it turns out that the FSI plays an indispensable role. In the paper by Z.-Y. Di and Z.-G. Wang, the $D\overline{D}^*K$ system is studied by employing QCD sum rules, and a resonance with mass $4.71^{+0.19}_{-0.11}$ GeV is predicted. The future measurement of invariant mass of $J/\psi\pi K$ in the decay channel $B \longrightarrow J/\psi\pi\pi K$ can test such prediction. Finally, R. Gao *et al.* study the nature of the resonances $Z_c(3900)$, $X(4020)$, $\chi_{c1}(4140)$, $\psi(4260)$, and $\psi(4660)$ every of which lies nearby a threshold of two open heavy-flavor hadrons. The effective range expansion is used and the scattering length (a) and effective range (r) are determined by reproducing the pole positions. The composite or elementary nature of these states is addressed by considering the values of a and r, as well as by calculating the compositeness coefficient X. Other interpretations of the latter coefficient in the literature are compared and critically reviewed.

Conflicts of Interest

We declare that we have no conflicts of interest.

Xian-Wei Kang
J. A. Oller
Ling-Yun Dai
Tao Luo

Hindawi
Advances in High Energy Physics
Volume 2019, Article ID 4651908, 6 pages
https://doi.org/10.1155/2019/4651908

Research Article

Effective-Range-Expansion Study of Near Threshold Heavy-Flavor Resonances

Rui Gao,[1] Zhi-Hui Guo,[1] Xian-Wei Kang,[2] and J. A. Oller[3]

[1]*Department of Physics and Hebei Advanced Thin Films Laboratory, Hebei Normal University, Shijiazhuang 050024, China*
[2]*College of Nuclear Science and Technology, Beijing Normal University, Beijing 100875, China*
[3]*Departamento de Física, Universidad de Murcia, E-30071 Murcia, Spain*

Correspondence should be addressed to Zhi-Hui Guo; zhguo@hebtu.edu.cn

Received 26 December 2018; Revised 5 April 2019; Accepted 15 May 2019; Published 16 June 2019

Academic Editor: Burak Bilki

In this work, we study the resonances near the thresholds of the open heavy-flavor hadrons using the effective-range-expansion method. The unitarity, analyticity, and compositeness coefficient are also taken into account in our theoretical formalism. We consider the $Z_c(3900)$, $X(4020)$, $\chi_{c1}(4140)$, $\psi(4260)$, and $\psi(4660)$. The scattering lengths and effective ranges from the relevant elastic S-wave scattering amplitudes are determined. Tentative discussions on the inner structures of the aforementioned resonances are given.

1. Introduction

Since the discovery of the $X(3872)$ [1], the study of the exotic hidden heavy-flavor hadrons has become one of the most important and active research topics in particle physics. Up to now more than twenty of the so-called XYZ hadrons are observed by experiments [2] and we refer to [3, 4] for recent comprehensive reviews on this subject. One of the most important features of the newly observed hadrons is that they are usually close to the nearby thresholds of the open heavy-flavor states. As a result typically one needs to properly take into account the threshold effects when studying those possible exotic states. The effective range expansion (ERE), which is based on the three-momentum expansion near the threshold, provides a useful tool to address the dynamics in the energy region around the relevant threshold in question [5, 6].

By combining the ERE, unitarity, analyticity, and the compositeness coefficients developed in [7, 8], we have successfully analyzed several non-ordinary hadronic states that lie close to the thresholds of the underlying two-particle states, including the $\Lambda_c(2595)$ [9], $Z_b(10610)$, and $Z_b(10650)$ [10], and the newly observed pentaquark candidates $P_c(4312)$, $P_c(4440)$ and $P_c(4457)$ [11]. The essential idea of the formalism is that we construct the elastic unitarized partial-wave amplitude using the ERE as the kernel, which includes the scattering length a and effective range r as free parameters. The latter are determined by reproducing the values of the mass and width of the observed resonance. We always obtain real values consistently with the assumption of only one-channel scattering. Then the residue of the resonance pole, which corresponds to the coupling strength of the resonance to the interacting two-particle state, can be obtained as well. With all of these ingredients, we can apply the compositeness formalism to infer the probability to find the two-particle state inside the resonance. In this work we first briefly recapitulate the essentials of the theoretical formalism. Then we tentatively generalize this formalism to other newly observed hadronic states, including the $Z_c(3900)$ near the $D\overline{D}^* + c.c.$ (denoted shortly as $D\overline{D}^*$ in the following) threshold, the $X(4020)$ near the $D^*\overline{D}^*$ threshold, the $\chi_{c1}(4140)$ near the $D_s^{\pm}D_s^{*\mp}$ (denoted as $D_s\overline{D}_s^*$ in the following) threshold, the $\psi(4260)$ near the $D_1\overline{D} + c.c.$ (denoted shortly as $D_1\overline{D}$ in the following) threshold, and the $\psi(4660)$ near the $\Lambda_c\overline{\Lambda}_c$ threshold [2]. Historically, there is also a state named $X(4630)$ that we identify with the resonance $\psi(4660)$ as in the PDG [2] and [12–14].

2. Effective Range Expansion and Compositeness Coefficients of Resonances

The basic staring point of our theoretical formalism is the ERE up to the next-to-leading order:

$$t(E) = \frac{1}{-1/a + (1/2)rk^2 - ik}, \tag{1}$$

with a the scattering length, r the effective range, and k the three-momentum in the center of mass (CM) frame. At a given CM energy E around the threshold, one can write the nonrelativistic three-momentum as

$$k = \sqrt{2\mu_m (E - m_{\text{th}})}, \tag{2}$$

where the reduced mass of the system with masses m_1 and m_2 is $\mu_m = m_1 m_2/(m_1 + m_2)$ and the threshold is given by $m_{\text{th}} = m_1 + m_2$.

We mention that a more general expression to write the scattering amplitude near threshold is to include the so-called Castillejo-Dalitz-Dyson (CDD) poles. The standard ERE in (1) can be obtained by expanding the full expression with CDD poles [9, 10]. However when the CDD pole happens to be near the threshold, the expansion in terms of k^2 will be invalid, or at least quite limited to a tiny region. One of the prominent features in this situation is the huge effective range r, which usually becomes much larger than its standard value around 1 fm. If this is the case, one has to work explicitly with the CDD pole in the full expression, as done in [9, 10, 18].

The partial-wave amplitude given in (1) corresponds to the physical one in the first Riemann sheet (RS). Its expression in the second RS is given by

$$t_{\text{II}}(E) = \frac{1}{-1/a + (1/2)rk^2 + ik}. \tag{3}$$

The resonance poles only appear in the second RS. Comparing with (1) and (3), there is a change of sign for the k term. Notice that, in the conventions of (1) and (3), the three-momentum k should be evaluated with $\text{Im}\, k > 0$.

Let us now consider a resonance R whose pole position in the unphysical RS is located at $E = E_R$, with $E_R = M_R - i\Gamma_R/2$. For a conventional narrow-width resonance, one can identify M_R and Γ_R as its mass and width, respectively. The corresponding three-momentum at the resonance pole is then given by

$$k_R = \sqrt{2\mu_m (E_R - m_{\text{th}})}. \tag{4}$$

For later convenience, we further define

$$k_R = k_r + ik_i, \quad k_i > 0. \tag{5}$$

One has to be careful when evaluating k_R in terms of the threshold m_{th} and the resonance parameters M_R and Γ_R, specially distinguishing the sign of $M_R - m_{\text{th}}$. Detailed discussions can be found in [10].

The resonance pole corresponds to the zero of the denominator of $t_{\text{II}}(E)$; i.e., at the pole position one has

$$-\frac{1}{a} + \frac{1}{2}rk_R^2 + ik_R = 0. \tag{6}$$

By a straightforward algebraic manipulation, one can solve a and r in terms of k_r and k_i:

$$a = -\frac{2k_i}{|k_R|^2}, \tag{7}$$

$$r = -\frac{1}{k_i}. \tag{8}$$

Substituting (7) and (8) into (3), one can write the partial-wave amplitude around the resonance pole E_R as

$$t_{II}(k) = \frac{-k_i/k_r}{k - k_R} + \cdots, \tag{9}$$

where the ellipses stand for the neglected terms when expanding the denominator of (3) in terms of $k - k_R$. From (9), we can identify the residue at the pole in the variable k, which turns out to be

$$\gamma_k^2 = -\frac{k_i}{k_r} > 0, \tag{10}$$

since $k_r < 0$. Alternatively one can also expand the partial-wave amplitude around the pole as

$$t_{II}(E) = -\frac{\gamma^2}{s - E_R^2} + \cdots. \tag{11}$$

The residue γ^2 is related to γ_k^2 as

$$\gamma_k^2 = -\gamma^2 \left.\frac{dk}{ds}\right|_{k_R} = -\frac{\mu_m \gamma^2}{2E_R k_R}. \tag{12}$$

In [7], a probabilistic interpretation for the compositeness X of the two-particle state inside the resonance is derived. The value of X can be calculated once the resonance pole position and the corresponding residues are provided. Around the two-particle threshold, the probability X reduces to the following [10]:

$$X = |\gamma_k|^2. \tag{13}$$

However, we point out that the probabilistic interpretation of X is restricted to resonances with $M_R > m_{\text{th}}$ [7]. In [15–17, 19–24], other approaches to generalize the Weinberg's compositeness of bound states [25] to the resonances are discussed. We compare below our results with some of them in Section 3.

In the next section, we proceed to study several near-threshold resonances within the present ERE approach. Let us notice that if this type of ERE study is applied to a near-threshold resonance which is composite of the nearby channel (the so-called elastic one) then $X \simeq 1$. From here it also follows that if we apply this type of ERE study to a near-threshold resonance and it results that $X \ll 1$, then one can conclude for sure that this resonance is not a composite one of the elastic channel. On the other hand, if it results that $X \simeq 1$ then the interpretation of this resonance as a composite one of the elastic channel is favored (In a similar sense that a cloudy sky favors rainfall.).

Table 1: In the second and third columns, the masses and widths of the $Z_c(3900)$, $X(4020)$, $\psi(4260)$ and $\psi(4660)$ from the PDG are given. For the $\chi_{c1}(4140)$, we have distinguished three different determinations: LHCb, the average without LHCb (~~LHCb~~) and the PDG average. To make a conservative error estimate, the largest error bars are taken for the asymmetric ones in the values from the LHCb and PDG. We assume that the S-wave two-particle states shown in the fourth column are responsible for the resonance poles. The corresponding thresholds are also explicitly given. The elastic scattering lengths, effective ranges, and the compositeness coefficients are provided in the last three columns. Since the mass of the $\psi(4260)$ is below the $D_1\overline{D}$ threshold, the probabilistic interpretation of X does not hold in this situation [7].

Resonance	Mass (MeV)	Width (MeV)	Threshold (MeV)	a (fm)	r (fm)	X
$Z_c(3900)$	3886.6 ± 2.4	28.2 ± 2.6	$D\overline{D}^*$ (3875.8)	-0.94 ± 0.12	-2.40 ± 0.21	0.49 ± 0.06
$X(4020)$	4024.1 ± 1.9	13 ± 5	$D^*\overline{D}^*$ (4017.1)	-1.04 ± 0.26	-3.89 ± 1.42	0.39 ± 0.12
$\psi(4260)$	4230 ± 8	55 ± 19	$D_1\overline{D}$ (4289.2)	-1.04 ± 0.06	-0.54 ± 0.03	$---$
$\psi(4660)$	4643 ± 9	72 ± 11	$\Lambda_c\overline{\Lambda}_c$ (4572.9)	-0.22 ± 0.04	-1.98 ± 0.28	0.24 ± 0.04
$\chi_{c1}(4140)$ (LHCb)	4146.5 ± 6.4	83 ± 30	$D_s\overline{D}_s^*$ (4080.5)	-0.27 ± 0.06	-1.79 ± 0.61	0.29 ± 0.08
$\chi_{c1}(4140)$ (~~LHCb~~)	4147.1 ± 2.4	15.7 ± 6.3	$D_s\overline{D}_s^*$ (4080.5)	-0.06 ± 0.02	-9.10 ± 3.86	0.06 ± 0.02
$\chi_{c1}(4140)$ (PDG)	4146.8 ± 2.4	22 ± 8	$D_s\overline{D}_s^*$ (4080.5)	-0.09 ± 0.03	-6.49 ± 2.40	0.08 ± 0.03

3. Phenomenological Discussions

Before entering the detailed discussions, we stress that the theoretical approach developed is based on the elastic S-wave two-body scattering. Strictly speaking, the present formalism applies to the scattering of two stable hadrons. A rigorous approach to handle the presence of unstable hadrons in the scattering process is to perform the study within three- or even few-body scattering [26], which is clearly beyond the scope of the present work. Another indirect way to understand the role of the width in the unstable hadrons is to use a complex mass ($m_i \longrightarrow m_i - i\Gamma_i/2$) in the expression for the three-momentum, Eq. (4), which then reads

$$k_R = \sqrt{2\mu_m \left(E_R - m_{\text{th}} + i\frac{\Gamma}{2}\right)}. \tag{14}$$

In this way, one can take into account the self-energy effects of the decaying channels. This is applicable, as compared with a full three-body study, if Γ is much smaller than the difference between the mass of the resonance and the threshold of the decay channel, as indicated by the results from [26] concerning the $D\overline{D}^*$, $\overline{D}D^*$ and $D\overline{D}\pi$ scattering and the $X(3872)$ resonance. This is the case for the D_1 hadron, and the numerical results obtained with a complex mass are also indicated below. Another interesting point is that unstable hadrons could introduce additional crossed-channel contributions, comparing with stable ones; see, e.g., [26].

The crossed-channel effects, such as the light-flavor hadron exchanges, are neglected in (1), which is strictly valid in the near-threshold region before any other branch-point singularity, associated with the onset of crossed channels, sets in. Nonetheless, the theoretical formalism presented here can be used also to study the systems in which the crossed-channel dynamics can be treated perturbatively. In [9, 10], the resonances $\Lambda_c(2595)$, $Z_b(10610)$ and $Z_b(10650)$ have been successfully addressed within this formalism. In the following, we tentatively generalize the discussions to the $Z_c(3900)$, $X(4020)$, $\chi_{c1}(4140)$, $\psi(4260)$ and $\psi(4660)$, which may be composed by some specific S-wave open-charm two-body states and lie close to their thresholds.

The masses and widths of the $Z_c(3900)$, $X(4020)$, $\chi_{c1}(4140)$, $\psi(4260)$, and $\psi(4660)$ and the thresholds of the nearby two-body states are collected in Table 1. The spin and parity of the $Z_c(3900)$, $\chi_{c1}(4140)$, $\psi(4260)$, and $\psi(4660)$ given in the PDG [2] are compatible with the S-wave elastic scattering of $D\overline{D}^*$, $D_s\overline{D}_s^*$, $D_1\overline{D}$ and $\Lambda_c\overline{\Lambda}_c$, respectively. For the $X(4020)$, its spin and parity are not confirmed by experiments yet. By assuming the S-wave molecular nature of $D^*\overline{D}^*$, a possible quantum number J^{PC} of the $X(4020)$ would be 1^{+-}.

For the $Z_c(3900)$, we see that standard values of a and r, corresponding to the typical scale of the long-range force of strong interactions, result from the $D\overline{D}^*$ scattering, according to the results in Table 1. The component of $D\overline{D}^*$ inside the $Z_c(3900)$ is as important as the other degrees of freedom (d.o.f), according to the compositeness $X \sim 0.5$. This finding qualitatively agrees with the conclusion from the pole-counting-rule study [27]. We have used the error bars of the masses and widths of the resonances to estimate the uncertainties of the a, r, and X and neglected the tiny error bars of the thresholds. For the $X(4020)$, a somewhat large value for $|r|$ is obtained. Both the $D^*\overline{D}^*$ and other d.o.f play important roles in the formation of $X(4020)$.

It is proposed in [28, 29] that the $\psi(4260)$ could be a possible S-wave $D_1\overline{D}$ resonance. If one assumes that the S-wave $D_1\overline{D}$ is the only source which is responsible for the resonance pole, the resulting scattering length and effective range can be found in Table 1. Standard values of a and r around 1 fm are obtained. However, because the resonance pole of $\psi(4260)$ is below the $D_1\overline{D}$ threshold, we can not use the recipe in (13) for the probabilistic interpretation [7]. Nonetheless, since the presence of a close to threshold CDD pole is characterized by having a small scattering length and a big effective range in magnitudes, the natural values for a and r given in Table 1 favor the interpretation offered in [28, 29].

Table 2: Set of numbers $|X|$, $|\widetilde{X}|$ [15], $|\widehat{X}|$ [16] and U [15–17] for the resonances considered in Table 1. No criteria for the probabilistic interpretation of the compositeness is met in the case of the $\psi(4260)$ resonance.

Resonance	Asymptotic State	$\lvert X\rvert$	$\widetilde{X}$	$\widehat{X}$	U
$Z_c(3900)$	$D\overline{D}^*$	0.49 ± 0.06	0.18 ± 0.02	0.30 ± 0.02	0.60 ± 0.10
$X(4020)$	$D^*\overline{D}^*$	0.39 ± 0.12	0.16 ± 0.04	0.27 ± 0.06	0.47 ± 0.19
$\psi(4260)$	$D_1\overline{D}$	4.5 ± 1.6	0.45 ± 0.02	0.49 ± 0.01	8.1 ± 3.2
$\psi(4660)$	$\Lambda_c\overline{\Lambda}_c$	0.24 ± 0.04	0.11 ± 0.02	0.19 ± 0.03	0.27 ± 0.05
$\chi_{c1}(4140)$ (LHCb)	$D_s\overline{D}_s^*$	0.29 ± 0.08	0.12 ± 0.03	0.22 ± 0.05	0.33 ± 0.12
$\chi_{c1}(4140)$ (~~LHCb~~)	$D_s\overline{D}_s^*$	0.06 ± 0.02	0.03 ± 0.01	0.06 ± 0.02	0.06 ± 0.02
$\chi_{c1}(4140)$ (PDG)	$D_s\overline{D}_s^*$	0.08 ± 0.03	0.04 ± 0.01	0.08 ± 0.03	0.09 ± 0.03

As shown in [10] when the position of the CDD pole tends to threshold, $M_{\text{CDD}} \longrightarrow m_{\text{th}}$, the resulting a and r tend to

$$a \longrightarrow \frac{M_{\text{CDD}} - m_{\text{th}}}{\lambda},$$
$$r \longrightarrow -\frac{\lambda}{\mu_m \left(M_{\text{CDD}} - m_{\text{th}}\right)^2}, \tag{15}$$

where λ is the residue of the CDD pole. The bigger this residue is, the sooner this behavior sets in. When the finite width of the D_1 is included via (14), the scattering length a and effective range r are shifted to -1.10 ± 0.07 fm and -0.55 ± 0.04 fm, respectively, which are compatible with the results shown in Table 1 within uncertainties. Therefore the effects from the finite width of the D_1 are indeed small. We also note that in [30], the large coupling of $\psi(4260)$ to $\omega\chi_{c0}$ is pointed out. Employing this coupling [7] obtained that $X_{\omega\chi_{c0}} \sim 0.2$.

Due to the closeness of the $\psi(4660)$ to the $\Lambda_c\overline{\Lambda}_c$ threshold and the compatibility of its quantum numbers with the S-wave $\Lambda_c\overline{\Lambda}_c$, we also explore the possibility that the elastic S-wave $\Lambda_c\overline{\Lambda}_c$ scattering is responsible for the $\psi(4660)$ pole. However, the small value of compositeness coefficient X in Table 1 indicates that the $\Lambda_c\overline{\Lambda}_c$ component plays a minor role and other d.o.f plays a more important role inside the $\psi(4660)$.

The quantum numbers of the S-wave $D_s\overline{D}_s^*$ scattering is compatible with the preferred $J^{PC} = 1^{++}$ of the $\chi_{c1}(4140)$ [2]. Notice that the new determinations of the masses and widths from LHCb [31, 32] are obviously larger than the previous measurements. We explicitly give different values for the masses and widths of $\chi_{c1}(4140)$ in Table 1. In all cases, it seems that the $D_s\overline{D}_s^*$ component plays a minor role inside $\chi_{c1}(4140)$.

We have employed the approach of [7, 10] which conclude a probabilistic interpretation of $|X|$ for $M_R > m_{\text{th}}$. As explained in more detail in [7, 8], this result is based on a phase redefinition of the resonance couplings (whose phases are affected by the non-resonant terms around the pole [33]), and on a direct observation of the resonance-peak signal stemming from its Laurent series for physical values of the energy. In contrast, [15–17] propose some ad-hoc manipulations on the complex numbers X and $Z = 1 - X$ so as to end with positive definite values between 0 and 1. We compare our results with theirs below.

References [15, 17] construct from $|X|$ and $|Z|$ other numbers $\widetilde{X}$, $\widetilde{Z}$ and U, which are defined as

$$\widetilde{X} = \frac{1}{2} + \frac{|X| - |1 - X|}{2},$$
$$\widetilde{Z} = \frac{1}{2} + \frac{|1 - X| - |X|}{2}, \tag{16}$$
$$U = |X| + |1 - X| - 1.$$

By construction they fulfill that $\widetilde{X} + \widetilde{Z} = 1$ and $0 \le \widetilde{X}, \widetilde{Z} \le 1$. The parameter U measures the degree of cancellation between the complex numbers X and Z, whose sum is 1. By geometrical reasoning, see Figure 1 of [15], $\pm U/2$ is interpreted as the uncertainty in the probabilistic interpretation of $\widetilde{X}$.

In turn, [16] introduces other numbers $\widehat{X}$ and $\widehat{Z}$ defined by

$$\widehat{X} = \frac{|X|}{1 + U},$$
$$\widehat{Z} = \frac{|1 - X|}{1 + U}. \tag{17}$$

These numbers also fulfill by construction that $0 \le \widehat{X}, \widehat{Z} \le 1$ and $\widehat{X} + \widehat{Z} = 1$. This reference claims that $\widehat{X}$ and $\widehat{Z}$ have a probabilistic interpretation in connection with the weight of the different continuum states in a resonance if $U \ll 1$. It is also noticed that the difference between $\widetilde{X}$ and $\widehat{X}$ tends to zero linearly in U for $U \longrightarrow 0$.

We give in Table 2 the values of $|X|$, $\widetilde{X}$, $\widehat{X}$ and U for the resonances shown in Table 1. For the last two entries of the $\chi_{c1}(4140)$ one has that $U \ll 1$ and the same quantitative conclusion on the very small size of the compositeness of $D_s\overline{D}_s^*$ results from all these numbers. Still small values for $U \lesssim 0.3$ results for the first entry of the $\chi_{c1}(4140)$ and for the $\psi(4660)$, and a similar conclusion on the relatively small size of the weight of the two-body continuum states results from all the instances. Notice that it is always the case in these examples that $|X| \simeq \widehat{X}$, while $\widetilde{X}$ is different by around a factor of 2. This is because of the following [15]:

$$\left||X| - \widetilde{X}\right| = \frac{U}{2}, \tag{18}$$

as it is clear from (16), and U is as large as $|X|$ in these cases. Thus, the approach that we follow here, based on [7, 10] and summarized above, favors the use of $\widehat{X}$ of [16] over $\widetilde{X}$ of [15].

For the resonance $X(4020)$ one has that $U \approx 0.5$. Now, the difference between the central values of $|X|$ and $\widehat{X}$ is larger, although they drive to a similar conclusion on the weight of the continuum state. The value of U is larger for the $Z_c(3900)$, with $U/2 \approx 0.3$, and the uncertainty $U/2$ in the interpretation of the numbers $\widehat{X}$ and $\widetilde{X}$, as argued in [15], becomes very important, driving to values that differ between each other by around a factor of 2. Finally, any of the criteria for the probabilistic interpretation of the compositeness of the $\psi(4260)$ cannot be applied since now U is huge.

Let us also mention that the ERE for scattering up to and including the effective range, like in our study here, drives necessarily to purely imaginary values for X, since $X = i\gamma_k^2 = -ik_i/k_r$. This invalidates the interpretation of ReX as the compositeness for the case of a resonance, as advocated in [24], because it is always equal to zero in our case, no matter the nature of the resonance under study.

4. Summary and Conclusions

In this work, we have combined the effective range expansion, unitarity, analyticity, and the compositeness coefficient to study the resonance dynamics around the threshold energy region. We only focus on the elastic S-wave scattering throughout. In our formalism, the scattering length, effective range, and the compositeness coefficient can be straightforwardly calculated, if the mass and width of the resonance are provided.

We have applied the theoretical formalism to the $Z_c(3900)$, $X(4020)$, $\chi_{c1}(4140)$, $\psi(4260)$ and $\psi(4660)$. The resonance poles are assumed to be generated by the elastic S-wave scattering of $D\overline{D}^*$, $D^*\overline{D}^*$, $D_s\overline{D}_s^*$, $D_1\overline{D}$ and $\Lambda_c\overline{\Lambda}_c$, respectively. According to the values in Table 1, we tentatively conclude that both the $D\overline{D}^*$ and other degrees of freedom are equally important inside the $Z_c(3900)$. The $D^*\overline{D}^*$ component inside the $X(4020)$ is also important, while, for the $\chi_{c1}(4140)$ and $\psi(4660)$, the $D_s\overline{D}_s^*$ and $\Lambda_c\overline{\Lambda}_c$ components seem playing minor roles, respectively. In addition, the natural values for $a \simeq -1$ fm and $r \simeq -0.5$ fm in the case of the $\psi(4260)$ are compatible with its interpretation in [28, 29] as a $D_1\overline{D}$ molecular state.

Data Availability

The data used to support the findings of this study are included within the article.

Conflicts of Interest

The authors declare that they have no conflicts of interest.

Acknowledgments

Zhi-Hui Guo would like to thank En Wang for the informative communication on the $\chi_{c1}(4140)$. This work is funded in part by the NSFC under Grants nos. 11575052 and 11805012, the Natural Science Foundation of Hebei Province under Contract no. A2015205205, and the MINECO (Spain) and FEDER (EU) Grant FPA2016-77313-P.

References

[1] S. K. Choi, [Belle Collaboration] et al., "Observation of a Narrow Charmoniumlike State in Exclusive $B^{\pm} \longrightarrow K^{\pm}\pi^+\pi^- J/\psi$ Decays," *Physical Review Letters*, vol. 91, Article ID 262001, 2003.

[2] M. Tanabashi, K. Hagiwara, and K. Hikasa, "Review of particle physics," *Physical Review D: Particles, Fields, Gravitation and Cosmology*, vol. 98, no. 3, Article ID 030001, 2018.

[3] H. X. Chen, W. Chen, X. Liu, and S. L. Zhu, "The hidden-charm pentaquark and tetraquark states," *Physics Reports*, vol. 639, pp. 1–121, 2016.

[4] F. K. Guo, C. Hanhart, U. G. Meißner, Q. Wang, Q. Zhao, and B. S. Zou, "Hadronic molecules," *Reviews of Modern Physics*, vol. 90, no. 1, Article ID 015004, 2018.

[5] H. A. Bethe, "Theory of the effective range in nuclear scattering," *Physical Review Journals*, vol. 76, pp. 38–50, 1949.

[6] M. A. Preston and B. K. Bhaduri, *Structure of the Nucleus*, Addison-Wesley Publishing Company, Inc., Massachusetts, Mass, USA, 1975.

[7] Z. H. Guo and J. A. Oller, "Probabilistic interpretation of compositeness relation for resonances," *Physical Review D*, vol. 93, no. 9, Article ID 096001, 2016.

[8] J. A. Oller, "New results from a number operator interpretation of the compositeness of bound and resonant states," *Annals of Physics*, vol. 396, pp. 429–458, 2018.

[9] Z. H. Guo and J. A. Oller, "Resonance on top of thresholds: the $\Lambda_c(2595)^+$ as an extremely fine-tuned state," *Physical Review D*, vol. 93, no. 5, Article ID 054014, 2016.

[10] X. W. Kang, Z. H. Guo, and J. A. Oller, "General considerations on the nature of $Z_b(10610)$ and $Z_b(10650)$ from their pole positions," *Physical Review D: Particles, Fields, Gravitation and Cosmology*, vol. 94, no. 1, Article ID 014012, 2016.

[11] Z. H. Guo and J. A. Oller, "Anatomy of the newly observed hidden-charm pentaquark states: $P_c(4312)$, $P_c(4440)$ and $P_c(4457)$," *Physics Letters B*, vol. 793, pp. 144–149, 2019.

[12] L. Y. Dai, J. Haidenbauer, and U. G. Meißner, "Re-examining the X(4630) resonance in the reaction $e^+e^- \longrightarrow \Lambda_c^+\overline{\Lambda}_c^-$," *Physical Review D*, vol. 96, no. 11, Article ID 116001, 2017.

[13] G. Cotugno, R. Faccini, A. D. Polosa, and C. Sabelli, "Charmed baryonium," *Physical Review Letters*, vol. 104, no. 13, Article ID 132005, 2010.

[14] F. Guo, J. Haidenbauer, C. Hanhart, and U. Meißner, "Reconciling the $X(4630)$ with the $Y(4660)$," *Physical Review D: Particles, Fields, Gravitation and Cosmology*, vol. 82, no. 9, Article ID 094008, 2010.

[15] Y. Kamiya and T. Hyodo, "Generalized weak-binding relations of compositeness in effective field theory," *PTEP: Progress of Theoretical and Experimental Physics*, vol. 2017, no. 2, Article ID 023D02, 2017.

[16] T. Sekihara, T. Arai, J. Yamagata-Sekihara, and S. Yasui, "Compositeness of baryonic resonances: Application to the $\Delta(1232)$, $N(1535)$, and $N(1650)$ resonances," *Physical Review C: Nuclear Physics*, vol. 93, no. 3, Article ID 035204, 2016.

[17] Y. Kamiya, T. Hyodo, and C. Phys. Rev, "Structure of near-threshold quasibound states," *Physical Review C*, vol. 93, no. 3, Article ID 035203, 2016.

[18] X. Kang and J. A. Oller, "Different pole structures in line shapes of the $X(3872)$," *The European Physical Journal C*, vol. 77, no. 6, article 399, 2017.

[19] V. Baru, J. Haidenbauer, C. Hanhart, Y. Kalashnikova, and A. E. Kudryavtsev, "Evidence that the a(0)(980) and f(0)(980) are not elementary particles," *Physics Letters B*, vol. 586, no. 1-2, pp. 53–61, 2004.

[20] C. Hanhart, Y. S. Kalashnikova, and A. V. Nefediev, "Interplay of quark and meson degrees of freedom in a near-threshold resonance: multi-channel case," *The European Physical Journal A*, vol. 47, article 101, 2011.

[21] T. Hyodo, D. Jido, and A. Hosaka, "Compositeness of dynamically generated states in a chiral unitary approach," *Physical Review C: Nuclear Physics*, vol. 85, no. 1, Article ID 015201, 2012.

[22] F. Aceti and E. Oset, "Wave functions of composite hadron states and relationship to couplings of scattering amplitudes for general partial waves," *Physical Review D: Particles, Fields, Gravitation and Cosmology*, vol. 86, no. 1, Article ID 014012, 2012.

[23] T. Sekihara, T. Hyodo, and D. Jido, "Comprehensive analysis of the wave function of a hadronic resonance and its compositeness," *PTEP: Progress of Theoretical and Experimental Physics*, vol. 2015, no. 6, Article ID 063D04, 2015.

[24] F.-H. Liu, T. Tian, H. Zhao, and B.-C. Li, "Meson-baryon components in the states of the baryon decuplet," *The European Physical Journal A*, vol. 50, article 57, 2014.

[25] S. Weinberg, "Elementary particle theory of composite particles," *Physical Review A: Atomic, Molecular and Optical Physics*, vol. 130, no. 2, pp. 776–783, 1963.

[26] V. Baru, A. A. Filin, C. Hanhart, Y. S. Kalashnikova, A. E. Kudryavtsev, and A. V. Nefediev, "Three-body $D\overline{D}\pi$ dynamics for the $X(3872)$," *Physical Review D: Particles, Fields, Gravitation and Cosmology*, vol. 84, no. 7, Article ID 074029, 2011.

[27] Q. Gong, Z. Guo, C. Meng, G. Tang, Y. Wang, and H. Zheng, "$Z_c(3900)$ as a $\overline{D}D^*$ molecule from the pole counting rule," *Physical Review D: Particles, Fields, Gravitation and Cosmology*, vol. 94, no. 11, Article ID 114019, 2016.

[28] Q. Wang, C. Hanhart, and Q. Zhao, "Decoding the Riddle of $Y(4260)$ and $Z_c(3900)$," *Physical Review Letters*, vol. 111, no. 13, Article ID 132003, 2013.

[29] Q. Wang, M. Cleven, F. Guo et al., "$Y(4260)$: Hadronic molecule versus hadro-charmonium interpretation," *Physical Review D: Particles, Fields, Gravitation and Cosmology*, vol. 89, no. 3, Article ID 034001, 2014.

[30] L. Dai, M. Shi, G. Tang, and H. Zheng, "Nature of X(4260)," *Physical Review D: Particles, Fields, Gravitation and Cosmology*, vol. 92, no. 1, Article ID 014020, 2015.

[31] R. Aaij, B. Adeva, and M. Adinolfi, "Publisher's Note: First Experimental Study of Photon Polarization in Radiative B_s^0 Decays," *Physical Review Letters*, vol. 118, no. 2, Article ID 022003, 2017.

[32] R. Aaij et al., "Amplitude analysis of $B^+ \longrightarrow J/\psi\phi K^+$ decays," *Physical Review D: Particles, Fields, Gravitation and Cosmology*, vol. 95, no. 1, Article ID 012002, 2017.

[33] S. Weinberg, *The Quantum Field Theory of Fields. Volume I Foundations*, Cambridge University Press, New York, NY, USA, 1995.

Hindawi
Advances in High Energy Physics
Volume 2019, Article ID 3465159, 7 pages
https://doi.org/10.1155/2019/3465159

Research Article

Unquenching the Quark Model in a Nonperturbative Scheme

Pablo G. Ortega, David R. Entem, and Francisco Fernández

Grupo de Física Nuclear and Instituto Universitario de Física Fundamental y Matemáticas (IUFFyM), Universidad de Salamanca, E-37008 Salamanca, Spain

Correspondence should be addressed to David R. Entem; entem@usal.es

Received 8 January 2019; Revised 17 March 2019; Accepted 7 April 2019; Published 2 May 2019

Guest Editor: Xian-Wei Kang

In recent years, the discovery in quarkonium spectrum of several states not predicted by the naive quark model has awakened a lot of interest. A possible description of such states requires the enlargement of the quark model by introducing quark-antiquark pair creation or continuum coupling effects. The unquenching of the quark models is a way to take these new components into account. In the spirit of the Cornell Model, this is usually done by coupling perturbatively a quark-antiquark state with definite quantum numbers to the meson-meson channel with the closest threshold. In this work we present a method to coupled quark-antiquark states with meson-meson channels, taking into account effectively the nonperturbative coupling to all quark-antiquark states with the same quantum numbers. The method will be applied to the study of the X(3872) resonance and a comparison with the perturbative calculation will be performed.

1. Introduction

Constituent quark models (CQM) have been extremely successful in describing the properties of hadrons such as the spectrum and the magnetic moments. However, since the earliest days of the hadron spectroscopy, it was realized [1] that such models neglect the contribution of higher Fock components (virtual $q\bar{q}$ pairs, unitary loops, or hadron-hadron channels) predicted by QCD. Unquenching the quark model is a way to incorporate these components, in a similar way as unquenched lattice theories included dynamical quarks instead of static quarks (quenched theories). It is worth noticing, though, that the name "unquenched quark model" refers to different approaches to include these higher Fock components. Thus, Tornqvist and collaborators [2, 3] use a "unitarized" quark model to incorporate the effects of two meson channels to $c\bar{c}$ and $b\bar{b}$ spectrum. Van Beveren and Rupp [4, 5] showed the influence of continuum channels on the properties of hadrons, in a model which describes the meson as a system of one or more closed quark-antiquark states in interaction with several two meson channels. More recently, Bijker and Santopinto [6] developed an unquenched quark model for baryons, in which a constituent quark model is modified to include, as a perturbation, a QCD-inspired quark-antiquark creation mechanism. Under this assumption, the baryon wave function consists of a zeroth-order three-valence quark configuration plus a sum over baryon-meson loops.

The components beyond the naive constituent quark model became more relevant since 2003, when the $X(3872)$ and other XYZ states were discovered. At that time hadron spectroscopy begins to measure hadron states near two particle thresholds and in this situation loop corrections are relevant.

The $X(3872)$ resonance has been studied using different versions of the unquenched quark model in Ref. [7–9]. Eichten *et al.* [7] considered the influence of meson-meson channels using the Cornell coupled channels scheme [10], obtaining a perturbative mass shift of the $c\bar{c}$ configuration below threshold and an additional decay width for configurations above threshold. Using the Resonance Spectrum expansion [11] Coito *et al.* showed that the $X(3872)$ is compatible with a description in terms of a regular 2^3P_1 charmonium state with a renormalized mass, via opened and closed decay channels. Finally, in Ref. [12], it was shown that one can describe the $X(3872)$ as a $\chi_{c1}(2P)$ interpreted as a

$c\bar{c}$ core plus higher Fock components due to perturbative coupling to the meson-meson continuum.

A different point of view from the references mentioned above is presented in Ref. [13]. The authors of Ref. [13] also study the coupling of the $q\bar{q}$ states with meson-meson channels, but in this case the meson-meson interaction which originates by the underlying quark-quark interaction is fully taken into account, in contrast to other studies such as Ref. [14]. The approach of Ref. [13] allows to have bound states not only in the $q\bar{q}$ channels but, under certain circumstances, in the meson-meson channels. They start from a coupled channels approach for the $J^{PC} = 1^{++}$ channel, to study the influence of the $q\bar{q}$ channels in the meson-meson one. Solving the coupling for the $q\bar{q}$ states one arrives to a Schrödinger-type equation in which the meson-meson interaction gets modified by the coupling with the bare $q\bar{q}$ states, generating a resonance which can be identified with the $X(3872)$. Besides this state, one gets an orthogonal one which can be identified with the $X(3940)$. Both are different combinations of $q\bar{q}$ and meson-meson states.

Some models, as our previous work in Ref. [13], choose a particular $q\bar{q}$ state which gets modified by the interaction with the two meson channels. Usually, the states "closer" to the threshold of the meson-meson channel are chosen, but sometimes it is difficult to decide which ones are relevant. Moreover, in some models, this state is modified perturbatively.

In an attempt to improve these caveats, we have developed a new scheme in which the contributions of the complete tower of radial excitations corresponding to a given J^{PC} value of $q\bar{q}$ states are automatically taken into account. A similar approach was already done in Ref. [14], in which a model that can be solved analytically was used, but with no meson-meson interaction included. The rationale of the method is to leave the $q\bar{q}$ radial wave function as unknown to be determined dynamically. Afterwards, the contribution of each "quenched" state is determined by expanding the obtained wave function in a bare quark-antiquark base. In this way, one incorporates from scratch all possible $q\bar{q}$ states and also allows the deformation of the bare $q\bar{q}$ wave function due to interaction with the meson-meson channels. Although the method is general for baryons and mesons, for the sake of clarity in this paper we will develop it only for mesons.

The paper is organized as follows. In Section 2 we first discuss the coupled channel formalism and the coupling mechanism between the different channels and the basic ingredients of the constituent quark model. Results and comments are presented in Section 3. Finally, we summarize the main achievements of our calculation in Section 4.

2. The Model

2.1. The Constituent Quark Model. The constituent quark model used in this work has been extensively described elsewhere [15, 16] and therefore we will only summarize here its most relevant aspects. The chiral symmetry of the original QCD Lagrangian appears spontaneously broken in nature and, as a consequence, light quarks acquire a dynamical mass. The simplest Lagrangian invariant under chiral rotations must therefore contain chiral fields and can be expressed as

$$\mathscr{L} = \overline{\psi}\left(i\partial\!\!\!/ - M\left(q^2\right)U^{\gamma_5}\right)\psi \tag{1}$$

where $U^{\gamma_5} = e^{i(\lambda_a/f_\pi)\phi^a\gamma_5}$ is the Goldstone boson fields matrix and $M(q^2)$ is the dynamical (constituent) mass. This Lagrangian has been derived in Ref. [17] as the low-energy limit in the instanton liquid model. In this model the dynamical mass vanishes at large momenta and it is frozen at low momenta, for a value around 300 MeV. Similar results have also been obtained in lattice calculations [18]. To simulate this behavior we parametrize the dynamical mass as $M(q^2) = m_q F(q^2)$, where $m_q \simeq 300\ MeV$, and

$$F\left(q^2\right) = \left[\frac{\Lambda_\chi^2}{\Lambda_\chi^2 + q^2}\right]^{1/2}. \tag{2}$$

The cut-off Λ_χ fixes the chiral symmetry breaking scale.

The Goldstone boson field matrix U^{γ_5} can be expanded in terms of boson fields,

$$U^{\gamma_5} = 1 + \frac{i}{f_\pi}\gamma^5\lambda^a\pi^a - \frac{1}{2f_\pi^2}\pi^a\pi^a + \cdots \tag{3}$$

The first term of the expansion generates the constituent quark mass while the second gives rise to a one-boson exchange interaction between quarks. The main contribution of the third term comes from the two-pion exchange which has been simulated by means of a scalar exchange potential.

In the heavy quark sector chiral symmetry is explicitly broken and this type of interaction does not act. However it constrains the model parameters through the light meson phenomenology and provides a natural way to incorporate the pion exchange interaction in the open charm dynamics.

Below the chiral symmetry breaking scale quarks still interact through gluon exchanges described by the Lagrangian

$$\mathscr{L}_{gqq} = i\sqrt{4\pi\alpha_s}\overline{\psi}\gamma_\mu G_c^\mu\lambda_c\psi, \tag{4}$$

where λ_c are the SU(3) color generators and G_c^μ is the gluon field. The other QCD nonperturbative effect corresponds to confinement, which prevents from having colored hadrons. Such a term can be physically interpreted in a picture in which the quark and the antiquark are linked by a one-dimensional color flux-tube.

Lattice calculations have shown that, as far as the quarks get separated, virtual quark anti-quark pairs tend to modify the confinement potential, giving rise at some scale to a breakup of the color flux-tube [19]. Coupled channels and screening potential represent similar physics [20]. However, our approach is to couple those channels whose thresholds are near to the $q\bar{q}$ states we are studying in detail; therefore it should not be treated perturbatively, and, furthermore, averaging the effects of the rest of the thresholds through the following screened confinement potential,

$$V_{CON}\left(\vec{r}_{ij}\right) = \left\{-a_c\left(1 - e^{-\mu_c r_{ij}}\right) + \Delta\right\}\left(\vec{\lambda^c}_i \cdot \vec{\lambda^c}_j\right). \tag{5}$$

Explicit expressions for these interactions and the value of the parameters are given in Ref. [15, 16].

2.2. The Unquenched Meson Spectrum. Although over the time the procedure to incorporate new Fock components to the $q\overline{q}$ wave function has received several names (unitarized quark model [2], resonance spectrum expansion [11], and coupled channel formalism [1]) the basic idea behind the unquenched meson model is to assume that a hadron wave function with fixed J^P quantum numbers combines a zeroth-order configuration plus a sum over the possible higher Fock components due to the creation of $q\overline{q}$ pairs:

$$\left|\Psi_A\right\rangle = \mathcal{N}\left|A\right\rangle + \sum_{BClj}\int d\vec{K}k^2dk\left|BClj,\vec{K},k\right\rangle \times \frac{\left\langle BClj,\vec{K},k\right|T^+\left|A\right\rangle}{E_0 - E_B - E_C} \tag{6}$$

where T^+ stands for the operator which couples the different components, usually the $^3P_0$ quark-antiquark pair creator, and $|A\rangle$ is an eigenstate of the bare Hamiltonian $H_0|A\rangle = E_0|A\rangle$.

In practice what is done is to assume that the first Fock component, namely, the $q\overline{q}$ structure, is renormalized via the influence of nearby meson-meson channels and, thus, coupled channels calculation is performed including the bare $q\overline{q}$ state and the meson-meson channels. Solving the coupling with the meson-meson channels one obtains for the mass shift of the meson $|A\rangle$

$$\Sigma\left(E_A\right) = \sum_{BClj}\int dk^2dk\frac{\left|\left\langle BClj,\vec{K},k\right|T^+\left|A\right\rangle\right|^2}{E_A - E_{BC}} \tag{7}$$

where E_{BC} is the kinetic energy of the meson-meson pair.

As stated in the introduction, this method has two important shortcomings. First of all, it focuses the study on the modification of the $q\overline{q}$ channel, avoiding the study of the meson-meson channel where interesting structures may appear. Second, it is chosen from the beginning one $q\overline{q}$ channel to be modified, neglecting those $q\overline{q}$ channels which may be generated in the interaction with the meson-meson channel.

For these reasons, we have developed a new scheme in which the contributions of all states are initially taken into account, being the dynamics the responsible of selecting the contribution of each bound state.

The Hamiltonian we consider

$$H = H_0 + V \tag{8}$$

is the sum of an "unperturbed" part H_0 and a second part V which couples a $q\overline{q}$ system to a continuum made of meson-meson states.

Instead of expanding the wave function of the $q\overline{q}$ system in eigenstates of the H_0 Hamiltonian and then solving the coupled channels equation with the meson-meson channels, we use a general wave function for the $q\overline{q}$ system to solve the coupled channels problem and then develop the solution of the $q\overline{q}$ system in the base of the bare $q\overline{q}$ states. In this way, the dynamics of the system is the element which determines the contribution of each bare state to the eigenstate, obtained from the two-body Schrödinger equation which includes the effect of the dynamics of the nearby meson-meson channels.

The meson wave functions to be used all along this work will be expressed using the Gaussian Expansion Method [21] (GEM), expanding the radial wave function in terms of basis functions

$$\left|\Phi_\alpha\left(r\right)\right\rangle = \sum_{n=1}^{n_{max}} c_n^\alpha\left|\phi_{nl}^G\left(r\right)\right\rangle \tag{9}$$

where α refers to the channel quantum numbers and $|\phi_{nl}^G(r)\rangle$ are Gaussian trial functions with ranges in geometrical progression. This choice is useful for optimizing the ranges with a small number of free parameters [21]. In addition, the density of the distribution of the Gaussian ranges in geometrical progression at small ranges is suitable for making the wave function correlate with short range potentials.

To introduce higher Fock components in the $q\overline{q}$ wave function we assume that the hadronic state is

$$\left|\Psi\right\rangle = \left|\Phi_\alpha\right\rangle + \sum_\beta \chi_\beta\left(P\right)\left|\phi_A\phi_B\beta\right\rangle \tag{10}$$

where $|\Phi_\alpha\rangle$ is the $q\overline{q}$ wave function, ϕ_M are $q\overline{q}$ eigenstates describing the A and B mesons, $|\phi_A\phi_B\beta\rangle$ is the two-meson state with β quantum numbers coupled to total J^{PC} quantum numbers, and $\chi_\beta(P)$ is the relative wave function between the two mesons in the molecule. The meson-meson interaction will be derived from the qq interaction using the Resonating Group Method (RGM) [22].

We must notice that, although the Gaussian Expansion Method of the $q\overline{q}$ wave functions can be also used for the mesons constituting the molecular states, we will assume that the wave functions of these mesons are simple solutions of the Schrödinger two-body equation.

In order to couple both sectors, we use the QCD-inspired $^3P_0$ model [23], which gives a clear picture of the physical mechanism of the coupling. In this model, a quark pair is created from the vacuum with the vacuum quantum numbers. After the pair creation, a recombination of the quark-antiquark of the initial meson with the $^3P_0$ pair follows to give the two final mesons. The $^3P_0$ quark-antiquark pair-creation operator can be written as [24]

$$\mathcal{T} = -3\sqrt{2}\gamma'\sum_\mu\int d^3pd^3p'\delta^{(3)}\left(p+p'\right) \times\left[\mathcal{Y}_1\left(\frac{p-p'}{2}\right)b_\mu^\dagger\left(p\right)d_\nu^\dagger\left(p'\right)\right]^{C=1,I=0,S=1,J=0} \tag{11}$$

where μ ($\nu = \overline{\mu}$) are the quark (antiquark) quantum numbers and $\gamma' = 2^{5/2}\pi^{1/2}\gamma$ with $\gamma = g/2m$ is a dimensionless constant which gives the strength of the $q\overline{q}$ pair creation from the vacuum.

Finally, in the context of the $^3P_0$ model, the transition operator $h_{\beta\alpha}(P)$ can be defined from the $\mathcal{T}$ operator as

$$\left\langle \phi_{M_1}\phi_{M_2}\beta\right| \mathcal{T} \left|\Phi_\alpha\right\rangle = Ph_{\beta\alpha}(P)\,\delta^{(3)}\left(\vec{P}_{\mathrm{cm}}\right) \tag{12}$$

where P is the relative momentum of the two-meson state.

Now, we use Eq. (9) to decompose $h_{\beta\alpha}(P)$ as

$$h_{\beta\alpha}(P) = \sum_{n=1}^{n_{max}} c_n^\alpha h_{\beta\alpha}^n(P) \tag{13}$$

Then, the coefficients c_n^α of the $q\overline{q}$ meson wave function and the eigenenergy E are determined from the coupled-channel equations

$$\begin{aligned}&\sum_{\alpha,n}\left[\mathscr{H}_{n'n}^{\alpha'\alpha} - \mathscr{G}_{n'n}^{0\alpha'\alpha}(E)\right]c_n^\alpha = \sum_n EN_{n'n}^{\alpha'}c_n^{\alpha'}\\ &\sum_\beta \int H_{\beta'\beta}\left(P',P\right)\chi_\beta(P)\,P^2dP + \sum_\alpha h_{\beta'\alpha}\left(P'\right)\\ &\quad = E\chi_{\beta'}\left(P'\right)\end{aligned} \tag{14}$$

where $N_{n'n}^{\alpha'}$ is the normalization matrix of the GEM trial Gaussian functions, $\mathscr{H}_{n'n}^{\alpha'\alpha}$ is the interquark Hamiltonian that defines the bare $q\overline{q}$ meson spectrum, and $H_{\beta'\beta}$ is the RGM Hamiltonian for the two meson states, obtained from the $q\overline{q}$ interaction. In the previous equations we have defined the perturbative mass shift $\mathscr{G}_{n'n}^{0\alpha'\alpha}$ as

$$\mathscr{G}_{n'n}^{0\alpha'\alpha}(E) = -\delta^{\alpha'\alpha}\delta_{n'n}\sum_\beta \int h_{\alpha'\beta}^{n'}(P)\,\chi_\beta(P)\,P^2dP, \tag{15}$$

which codifies the coupling with molecular states. Apparently, the perturbative mass shift does not mix different $q\overline{q}$ channels, so the only operator which mixes them is the potential $V_{n'n}^{\alpha'\alpha}$ in $\mathscr{H}_{n'n}^{\alpha'\alpha}$. However, as will be detailed below, the molecular wave function is dependent on different meson channels.

The previous coupled channel equations can be solved in a more elegant way through the T matrix, solution of the Lippmann-Schwinger equation,

$$\begin{aligned}T^{\beta'\beta}\left(P',P;E\right) &= V^{\beta'\beta}\left(P',P;E\right)\\ &+ \sum_{\beta''}\int V^{\beta'\beta''}\left(P',P'';E\right)\\ &\cdot \frac{1}{E - E_{\beta''}(P'')}T^{\beta''\beta}\left(P'',P;E\right)P''^2dP''\end{aligned} \tag{16}$$

where $V^{\beta'\beta}(P',P)$ is the RGM potential.

Using the T matrix, we end up with a Schrödinger-like equation for the c_n^α coefficients,

$$\sum_{\alpha,n}\left[\mathscr{H}_{n'n}^{\alpha'\alpha} - \mathscr{G}_{n'n}^{\alpha'\alpha}(E)\right]c_n^\alpha = \sum_n EN_{n'n}^{\alpha'}c_n^{\alpha'}. \tag{17}$$

In the previous equation we identify $\mathscr{G}_{n'n}^{\alpha'\alpha}$ as the energy-dependent complete mass-shift matrix

$$\mathscr{G}_{n'n}^{\alpha'\alpha}(E) = \sum_\beta \int dqq^2\frac{\overline{h}_{\alpha'\beta}^{n'}(q,E)\,h_{\beta\alpha}^n(q)}{q^2/2\mu - E - i0^+}, \tag{18}$$

where $\overline{h}^{\alpha'\beta}$ is the ${}^3P_0$ potential dressed by the RGM meson-meson interaction,

$$\begin{aligned}\overline{h}^{\alpha\beta'}(p,E) &= h_{\alpha\beta'}(p)\\ &- \sum_\beta \int d^3q\frac{T^{\beta'\beta}(p,q,E)\,h_{\alpha\beta}(q)}{q^2/2\mu - E - i0^+},\end{aligned} \tag{19}$$

which can be decomposed in the GEM basis as $h^{\alpha\beta}$ in Eq. (13).

In order to find molecular states above and below thresholds in the same formalism we have to analytically continue all the potentials for complex momenta. Therefore, resonances are solutions of Eq. (17), with the pole position solved by the Broyden method [25].

The molecular wave function is related with the c_n^α coefficients of the meson $q\overline{q}$ state,

$$\chi_\beta(p) = -\sum_{\alpha,n}\frac{\overline{h}_{\alpha\beta}^n(p,E)\,c_n^\alpha(E)}{p^2/2\mu - E - i0^+} \tag{20}$$

with the normalization given by

$$1 = \sum_{\alpha,\alpha',n,n'} c_{n'}^{\alpha'}N_{n'n}^{\alpha'\alpha}c_n^\alpha + \left\langle \chi_\beta \mid \chi_\beta\right\rangle \tag{21}$$

The partial decay widths can be defined through the complete S-matrix of the mix channel, as detailed in [26].

3. Calculations, Results, and Discussions

In order to compare the results of the proposed scheme with the perturbative one we perform a similar calculation as in Ref. [13], namely, a coupled channel calculation including the 1^{++} $q\overline{q}$ sector and the $D^0\overline{D}^{0*}$ and $D^\pm D^{*\mp}$ channels. We, first of all, perform a calculation with the same parameters as [13] in the charge basis

$$\left|D^\pm D^{*\mp}\right\rangle = \frac{1}{\sqrt{2}}\left(\left|D\overline{D}^*\,I=0\right\rangle - \left|D\overline{D}^*\,I=1\right\rangle\right) \tag{22}$$

$$\left|D^0\overline{D}^{*0}\right\rangle = \frac{1}{\sqrt{2}}\left(\left|D\overline{D}^*\,I=0\right\rangle + \left|D\overline{D}^*\,I=1\right\rangle\right) \tag{23}$$

Isospin symmetry is explicitly broken taking the experimental threshold difference into account in our equations and solving for the charged and the neutral components.

One can see in Table 2 that when we use the value of $\gamma = 0.26$ we get three states with energies close to the $X(3940)$, the $X(3872)$, and the $c\overline{c}$ $M = 3510$ MeV/c^2. The first two states are mixtures of $c\overline{c}$ and $D\overline{D}^*$ components, being the $X(3940)$ predominantly $c\overline{c}$ and the $X(3872)$ mostly $D\overline{D}^*$. The third state is clearly a $q\overline{q}$ state. If we project the $q\overline{q}$ component in the base of bare $c\overline{c}$ states (Table 3) we realize that this third state is an almost pure 1^3P_1 $c\overline{c}$ state whereas the other two are predominantly 2^3P_1. In order to compare with the bare H_0 spectrum we show in Table 1 the charmonium states in the vicinity of the $X(3872)$, only up to the first radial excitation.

Table 1: H_0 spectrum for the $J^{PC} = 1^{++}$ sector in the vicinity of the $X(3872)$ resonance. A more complete description of the bare charmonium spectrum can be found in Ref. [27].

$c\overline{c}$ State	Mass [MeV]
1^3P_1	3503.9
2^3P_1	3947.4

One can analyze the isospin content of the $D\overline{D}^*$ component of the different states. The only one which shows a sizable $I = 1$ component is the one we have identified with the $X(3872)$. The other two are basically $I = 0$ states. Notice that all the interactions are isospin conserving interactions and the reason to have a non-zero $I = 1$ component for the $X(3872)$ is that the binding energy of the $D\overline{D}^*$ component for this state is smaller than the isospin breaking of the $D^{(*)0}$ and $D^{(*)\pm}$ masses which enhances the $D^0\overline{D}^{*0}$ component at large distances.

As in Ref. [13], we have fine-tuned the $^3P_0$ parameter to get the right binding energy of the $X(3872)$. The results are shown in the second part of Table 2. We get again three states. The first one, with a mass of $M = 3943.9$ MeV/c^2, can be identified with the $X(3940)$ [28] and is a mixture of 57% of $q\overline{q}$ and 43% of $D\overline{D}^*$ molecule with isospin $I = 0$. The $q\overline{q}$ component is basically a 2^3P_1 state. The second state has now the right energy of the $X(3872)$ resonance. The $D^0\overline{D}^{*0}$ clearly dominates its structure with a 94% probability, giving a 55% probability for the isospin 0 component and 39% for isospin 1, which is enhanced in this case because the binding energy is much smaller compared with mass difference of the neutral and charged $D\overline{D}^*$ components. As the isospin breaking is a threshold effect, it grows as we get closer to the $X(3872)$ physical mass. The $q\overline{q}$ component is, as in the previous state, a 2^3P_1 bare state. Finally we get an almost pure $I = 0$ 1^3P_1 state with a mass of $M = 3480.75$ MeV/c^2.

The scenario drawn by these results consists of two bare states (a molecule and a 2^3P_1 $q\overline{q}$ state), which mix together to give the two physical states, and a third state which participates slightly into the game, although, as we will see, its contribution is important. The result is similar to those of Ref. [13], within the uncertainties of the model, but now it appears dynamically without the need to make educated guesses about the bare states involved in the calculation. In this way we are confident that all the physics is included into the model.

Although not addressed in Ref. [13], we have calculated with our wave functions the two decay rates that represent a challenge in the description of the $X(3782)$ structure, namely,

$$R_I = \frac{\mathcal{B}\left(X\left(3872\right) \longrightarrow \omega J/\psi\right)}{\mathcal{B}\left(X\left(3872\right) \longrightarrow \pi^-\pi^+ J/\psi\right)} \tag{24}$$

$$R_\gamma = \frac{\mathcal{B}\left(X\left(3872\right) \longrightarrow \psi\left(2S\right)\gamma\right)}{\mathcal{B}\left(X\left(3872\right) \longrightarrow J/\psi\gamma\right)} \tag{25}$$

R_I has been measured by BaBar Collaboration [29] obtaining $R_I = 0.8 \pm 0.3$. A value of $R_\gamma = 2.46 \pm 0.64 \pm 0.29$ has been recently reported by LHCb Collaboration [30].

Whereas R_I, which showed a large isospin symmetry breaking, has been used to justify that the $X(3872)$ should be hadronic molecule, the high value of R_γ was interpreted as a strong evidence that the $X(3872)$ cannot be a pure hadronic molecule, based on the claim that the contributions of the molecular component to this ratio should be small [31].

Our $X(3872)$ wave function allows for a simultaneous description of both ratios. To calculate R_γ we have assumed that the decay proceeds through the $q\overline{q}$ component, obtaining the value $R_\gamma = 0.39$ which is clearly far from the experimental value. A similar result is obtained in [32], where it is shown that if the 1^3P_1 states are neglected the ratio approaches to the experimental value. In our approach the 1^3P_1 appears automatically. Then, it seems that a more careful calculation of this decay in the line of Ref. [33, 34] should be done.

The obtained value for the first ratio is $R_I = 1.5$ that is close to the experimental result, similar to the values obtained in Ref. [35–37].

4. Summary

In this work we present a method to coupled quark-antiquark states with meson-meson channels, taking into account effectively the nonperturbative coupling to all quark-antiquark states with the same quantum numbers. Instead of expanding the wave function of the $q\overline{q}$ system in eigenstates of the H_0 Hamiltonian and then solving the coupled channels equation with the meson-meson channels, we use a general wave function for the $q\overline{q}$ system to solve the coupled channels problem and then develop the solution of the $q\overline{q}$ system in the base of the bare $q\overline{q}$ states. The method is applied to the coupling of the $X(3872)$ resonance to the 1^{++} $q\overline{q}$ states and the results were compared with those of the perturbative calculation of Ref. [13].

Data Availability

The data used to support the findings of this study are included within the article.

Conflicts of Interest

The authors declare that they have no conflicts of interest.

Acknowledgments

This work has been funded by Ministerio de Economía, Industria y Competitividad under Contract No. FPA2016-77177-C2-2-P. Pablo G. Ortega acknowledges the financial support from Spanish MINECO's Juan de la Cierva-Incorporación program, Grant Agreement No. IJCI-2016-28525.

Table 2: Mass and channel probabilities for the three states in the present approach using the two values of the $^3P_0$ strength parameter as explained in the text.

γ^3P_0	M (MeV)	$c\bar{c}$	$D^0\overline{D}^{*0}$	$D^{\pm}D^{*\pm}$	I=0	I=1
	3948.89	56.71%	22.47%	20.82%	43.10%	0.25%
0.260	3867.36	30.22%	51.37%	18.40%	64.72%	5.06%
	3468.29	95.70%	2.18%	2.12%	4.30%	0.0%
	3944.58	57.03%	22.07%	20.89%	42.72%	0.43%
0.218	3871.76	3.62%	93.99%	2.39%	54.98%	39.34%
	3478.55	96.84%	1.60%	1.56%	3.16%	0.0%

Table 3: Decomposition of the $c\bar{c}$ component of the states in Table 2 in the bare $c\bar{c}$ basis.

γ^3P_0	M (MeV)	$c\bar{c}$	1^3P_1	2^3P_1	3^3P_1	4^3P_1
	3948.89	56.71%	1.61%	96.33%	1.28%	0.78%
0.260	3867.36	30.22%	1.80%	98.14%	0.06%	0.0%
	3468.29	95.70%	99.99%	0.01%	0.0%	0.0%
	3944.58	57.03%	0.23%	99.49%	0.28%	0.0%
0.218	3871.76	3.62%	2.11%	97.75%	0.14%	0.0%
	3478.55	96.84%	100.0%	0.0%	0.0%	0.0%

References

[1] E. Eichten, K. Gottfried, T. Kinoshita, K. D. Lane, and T.-M. Yan, "Charmonium: the model," *Physical Review D: Particles, Fields, Gravitation and Cosmology*, vol. 17, no. 11, pp. 3090–3117, 1978.

[2] K. Heikkilä, N. A. Törnqvist, and S. Ono, "Heavy $c\bar{c}$ and $b\bar{b}$ quarkonium states and unitarity effects," *Physical Review D: Particles, Fields, Gravitation and Cosmology*, vol. 29, no. 110, pp. 2136-2136, 1984, Erratum: Phys. Rev.D29,2136(1984).

[3] S. Ono and N. A. Tornqvist, "Continuum mixing and coupled channel effects in $c\bar{c}$ and $b\bar{b}$ quarkonium," *Zeitschrift für Physik C Particles and Fields*, vol. 23, no. 1, pp. 59–66, 1984.

[4] E. van Beveren, C. Dullemond, and G. Rupp, "Spectra and strong decays of $c\bar{c}$ and $b\bar{b}$ states," *Physical Review D: Particles and Fields*, vol. 21, no. 3, pp. 772–778, 1980.

[5] E. Van Beveren, G. Rupp, T. A. Rijken, and C. Dullemond, "Radial spectra and hadronic decay widths of light and heavy mesons," *Physical Review D: Particles, Fields, Gravitation and Cosmology*, vol. 27, no. 7, pp. 1527–1543, 1983.

[6] R. Bijker and E. Santopinto, "Unquenched quark model for baryons: magnetic moments, spins, and orbital angular momenta," *Physical Review C Nuclear Physics*, vol. 80, no. 6, 2009.

[7] E. J. Eichten, K. Lane, and C. Quigg, "Charmonium levels near threshold and the narrow state $X(3872)\longrightarrow \pi^+\pi^- J/\psi$," *Physical Review D: Particles, Fields, Gravitation and Cosmology*, vol. 69, no. 9, 2004.

[8] S. Coito, G. Rupp, and E. van Beveren, "$X(3872)$ is not a true molecule," *The European Physical Journal C*, vol. 73, no. 3, 2013.

[9] J. Ferretti, G. Galatà, and E. Santopinto, "Interpretation of the $X(3872)$ as a charmonium state plus an extra component due to the coupling to the meson-meson continuum," *Physical Review C: Nuclear Physics*, vol. 88, no. 1, 2013.

[10] E. Eichten, K. Gottfried, T. Kinoshita, K. D. Lane, and T. M. Yan, "Charmonium: comparison with experiment," *Physical Review D: Particles, Fields, Gravitation and Cosmology*, vol. 21, no. 1, pp. 203–233, 1980.

[11] E. van Beveren and G. Rupp, "Reconciling the light scalar mesons with Breit-Wigner resonances as well as the quark model," *International Journal of Theoretical Physics, Group Theory, and Nonlinear Optics*, vol. 11, pp. 179–206, 2006 (Portuguese), arXiv:hep-ph/0304105.

[12] J. Ferretti, G. Galatà, and E. Santopinto, "Quark structure of the $X(3872)$ and $\chi_b(3P)$ resonances," *Physical Review D: Particles, Fields, Gravitation and Cosmology*, vol. 90, no. 5, 2014.

[13] P. G. Ortega, J. Segovia, D. R. Entem, and F. Fernández, "Coupled channel approach to the structure of the $X(3872)$," *Physical Review D: Particles, Fields, Gravitation and Cosmology*, vol. 81, no. 5, 2010.

[14] E. van Beveren, C. Dullemond, and T. A. Rijken, "On the influence of hadronic decay on the properties of hadrons," *Zeitschrift für Physik C Particles and Fields*, vol. 19, no. 3, pp. 275–281, 1983.

[15] J. Vijande, F. Fernández, and A. Valcarce, "Constituent quark model study of the meson spectra," *Journal of Physics G: Nuclear and Particle Physics*, vol. 31, no. 5, pp. 481–506, 2005.

[16] J. Segovia, A. M. Yasser, D. R. Entem, and F. Fernández, "$J^{PC}=1^-$ hidden charm resonances," *Physical Review D: Particles, Fields, Gravitation and Cosmology*, vol. 78, no. 11, 2008.

[17] D. Diakonov, "Instantons at work," *Progress in Particle and Nuclear Physics*, vol. 51, no. 1, pp. 173–222, 2003.

[18] P. O. Bowman, U. M. Heller, D. B. Leinweber, M. B. Parappilly, A. G. Williams, and J. Zhang, "Unquenched quark propagator in Landau gauge," *Physical Review D: Particles, Fields, Gravitation and Cosmology*, vol. 71, no. 5, 2005.

[19] G. S. Bali, H. Neff, T. Düssel, T. Lippert, and K. Schilling, "Observation of string breaking in QCD," *Physical Review D: Particles, Fields, Gravitation and Cosmology*, vol. 71, no. 11, 2005.

[20] B. Li, C. Meng, and K. Chao, "Coupled-channel and screening effects in charmonium spectrum," *Physical Review D: Particles, Fields, Gravitation and Cosmology*, vol. 80, no. 1, 2009.

[21] E. Hiyama, Y. Kino, and M. Kamimura, "Gaussian expansion method for few-body systems," *Progress in Particle and Nuclear Physics*, vol. 51, no. 1, pp. 223–307, 2003.

[22] Y. C. Tang, M. LeMere, and D. R. Thompsom, "Resonating-group method for nuclear many-body problems," *Physics Reports*, vol. 47, no. 3, pp. 167–223, 1978.

[23] A. Le Yaouanc, L. Oliver, O. Pène, and J.-C. Raynal, ""Naive" quark-pair-creation model of strong-interaction vertices," *Physical Review D: Particles, Fields, Gravitation and Cosmology*, vol. 8, no. 7, pp. 2223–2234, 1973.

[24] R. Bonnaz and B. Silvestre-Brac, "Discussion of the $^3P_0$ model applied to the decay of mesons into two mesons," *Few-Body Systems*, vol. 27, no. 3-4, pp. 163–187, 1999.

[25] C. G. Broyden, "A class of methods for solving nonlinear simultaneous equations," *Mathematics of Computation*, vol. 19, no. 92, pp. 577–593, 1965.

[26] P. Ortega, D. Entem, and F. Fernandez, "Molecular structures in charmonium spectrum: the *XYZ* puzzle," *Journal of Physics G Nuclear and Particle Physics*, vol. 40, no. 6, Article ID 065107, 2012.

[27] J. Segovia, D. R. Entem, F. Fernandez, and E. Hernandez, "Constituent quark model description of charmonium phenomenology," *International Journal of Modern Physics E*, vol. 22, no. 10, 2013.

[28] K. Olive, K. Agashe, and C. Amsler, "Review of particle physics," *Chinese Physics C*, vol. 38, no. 9, 2014.

[29] P. del Amo Sanchez and etal (The BABAR Collaboration), "Evidence for the decay X(3872)⟶J/$\psi\omega$," *Physical Review D: Particles, Fields, Gravitation and Cosmology*, vol. 82, no. 1, 2010.

[30] R. Aaij and etal (LHCb Collaboration), "Evidence for the decay X(3872) ⟶ ψ(2S)γ," *Nuclear Physics B*, vol. 886, pp. 665–680, 2014.

[31] E. S. Swanson, "Diagnostic Decays of the $X(3872)$," *Physics Letters B*, vol. 598, no. 3-4, pp. 197–202, 2004.

[32] M. Takizawa, S. Takeuchi, and K. Shimizu, "Radiative $X(3872)$ decays in charmonium-molecule hybrid model," *Few-Body Systems*, vol. 55, no. 8-10, pp. 779–782, 2014, Proceed-Proceedings of the 22nd European Conference on Few-Body Problemsin Physics (EFB22).

[33] M. Cardoso, G. Rupp, and E. van Beveren, "Unquenched quark-model calculation of $X(3872)$ electromagnetic decays," *The European Physical Journal C*, vol. 75, no. 1, 2015.

[34] F. De Fazio, "Radiative transitions of heavy quarkonium states," *Physical Review D: Particles, Fields, Gravitation and Cosmology*, vol. 79, 2009, [Erratum: Phys. Rev.D83,099901(2011)].

[35] S. Takeuchi, M. Takizawa, and K. Shimizu, "On the Origin of the Narrow Peak and the Isospin Symmetry Breaking of the $X(3872)$," *Acta Physica Polonica B Proceedings Supplement*, vol. 8, no. 1, p. 253, 2015, Proceedings of the Workshop on Unquenched Hadron Spectroscopy: Non-Perturbative Models and Methods of QCD vs. Experiment. At the occasion of Eef van Beveren's 70th birthday (EEF70), Coimbra, Portugal, September 1-5, 2014.

[36] E. Cincioglu, J. Nieves, A. Ozpineci, and A. U. Yilmazer, "Quarkonium Contribution to Meson Molecules," *The European Physical Journal C*, vol. 76, no. 10, 2016.

[37] J. Ferretti and E. Santopinto, "Threshold corrections of $\chi_c(2P)$ and $\chi_b(3P)$ states and $J/\psi\rho$ and $J/\psi\omega$ transitions of the $X(3872)$ in a coupled-channel model," *Physics Letters B*, vol. 789, pp. 550–555, 2019.

Hindawi
Advances in High Energy Physics
Volume 2019, Article ID 7650678, 5 pages
https://doi.org/10.1155/2019/7650678

Research Article

Chromopolarizability of Charmonium and $\pi\pi$ Final State Interaction Revisited

Yun-Hua Chen

School of Mathematics and Physics, University of Science and Technology Beijing, Beijing 100083, China

Correspondence should be addressed to Yun-Hua Chen; yhchen@ustb.edu.cn

Received 16 January 2019; Accepted 7 March 2019; Published 23 April 2019

Guest Editor: Tao Luo

The chromopolarizability of a quarkonium describes the quarkonium's interaction with soft gluonic fields and can be measured in the heavy quarkonium decay. Within the framework of dispersion theory which considers the $\pi\pi$ final state interaction (FSI) model-independently, we analyze the transition $\psi' \longrightarrow J/\psi\pi^+\pi^-$ and obtain the chromopolarizability $\alpha_{\psi'\psi}$ and the parameter κ. It is found that the $\pi\pi$ FSI plays an important role in extracting the chromopolarizability from the experimental data. The obtained chromopolarizability with the FSI is reduced to about 1/2 of that without the FSI. With the FSI, we determine the chromopolarizability $|\alpha_{\psi'\psi}| = (1.44 \pm 0.02)$ GeV^{-3} and the parameter $\kappa = 0.139 \pm 0.005$. Our results could be useful in studying the interactions of charmonium with light hadrons.

1. Introduction

The chromopolarizability α of a quarkonium parametrizes the quarkonium's effective interaction with soft gluons, and it is an important quantity in the heavy quark effective theory. Within the multipole expansion in QCD in terms of the chromopolarizability, many processes can be described, including the hadronic transitions between quarkonium resonances [1, 2] and the interaction of slow quarkonium with a nuclear medium [3]. A recent interest of the chromopolarizabilities of J/ψ and ψ' comes from the hadrocharmonium [3–8] interpretation of the $P_c^+(4380)$ and $P_c^+(4450)$ observed by the LHCb Collaboration, and it is found that the $P_c^+(4450)$ can be interpreted as a ψ'-nucleon bound state if $\alpha_{\psi'}/\alpha_{J/\psi} \simeq 15$ [9].

There are a few studies of the chromopolarizabilities of J/ψ and ψ', some of which are not in line with each other. Calculated in the large-N_c limit in the heavy quark approximation, the values of the chromopolarizabilities of the J/ψ and ψ' are obtained: $\alpha_{J/\psi} \approx 0.2$ GeV^{-3} and $\alpha_{\psi'} \approx 12$ GeV^{-3} [6, 7, 10, 11]. Within a quarkonium-nucleon effective field theory, the chromopolarizability of the J/ψ is determined through fitting the lattice QCD data [12] of the J/ψ-nucleon potential, and the result is $\alpha_{J/\psi} = 0.24$ GeV^{-3} [13, 14]. Based on an effective potential formalism given in [15] and a recent lattice QCD calculation [16], the chromopolarizabilities of J/ψ are extracted to be $\alpha_{J/\psi} = (1.6 \pm 0.8)$ GeV^{-3} [9]. On the other hand, the determination of the transitional chromopolarizability $\alpha_{\psi'\psi} \equiv \alpha_{\psi'\longrightarrow J/\psi}$ is of importance since it acts a reference benchmark for either of the diagonal terms due to the Schwartz inequality: $\alpha_{J/\psi}\alpha_{\psi'} \geq \alpha_{\psi'\psi}^2$ [4]. The perturbative prediction in the large N_c limit is $\alpha_{\psi'\psi} \approx -0.6$ GeV^{-3} [6, 7, 10, 11]. While being extracted from the process of $\psi' \longrightarrow J/\psi\pi\pi$, the result is $|\alpha_{\psi'\psi}| \approx 2$ GeV^{-3} [4, 17]. Taking account of the $\pi\pi$ FSI in a chiral unitary approach, it is found that the value of $|\alpha_{\psi'\psi}|$ may be reduced to about 1/3 of that without the $\pi\pi$ FSI [18].

Since the FSI plays an important role in the heavy quarkonium transitions and modifies the value of $\alpha_{\psi'\psi}$ significantly, it is thus necessary to account for the FSI properly. In this work we will use the dispersion theory to take into account of the $\pi\pi$ FSI and extract the value of $\alpha_{\psi'\psi}$. Instead of the chiral unitary approach [18, 19], in which the scalar mesons (σ, $f_0(980)$, and $a_0(980)$) are dynamically generated, in the dispersion theory the $\pi\pi$ FSI is treated in a model-independent way consistent with $\pi\pi$ scattering data. Another update of our calculation is that we consider the FSIs of separate partial waves, namely, the S- and D-waves, instead

of only accounting for the S-wave as in the parametrization in [17, 18].

The theoretical framework is described in detail in Section 2. In Section 3, we fit the decay amplitudes to the data for the $\psi' \longrightarrow J/\psi\pi^+\pi^-$ transition and determine the chromopolarizability $\alpha_{\psi'\psi}$ and the parameter κ. A brief summary will be presented in Section 4.

2. Theoretical Framework

First we define the Mandelstam variables of the decay process $\psi'(p_a) \longrightarrow J/\psi(p_b)\pi(p_c)\pi(p_d)$

$$\begin{aligned} s &= (p_c + p_d)^2, \\ t &= (p_a - p_c)^2, \\ u &= (p_a - p_d)^2. \end{aligned} \tag{1}$$

The amplitude for the $\pi^+\pi^-$ transition between S-wave states A and B of heavy quarkonium can be written as [4, 13]

$$\begin{aligned} M_{AB} &= 2\sqrt{m_A m_B}\alpha_{AB}\left\langle \pi^+(p_c)\pi^-(p_d)\left|\frac{1}{2}\mathbf{E}^a\cdot\mathbf{E}^a\right|0\right\rangle \\ &= \frac{8\pi^2}{b}\sqrt{m_A m_B}\alpha_{AB}\left(\kappa_1 p_c^0 p_d^0 - \kappa_2 p_c^i p_d^i\right), \end{aligned} \tag{2}$$

where the factor $2\sqrt{m_A m_B}$ appears due to the relativistic normalization of the decay amplitude, α_{AB} is the chromopolarizability, and $\mathbf{E}^a$ denotes the chromoelectric field. b is the first coefficient of the QCD beta function, $b = (11/3)N_c - (2/3)N_f$, where $N_c = 3$ and $N_f = 3$ are the number of colors and of light flavors, respectively. $\kappa_1 = 2 - 9\kappa/2$, and $\kappa_2 = 2 + 3\kappa/2$, where κ is a parameter that can be determined from the data.

The above result of the QCD multipole expansion together with the soft-pion theorem can be reproduced by constructing a chiral effective Lagrangian for the $\psi' \longrightarrow J/\psi\pi\pi$ transition. Since the spin-dependent interactions are suppressed by the charm mass, the heavy quarkonia can be expressed in terms of spin multiplets, and one has $J \equiv \psi\cdot\boldsymbol{\sigma} + \eta_c$, where $\boldsymbol{\sigma}$ contains the Pauli matrices and ψ and η_c annihilates the ψ and η_c states, respectively [20]. The effective Lagrangian, at the leading order in the chiral as well as the heavy quark nonrelativistic expansion, reads [21–23]

$$\begin{aligned} \mathscr{L}_{\psi\psi'\pi\pi} = {} & \frac{c_1}{2}\left\langle J^\dagger J'\right\rangle\left\langle u_\mu u^\mu\right\rangle + \frac{c_2}{2}\left\langle J^\dagger J'\right\rangle\left\langle u_\mu u_\nu\right\rangle v^\mu v^\nu \\ & + \text{h.c.}, \end{aligned} \tag{3}$$

where $v^\mu = (1, \mathbf{0})$ is the velocity of the heavy quark. The Goldstone bosons of the spontaneous breaking of chiral symmetry can be parametrized according to

$$\begin{aligned} u_\mu &= i\left(u^\dagger\partial_\mu u - u\partial_\mu u^\dagger\right), \\ u^2 &= e^{i\Phi/F_\pi}, \quad \Phi = \begin{pmatrix} \pi^0 & \sqrt{2}\pi^+ \\ \sqrt{2}\pi^- & -\pi^0 \end{pmatrix}, \end{aligned} \tag{4}$$

where $F_\pi = 92.2$ MeV denotes the pion decay constant.

The amplitude obtained by using the effective Lagrangians in (3) is

$$M(s,t,u) = -\frac{4}{F_\pi^2}\left(c_1 p_c\cdot p_d + c_2 p_c^0 p_d^0\right). \tag{5}$$

Matching the amplitude in (2) to that in (5), we can express the low-energy couplings in the chiral effective Lagrangian in terms of the chromopolarizability α_{AB} and the parameter κ

$$\begin{aligned} c_1 &= -\frac{\pi^2\sqrt{m_{\psi'}m_\psi}F_\pi^2}{b}\alpha_{\psi'\psi}(4+3\kappa), \\ c_2 &= \frac{12\pi^2\sqrt{m_{\psi'}m_\psi}F_\pi^2}{b}\alpha_{\psi'\psi}\kappa. \end{aligned} \tag{6}$$

The partial-wave decomposition of $M(s,t,u)$ can be easily performed by using the relation

$$p_c^0 p_d^0 = \frac{1}{4}\left(s + \mathbf{q}^2\right) - \frac{1}{4}\mathbf{q}^2\sigma_\pi^2\cos^2\theta, \tag{7}$$

where $\mathbf{q}$ is the 3-momentum of the final vector meson in the rest frame of the initial state with $|\mathbf{q}| = \{[(m_{\psi'} + m_\psi)^2 - s]/[(m_{\psi'} - m_\psi)^2 - s]\}^{1/2}/(2m_{\psi'})$, $\sigma_\pi \equiv \sqrt{1 - 4m_\pi^2/s}$, and θ is the angle between the 3-momentum of the π^+ in the rest frame of the $\pi\pi$ system and that of the $\pi\pi$ system in the rest frame of the initial ψ'.

Parity and C-parity conservations require the pion pair to have even relative angular momentum l. We only consider the S- and D-wave components in this study, neglecting the effects of higher partial waves. Explicitly, the S- and D-wave components of the amplitude read

$$\begin{aligned} & M_0^\chi(s) \\ & \quad = -\frac{2}{F_\pi^2}\left\{c_1\left(s - 2m_\pi^2\right) + \frac{c_2}{2}\left[s + \mathbf{q}^2\left(1 - \frac{\sigma_\pi^2}{3}\right)\right]\right\}, \\ & M_2^\chi(s) = \frac{2}{3F_\pi^2}c_2\mathbf{q}^2\sigma_\pi^2. \end{aligned} \tag{8}$$

There are strong FSI in the $\pi\pi$ system especially in the isospin-0 S-wave, which can be taken into account model-independently using dispersion theory [22–31]. We will use the Omnès solution to obtain the amplitude including FSI. In the region of elastic $\pi\pi$ rescattering, the partial-wave unitarity conditions read

$$\operatorname{Im} M_l(s) = M_l(s)\sin\delta_l^0(s)\, e^{-i\delta_l^0(s)}. \tag{9}$$

Below the inelastic threshold, the phases δ_l^I of the partial-wave amplitudes of isospin I and angular momentum l coincide with the $\pi\pi$ elastic phase shifts modulo $n\pi$, as required by Watson's theorem [32, 33]. It is known that the standard Omnès solution of (9) is as follows:

$$M_l(s) = P_l^n(s)\,\Omega_l^0(s), \tag{10}$$

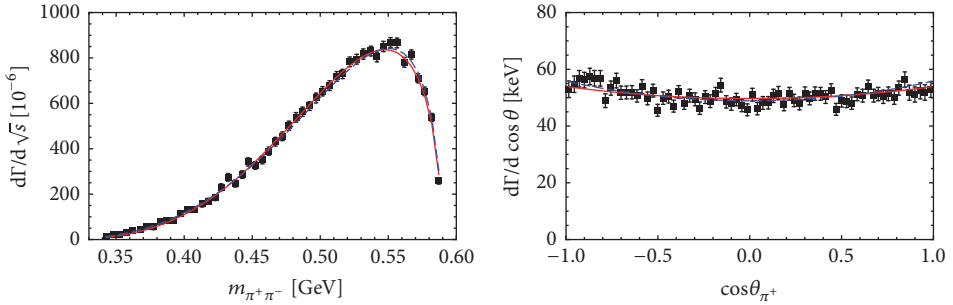

FIGURE 1: Simultaneous fit to the $\pi\pi$ invariant mass distributions and the helicity angle distributions in $\psi' \longrightarrow J/\psi\pi^+\pi^-$. The red solid and blue dashed curves represent the theoretical fit results with $\pi\pi$ FSI and without $\pi\pi$ FSI cases, respectively. The data are taken from [37].

where the $P_l^n(s)$ is a polynomial, and the Omnès function is defined as [34]

$$\Omega_l^I(s) = \exp\left\{\frac{s}{\pi}\int_{4m_\pi^2}^{\infty}\frac{dx}{x}\frac{\delta_l^I(x)}{x-s}\right\}. \tag{11}$$

At low energies, $M_0(s)$ and $M_2(s)$ can be matched to the chiral representation. Namely, in the limit of switching off the $\pi\pi$ FSI, i.e., $\Omega_l^0(s) \equiv 1$, the polynomials $P_l^n(s)$ can be identified exactly with the expressions given in (8). Therefore, the amplitudes including the FSI take the form

$$M_0(s) = -\frac{2}{F_\pi^2}\left[c_1\left(s-2m_\pi^2\right)+\frac{c_2}{2}\left(s+\mathbf{q}^2\left(1-\frac{\sigma_\pi^2}{3}\right)\right)\right] \cdot \Omega_0^0(s), \tag{12}$$

$$M_2(s) = \frac{2}{3F_\pi^2}c_2\mathbf{q}^2\sigma_\pi^2\Omega_2^0(s). \tag{13}$$

Now we discuss the $\pi\pi$ phase shifts used in the calculation of the Omnès functions. For the S-wave, we use the phase of the nonstrange pion scalar form factor as determined in [35], which yields a good description below the onset of the $K\overline{K}$ threshold. For the D-wave, we employ the parametrization for δ_2^0 given by the Madrid–Kraków collaboration [36]. Both phases are guided smoothly to π for $s \longrightarrow \infty$.

It is then straightforward to calculate the $\pi\pi$ invariant mass spectrum and helicity angular distribution for $\psi' \longrightarrow J/\psi\pi^+\pi^-$ using

$$\frac{d\Gamma}{d\sqrt{s}\,d\cos\theta} = \frac{\sqrt{s}\sigma_\pi|\mathbf{q}|}{128\pi^3 m_{\psi'}^2}\left|M_0(s)+M_2(s)P_2(\cos\theta)\right|^2, \tag{14}$$

where the Legendre polynomial $P_2(\cos\theta) = (3\cos^2\theta - 1)/2$.

3. Phenomenological Discussion

The unknown parameters are the low-energy constants c_1 and c_2 in the chiral Lagrangian (3), which can be expressed in terms of the chromopolarizability $\alpha_{\psi'\psi}$ and the parameter κ as in (6). In order to determine $\alpha_{\psi'\psi}$ and κ, we fit the theoretical results to the experimental $\pi^+\pi^-$ invariant mass spectra and the helicity angular distribution from the BES $\psi' \longrightarrow J/\psi\pi^+\pi^-$ decay data [37] and the corresponding decay width $\Gamma(\psi' \longrightarrow J/\psi\pi^+\pi^-)$ [38]. The fit results are plotted in Figure 1, where the red solid and blue dashed curves represent the results with or without the $\pi\pi$ FSI, respectively. The fit parameters as well as the χ^2/d.o.f. are shown in Table 1. One observes that the experimental data can be well described regardless of whether the FSI is included. This is due to the simple shapes of the $\pi\pi$ invariant mass distribution and the helicity angular distribution in this process and does not mean the FSI is not important. Since the dipion mass invariant mass reaches about 600 MeV in such a decay, the $\pi\pi$ FSI is known to be strong in this energy range and needs to be considered. On the other hand, one can readily see from (6) and (8) that while the chromopolarizability $\alpha_{\psi'\psi}$ determines the overall decay rate, the parameter κ characterizes the D-wave contribution, and we do not find significant correlation between $\alpha_{\psi'\psi}$ and κ.

TABLE 1: The parameter results from the fits of the $\psi' \longrightarrow \psi\pi\pi$ processes with and without the $\pi\pi$ FSI.

	Without $\pi\pi$ FSI	With $\pi\pi$ FSI
$\lvert\alpha_{\psi'\psi}\rvert$ (GeV^{-3})	2.37 ± 0.02	1.44 ± 0.02
κ	0.135 ± 0.005	0.139 ± 0.005
$\frac{\chi^2}{\text{d.o.f}}$	$\frac{115.3}{120-2} = 0.98$	$\frac{117.6}{120-2} = 1.00$

We observe that the $\pi\pi$ FSI modifies the value of the chromopolarizability $\alpha_{\psi'\psi}$ significantly, and resultant value with the FSI is almost 1/2 of that without the FSI. The obtained value with the FSI, $|\alpha_{\psi'\psi}| = (1.44 \pm 0.02)$ GeV^{-3}, coincides with the suspicion $\alpha_{J/\psi} \geq |\alpha_{\psi'\psi}|$ [3] with the value $\alpha_{J/\psi} = (1.6 \pm 0.8)$ GeV^{-3} from the calculation [9] based on the recent lattice QCD data of J/ψ-nucleon potential [16]. It should be mentioned that the value of $\alpha_{\psi'\psi}$ with the FSI obtained here is different from the one in [18], $|\alpha_{\psi'\psi}| = (0.83 \pm 0.01)$ GeV^{-3}, and also our result without the FSI slightly differs from those in [17, 18]. The reasons are that the chiral unitary approach instead of dispersion theory is used to account for the FSI

in [18], and we use the updated experimental data [37, 38] and a general theoretical amplitude rather than the one only containing the S-wave as employed in [17, 18].

For the parameter κ, as shown in Table 1 its value is affected little by the $\pi\pi$ FSI. One notes that a detailed study of the $\psi' \longrightarrow J/\psi\pi^+\pi^-$ process using the Novikov-Shifman model [2] has been performed by BES [39], and based on the joint $m_{\pi^+\pi^-}$-$\cos\theta_{\pi^+}$ distribution this parameter was determined as $\kappa = 0.183 \pm 0.002 \pm 0.003$. We have tried fitting the same old BES data [39] and our κ changes slightly and is still much smaller than the BES one. In the Novikov-Shifman model, the $\psi' \longrightarrow J/\psi\pi^+\pi^-$ amplitude reads [2]

$$M \propto \left\{ s - \kappa \left(m_{\psi'} - m_{\psi}\right)^2 \left(1 + \frac{2m_\pi^2}{s}\right) + \frac{3}{2}\kappa \left[\left(m_{\psi'} - m_{\psi}\right)^2 - s\right] \sigma_\pi^2 \left(\cos^2\theta - \frac{1}{3}\right) \right\}. \tag{15}$$

If we make the same approximation, namely, neglect the $O(m_\pi^2)$ terms except the m_π^2/s ones, as in [2] and set $(m_{\psi'} + m_{\psi})^2 - s \approx (m_{\psi'} + m_{\psi})^2$ in the expression of 3-momentum $\mathbf{q}$, our amplitude without the $\pi\pi$ FSI agrees with (15). While numerically we find that some neglected $O(m_\pi^2)$ terms are at the same order as the $\kappa(m_{\psi'} - m_{\psi})^2$ term in (15), this may account for the difference of κ between ours and that in [39]. On the other hand, we have checked that the contribution of the D-wave, which is characterized by the parameter κ, to the total rate is less than two percent, and the same observation has been made in [39].

4. Conclusions

We have used dispersion theory to study the $\pi\pi$ FSI in the decay $\psi' \longrightarrow J/\psi\pi^+\pi^-$. Through fitting the data of the $\pi\pi$ mass spectra and the angular $\cos\theta$ distributions, the values of the chromopolarizability $\alpha_{\psi'\psi}$ and the parameter κ are determined. It is found that the effect of the $\pi\pi$ FSI is quite sizeable in the chromopolarizability $\alpha_{\psi'\psi}$, and the one with FSI is almost 1/2 of that without FSI. The parameter κ, which accounts for the D-wave contribution, is affected little by the $\pi\pi$ FSI. The results obtained in this work would be valuable to understand the chromopolarizability of charmonia and will have applications for the studies of the nucleon-charmonia interaction.

Data Availability

All the data used in this work are from [37, 38].

Conflicts of Interest

The author declares that they have no conflicts of interest.

Acknowledgments

We acknowledge Feng-Kun Guo for the proposal for this work and for the useful comments on the manuscript. This research is supported in part by the Fundamental Research Funds for the Central Universities under Grant no. 06500077.

References

[1] M. Voloshin and V. Zakharov, "Measuring quantum-chromodynamic anomalies in hadronic transitions between quarkonium states," *Physical Review Letters*, vol. 45, no. 9, pp. 688–691, 1980.

[2] V. A. Novikov and M. A. Shifman, "Comment on the $\psi' \longrightarrow J/\psi\pi\pi$ decay," *Zeitschrift für Physik C Particles and Fields*, vol. 8, no. 1, pp. 43–47, 1981.

[3] A. Sibirtsev and M. B. Voloshin, "Interaction of slow J/ψ and ψ' with nucleons," *Physical Review D*, vol. 71, Article ID 076005, 2005.

[4] M. B. Voloshin, "Charmonium," *Progress in Particle and Nuclear Physics*, vol. 61, no. 455, 2008.

[5] S. Dubynskiy and M. Voloshin, "Hadro-charmonium," *Physics Letters B*, vol. 666, no. 4, pp. 344–346, 2008.

[6] M. I. Eides, V. Y. Petrov, and M. V. Polyakov, "Narrow nucleon-ψ(2S) bound state and LHCb pentaquarks," *Physical Review D: Particles, Fields, Gravitation and Cosmology*, vol. 93, Article ID 054039, 2016.

[7] M. I. Eides, V. Y. Petrov, and M. V. Polyakov, "Pentaquarks with hidden charm as hadroquarkonia," *The European Physical Journal C*, vol. 78, no. 36, 2018.

[8] K. Tsushima, D. H. Lu, G. Krein, and A. W. Thomas, "J/Ψ-nuclear bound states," *Physical Review C: Nuclear Physics*, vol. 83, no. 6, Article ID 065208, 2011.

[9] M. V. Polyakov and P. Schweitzer, "Determination of J/ψ chromoelectric polarizability from lattice data," *Physical Review D*, vol. 98, no. 3, Article ID 034030, pp. 1–7, 2018.

[10] M. E. Peskin, "Short-distance analysis for heavy-quark systems: (I). Diagrammatics," *Nuclear Physics B*, vol. 156, no. 3, pp. 365–390, 1979.

[11] G. Bhanot and M. E. Peskin, "Short-distance analysis for heavy-quark systems: (I). Diagrammatics," *Nuclear Physics B*, vol. 156, no. 3, pp. 365–390, 1979.

[12] T. Kawanai and S. Sasaki, "Charmonium-nucleon potential from lattice QCD," *Physical Review D*, vol. 82, no. 9, Article ID 091501, 2010.

[13] N. Brambilla, G. Krein, J. Tarrús Castellà, and A. Vairo, "Long-range properties of 1S bottomonium states," *Physical Review D: Particles, Fields, Gravitation and Cosmology*, vol. 93, Article ID 054002, 2016.

[14] J. Tarrs Castell and G. Krein, "Effective field theory for the nucleon-quarkonium interaction," *Physical Review D*, vol. 98, no. 1, Article ID 014029, 2018.

[15] M. B. Voloshin, "Precoulombic asymptotics for energy levels of heavy quarkonium," *Soviet Journal of Nuclear Physics*, vol. 36, no. 143, pp. 247–255, 1982.

[16] T. Sugiura, Y. Ikeda, and N. Ishii, "Charmonium-nucleon interactions from the time-dependent HAL QCD method," in *Proceedings of the 35th International Symposium on Lattice Field Theory (Lattice 2017)*, vol. 175, pp. 1–8, 2018.

[17] M. B. Voloshin, "Quarkonium chromo-polarizability from the decays $J/\psi(\Upsilon) \longrightarrow \pi\pi\ell^+\ell^-$," *Modern Physics Letters A*, vol. 19, no. 9, pp. 665–670, 2004.

[18] F. K. Guo, P. N. Shen, and H. C. Chiang, "Chromopolarizability and $\pi\pi$ final state interaction," *Physical Review D*, vol. 74, Article ID 014011, pp. 11–15, 2006.

[19] J. A. Oller and E. Oset, "Chiral symmetry amplitudes in the S-wave isoscalar and isovector channels and the σ, $f_0(980)$, a0(980) scalar mesons," *Nuclear Physics A*, vol. 620, pp. 438–456, 1997.

[20] M. Cleven, F.-K. Guo, C. Hanhart, and U.-G. Meißner, "Bound state nature of the exotic Z_b states," *The European Physical Journal A*, vol. 47, no. 120, 2011.

[21] T. Mannel and R. Urech, "Hadronic decays of excited heavy quarkonia," *Zeitschrift für Physik C Particles and Fields*, vol. 73, no. 541, 1997.

[22] Y. Chen, J. T. Daub, F. Guo, B. Kubis, U. Meißner, and B. Zou, "Effect of Z_b states on $\Upsilon(3S) \longrightarrow \Upsilon(1S)\pi\pi$ decays," *Physical Review D*, vol. 93, no. 3, Article ID 034030, 2016.

[23] Y. Chen, M. Cleven, J. T. Daub et al., "Effects of Z_b states and bottom meson loops on $\Upsilon(4S) \longrightarrow \Upsilon(1S, 2S)\pi^+\pi^-$ transitions," *Physical Review D*, vol. 95, Article ID 034022, 2017.

[24] X. Kang, B. Kubis, C. Hanhart, and U. Meissner, "B_{l4} decays and the extraction of $|V_{ub}|$," *Physical Review D*, vol. 89, no. 5, Article ID 053015, 2014.

[25] B. Kubis and J. Plenter, "Anomalous decay and scattering processes of the η meson," *The European Physical Journal C*, vol. 75, no. 283, 2015.

[26] T. Isken, B. Kubis, S. P. Schneider, and P. Stoffer, "Dispersion relations for $\eta' \longrightarrow \eta\pi\pi$," *The European Physical Journal*, vol. 77, p. 489, 2017.

[27] S. Ropertz, C. Hanhart, and B. Kubis, "A new parametrization for the scalar pion form factors," *The European Physical Journal C*, vol. 78, no. 12, article no. 1000, 2018.

[28] L.-Y. Dai and M. R. Pennington, "Two photon couplings of the lightest isoscalars from BELLE data," *Physics Letters B*, vol. 736, pp. 11–15, 2014.

[29] L.-Y. Dai and M. R. Pennington, "Comprehensive amplitude analysis of $\gamma\gamma \longrightarrow \pi^+\pi^-, \pi^0\pi^0$ and $\overline{K}K$ below 1.5 GeV," *Physical Review D*, vol. 90, Article ID 036004, 2014.

[30] L.-Y. Dai and M. R. Pennington, "Pion polarizabilities from a $\gamma\gamma \longrightarrow \pi\pi$ analysis," *Physical Review D: Particles, Fields, Gravitation and Cosmology*, vol. 94, no. 4, Article ID 116021, 2016.

[31] L.-Y. Dai and M. R. Pennington, "Pascalutsa-Vanderhaeghen light-by-light sum rule from photon-photon collisions," *Physical Review D*, vol. 97, Article ID 036012, 2018.

[32] K. M. Watson, "The effect of final state interactions on reaction cross sections," *Physical Review*, vol. 88, no. 1163, 1952.

[33] K. M. Watson, "Some general relations between the photoproduction and scattering of π mesons," *Physical Review A: Atomic, Molecular and Optical Physics*, vol. 95, no. 228, 1954.

[34] R. Omnès, "On the solution of certain singular integral equations of quantum field theory," *Nuovo Cimento*, vol. 8, pp. 316–326, 1958.

[35] M. Hoferichter, C. Ditsche, B. Kubis, U.-G. Mei, and U.-G. Meißner, "Dispersive analysis of the scalar form factor of the nucleon," *Journal of High Energy Physics*, vol. 06, article no. 063, 2012.

[36] R. García-Martín, R. Kamiński, J. R. Peláez, J. Ruiz de Elvira, and F. J. Ynduráin, "Pion-pion scattering amplitude. IV: improved analysis with once subtracted roy-like equations up to 1100 MeV," *Physical Review D*, vol. 83, no. 7, Article ID 074004, 2011.

[37] M. Ablikim, J. Z. Bai, Y. Ban et al., "Production of σ in $\psi(2S) \longrightarrow \pi^+\pi^- J/\psi$," *Physics Letters B*, vol. 645, no. 19, 2007.

[38] M. Tanabashi, U. Nagoya, K. M. I. Nagoya et al., "Review of Particle Physics," *Physical Review D*, vol. 98, no. 3, Article ID 030001, 2018.

[39] J. Z. Bai, Y. Ban, J. G. Bian et al., "$\psi(2S) \longrightarrow \pi^+\pi^- J/\psi$ decay distributions," *Physical Review D*, vol. 62, Article ID 032002, 2000.

Hindawi
Advances in High Energy Physics
Volume 2019, Article ID 8958079, 6 pages
https://doi.org/10.1155/2019/8958079

Research Article

Analysis of the $D\overline{D}^*K$ System with QCD Sum Rules

Zun-Yan Di[1,2] and Zhi-Gang Wang[1]

[1]*Department of Physics, North China Electric Power University, Baoding 071003, China*
[2]*School of Nuclear Science and Engineering, North China Electric Power University, Beijing 102206, China*

Correspondence should be addressed to Zhi-Gang Wang; zgwang@aliyun.com

Received 16 January 2019; Accepted 27 February 2019; Published 1 April 2019

Guest Editor: Ling-Yun Dai

In this article, we construct the color singlet-singlet-singlet interpolating current with $I(J^P) = (3/2)(1^-)$ to study the $D\overline{D}^*K$ system through QCD sum rules approach. In calculations, we consider the contributions of the vacuum condensates up to dimension-16 and employ the formula $\mu = \sqrt{M^2_{X/Y/Z} - (2\mathbb{M}_c)^2}$ to choose the optimal energy scale of the QCD spectral density. The numerical result $M_Z = 4.71^{+0.19}_{-0.11}$ GeV indicates that there exists a resonance state Z lying above the $D\overline{D}^*K$ threshold to saturate the QCD sum rules. This resonance state Z may be found by focusing on the channel $J/\psi\pi K$ of the decay $B \longrightarrow J/\psi\pi\pi K$ in the future.

1. Introduction

Since the observation of the $X(3872)$ by the Belle collaboration in 2003 [1], more and more exotic hadrons have been observed and confirmed experimentally, such as the charmonium-like X, Y, Z states, hidden-charm pentaquarks, etc. [2–4]. Those exotic hadron states, which cannot be interpreted as the quark-antiquark mesons or three-quark baryons in the naive quark model [5], are good candidates of the multiquark states [6, 7]. The multiquark states are color-neutral objects because of the color confinement and provide an important platform to explore the low energy behaviors of QCD, as no free particles carrying net color charges have ever been experimentally observed. Compared to the conventional hadrons, the dynamics of the multiquark states is poorly understood and calls for more works.

Some exotic hadrons can be understood as hadronic molecular states [8], which are analogous to the deuteron as a loosely bound state of the proton and neutron. The most impressive example is the original exotic state, the $X(3872)$, which has been studied as the $D\overline{D}^*$ molecular state by many theoretical groups [9–17]. Another impressive example is the $P_c(4380)$ and $P_c(4450)$ pentaquark states observed by the LHCb collaboration in 2015, which are good candidates for the $\overline{D}\Sigma_c^*$, $\overline{D}^*\Sigma_c$, $\overline{D}^*\Sigma_c^*$ molecular states [8]. In additional to the meson-meson type and meson-baryon type molecular state, there may also exist meson-meson-meson type molecular states; in other words, there may exist three-meson hadronic molecules.

In [18, 19], the authors explore the possible existence of three-meson system $D\overline{D}^*K$ molecule according to the attractive interactions of the two-body subsystems DK, $\overline{D}K$, D^*K, $\overline{D}^*K$, and $D\overline{D}^*$ with the Born-Oppenheimer approximation and the fixed center approximation, respectively. In this article, we study the $D\overline{D}^*K$ system with QCD sum rules.

The QCD sum rules method is a powerful tool in studying the exotic hadrons [20–25] and has given many successful descriptions; for example, the mass and width of the $Z_c(3900)$ have been successfully reproduced as an axial vector tetraquark state [26, 27]. In QCD sum rules, we expand the time-ordered currents into a series of quark and gluon condensates via the operator product expansion method. These quark and gluon condensates parameterize the nonperturbative properties of the QCD vacuum. According to the quark-hadron duality, the copious information about the hadronic parameters can be obtained on the phenomenological side [28, 29].

In this article, the color singlet-singlet-singlet interpolating current with $I(J^P) = (3/2)(1^-)$ is constructed to study

the $D\overline{D}^{*}K$ system. In calculations, the contributions of the vacuum condensates are considered up to dimension-16 in the operator product expansion and the energy-scale formula $\mu = \sqrt{M^2_{X/Y/Z} - (2\mathbb{M}_c)^2}$ is used to seek the ideal energy scale of the QCD spectral density.

The rest of this article is arranged as follows: in Section 2, we derive the QCD sum rules for the mass and pole residue of the $D\overline{D}^{*}K$ state; in Section 3, we present the numerical results and discussions; Section 4 is reserved for our conclusion.

2. QCD Sum Rules for the $D\overline{D}^{*}K$ State

In QCD sum rules, we consider the two-point correlation function,

$$\Pi_{\mu\nu}(p) = i\int d^4x e^{ip\cdot x}\langle 0|T\left\{J_\mu(x)J_\nu^{\dagger}(0)\right\}|0\rangle, \tag{1}$$

where

$$\begin{aligned} J_\mu(x) &= \overline{u}^m(x)\,i\gamma_5 c^m(x)\,\overline{c}^n(x)\,\gamma_\mu d^n(x)\,\overline{u}^k(x)\,i\gamma_5 s^k(x), \end{aligned} \tag{2}$$

and the m, n, and k are color indexes. The color singlet-singlet-singlet current operator $J_\mu(x)$ has the same quantum numbers $I(J^P) = (3/2)(1^-)$ as the $D\overline{D}^{*}K$ system.

On the phenomenological side, a complete set of intermediate hadronic states, which has the same quantum numbers as the current operator $J_\mu(x)$, is inserted into the correlation function $\Pi_{\mu\nu}(p)$ to obtain the hadronic representation [28, 29]. We isolate the ground state contribution Z from the pole term, and get the result:

$$\begin{aligned} \Pi_{\mu\nu}(p) &= \frac{\lambda_Z^2}{M_Z^2 - p^2}\left(-g_{\mu\nu} + \frac{p_\mu p_\nu}{p^2}\right) + \cdots \\ &= \Pi\left(p^2\right)\left(-g_{\mu\nu} + \frac{p_\mu p_\nu}{p^2}\right) + \cdots, \end{aligned} \tag{3}$$

where the pole residue λ_Z is defined by $\langle 0|J_\mu(0)|Z(p)\rangle = \lambda_Z\varepsilon_\mu$, the ε_μ is the polarization vector of the vector hexaquark state Z.

At the quark level, we calculate the correlation function $\Pi_{\mu\nu}(p)$ via the operator product expansion method in perturbative QCD. The u, d, s, and c quark fields are contracted with the Wick theorem, and the following result is obtained:

$$\begin{aligned} \Pi_{\mu\nu}(p) = -i\int d^4x e^{ip\cdot x}\Big\{ &\mathrm{Tr}\left[\gamma_\mu D^{nn'}(x)\,\gamma_\nu C^{n'n}(-x)\right] \\ &\cdot \mathrm{Tr}\left[i\gamma_5 C^{mm'}(x)\,i\gamma_5 U^{m'm}(-x)\right]\mathrm{Tr}\left[i\gamma_5 S^{kk'}(x)\right. \\ &\left.\cdot\, i\gamma_5 U^{k'k}(-x)\right] - \mathrm{Tr}\left[\gamma_\mu D^{nn'}(x)\,\gamma_\nu C^{n'n}(-x)\right] \\ &\cdot \mathrm{Tr}\left[i\gamma_5 C^{mm'}(x)\,i\gamma_5 U^{m'k}(-x)\,i\gamma_5 S^{kk'}(x)\right. \\ &\left.\cdot\, i\gamma_5 U^{k'm}(-x)\right]\Big\}, \end{aligned} \tag{4}$$

where the $U_{ij}(x)$, $D_{ij}(x)$, $S_{ij}(x)$, and $C_{ij}(x)$ are the full u, d, s, and c quark propagators, respectively. We give the full quark propagators explicitly in the following, (the $P_{ij}(x)$ denotes the $U_{ij}(x)$ or $D_{ij}(x)$),

$$\begin{aligned} P_{ij}(x) = {} & \frac{i\delta_{ij}\not{x}}{2\pi^2x^4} - \frac{\delta_{ij}\langle\overline{q}q\rangle}{12} - \frac{\delta_{ij}x^2\langle\overline{q}g_s\sigma Gq\rangle}{192} \\ & - \frac{ig_sG^n_{\alpha\beta}t^n_{ij}\left(\not{x}\sigma^{\alpha\beta} + \sigma^{\alpha\beta}\not{x}\right)}{32\pi^2x^2} - \frac{1}{8}\left\langle\overline{q}_j\sigma^{\alpha\beta}q_i\right\rangle\sigma_{\alpha\beta} \\ & + \cdots, \end{aligned} \tag{5}$$

$$\begin{aligned} S_{ij}(x) = {} & \frac{i\delta_{ij}\not{x}}{2\pi^2x^4} - \frac{\delta_{ij}m_s}{4\pi^2x^2} - \frac{\delta_{ij}\langle\overline{s}s\rangle}{12} + \frac{i\delta_{ij}\not{x}m_s\langle\overline{s}s\rangle}{48} \\ & - \frac{\delta_{ij}x^2\langle\overline{s}g_s\sigma Gs\rangle}{192} + \frac{i\delta_{ij}x^2\not{x}m_s\langle\overline{s}g_s\sigma Gs\rangle}{1152} \\ & - \frac{ig_sG^n_{\alpha\beta}t^n_{ij}\left(\not{x}\sigma^{\alpha\beta} + \sigma^{\alpha\beta}\not{x}\right)}{32\pi^2x^2} - \frac{1}{8}\left\langle\overline{s}_j\sigma^{\alpha\beta}s_i\right\rangle\sigma_{\alpha\beta} + \cdots, \end{aligned} \tag{6}$$

$$\begin{aligned} C_{ij}(x) = {} & \frac{i}{(2\pi)^4}\int d^4k e^{-ik\cdot x}\left\{\frac{\not{k} + m_c}{k^2 - m_c^2}\delta_{ij}\right. \\ & - g_st^n_{ij}G^n_{\alpha\beta}\frac{(\not{k} + m_c)\sigma^{\alpha\beta} + \sigma^{\alpha\beta}(\not{k} + m_c)}{4\left(k^2 - m_c^2\right)^2} \\ & - \frac{g_s^2\left(t^nt^m\right)_{ij}G^n_{\alpha\beta}G^n_{\mu\nu}\left(f^{\alpha\beta\mu\nu} + f^{\alpha\mu\beta\nu} + f^{\alpha\mu\nu\beta}\right)}{4\left(k^2 - m_c^2\right)^5} \\ & \left. + \cdots\right\}, \end{aligned} \tag{7}$$

$$\begin{aligned} f^{\lambda\alpha\beta} &= (\not{k} + m_c)\gamma^\lambda(\not{k} + m_c)\gamma^\alpha(\not{k} + m_c)\gamma^\beta(\not{k} + m_c), \\ f^{\alpha\beta\mu\nu} &= (\not{k} + m_c)\gamma^\alpha(\not{k} + m_c)\gamma^\beta(\not{k} + m_c)\gamma^\mu(\not{k} + m_c) \\ &\quad\cdot\gamma^\nu(\not{k} + m_c), \end{aligned} \tag{8}$$

and $t^n = \lambda^n/2$; the λ^n is the Gell-Mann matrix [29]. We compute the integrals in the coordinate space for the light quark propagators and in the momentum space for the charm quark propagators and obtain the QCD spectral density $\rho(s)$ via taking the imaginary part of the correlation function: $\rho(s) = \lim_{\varepsilon\longrightarrow 0}(\mathrm{Im}\,\Pi(s + i\varepsilon)/\pi)$ [26]. In the operator product expansion, we take into account the contributions of vacuum condensates up to dimension-16 and keep the terms which are linear in the strange quark mass m_s. We take the truncation $k \leq 1$ for the operators of the order $\mathcal{O}(\alpha_s^k)$ in a consistent way and discard the perturbative corrections. Furthermore, the condensates $\langle\overline{q}q\rangle\langle\alpha_sGG/\pi\rangle$, $\langle\overline{q}q\rangle^2\langle\alpha_sGG/\pi\rangle$, and $\langle\overline{q}q\rangle^3\langle\alpha_sGG/\pi\rangle$ play a minor important role and are neglected.

According to the quark-hadron duality, we match the correlation function $\Pi(p^2)$ gotten on the hadron side and at the quark level below the continuum threshold s_0 and

perform Borel transform with respect to the variable $P^2 = -p^2$ to obtain the QCD sum rule:

$$\lambda_Z^2 \exp\left(-\frac{M_Z^2}{T^2}\right) = \int_{4m_c^2}^{s_0} ds\rho(s) \exp\left(-\frac{s}{T^2}\right), \quad (9)$$

where the QCD spectral density is

$$\begin{aligned}\rho(s) &= \rho_0(s) + \rho_3(s) + \rho_4(s) + \rho_5(s) + \rho_6(s) + \rho_8(s) \\ &+ \rho_9(s) + \rho_{10}(s) + \rho_{11}(s) + \rho_{12}(s) + \rho_{13}(s) \\ &+ \rho_{14}(s) + \rho_{16}(s),\end{aligned} \quad (10)$$

and the subscripts 0, 3, 4, 5, 6, 8, 9, 10, 11, 12, 13, 14, and 16 denote the dimensions of the vacuum condensates, the T^2 is the Borel parameter, and the lengthy and complicated expressions are neglected for simplicity. However, for the explicit expressions of the QCD special densities, the interested readers can obtain them through emailing us.

We derive (9) with respect to $1/T^2$ and eliminate the pole residue λ_Z to extract the QCD sum rule for the mass:

$$M_Z^2 = \frac{\int_{4m_c^2}^{s_0} ds \left(d/d\left(-1/T^2\right)\right)\rho(s)\exp\left(-s/T^2\right)}{\int_{4m_c^2}^{s_0} ds\rho(s)\exp\left(-s/T^2\right)}. \quad (11)$$

3. Numerical Results and Discussions

In this section, we perform the numerical analysis. To extract the numerical values of M_Z, we take the values of the vacuum condensates $\langle\overline{q}q\rangle = -(0.24 \pm 0.01\,\text{GeV})^3$, $\langle\overline{s}s\rangle = (0.8 \pm 0.1)\langle\overline{q}q\rangle$, $\langle\overline{q}g_s\sigma Gq\rangle = m_0^2\langle\overline{q}q\rangle$, $\langle\overline{s}g_s\sigma Gs\rangle = m_0^2\langle\overline{s}s\rangle$, $m_0^2 = (0.8 \pm 0.1)\,\text{GeV}^2$, $\langle\alpha_s GG/\pi\rangle = (0.33\,\text{GeV})^4$ at the energy scale $\mu = 1\,\text{GeV}$ [28–30], choose the $\overline{MS}$ masses $m_c(m_c) = (1.275 \pm 0.025)\,\text{GeV}$, $m_s(\mu = 2\,\text{GeV}) = (0.095^{+0.009}_{-0.003})\,\text{GeV}$ from the Particle Data Group [2], and neglect the up and down quark masses, i.e., $m_u = m_d = 0$. Moreover, we consider the energy-scale dependence of the input parameters on the QCD side from the renormalization group equation,

$$\begin{aligned}\langle\overline{q}q\rangle(\mu) &= \langle\overline{q}q\rangle(1\text{GeV})\left[\frac{\alpha_s(1\text{GeV})}{\alpha_s(\mu)}\right]^{4/9}, \\ \langle\overline{s}s\rangle(\mu) &= \langle\overline{s}s\rangle(1\text{GeV})\left[\frac{\alpha_s(1\text{GeV})}{\alpha_s(\mu)}\right]^{4/9}, \\ \langle\overline{q}g_s\sigma Gq\rangle(\mu) &= \langle\overline{q}g_s\sigma Gq\rangle(1\text{GeV})\left[\frac{\alpha_s(1\text{GeV})}{\alpha_s(\mu)}\right]^{2/27}, \\ \langle\overline{s}g_s\sigma Gs\rangle(\mu) &= \langle\overline{s}g_s\sigma Gs\rangle(1\text{GeV})\left[\frac{\alpha_s(1\text{GeV})}{\alpha_s(\mu)}\right]^{2/27}, \\ m_s(\mu) &= m_s(2\,\text{GeV})\left[\frac{\alpha_s(\mu)}{\alpha_s(2\,\text{GeV})}\right]^{4/9}, \\ m_c(\mu) &= m_c(m_c)\left[\frac{\alpha_s(\mu)}{\alpha_s(m_c)}\right]^{12/25}, \\ \alpha_s(\mu) &= \frac{1}{b_0 t}\left[1 - \frac{b_1}{b_0^2}\frac{\log t}{t} + \frac{b_1^2\left(\log^2 t - \log t - 1\right) + b_0 b_2}{b_0^4 t^2}\right],\end{aligned} \quad (12)$$

where $t = \log(\mu^2/\Lambda^2)$, $b_0 = (33 - 2n_f)/12\pi$, $b_1 = (153 - 19n_f)/24\pi^2$, $b_2 = (2857 - (5033/9)n_f + (325/27)n_f^2)/128\pi^3$, $\Lambda = 213\,\text{MeV}$, 296 MeV and 339 MeV for the flavors $n_f = 5$, 4 and 3, respectively [2].

For the hadron mass, it is independent of the energy scale because of its observability. However, in calculations, the perturbative corrections are neglected, the operators of the orders $\mathcal{O}_n(\alpha_s^k)$ with $k > 1$ or the dimensions $n > 16$ are discarded, and some higher dimensional vacuum condensates are factorized into lower dimensional ones; therefore, the corresponding energy-scale dependence is modified. We have to take into account the energy-scale dependence of the QCD sum rules.

In [26, 31–34], the energy-scale dependence of the QCD sum rules is studied in detail for the hidden-charm tetraquark states and molecular states, and an energy-scale formula $\mu = \sqrt{M^2_{X/Y/Z} - (2\mathbb{M}_c)^2}$ is come up with to determine the optimal energy scale. This energy-scale formula enhances the pole contribution remarkably, improves the convergent behaviors in the operator product expansion, and works well for the exotic hadron states. In this article, we explore the $D\overline{D}^*K$ state Z through constructing the color singlet-singlet-singlet type current based on the color-singlet $q\overline{q}$ substructure. For the two-meson molecular states, the basic constituent is also the color-singlet $q\overline{q}$ substructure [33, 34]. Hence, the previous works can be extended to study the $D\overline{D}^*K$ state. We employ the energy-scale formula $\mu = \sqrt{M^2_{X/Y/Z} - (2\mathbb{M}_c)^2}$ with the updated value of the effective c-quark mass $\mathbb{M}_c = 1.85\,\text{GeV}$ to take the ideal energy scale of the QCD spectral density.

At the present time, no candidate is observed experimentally for the hexaquark state Z with the symbolic quark constituent $c\overline{c}d\overline{u}s\overline{u}$. However, in the scenario of four-quark states, the $Z_c(3900)$ and $Z(4430)$ can be tentatively assigned to be the ground state and the first radial excited state of the axial vector four-quark states, respectively [35], while the $X(3915)$ and $X(4500)$ can be tentatively assigned to be the ground state and the first radial excited state of the scalar four-quark states, respectively [36, 37]. By comparison, the energy gap is about 0.6 GeV between the ground state and the first radial excited state of the hidden-charm four-quark states. Here, we suppose the energy gap is also about 0.6 GeV between the ground state and the first radial excited state of the hidden-charm six-quark states and take the relation $\sqrt{s_0} = M_Z + (0.4 - 0.6)\,\text{GeV}$ as a constraint to obey.

In (11), there are two free parameters: the Borel parameter T^2 and the continuum threshold parameter s_0. The extracted hadron mass is a function of the Borel parameter T^2 and the

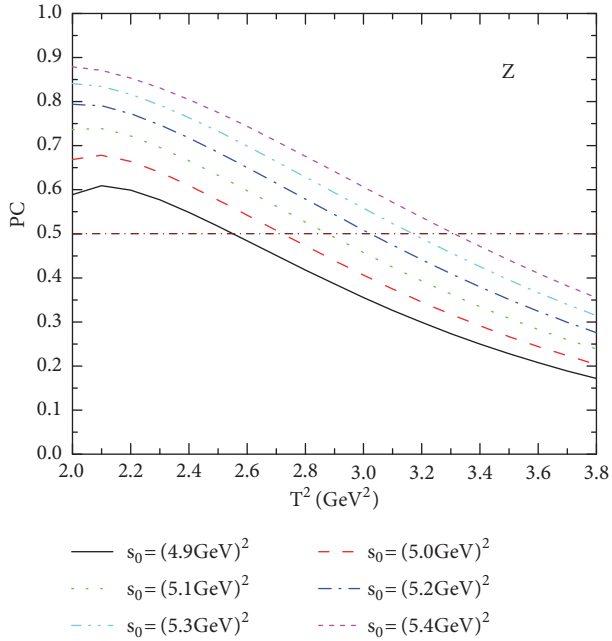

Figure 1: The pole contribution with variation of the Borel parameter T^2.

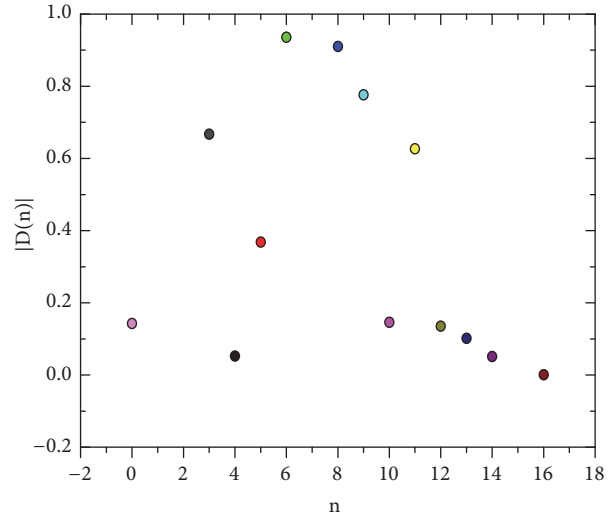

Figure 2: The absolute contributions of the vacuum condensates with dimension n in the operator product expansion.

continuum threshold parameter s_0. To obtain a reliable mass sum rule analysis, we obey two criteria to choose suitable working ranges for the two free parameters. One criterion is the pole dominance on the phenomenological side, which requires the pole contribution (PC) to be about $(40 - 60)\%$. The PC is defined as

$$\text{PC} = \frac{\int_{4m_c^2}^{s_0} ds\rho(s) \exp\left(-s/T^2\right)}{\int_{4m_c^2}^{\infty} ds\rho(s) \exp\left(-s/T^2\right)}. \tag{13}$$

The other criterion is the convergence of the operator product expansion. To judge the convergence, we compute the contributions of the vacuum condensates $D(n)$ in the operator product expansion with the formula:

$$D(n) = \frac{\int_{4m_c^2}^{s_0} ds\rho_n(s) \exp\left(-s/T^2\right)}{\int_{4m_c^2}^{s_0} ds\rho(s) \exp\left(-s/T^2\right)}, \tag{14}$$

where the n is the dimension of the vacuum condensates.

In Figure 1, we show the variation of the PC with respect to the Borel parameter T^2 for different values of the continuum threshold parameter s_0 at the energy scale $\mu = 2.9\,\text{GeV}$. From the figure, we can see that the value $\sqrt{s_0} \leq 5.0\,\text{GeV}$ is too tiny to obey the pole dominance criterion and result in sound Borel window for the state Z. To warrant the Borel platform for the mass m_Z, we take the value $T^2 = (2.8 - 3.2)\,\text{GeV}^2$. In the above Borel window, if we choose the value $\sqrt{s_0} = (5.1 - 5.3)\,\text{GeV}$, the PC is about $(39 - 63)\%$. The pole dominance condition is well satisfied.

In Figure 2, we draw the absolute contribution values of the vacuum condensates $|D(n)|$ at central values of the above input parameters. From the figure, we can observe that the contribution of the perturbative term $D(0)$ is not the dominant contribution; the contributions of the vacuum condensates with dimensions 3, 6, 8, 9, and 11 are very great. If we take the contribution of the vacuum condensate with dimension 11 as a milestone, the absolute contribution values of the vacuum condensates $|D(n)|$ decrease quickly with the increase of the dimensions n, and the operator product expansion converges nicely.

Thus, we obtain the values $T^2 = (2.8 - 3.2)\,\text{GeV}^2$, $\sqrt{s_0} = (5.1 - 5.3)\,\text{GeV}$ and $\mu = 2.9\,\text{GeV}$ for the state Z. Considering all uncertainties of the input parameters, we get the values of the mass and pole residue of the state Z:

$$\begin{aligned} M_Z &= 4.71^{+0.19}_{-0.11}\,\text{GeV}, \\ \lambda_Z &= \left(4.60^{+1.15}_{-0.69}\right) \times 10^{-4}\,\text{GeV}^8, \end{aligned} \tag{15}$$

which are shown explicitly in Figures 3 and 4. Obviously, the energy-scale formula $\mu = \sqrt{M^2_{X/Y/Z} - (2\mathbb{M}_c)^2}$ and the relation $\sqrt{s_0} = M_Z + (0.4 - 0.6)\,\text{GeV}$ are also well satisfied. The central value $M_Z = 4.71\,\text{GeV}$ is about 337 MeV above the threshold $M_{K+D+\overline{D}^*} = 497.6 + 1865 + 2010 = 4372.6\,\text{MeV}$, which indicates that the Z is probably a resonance state. For some exotic resonances, the authors have combined the effective range expansion, unitarity, analyticity, and compositeness coefficient to probe their inner structure in [38, 39]. Their studies indicated that the underlying two-particle component (in the present case, corresponding to three-particle component) plays an important or minor role; in other words, there are the other hadronic degrees of freedom inside the corresponding resonance. Hence, a resonance state embodies the net effect. Considering the conservation of the angular momentum, parity and isospin, we list out the possible hadronic decay patterns of the hexaquark state Z:

$$Z \longrightarrow J/\psi\pi K, \eta_c\rho(770)K, D\overline{D}^* K. \tag{16}$$

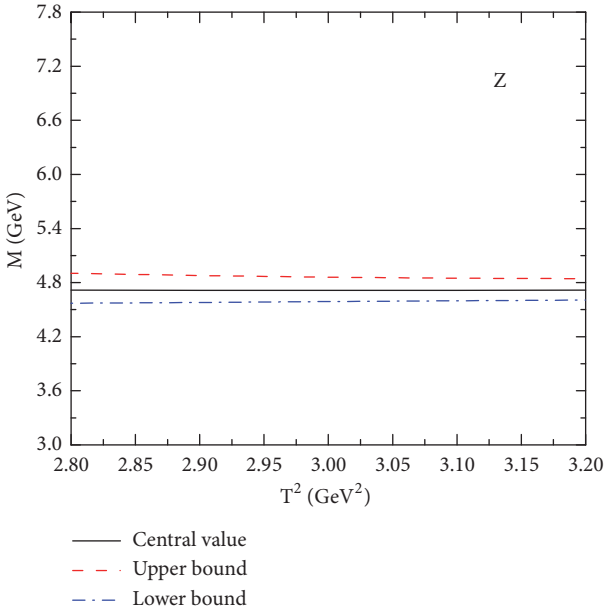

Figure 3: The mass with variation of the Borel parameter T^2.

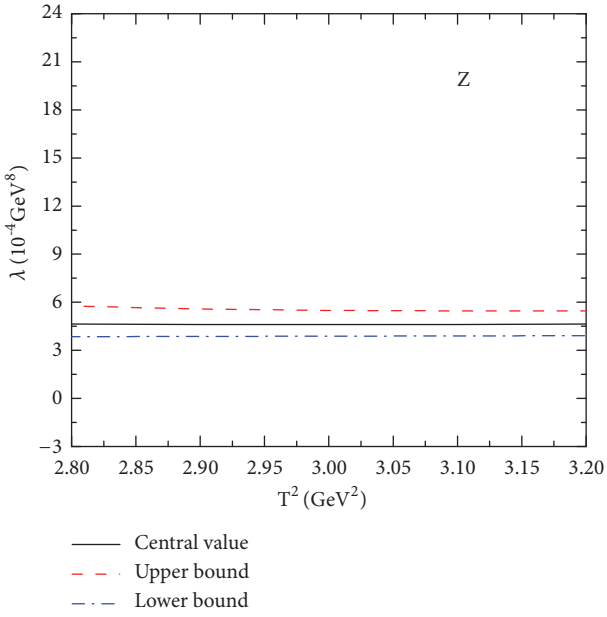

Figure 4: The pole residue with variation of the Borel parameters T^2.

To search for the X(3872), Belle, BaBar, and LHCb have collected numerous data in the decay $B \longrightarrow J/\psi\pi\pi K$. Thus, the hexaquark state Z may be found by focusing on the easiest channel $J/\psi\pi K$ in the experiment.

4. Conclusion

In this article, we construct the color singlet-singlet-singlet interpolating current operator with $I(J^P) = (3/2)(1^-)$ to study the $D\overline{D}^* K$ system through QCD sum rules approach by taking into account the contributions of the vacuum condensates up to dimension-16 in the operator product expansion. In numerical calculations, we saturate the hadron side of the QCD sum rule with a hexaquark molecular state, employ the energy-scale formula $\mu = \sqrt{M^2_{X/Y/Z} - (2\mathbb{M}_c)^2}$ to take the optimal energy scale of the QCD spectral density, and seek the ideal Borel parameter T^2 and continuum threshold s_0 by obeying two criteria of QCD sum rules for multiquark states. Finally, we obtain the mass and pole residue of the corresponding hexaquark molecular state Z. The predicted mass, $M_Z = 4.71^{+0.19}_{-0.11}$ GeV, which lies above the $D\overline{D}^* K$ threshold, indicates that the Z is probably a resonance state. This resonance state Z may be found by focusing on the channel $J/\psi\pi K$ of the decay $B \longrightarrow J/\psi\pi\pi K$ in the future.

Data Availability

The data used to support the findings of this study are available from the corresponding author upon request.

Conflicts of Interest

The authors declare that they have no conflicts of interest.

Acknowledgments

This work is supported by National Natural Science Foundation, Grant Number 11775079.

References

[1] S. K. Choi, "Observation of a narrow charmoniumlike state in exclusive $B^{\pm} \longrightarrow K^{\pm}\pi^+\pi^- J/\psi$ decays," *Physical Review Letters*, vol. 91, Article ID 262001, 2003.

[2] K. A. Olive, "Review of particle physics," *Chinese Physics C*, vol. 38, Article ID 090001, 2014.

[3] S. L. Olsen, T. Skwarnicki, and D. Zieminska, "Nonstandard heavy mesons and baryons: experimental evidence," *Reviews of Modern Physics*, vol. 90, no. 1, Article ID 15003, 2018.

[4] N. Brambilla, "Heavy quarkonium: progress, puzzles, and opportunities," *European Physical Journal C*, vol. 71, Article ID 1534, 2011.

[5] S. Godfrey and N. Isgur, "Mesons in a relativized quark model with chromodynamics," *Physical Review D: Particles, Fields, Gravitation and Cosmology*, vol. 32, no. 1, pp. 189–231, 1985.

[6] H.-X. Chen, W. Chen, X. Liu, and S.-L. Zhu, "The hidden-charm pentaquark and tetraquark states," *Physics Reports*, vol. 639, p. 1, 2016.

[7] J. He, "$\overline{D}\Sigma_c^*$ and $\overline{D}^*\Sigma_c$ interactions and the LHCb hidden-charmed pentaquarks," *Physics Letters B*, vol. 753, pp. 547–551, 2016.

[8] F. K. Guo, C. Hanhart, U. G. Meißner, Q. Wang, Q. Zhao, and B. S. Zou, "Hadronic molecules," *Reviews of Modern Physics*, vol. 90, no. 1, Article ID 015004, 2018.

[9] C. Y. Wong, "Molecular states of heavy quark mesons," *Physical Review C*, vol. 69, Article ID 055202, 2004.

[10] E. S. Swanson, "Short range structure in the X(3872)," *Physics Letters B*, vol. 588, pp. 189–195, 2004.

[11] M. Suzuki, "X(3872) boson: Molecule or charmonium," *Physical Review D*, vol. 72, Article ID 114013, 2005.

[12] M. T. AlFiky, F. Gabbiani, and A. A. Petrov, "X(3872) Hadronic molecules in effective field theory," *Physics Letters B*, vol. 640, p. 238, 2006.

[13] S. Fleming, M. Kusunoki, T. Mehen, and U. van Kolck, "Pion interactions in the X(3872)," *Physical Review D*, vol. 76, Article ID 034006, 2007.

[14] E. Braaten, M. Lu, and J. Lee, "Weakly-bound hadronic molecule near a 3-body threshold," *Physical Review D*, vol. 76, Article ID 054010, 2007.

[15] C. Hanhart, Y. S. Kalashnikova, A. E. Kudryavtsev, and A. V. Nefediev, "Reconciling the X(3872) with the near-threshold enhancement in the $D^0\overline{D}^{*0}$ final state," *Physical Review D*, vol. 76, Article ID 034007, 2007.

[16] M. B. Voloshin, "sospin properties of the X state near the $D\overline{D}^*$ threshold," *Physical Review D*, vol. 76, Article ID 014007, 2007.

[17] P. Colangelo, F. De Fazio, and S. Nicotri, "$X(3872) \longrightarrow D\overline{D}\gamma$ decays and the structure of $X(3872)$," *Physics Letters B*, vol. 650, pp. 166–171, 2007.

[18] L. Ma, Q. Wang, and U.-G. Meissner, "Double heavy tri-hadron bound state via delocalized π bond," *Chinese Physics C*, vol. 43, Article ID 014012, 2019.

[19] X. L. Ren, B. B. Malabarba, L. S. Geng, K. P. Khemchandani, and A. M. Torres, "K^* mesons with hidden charm arising from KX(3872) and $KZ_c(3900)$ dynamics," *Physics Letters B*, vol. 785, pp. 112–117, 2018.

[20] R. M. Albuquerque, K. P. Khemchandani, J. M. Dias et al., "QCD sum rules approach to the *X*, *Y* and *Z* states," https://arxiv.org/abs/1812.08207.

[21] W. Chen and S. L. Zhu, "The vector and axial-vector charmonium-like states," *Physical Review D*, vol. 83, Article ID 034010, 2011.

[22] W. Chen, T. G. Steele, H. X. Chen, and S. L. Zhu, "$Z_c(4200)^+$ decay width as a charmonium-like tetraquark state," *The European Physical Journal C*, vol. 75, p. 338, 2015.

[23] J. R. Zhang and M. Q. Huang, "$\{Q\bar{s}\bar{Q}(')s\}$ molecular states in QCD sum rules," *Communications in Theoretical Physics*, vol. 54, pp. 1075–1090, 2010.

[24] Z. Y. Di, Z. G. Wang, J. X. Zhang, and G. L. Yu, "Scalar hidden-charm tetraquark states with QCD sum rules," *Communications in Theoretical Physics*, vol. 69, p. 191, 2018.

[25] Z. G. Wang, "The lowest hidden charmed tetraquark state from QCD sum rules," *Modern Physics Letters A*, vol. 29, Article ID 1450207., 2014.

[26] Z. G. Wang and T. Huang, "Analysis of the X(3872), $Z_c(3900)$, and $Z_c(3885)$ as axial-vector tetraquark states with QCD sum rules," *Physical Review D*, vol. 89, Article ID 054019, 2014.

[27] Z. G. Wang and J. X. Zhang, "Possible pentaquark candidates: new excited Ω_c states," *European Physical Journal C*, vol. 78, p. 14, 2018.

[28] M. A. Shifman, A. I. Vainshtein, and V. I. Zakharov, "QCD and resonance physics. Applications," *Nuclear Physics B*, vol. 147, no. 5, pp. 448–518, 1979.

[29] L. J. Reinders, H. Rubinstein, and S. Yazaki, "Hadron properties from QCD sum rules," *Physics Reports*, vol. 127, no. 1, p. 1, 1985.

[30] P. Colangelo and A. Khodjamirian, *At the Frontier of Particle Physics: Handbook of QCD*, M. Shifman, Ed., vol. 3, World Scientific, Singapore, 2001.

[31] Z. G. Wang, "Analysis of the $Z_c(4020)$, $Z_c(4025)$, Y(4360), and (Y4660) as vector tetraquark states with QCD sum rules," *European Physical Journal C*, vol. 74, p. 2874, 2014.

[32] Z. G. Wang and T. Huang, "The $Z_b(10610)$ and $Z_b(10650)$ as axial-vector tetraquark states in the QCD sum rules," *Nuclear Physics A*, vol. 930, pp. 63–85, 2014.

[33] Z. G. Wang and T. Huang, "Possible assignments of the X(3872), $Z_c(3900)$, and $Z_b(10610)$ as axial-vector molecular states," *European Physical Journal C*, vol. 74, p. 2891, 2014.

[34] Z. G. Wang, "Reanalysis of the Y(3940), Y(4140), Zc(4020), $Z_c(4025)$, and $Z_b(10650)$ as molecular states with QCD sum rules," *European Physical Journal C*, vol. 74, p. 2963, 2014.

[35] Z. G. Wang, "Analysis of the Z(4430) as the First Radial Excitation of the $Z_c(3900)$," *Communications in Theoretical Physics*, vol. 63, p. 325, 2015.

[36] Z. G. Wang, "Scalar tetraquark state candidates: X(3915), X(4500) and X(4700)," *European Physical Journal C*, vol. 77, p. 78, 2017.

[37] Z. G. Wang, "Reanalysis of the X(3915) , X(4500) and X(4700) with QCD sum rules," *European Physical Journal A*, vol. 53, p. 19, 2017.

[38] X. W. Kang, Z. H. Guo, and J. A. Oller, "General considerations on the natureof $Z_b(10610)$ and $Z_b(10650)$ from their pole positions," *Physical Review D*, vol. 94, Article ID 014012, 2016.

[39] R. Gao, Z. H. Guo, X. W. Kang, and J. A. Oller, "Effective-range-expansion study of near threshold heavy-flavor resonances," https://arxiv.org/abs/1812.07323.

Hindawi
Advances in High Energy Physics
Volume 2019, Article ID 7576254, 6 pages
https://doi.org/10.1155/2019/7576254

Research Article

Studying the Bound State of the $B\overline{K}$ System in the Bethe-Salpeter Formalism

Zhen-Yang Wang,[1] Jing-Juan Qi,[2] and Xin-Heng Guo[2]

[1]*Physics Department, Ningbo University, Zhejiang 315211, China*
[2]*College of Nuclear Science and Technology, Beijing Normal University, Beijing 100875, China*

Correspondence should be addressed to Xin-Heng Guo; xhguo@bnu.edu.cn

Received 7 January 2019; Accepted 17 February 2019; Published 4 March 2019

Guest Editor: Tao Luo

In this work, we study the $B\overline{K}$ molecule in the Bethe-Salpeter (BS) equation approach. With the kernel containing one-particle-exchange diagrams and introducing two different form factors (monopole form factor and dipole form factor) in the vertex, we solve the BS equation numerically in the covariant instantaneous approximation. We investigate the isoscalar and isovector $B\overline{K}$ systems, and we find that $X(5568)$ cannot be a $B\overline{K}$ molecule.

1. Introduction

The physics of exotic multiquark states has been a subject of intense interest in recent years. One reason for this is that the experimental data are being accumulated on charmonium-like XYZ states and P_c pentaquark states (see the review papers [1–3] for details) and more and more experimental data will be found in near future.

In 2016, the D0 Collaboration announced a new enhancement structure $X(5568)$ with the statistical significance of 5.1σ in the $B_s^0\pi^\pm$ invariant mass spectrum, which has the mass $5567.8 \pm 2.9(\text{stat})^{+0.9}_{-1.9}(\text{syst})$ MeV and width $\Gamma = 21.9 \pm 6.4(\text{stat})^{+5.0}_{-2.5}(\text{syst})$ MeV [4]. The observed channel indicates that the isospin of the $X(5568)$ is 1 and if it decays into $B^0\pi^\pm$ via a S-wave, the quantum numbers of the $X(5568)$ should be $J^P = 0^+$. Subsequent analyses by the LHCb [5], CMS [6], and ATLAS [7] Collaborations have not found evidence for the $X(5568)$ in proton-proton interactions at $\sqrt{s}$= 7 and 8 TeV. The CDF Collaboration has recently reported no evidence for $X(5568)$ in proton-antiproton collisions at $\sqrt{s} = 1.96$ TeV [8] with different kinematic. Recently, the D0 Collaboration reported a further evidence about this state in the decay of B with a significance of 6.7σ [9] which is consistent with their previous measurement in the hadronic decay mode [4]. Therefore, the experimental status of the $X(5568)$ resonance remains unclear and controversial.

No matter whether the structure exists or not, it has been attracting a lot of attention from both experimental and theoretical sides. Many theoretical groups have studied possible ways to explain $X(5568)$ as a tetraquark state, a molecular state, etc., within various models, and they obtained different results. In Refs. [10–18], the authors based on QCD sum rules obtained the mass and/or decay width which are in agreement with the experimental data. In Refs. [19, 20], the authors showed that $X(5568)$ or $X(5616)$ could not be assigned to be an $B\overline{K}$ or $B^*\overline{K}$ molecular state. $X(5568)$ is also disfavored as a P-wave coupled-channel scattering molecule involving the states $B_s\pi$, $B_s^*\pi$, $B\overline{K}$, and $B^*\overline{K}$ in Ref. [21]. The authors of Ref. [22] pointed out that the $B_s\pi$ and $B\overline{K}$ interactions were weak and $X(5568)$ could not be a S-wave $B_s\pi$ and $B\overline{K}$ molecular state. Based on the lattice QCD, there is no candidate for $X(5568)$ with $J^P = 0^+$ [23]. The authors found that threshold, cusp, molecular, and tetraquark models were all unfavoured for $X(5568)$ [24]. $X(5568)$ as $B\overline{K}$ molecule and diquark-diquark model are considered in Ref. [25] using QCD two-point and light-cone sum rules, and their results strengthen the diquark-antidiquark picture for the $X(5568)$ state rather than a meson molecule structure.

But the authors of Ref. [26] found that the $X(5568)$ signal can be reproduced by using $B_s\pi - B\overline{K}$ coupled channel analysis, if the corresponding cutoff value was larger than a natural value $\Lambda \sim 1$ GeV. In Ref. [27], the authors demonstrated that $X(5568)$ could be a kinematic reflection and explained the absence of $X(5568)$ in LHCb and CMS Collaborations. Based on the quark model, $X(5568)$ could exist as a mixture of a tetraquark and hadronic molecule [28].

By this chance, we will systematically study the $B\overline{K}$ molecular state in the BS equation approach. We investigate the S-wave $B\overline{K}$ systems with both isospins $I = 0, 1$ being considered. We will vary $E_b(E_b = E - M_B - M_K)$ in a much wider range and search for all the possible solutions. In this process, we naturally check whether $X(5568)$ can exist as S-wave $B\overline{K}$ molecular state, or not.

The remainder of this paper is organized as follows. In Section 2, we discuss the BS equation for two pseudoscalar mesons and establish the one-dimensional BS function for this system. The numerical results of the $B\overline{K}$ systems are presented in Section 3. In the last section, we give a summary and some discussions.

2. The Bethe-Salpeter Formalism for $B\overline{K}$ System

In this section, we will review the general formalism of the BS equation and establish the BS equation for the system of two pseudoscalar mesons. Let us start by defining the BS wave function for the bound state $|P\rangle$ as the following:

$$\chi\left(x_1, x_2, P\right) = \langle 0| TB\left(x_1\right)\overline{K}\left(x_2\right)|P\rangle, \tag{1}$$

where $B(x_1)$ and $\overline{K}(x_2)$ are the field operators of the B and $\overline{K}$ mesons at space coordinates x_1 and x_2, respectively, and P denotes the total momentum of the bound state with mass M and velocity v. The BS wave function in momentum space is defined as

$$\chi_P\left(x_1, x_2, P\right) = e^{-iPX}\int \frac{d^4p}{(2\pi)^4} e^{-ipx}\chi_P\left(p\right), \tag{2}$$

where p represents the relative momentum of the two constituents and $p = \lambda_2 p_1 - \lambda_1 p_2$ (or $p_1 = \lambda_1 P + p$, $p_2 = \lambda_2 P - p$). The relative coordinate x and the center-of-mass coordinate X are defined by

$$\begin{aligned} X &= \lambda_1 x_1 + \lambda_2 x_2, \\ x &= x_1 - x_2, \end{aligned} \tag{3}$$

or inversely,

$$\begin{aligned} x_1 &= X + \lambda_2 x, \\ x_2 &= X - \lambda_1 x, \end{aligned} \tag{4}$$

where $\lambda_1 = m_B/(m_B + m_K)$ and $\lambda_2 = m_K/(m_B + m_K)$, and m_B and m_K are the masses of B and K mesons.

It can be shown that the BS wave function of $B\overline{K}$ bound state satisfies the following BS equation [29]:

$$\chi_P\left(p\right) = S_B\left(p_1\right)\int \frac{d^4q}{(2\pi)^4} K\left(P, p, q\right)\chi_P\left(q\right) S_{\overline{K}}\left(p_2\right), \tag{5}$$

where S_B and $S_{\overline{K}}(p_2)$ are the propagators of B and $\overline{K}$, respectively, and $K(P, p, q)$ is the kernel, which is defined as the sum of all the two particle irreducible diagrams with respect to B and $\overline{K}$ mesons. For convenience, in the following we use the variables $p_l(= p \cdot v)$ and $p_t(= p - p_l v)$ to be the longitudinal and transverse projections of the relative momentum (p) along the bound state momentum (P). Then, the propagator of B mesons can be expressed as

$$S_B\left(\lambda_1 P + p\right) = \frac{i}{\left(\lambda_1 M + p_l\right)^2 - \omega_1^2 + i\epsilon}, \tag{6}$$

and the propagator of the $\overline{K}$ is

$$S_K\left(\lambda_2 P - p\right) = \frac{i}{\left(\lambda_2 M - p_l\right)^2 - \omega_2^2 + i\epsilon}, \tag{7}$$

where $\omega_{1(2)} = \sqrt{m_{B(K)}^2 + p_t^2}$ (we have defined $p_t^2 = -p_t \cdot p_t$).

As discussed in the introduction, we will study the S-wave bound state of $B\overline{K}$ system. The field doublets (B^+, B^-), $(B^0, \overline{B}^0)$, (K^+, K^-), and $(K^0, \overline{K}^0)$ have the following expansions in momentum space:

$$\begin{aligned} B_1\left(x\right) &= \int \frac{d^3p}{(2\pi)^3\sqrt{2E_B^{\pm}}}\left(a_{B^+}e^{-ipx} + a_{B^-}^{\dagger}e^{ipx}\right), \\ B_2\left(x\right) &= \int \frac{d^3p}{(2\pi)^3\sqrt{2E_B^{0}}}\left(a_{B^0}e^{-ipx} + a_{\overline{B}^0}^{\dagger}e^{ipx}\right), \\ K_1\left(x\right) &= \int \frac{d^3p}{(2\pi)^3\sqrt{2E_K^{\pm}}}\left(a_{K^-}e^{-ipx} + a_{\overline{K}^+}^{\dagger}e^{ipx}\right), \\ K_2\left(x\right) &= \int \frac{d^3p}{(2\pi)^3\sqrt{2E_K^{0}}}\left(a_{K^0}e^{-ipx} + a_{\overline{K}^0}^{\dagger}e^{ipx}\right), \end{aligned} \tag{8}$$

where $E_{B(K)} = \sqrt{p_{1(2)}^2 + m_{B(K)}^2}$ is the energy of the particle.

The isospin of $B\overline{K}$ can be 0 or 1 for $B\overline{K}$ system, and the flavor wave function for the isoscalar bound state can be written as

$$|P\rangle_{0,0} = \frac{1}{\sqrt{2}}\left|B^+K^- + B^0\overline{K}^0\right\rangle, \tag{9}$$

and the flavor wave functions of the isovector states for $B\overline{K}$ system are

$$\begin{aligned} |P\rangle_{1,1} &= \left|B^+\overline{K}^0\right\rangle, \\ |P\rangle_{1,0} &= \frac{1}{\sqrt{2}}\left|B^+K^- - B^0\overline{K}^0\right\rangle, \\ |P\rangle_{1,-1} &= \left|B^0K^-\right\rangle. \end{aligned} \tag{10}$$

Let us now project the bound states on the field operators $B_1(x)$, $B_2(x)$, $K_1(x)$, and $K_2(x)$. Then we have

$$\langle 0| TB_i\left(x_1\right)K_j\left(x_2\right)|P\rangle_{I,I_3} = C_{(I,I_3)}^{ij}\chi_P^{(\mu)I}\left(x_1, x_2\right), \tag{11}$$

where χ_P^I is the common BS wave function for the bound state with isospin I which depends only on I but not I_3 of the state $|P\rangle_{I,I_3}$. The isospin coefficients $C^{ij}_{(I,I_3)}$ for the isoscalar state are

$$C^{11}_{(0,0)} = C^{22}_{(0,0)} = \frac{1}{\sqrt{2}}, \quad \text{else} = 0, \tag{12}$$

and for the isovector states we have

$$\begin{aligned} C^{12}_{(1,1)} &= C^{21}_{(1,-1)} = 1, \\ C^{11}_{(1,0)} &= -C^{22}_{(1,0)} = \frac{1}{\sqrt{2}}, \\ &\text{else} = 0. \end{aligned} \tag{13}$$

Now considering the kernel, Eq. (5) can be written down schematically,

$$\begin{aligned} C^{ij}_{(I,I_3)}\chi_P^{(\mu)I}(p) &= S_B(\lambda_1 P + p) \\ &\cdot \int \frac{d^4q}{(2\pi)^4} K^{ij,lk}(P,p,q)\, C^{lk}_{(I,I_3)}\chi_P^I(q)\, S_{\overline{K}}(\lambda_2 P - p). \end{aligned} \tag{14}$$

Then, from Eq. (12), for the isoscalar case, we have (take $ij = 11$ as an example)

$$\begin{aligned} \chi_P^0(p) &= S_B(\lambda_1 P + p) \\ &\cdot \int \frac{d^4q}{(2\pi)^4} \left[K^{11,11} + K^{11,22}\right] \chi_P^0(q)\, S_{\overline{K}}(\lambda_2 P - p). \end{aligned} \tag{15}$$

Similarly, for the isovector case, taking the $I_3 = 0$ component as an example, we have

$$\begin{aligned} \chi_P^1(p) &= S_B(\lambda_1 P + p) \\ &\cdot \int \frac{d^4q}{(2\pi)^4} \left[K^{11,11} - K^{11,22}\right] \chi_P^1(q)\, S_{\overline{K}}(\lambda_2 P - p). \end{aligned} \tag{16}$$

In the BS equation approach, the interaction between B and $\overline{K}$ mesons can be due to the light vector-meson (ρ and ω) exchanges. The corresponding effective Lagrangians describing the couplings of $BB\rho(\omega)$ [30, 31] and $KK\rho(\omega)$ [32, 33] are

$$\begin{aligned} \mathscr{L}_{BB\mathbb{V}} &= -ig_{BB\mathbb{V}} B_a^\dagger \overleftrightarrow{\partial} B_b \mathbb{V}^\mu_{ba}, \\ \mathscr{L}_{KK\rho} &= ig_{KK\rho}\left[K^\dagger \overrightarrow{\tau}\left(\partial_\mu K\right) - \left(\partial_\mu K^\dagger\right)\overrightarrow{\tau} K\right]\cdot\overrightarrow{\rho}^\mu, \\ \mathscr{L}_{KK\omega} &= ig_{KK\omega}\left[K^\dagger\left(\partial_\mu K\right) - \left(\partial_\mu K^\dagger\right)K\right]\omega^\mu, \end{aligned} \tag{17}$$

where the nonet vector meson matrix reads as

$$\mathbb{V} = \begin{pmatrix} \frac{\rho^0}{\sqrt{2}} + \frac{\omega}{\sqrt{2}} & \rho^+ & K^{*+} \\ \rho^- & -\frac{\rho^0}{\sqrt{2}} + \frac{\omega}{\sqrt{2}} & K^{*0} \\ K^{*-} & \overline{K}^{*0} & \phi \end{pmatrix}. \tag{18}$$

In addition, the coupling constants involved in Eq. (17) are taken as $g_{BB\mathbb{V}} = \beta g_v/\sqrt{2}$ with $g_v = 5.8$, $\beta = 0.9$, while the coupling constants $g_{KK\mathbb{V}}$ satisfy the relations $g_{KK\rho} = g_{KK\omega} = g_{\rho\pi\pi}/2$ in the $SU(3)_f$ limit, and $g_{\rho\pi\pi} \simeq m_\rho/f_\pi \simeq 5.8$ [32].

From the above observations, at the tree level, in the t-channel the kernel for the BS equation of the interaction between B and $\overline{K}$ in the so-called ladder approximation is taken to have the following form:

$$\begin{aligned} K_V(P,p,q) &= (2\pi)^4\delta^4(q_1 + q_2 - p_1 - p_2) \\ &\cdot c_I g_{BBV} g_{KKV}(p_1 + q_1)_\mu (p_2 + q_2)_\nu \\ &\cdot \Delta^{\mu\nu}(k, m_V), \end{aligned} \tag{19}$$

where m_V represent the masses of the exchanged light vector mesons ρ and ω, and c_I is the isospin coefficient: $c_0 = 3, 1$ and $c_1 = 1, 1$ for ρ, ω, and $\Delta^{\mu\nu}$ represents the propagator for vector meson.

In order to manipulate the off shell effect of the exchanged mesons ρ and ω and finite size effect of the interacting hadrons, we introduce a form factor $\mathscr{F}(k^2)$ at each vertex. Generally, the form factor has the monopole form and dipole form as shown in Ref. [34]:

$$\mathscr{F}_M(k^2) = \frac{\Lambda^2 - m^2}{\Lambda^2 - k^2}, \tag{20}$$

$$\mathscr{F}_D(k^2) = \frac{\left(\Lambda^2 - m^2\right)^2}{\left(\Lambda^2 - k^2\right)^2}, \tag{21}$$

where Λ, m, and k represent the cutoff parameter, mass of the exchanged meson, and momentum of the exchanged meson, respectively. These two kinds of form factors are normalized at the on shell momentum of $k^2 = m^2$. On the other hand, if k^2 were taken to be infinitely large ($-\infty$), the form factors, which can be expressed as the overlap integral of the wave functions of the hadrons at the vertex, would approach zero.

For the $B\overline{K}$ system, substituting Eqs. (6), (7), and (19) and aforementioned form factors Eqs. (20) and (21) into Eq. (5) and using the so-called covariant instantaneous approximation [35], $p_l = q_l$ (which ensures that the BS equation is still covariant after this approximation). Then one obtains the expression

$$\begin{aligned} \chi(p) &= \frac{ic_I g_{BBV} g_{KKV}}{\left[(\lambda_1 M + p_l)^2 - \omega_1^2 + i\epsilon\right]\left[(\lambda_2 M - p_l)^2 - \omega_2^2 + i\epsilon\right]} \\ &\cdot \int \frac{d^4q}{(2\pi)^4} \frac{4(\lambda_1 M + p_l)(\lambda_2 M - p_l) + (p_t + q_t)^2 + \left(p_t^2 - q_t^2\right)^2/m_V^2}{-(p_t - q_t)^2 - m_V^2} \mathscr{F}^2(k_t)\chi(q). \end{aligned} \tag{22}$$

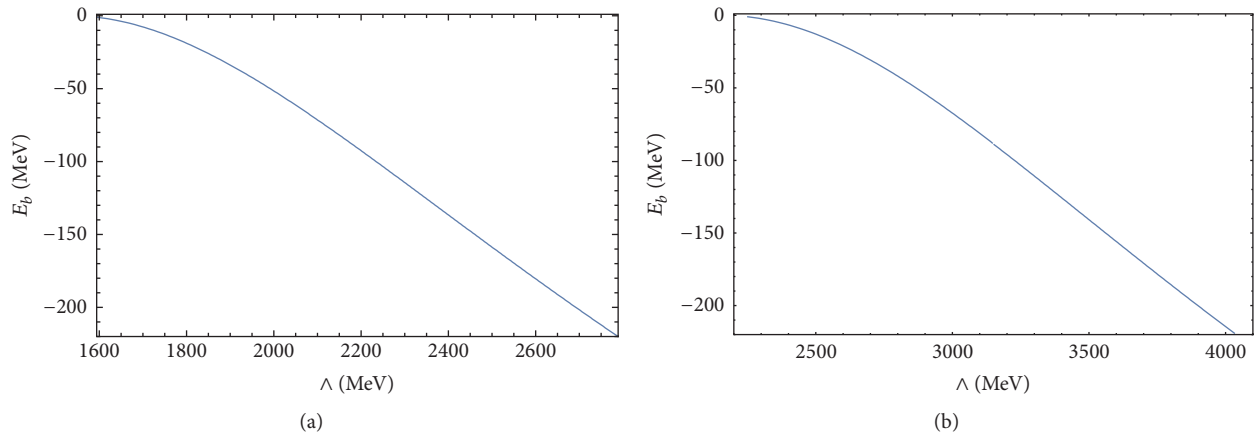

Figure 1: Relation of the cutoff Λ and the binding energy E_b with (a) the monopole form factor and (b) the dipole form factor for $I = 0$.

In Eq. (22) there are poles in $-\lambda_1 M - \omega_1 - i\epsilon$, $-\lambda_1 M + \omega_1 - i\epsilon$, $\lambda_2 M + \omega_2 - i\epsilon$, and $\lambda_2 M - \omega_2 + i\epsilon$. By choosing the appropriate contour, we integrate over p_l on both sides of Eq. (22) in the rest frame, and we will obtain the following equation:

$$\begin{aligned}\widetilde{\chi}(p_t) = {} & \frac{c_I g_{BBV} g_{KKV}}{2(M+\omega_1-\omega_2)} \int \frac{d^3 p_t}{(2\pi)^3} \\ & \cdot \left[\frac{-4\omega_1 (M+\omega_1) + (p_t+q_t)^2 + \left(p_t^2 - q_t^2\right)^2 / m_V^2}{\omega_1 (M+\omega_1+\omega_2)\left[-(p_t-q_t)^2 - m_V^2\right]} \right. \\ & \left. - \frac{4\omega_2 (M-\omega_2) + (p_t+q_t)^2 + \left(p_t^2 - q_t^2\right)^2 / m_V^2}{\omega_2 (M-\omega_1-\omega_2)\left[-(p_t-q_t)^2 - m_V^2\right]} \right] \\ & \cdot \mathcal{F}^2(k_t)\, \widetilde{\chi}(q_t),\end{aligned} \tag{23}$$

where $\widetilde{\chi}(p_t) = \int dp_l \chi(p)$.

3. Numerical Results

In this part, we will solve the BS equation numerically and study whether the S-wave $B\overline{K}$ bound state exists or not. It can be seen from Eq. (23) that there is only one free parameter in our model, the cutoff Λ, it cannot be uniquely determined, and various forms and cutoff Λ are chosen phenomenologically. It contains the information about the nonpoint interaction due to the structures of hadrons. The value of Λ is near 1 GeV which is the typical scale of nonperturbative QCD interaction. In this work, we shall treat the cutoff Λ in the form factors as a parameter varying in a much wider range 0.8-4.8 GeV, in which we will try to search for all the possible solutions of the $B\overline{K}$ bound states. For each pair of trial values of the cutoff Λ and the binding energy E_b of the $B\overline{K}$ system (which is defined as $E_b = E - m_1 - m_2$), we will obtain all the eigenvalues of this eigenvalue equation. The eigenvalue closest to 1.0 for a pair of Λ and E_b will be selected out and called the trial eigenvalue. Fixing a value of the cutoff Λ and varying the binding energy E_b (from 0 to -220 MeV) we will obtain a series of the trial eigenvalues.

Since the BS wave function for the ground state is in fact rotationally invariant, $\widetilde{\chi}(p_t)$ depends only on $|p_t|$. Generally, $|p_t|$ varies from 0 to $+\infty$ and $\widetilde{\chi}(p_t)$ would decrease to zero when $|p_t| \longrightarrow +\infty$. We replace $|p_t|$ by the variable, t:

$$|p_t| = \epsilon + w \log\left[1 + y\frac{1+t}{1-t}\right], \tag{24}$$

where ϵ is a parameter introduced to avoid divergence in numerical calculations, w and y are parameters used in controlling the slope of wave functions and finding the proper solutions for these functions, and t varies from -1 to 1. We then discretize Eq. (23) into n pieces (n is large enough) through the Gauss quadrature rule. The BS wave function can be written as n-dimension vectors, $\widetilde{\chi}(p_t)$. The coupled integral equation becomes a matrix equation $\widetilde{\chi}(|p_t|(n)) = A(n\times n)\cdot\widetilde{\chi}(|q_t|(n))$ ($A(n\times n)$ corresponding to the coefficients in Eq. (23)). Similar methods are also adopted in solving d Lippmann-Schwinger equation for $p\overline{p}$ [36–41] and $\Lambda_c\overline{\Lambda}_c$ [42].

In our calculation, we choose to work in the rest frame of the bound state in which $P = (M, 0)$. We take the averaged masses of the mesons from the PDG [43], M_B = 5279.41 MeV, M_K = 494.98 MeV, M_ρ = 775.26 MeV, and M_ω = 782.65 MeV. With the above preparation, we try to search for the all the possible solutions by solving the BS equation. The relations between Λ and E_b for the $B\overline{K}$ with $I = 0, 1$ are depicted in Figures 1 and 2, respectively.

4. Summary

Stimulated by $X(5568)$, which is recently discovered by the D0 Collaboration, we carried out a study of the interaction of $B\overline{K}$ system with isospin I =0, 1 in the Bethe-Salpeter equation approach. In order to solve the BS equation, we have used the ladder approximation and the instantaneous approximation. The value of Λ is near 1 GeV which is the typical scale of nonperturbative QCD interaction. Thus, if

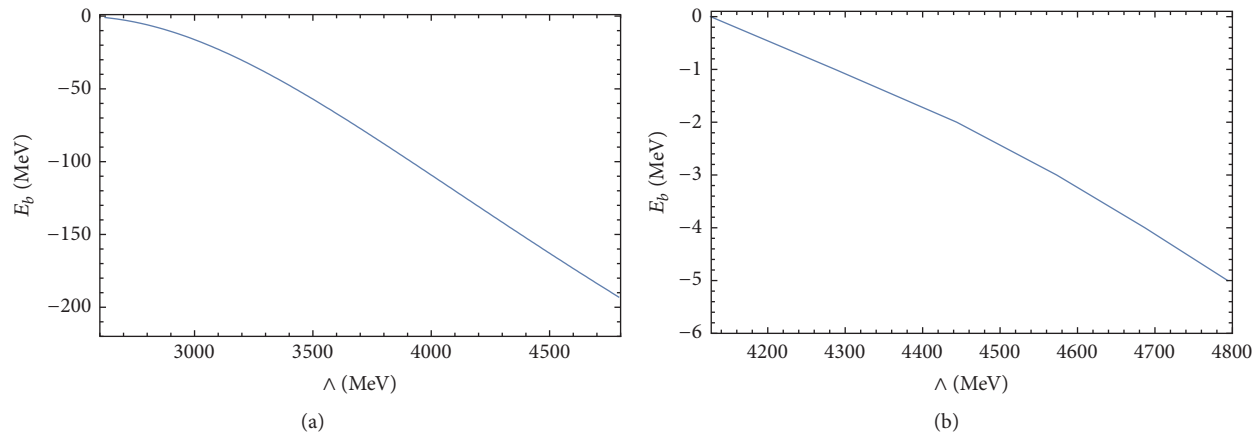

FIGURE 2: Relation of the cutoff Λ and the binding energy E_b with (a) the monopole form factor and (b) the dipole form factor for $I = 1$.

strictly considering this criterion of the value of Λ, we conclude that there does not exist isovector $B\overline{K}$ molecular state. And the $X(5568)$ cannot be the $B\overline{K}$ molecular state. The relations between Λ and E_b for the $B\overline{K}$ with $I = 0, 1$ are depicted in Figures 1 and 2, respectively.

Data Availability

The numerical data used to support the findings of this study are included within the article.

Conflicts of Interest

The authors declare that they have no conflicts of interest.

Acknowledgments

One of the authors (Z.-Y. Wang) thanks Dr. Xian-Wei Kang for a very careful reading of this manuscript. This work was supported by National Natural Science Foundation of China (Projects No. 11275025, No. 11775024, and No. 11605150) and K.C.Wong Magna Fund in Ningbo University.

References

[1] F. K. Guo, C. Hanhart, U. G. Meißner, Q. Wang, Q. Zhao, and B. S. Zou, "Hadronic molecules," *Reviews of Modern Physics*, vol. 90, no. 1, Article ID 015004, 2018.

[2] A. Esposito, A. Pilloni, and A. D. Polosa, "Multiquark resonances," *Physics Reports*, vol. 668, pp. 1–97, 2017.

[3] H. X. Chen, W. Chen, X. Liu, Y. R. Liu, and S. L. Zhu, "A review of the open charm and open bottom systems," *Reports on Progress in Physics*, vol. 80, no. 7, Article ID 076201, 2017.

[4] V. M. Abazov, B. Abbott, B. S. Acharya et al., "Evidence for a $B_s^0\pi^\pm$ state," *Physical Review Letters*, vol. 117, Article ID 022003, 2016.

[5] R. Aaij, B. Adeva, M. Adinolfi et al., "Search for structure in the $B_s^0\pi^\pm$ invariant mass spectrum," *Physical Review Letters*, vol. 117, Article ID 152003, 2016.

[6] A. M. Sirunyan, A. Tumasyan, W. Adam et al., "Search for the $X(5568)$ state decaying into $B_s^0\pi^\pm$ in proton-proton collisions at $\sqrt{s} = 8$ TeV," *Physical Review Letters*, vol. 120, Article ID 202005, 2018.

[7] M. Aaboud, G. Aad, B. Abbott et al., "Search for a structure in the $B_s^0\pi^\pm$ invariant mass spectrum with the ATLAS experiment," *Physical Review Letters*, vol. 120, Article ID 202007, 2018.

[8] T. Aaltonen, S. Amerio, D. Amidei et al., "Search for the exotic meson $X(5568)$ with the collider detector at Fermilab," *Physical Review Letters*, vol. 120, Article ID 202006, 2018.

[9] V. M. Abazov, B. Abbott, B. S. Acharya et al., "Study of the $X^\pm(5568)$ state with semileptonic decays of the B_s^0 meson," *Physical Review D*, vol. 97, Article ID 092004, 2004.

[10] S. Agaev, K. Azizi, and H. Sundu, "Mass and decay constant of the newly observed exotic $X(5568)$ state," *Physical Review D*, vol. 93, no. 7, Article ID 074024, 2016.

[11] C. M. Zanetti, M. Nielsen, and K. P. Khemchandani, "QCD sum rule study of a charged bottom-strange scalar meson," *Physical Review D*, vol. 93, Article ID 096011, 2016.

[12] W. Chen, H. X. Chen, X. Liu, T. G. Steele, and S. L. Zhu, "Decoding the $X(5568)$ as a fully open-flavor $su\overline{bd}$ tetraquark state," *Physical Review Letters*, vol. 117, Article ID 022002, 2016.

[13] S. S. Agaev, K. Azizi, and H. Sundu, "Width of the exotic $X_b(5568)$ state through its strong decay to $B_s^0\pi^+$," *Physical Review D*, vol. 93, Article ID 114007, 2016.

[14] J. Dias, K. Khemchandani, A. Martínez Torres, M. Nielsen, and C. Zanetti, "A QCD sum rule calculation of the $X^\pm(5568) \longrightarrow B_s^0\pi^\pm$ decay width," *Physics Letters B*, vol. 758, pp. 235–238, 2016.

[15] Z. G. Wang, "Analysis of the strong decay $X(5568) \longrightarrow B_s^0\pi^+$ with QCD sum rules," *The European Physical Journal C*, vol. 76, no. 5, p. 279, 2016.

[16] L. Tang and C. F. Qiao, "Tetraquark states with open flavors," *The European Physical Journal C*, vol. 76, p. 558, 2016.

[17] S. S. Agaev, K. Azizi, B. Barsbay, and H. Sundu, "Resonance $X(5568)$ as an exotic axial-vector state," *The European Physical Journal A*, vol. 53, p. 11, 2017.

[18] J. R. Zhang, J. L. Zou, and J. Y. Wu, "0^+ tetraquark states from improved QCD sum rules: delving into $X(5568)$," *Chinese Physics C*, vol. 42, no. 4, Article ID 043101, 2018.

[19] C. J. Xiao and D. Y. Chen, "Possible $B^{(*)}\overline{K}$ hadronic molecule state," *The European Physical Journal A*, vol. 53, p. 127, 2017.

[20] R. Chen and X. Liu, "Is the newly reported $X(5568)$ a $B\overline{K}$ molecular state?" *Physical Review D*, vol. 94, Article ID 034006, 2016.

[21] X. W. Kang and J. A. Oller, "P-wave coupled-channel scattering of $B_s\pi$, $B_s^*\pi$, $B\overline{K}$, $B^*\overline{K}$ and the puzzling $X(5568)$," *Physical Review D*, vol. 94, Article ID 054010, 2016.

[22] J. X. Lu, X. L. Ren, and L. S. Geng, "$B_s\pi - B\overline{K}$ interactions in finite volume and $X(5568)$," *The European Physical Journal C*, vol. 77, p. 94, 2017.

[23] C. B. Lang, D. Mohler, and S. Prelovsek, "$B_s\pi^+$ scattering and search for $X(5568)$ with lattice QCD," *Physical Review D*, vol. 94, Article ID 074509, 2016.

[24] T. J. Burns and E. S. Swanson, "Interpreting the $X(5568)$," *Physics Letters B*, vol. 760, p. 627, 2016.

[25] S. S. Agaev, K. Azizi, and H. Sundu, "Exploring $X(5568)$ as a meson molecule," *The European Physical Journal Plus*, vol. 131, no. 10, p. 351, 2016.

[26] M. Albaladejo, J. Nieves, E. Oset, Z. F. Sun, and X. Liu, "Can $X(5568)$ be described as a $B_s\pi$, $B\overline{K}$ resonant state?" *Physics Letters B*, vol. 757, p. 515, 2016.

[27] Z. Yang, Q. Wang, U. G. Mei, and U. G. Meißner, "Where does the $X(5568)$ structure come from?" *Physics Letters B*, vol. 767, p. 470, 2017.

[28] H. W. Ke and X. Q. Li, "How can $X^{\pm}(5568)$ escape detection?" *Physics Letters B*, vol. 785, p. 301, 2018.

[29] D. Lurie, *Particles and Fields*, Interscience Publishers, New York, NY, USA, 1968.

[30] J. He, "Study of $B\overline{B}^*/D\overline{D}^*$ bound states in a Bethe-Salpeter approach," *Physical Review D*, vol. 90, Article ID 076008, 2014.

[31] G. Q. Feng, Z. X. Xie, and X. H. Guo, "Possible $B\overline{K}$ molecular structure of $B_{s0}^*(5725)$ in the Bethe-Salpeter approach," *Physical Review D*, vol. 83, Article ID 016003, 2011.

[32] G. Q. Feng and X. H. Guo, "DK molecule in the Bethe-Salpeter equation approach in the heavy quark limit," *Physical Review D*, vol. 86, Article ID 036004, 2012.

[33] R. Chen, A. Hosaka, and X. Liu, "Searching for possible Ω_c-like molecular states from meson-baryon interaction," *Physical Review D*, vol. 97, Article ID 036016, 2018.

[34] R. Chen, A. Hosaka, and X. Liu, "Heavy molecules and one-σ/ω-exchange model," *Physical Review D*, vol. 96, Article ID 116012, 2017.

[35] X. H. Guo and T. Muta, "Isgur-Wise function for $\Lambda_b \longrightarrow \Lambda_c$ in the BS approach," *Physical Review D*, vol. 54, no. 7, Article ID 4629, 1996.

[36] X. W. Kang, J. Haidenbauer, and U. G. Meißner, "Antinucleon-nucleon interaction in chiral effective field theory," *Journal of High Energy Physics*, vol. 1402, p. 113, 2014.

[37] J. Haidenbauer, X.-W. Kang, and U.-G. Meißner, "The electromagnetic form factors of the proton in the timelike region," *Nuclear Physics A*, vol. 929, p. 102, 2014.

[38] X. Kang, J. Haidenbauer, and U. Meißner, "Near-threshold $\overline{p}p$ invariant mass spectrum measured in J/ψ and ψ' decays," *Physical Review D*, vol. 91, no. 7, Article ID 074003, 2015.

[39] J. Haidenbauer, C. Hanhart, X. Kang, and U. Meißner, "Origin of the structures observed in e^+e^- annihilation into multipion states around the $\overline{p}p$ threshold," *Physical Review D*, vol. 92, no. 5, Article ID 054032, 2015.

[40] L. Y. Dai, J. Haidenbauer, and U. G. Meißner, "Antinucleon-nucleon interaction at next-to-next-to-next-to-leading order in chiral effective field theory," *Journal of High Energy Physics*, vol. 1707, p. 78, 2017.

[41] L. Y. Dai, J. Haidenbauer, and U. G. Meißner, "$J/\psi \longrightarrow \gamma\eta'\pi^+\pi^-$ and the structure observed around the $\overline{p}p$ threshold," *Physical Review D*, vol. 98, Article ID 014005, 2018.

[42] L. Y. Dai, J. Haidenbauer, and U. G. Meißner, "Re-examining the $X(4630)$ resonance in the reaction $e^+e^- \longrightarrow \Lambda_c^+\overline{\Lambda}_c^-$," *Physical Review D*, vol. 96, Article ID 116001, 2017.

[43] M. Tanabashi, K. Hagiwara, K. Hikasa et al., "Review of particle physics," *Physical Review D*, vol. 98, no. 3, Article ID 030001, 2018.

Hindawi
Advances in High Energy Physics
Volume 2019, Article ID 2567070, 5 pages
https://doi.org/10.1155/2019/2567070

Research Article

A Method for the Direct Absolute Measurement of J/ψ Decay with $\psi(3686)$ Data Set

Fang Yan and Bo Zheng

School of Nuclear Science and Technology, University of South China, Hengyang, Hunan 421001, China

Correspondence should be addressed to Bo Zheng; zhengbo_usc@163.com

Received 9 November 2018; Accepted 12 December 2018; Published 17 January 2019

Guest Editor: Ling-Yun Dai

To take the full advantage of the $\psi(3686)$ data set collected at e^+e^- collider at τ−charm energy region, a tag method is developed to directly measure the J/ψ meson decay branching fractions absolutely. The J/ψ meson decay can be measured with the J/ψ sample tagged by the two soft charged pions from the decay $\psi(3686) \longrightarrow J/\psi\pi^+\pi^-$. This method is illustrated by comparing the input and output branching fractions of $J/\psi \longrightarrow \gamma\eta$ with 106 million inclusive $\psi(3686)$ Monte Carlo samples. The consistent result confirms the validity of the tag method.

1. Introduction

The firstly discovered charmonium J/ψ [1, 2], $J^{PC} = 1^{--}$, is the lowest one among those which can be produced directly in e^+e^- annihilation. Many experiments [3–14] have been performed to study its production and decay properties. However, the summation of the measured J/ψ decay branching fraction is not more than 60% [15] without considering the interference between resonance and continuum amplitudes until now, which hampers the understanding of its properties. The precisely measured branching fractions of J/ψ decay not only provide information to understand the J/ψ properties, but also can test OZI (Okubo-Zweig-Iizuka) rule, flavor SU(3) symmetry, and perturbative QCD [16].

The J/ψ production and decay property are studied by using the data collected from e^+e^- collisions at the J/ψ resonance traditionally. At this energy, the events consist mostly of $e^+e^- \longrightarrow J/\psi$, $e^+e^- \longrightarrow l^+l^-$ (l represents e, μ), with small amounts of three-flavor continuum and other processes such as γV, where V represents vector meson. Due to some unavoidable influences, such as interference effect and undistinguishable backgrounds, some J/ψ decay channels can not be studied by using this kind of data sample. An energy scan experiment performed around the J/ψ resonance can solve the problem induced by interference effect, while it is not effective for the final states with undistinguishable backgrounds from other processes. Usually, a large data set will be taken at $\psi(3686)$ resonance for τ−charm factory. Taking the Beijing Spectrometer III (BESIII) [17] at the Beijing Electron Positron Collider II (BEPCII) [17] as an example, a goal of 3.2 billion $\psi(3686)$ events is set to be taken before its closure. Considering the large branching fraction of $\psi(3686) \longrightarrow J/\psi\pi^+\pi^-$, $(34.67 \pm 0.30)\%$ [15], this sample can naturally be used to study the J/ψ decay.

In this paper, we propose a method to construct a J/ψ sample by tagging the J/ψ meson with the two soft charged pions from $\psi(3686) \longrightarrow J/\psi\pi^+\pi^-$ (called tag method for convenient) in the $\psi(3686)$ data sample. The feasibility of the method is then verified by examining the input and output branching fractions of $J/\psi \longrightarrow \gamma\eta$ in the inclusive $\psi(3686)$ Monte Carlo (MC) sample.

2. BESIII Detector and Simulation

There are four subdetectors at BESIII detector, which has been described elsewhere [17]. From the inner to the outside is Main Drift Chamber (MDC), Time of Flight (TOF), Electromagnetic Calorimeter (EMC), and Muon Counter

(MUC). The information from four subdetectors is used to identify and select candidate particles. The Superconducting Magnet, between EMC and MUC, provides 1 T magnetic field.

The work is performed in the framework of the BESIII Offline Software System (BOSS) [18], the GAUDI [19] based, which contains five subprojects such as framework, simulation, calibration, reconstruction, and analysis tools. Monte Carlo (MC) simulations are used to optimize the event selection and background estimation. The simulation software, the GEANT4-based, includes the geometric and material description of the BESIII detector, the detector response, running conditions, and performance. The production of $\psi(3686)$ is simulated by the KKMC [20, 21] generator, while its decay is generated by EVTGEN [22, 23] for known decay channels with branching fractions being set to the PDG [15] values, and by LUNDCHARM [24, 25] for the remaining unknown decay. In this work, 106 million inclusive $\psi(3686)$ events generated by data production group of BESIII are used. In addition, 100 000 exclusive $\psi(3686) \longrightarrow J/\psi\pi^+\pi^-$ with $J/\psi \longrightarrow \gamma\eta$ and $\eta \longrightarrow \gamma\gamma$ events are generated with JPIPI generator [22, 23] for $\psi(3686) \longrightarrow J/\psi\pi^+\pi^-$ and phase space generator for $J/\psi \longrightarrow \gamma\eta$ and $\eta \longrightarrow \gamma\gamma$.

3. Introduction of the Method

Usually, the $\psi(3686) \longrightarrow J/\psi\pi^+\pi^-$ is used to study J/ψ decay experimentally by calculating the branching fraction of $J/\psi \longrightarrow f$ (f denotes the studied final states) with formula

$$\mathscr{B}(J/\psi \longrightarrow f) = \frac{N^{\text{obs}}}{\epsilon \times N^{\text{tot}}_{\psi(3686)} \times \mathscr{B}(\psi(3686) \longrightarrow J/\psi\pi^+\pi^-)}, \quad (1)$$

where $\mathscr{B}$, N^{obs}, ϵ, and $N^{\text{tot}}_{\psi(3686)}$ represent the branching fraction, the number of observed events, the detection efficiency for the whole process ($\psi(3686) \longrightarrow J/\psi\pi^+\pi^-$) with $J/\psi \longrightarrow f$), and the total number of $\psi(3686)$ events. This is an indirect measurement, which replies on the input $\mathscr{B}(\psi(3686) \longrightarrow J/\psi\pi^+\pi^-)$. While an update measurement of $\mathscr{B}(\psi(3686) \longrightarrow J/\psi\pi^+\pi^-)$ is made, the $\mathscr{B}(J/\psi \longrightarrow f)$ should be updated accordingly.

To solve this problem, a tag method can be employed to determine the $\mathscr{B}(J/\psi \longrightarrow f)$, which is a direct measurement method. With the dominant $\psi(3686)$ decay channel, $\psi(3686) \longrightarrow J/\psi\pi^+\pi^-$, the J/ψ meson can be tagged with the two soft opposite charged pions. If the two pions are reconstructed correctly, there must be a J/ψ meson in the event, then the J/ψ decay can be studied. With this method, the branching fraction can be calculated directly by

$$\mathscr{B}(J/\psi \longrightarrow f) = \frac{N^{\text{obs}}}{\epsilon \times N^{\text{tag}}_{J/\psi}}, \quad (2)$$

where $N^{\text{tag}}_{J/\psi}$ is the number of tagged J/ψ mesons in $\psi(3686)$ sample and ϵ is the detection efficiency of $J/\psi \longrightarrow f$. In the following, we take the determination of $\mathscr{B}(J/\psi \longrightarrow \gamma\eta)$ as an example to illustrate and validate this method.

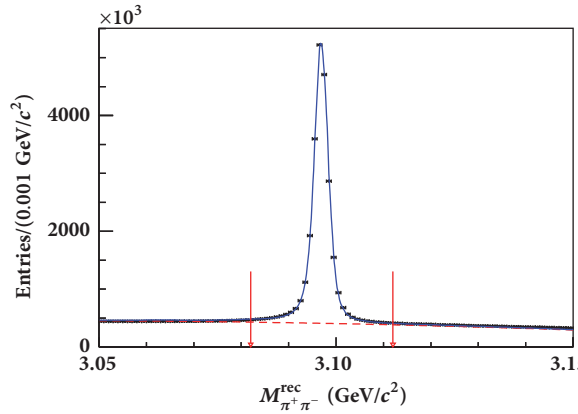

FIGURE 1: The $M^{\text{rec}}_{\pi^+\pi^-}$ spectra of candidate events from inclusive $\psi(3686)$ MC sample (the dots with error bars). The solid line shows the best fit to the spectra and the dashed line shows the background. The J/ψ signal region is shown between the two arrows.

4. General Track Selection

To be accepted as a good photon candidate, a neutral electromagnetic shower in the EMC must satisfy fiducial and shower-quality requirement. The good photon candidate showers reconstructed from the barrel EMC ($|\cos\theta| < 0.80$) must have a minimum energy of 25 MeV, while those in the end caps ($0.86 < |\cos\theta| < 0.92$) must have at least 50 MeV, where the energies deposited in nearby TOF counters are included. Showers in the region between the barrel and the end caps are poorly measured and excluded. To eliminate showers from charged particle, a photon candidate must be separated by at least 10° from any charged track. The time of EMC cluster (T_{EMC}) requirements is used to suppress electronic noise, which is $0 \le T_{\text{EMC}} \le 14$ (in unit of 50 ns).

Charged tracks in BESIII detector are reconstructed from MDC hits. Each charged track is required to satisfy $V_z < 10$ cm, $R_{xy} < 1$ cm and $|\cos\theta| < 0.93$, where V_z and R_{xy} are the closest approach to the beam axis in z direction and $x-y$ plane and θ is the polar angle.

5. Reconstruction of Tag Side

The two charged tracks in the tag side are required to satisfy $|\vec{p}| < 0.45$ GeV/c and $\cos\theta_{+-} < 0.95$, where $\vec{p}$ is the momentum of the candidate track and θ_{+-} is the angle between positive and negative charged tracks. The candidate tracks are assumed to be pions. The recoil mass of $\pi^+\pi^-$, $M^{\text{rec}}_{\pi^+\pi^-}$, is calculated by

$$M^{\text{rec}}_{\pi^+\pi^-} = \sqrt{(p_{\text{tot}} - p_{\pi^+} - p_{\pi^-})^2}, \quad (3)$$

where p_{tot}, p_{π^+}, and p_{π^-} are the four momenta of e^+e^-, π^+, and π^-. To reject the obvious background events, we only keep the events satisfying $3.03 < M^{\text{rec}}_{\pi^+\pi^-} < 3.17$ GeV/c^2. The $M^{\text{rec}}_{\pi^+\pi^-}$ spectra of candidate events are shown in Figure 1, which shows a clear J/ψ peak over a smooth background.

We fit the distribution of $M^{\text{rec}}_{\pi^+\pi^-}$ with the signal shape obtained from exclusive decay of $\psi(3686) \longrightarrow$

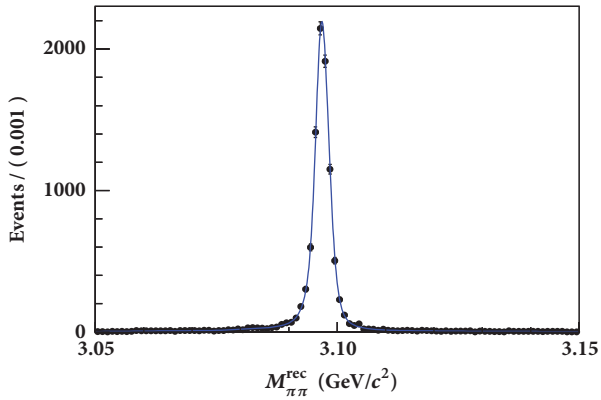

Figure 2: The $M^{rec}_{\pi^+\pi^-}$ spectra of the signal events from pure $\psi(3686) \longrightarrow J/\psi\pi^+\pi^-, J/\psi \longrightarrow \mu^+\mu^-$ sample (the dots with error bars) and the signal shape (the solid blue line).

$J/\psi\pi^+\pi^-, J/\psi \longrightarrow \mu^+\mu^-$, which is shown in Figure 2, and a polynomial background. In Figure 2, the dots with error bar show the distribution of $M^{rec}_{\pi^+\pi^-}$ from pure $\psi(3686) \longrightarrow J/\psi\pi^+\pi^-, J/\psi \longrightarrow \mu^+\mu^-$ MC events, and the solid line shows the extracted shape. Fitting the $M^{rec}_{\pi^+\pi^-}$ spectra of candidate events from 106 million inclusive $\psi(3686)$ MC samples with maximum likelihood method, the number of tagged J/ψ mesons can be obtained. The fitting results are shown in Figure 1, where the dots with error bar represent the numbers of events, the solid curve shows the total fitting result, and the dashed line shows the background. The fitting results given $(2.2515 \pm 0.0005) \times 10^7$ tagged J/ψ mesons. Considering the input $\mathcal{B}(\psi(3686) \longrightarrow J/\psi\pi^+\pi^-) = 32.6\%$, the tag efficiency is 65.2%.

To study the J/ψ decay in the recoil side, the $M^{rec}_{\pi^+\pi^-}$ is required to be located in J/ψ signal region, which is defined as from 3.082 to 3.112 GeV/c^2 according to the resolution of $M^{rec}_{\pi^+\pi^-}$ from the fitting. Integrating the signal distribution in the signal region, we obtain $(2.1120 \pm 0.0005) \times 10^7 J/\psi$ mesons.

6. Analysis of the J/ψ Decay

We choose the channel $J/\psi \longrightarrow \gamma\eta$ to study the validation of this method. The η meson is reconstructed with $\eta \longrightarrow \gamma\gamma$ and therefore there are three photons in the final states, one energetic radiative photon (denote by γ_1) and other two relative soft photons (denote by γ_2 and γ_3). Exactly three photons are required in each candidate event. For the energetic radiative photon, the deposited energy in EMC is required to be greater than 1.0 GeV in J/ψ rest frame. For the other two photons, the invariant mass of them ($M_{\gamma_2\gamma_3}$) is required to satisfy $0.45 < M_{\gamma_2\gamma_3} < 0.65$ GeV/c^2. To exclude the background from $\psi(3686) \longrightarrow \gamma\eta', \eta' \longrightarrow \eta\pi^+\pi^-$, the invariant mass of $\gamma_2\gamma_3$ and two soft pions ($M_{\gamma_2\gamma_3\pi^+\pi^-}$) is required to be greater than 1.0 GeV/c^2. A four-momentum constraint kinematic fit is performed to the candidate tracks and the χ^2 of the kinematic fit is required to be less than 40. The survived events are treated as $J/\psi \longrightarrow \gamma\eta$ candidates.

Table 1: The background of $J/\psi \longrightarrow \gamma\eta, \eta \longrightarrow \gamma\gamma$. N denotes the number of events passed from each decay chain.

decay chain	N
$\psi(3686) \longrightarrow J/\psi\pi^+\pi^-, J/\psi \longrightarrow \gamma\eta', \eta' \longrightarrow \gamma\gamma$	51
$\psi(3686) \longrightarrow J/\psi\pi^+\pi^-, J/\psi \longrightarrow \gamma\pi^0$	20
$\psi(3686) \longrightarrow J/\psi\pi^+\pi^-, J/\psi \longrightarrow \gamma f_4, f_4 \longrightarrow \pi^0\pi^0$	7
$\psi(3686) \longrightarrow \gamma_{FSR}e^+e^-\gamma_{FSR}$	1
$\psi(3686) \longrightarrow J/\psi\pi^+\pi^-, J/\psi \longrightarrow \gamma\eta\pi^0, \eta \longrightarrow \gamma\gamma$	1
$\psi(3686) \longrightarrow J/\psi\pi^+\pi^-, J/\psi \longrightarrow \gamma f_2, f_2 \longrightarrow \pi^0\pi^0$	1
$\psi(3686) \longrightarrow \gamma\eta', \eta' \longrightarrow \pi^+\pi^-\eta, \eta \longrightarrow \gamma\gamma$	1
$\psi(3686) \longrightarrow \pi^+\pi^-\pi^0\eta, \eta \longrightarrow \gamma\gamma$	1
$\psi(3686) \longrightarrow \pi^0 h_1, h_1 \longrightarrow \rho^+\pi^-, \rho^+ \longrightarrow \pi^+\pi^0$	1
$\psi(3686) \longrightarrow \rho^+ a_0^-, \rho^+ \longrightarrow \pi^+\pi^0, a_0^- \longrightarrow \pi^-\eta, \eta \longrightarrow \gamma\gamma$	1

Table 2: The input and output results.

	input	output
N^{tag}		$(2.1120 \pm 0.0005) \times 10^7$
N^{obs}		3399 ± 60
ϵ		$(41.49 \pm 0.39)\%$
$\mathcal{B}(J/\psi \longrightarrow \gamma\eta)$	9.8×10^{-4}	$(9.9 \pm 0.2) \times 10^{-4}$

The $M_{\gamma_2\gamma_3}$ spectra are examined to determine the number of signal events.

There are backgrounds from other decay channels. The MC truth information is used to study the background. Table 1 shows the decay chain of background channels for $J/\psi \longrightarrow \gamma\eta, \eta \longrightarrow \gamma\gamma$, and the number of background events from each channel is listed in the last column. The $M_{\gamma_2\gamma_3}$ spectra of background events are shown in Figure 3, where the signal region is between two arrows. The figure shows that there is no peak background contribution to $J/\psi \longrightarrow \gamma\eta$; the $\gamma_2\gamma_3$ spectra from background events can be described with smooth function.

7. Results

The $M_{\gamma_2\gamma_3}$ distribution from signal MC sample is shown in Figure 4 in dots with error bar, and the solid curve in the figure shows the probability density function extracted from the shape. The $M_{\gamma_2\gamma_3}$ spectra for the candidate events from inclusive $\psi(3686)$ sample are shown in Figure 5. We fit the spectra with the shape of $M_{\gamma_2\gamma_3}$ from signal MC sample to describe the signal and 1st order Chebychev polynomial to describe the background. The fitting results are shown in Figure 5, where the dots with error bars represent the number of events, the solid curve shows the total fit results, and the dashed line shows the background. The detection efficiency ϵ can be determined with signal MC sample, which is listed in the Table 2. Inserting the numbers into (2), considering the input $\mathcal{B}(\eta \longrightarrow \gamma\gamma) = 0.3925$, we can calculate $\mathcal{B}(J/\psi \longrightarrow \gamma\eta)$,

$$\mathcal{B}(J/\psi \longrightarrow \gamma\eta) = \frac{3399 \pm 60}{0.4149 \times 2.1120 \times 10^7 \times 0.3925} = (9.9 \pm 0.2) \times 10^{-4} \quad (4)$$

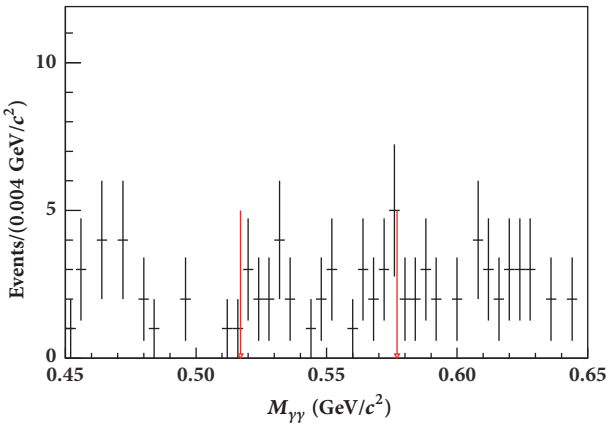

FIGURE 3: The $M_{\gamma_2\gamma_3}$ spectra of background events. The signal region of $M_{\gamma_2\gamma_3}$ is shown between the two arrows.

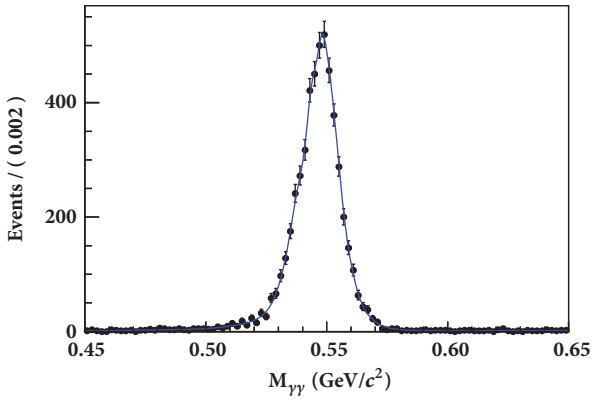

FIGURE 4: The $M_{\gamma_2\gamma_3}$ spectra of signal events from $J/\psi \longrightarrow \gamma\eta$ MC sample (dots with error bar) and the shape used to fit the $M_{\gamma_2\gamma_3}$ (solid blue line).

which is consistent with the input branching fraction 9.8×10^{-4}.

When considering the systematic uncertainty in the measurement of $J/\psi \longrightarrow \gamma\eta$, three sources, which are from the total number of $\psi(3686)$, the tracking efficiency of two soft pions, and the $\mathcal{B}(\psi(3686) \longrightarrow J/\psi\pi^+\pi^-)$, should be considered when the traditional method is used, but will not present in the tag method. The numbers for theses sources are 0.7% [26], 2.0% [27] in the BESIII experiment, and 0.9% [15], respectively. Therefore the total systematic uncertainty of the branching fraction measurement of this channel by using the tag method will be less than that of the traditional one.

8. Conclusion

In conclusion, we have developed a method to study the J/ψ decay with the $\psi(3686)$ data set. The two soft opposite charged pions from $\psi(3686) \longrightarrow J/\psi\pi^+\pi^-$ are used to tag the J/ψ meson. With the tagged J/ψ mesons from 106 million inclusive $\psi(3686)$ MC samples, the output branching fraction of $J/\psi \longrightarrow \gamma\eta$ is in good agreement with the input one, which gives a solid validation of this method. By employing this method, the J/ψ decay branching fractions can be precisely

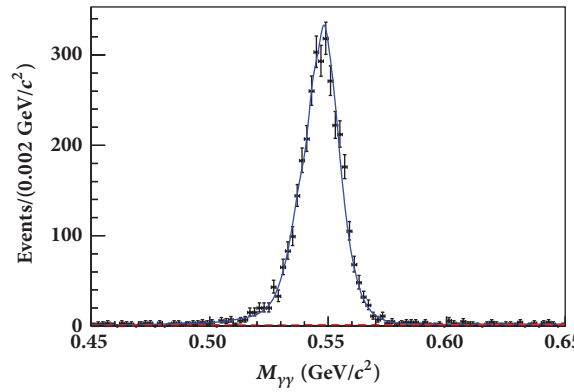

FIGURE 5: The $M_{\gamma_2\gamma_3}$ spectra of candidate events from 106 million inclusive $\psi(3686)$ MC samples (dots with error bar). The solid line shows the best fitting to the spectra and the dashed line shows the background.

measured absolutely with the large data set accumulated with BESIII and other detectors which will be run in charm energy region in the future [28] for the channels affected by interference effect or with undistinguishable background.

Data Availability

No data were used to support this study.

Conflicts of Interest

The authors declare that there are no conflicts of interest regarding the publication of this paper.

Acknowledgments

This work was partially supported by National Natural Science Foundation of China (Project Nos. 11575077 and 11475090), the Graduate Student Innovation Foundation (2018KYY033) and the Innovation Group of Nuclear and Particle Physics in USC.

References

[1] J. J. Aubert, U. Becker, P. J. Biggs et al., "Experimental Observation of a Heavy Particle J," *Physical Review Letters*, vol. 33, no. 23, p. 1404, 1974.

[2] J.-E. Augustin et al., "Discovery of a narrow resonance in e+e- annihilation," *Physical Review Letters*, vol. 33, no. 23, p. 1406, 1974.

[3] R. Brandelik, W. Braunschweig, H.-U. Martyn et al., "Results from DASP on e^+e^- annihilation between 3.1 and 5.2 GeV," *Zeitschrift für Physik C Particles and Fields*, vol. 1, no. 3, pp. 233–256, 1979.

[4] A. A. Zholentz, L. M. Kurdadze, M. Y. Lelchuk et al., "High precision measurement of the Ψ- and Ψ′-meson masses," *Physics Letters B*, vol. 96, no. 1-2, pp. 214–216, 1980.

[5] Y. Lemoigne, R. Barate, P. Bareyre et al., "Measurement of hadronic production of the χ1++(3507) and the χ2++(3553)

through their radiative decay to Jϕ," *Physics Letters B*, vol. 113, no. 6, pp. 509–512, 1982.

[6] C. Baglin, G. Bassompierre, J. C. Brient et al., "J/Ψ resonant formation and mass measurement in antiproton-proton annihilations," *Nuclear Physics B*, vol. 286, pp. 592–634, 1987.

[7] T. A. Armstrong et al., "Measurement of the J/ψ and ψ' resonance parameters in $\overline{p}p$ annihilation," *Physical Review D*, vol. 47, no. 3, p. 772, 1993.

[8] J. Z. Bai, G. P. Chen, H. F. Chen et al., "A measurement of Jψ decay widths," *Physics Letters B*, vol. 355, no. 1-2, pp. 374–380, 1995.

[9] A. Gribushin et al., "Production of J/ψ and ψ(2S) mesons in π− Be collisions at 515 GeV/c," *Physical Review D*, vol. 53, no. 6, p. 4723, 1996.

[10] A. S. Artamonov, S. E. Baru, A. E. Blinov et al., "High precision mass measurements in Ψ and ϒ families revisited," *Physics Letters B*, vol. 474, no. 3-4, pp. 427–429, 2000.

[11] V. M. Aulchenko, S. A. Balashov, E. M. Baldin et al., "New precision measurement of the J/ψ- and $\psi\prime$-meson masses," *Physics Letters B*, vol. 573, pp. 63–79, 2003.

[12] A. Bernard et al., "J/ψ production via initial state radiation in $e^+e^- \longrightarrow \mu^+\mu^-\gamma$ at an e^+e^- center-of-mass energy near 10.6 GeV," *Physical Review D*, vol. 69, no. 1, Article ID 011103(R), 2004.

[13] G. S. Adams et al., "Measurement of Γ_{ee}(J/ψ), Γ_{tot}(J/ψ), and $\Gamma_{ee}[\psi(2S)]/\Gamma_{ee}$(J/$\psi$)," *Physical Review D*, vol. 73, no. 5, Article ID 051103(R), 2006.

[14] V. V. Anashin, V. M. Aulchenko, E. M. Baldin et al., "Measurement of Γee(J/ψ)·B(J/$\psi \longrightarrow e^+e^-$) and Γee(J/$\psi$)·B(J/$\psi \longrightarrow \mu^+\mu^-$)," *Physics Letters B*, vol. 685, no. 2-3, pp. 134–140, 2010.

[15] M. Tanabashi et al., "Review of Particle Physics," *Physical Review D*, vol. 98, Article ID 030001, 2018.

[16] K. T. Chao and Y. F. Wang, "Physics at BES-III," *International Journal of Modern Physics A*, vol. 24, no. supp01, 2009.

[17] M. Ablikim, Z. H. An, J. Z. Bai et al., "Nuclear Instruments and Methods in Physics Research Section A: Accelerators, Spectrometers, Detectors and Associated Equipment," *Nuclear Instruments and Methods in Physics Research A*, vol. 614, no. 3, pp. 345–399, 2010.

[18] W. D. Li, "The BESIII offline software system," in *Proceedings of the International Conference on Computing in High Energy and Nuclear Physics*, vol. 225, 2006.

[19] G. Barrand, I. Belyaev, P. Binko et al., "GAUDI — A software architecture and framework for building HEP data processing applications," *Computer Physics Communications*, vol. 140, no. 1-2, pp. 45–55, 2001.

[20] S. Jadach, B. F. L. Ward, and Z. Was, "The precision Monte Carlo event generator KK for two-fermion final states in e^+e^- collisions," *Computer Physics Communications*, vol. 130, no. 3, pp. 260–325, 2000.

[21] S. Jadach, B. F. L. Ward, and Z. Wa, "Coherent exclusive exponentiation for precision Monte Carlo calculations," *Physical Review D*, vol. 63, no. 11, Article ID 113009, 2001.

[22] R. G. Ping, "Event generators at BESIII*," *Chinese Physics C*, vol. 32, no. 8, pp. 599–602, 2008.

[23] D. J. Lange, "The EvtGen particle decay simulation package," *Nuclear Instruments and Methods in Physics*, vol. 462, no. 1-2, pp. 152–155, 2001.

[24] J. C. Chen, G. S. Huang, X. R. Qi, D. H. Zhang, and Y. S. Zhu, "Event generator for J/ψ and $\psi(2S)$decay," *Physical Review D*, vol. 62, no. 3, Article ID 034003, 2000.

[25] R. L. Yang, R. G. Ping, and H. Chen, "Tuning and Validation of the Lundcharm Model with J/ψ Decays," *Chinese Physics Letters*, vol. 31, no. 6, Article ID 061301, 2014.

[26] M. Ablikim et al., "Determination of the number of ψ(3686) events at BESIII," *Chinese Physics C*, vol. 42, no. 2, Article ID 023001, 2018.

[27] M. Ablikim et al., "Measurements of $\psi(3686) \longrightarrow K^-\Lambda$ anti-Ξ^+ + c.c. and $\psi(3686) \longrightarrow \gamma\ K^-\Lambda$ anti- Ξ^+ + c.c," *Physical Review D*, vol. 91, no. 9, Article ID 092006, 2015.

[28] A. E. Bondar, "Project of a Super Charm-Tau factory at the Budker Institute of Nuclear Physics in Novosibirsk," *Physics of Atomic Nuclei*, vol. 76, no. 9, pp. 1072–1085, 2013.

Hindawi
Advances in High Energy Physics
Volume 2018, Article ID 5961031, 12 pages
https://doi.org/10.1155/2018/5961031

Research Article

S-Wave Heavy Quarkonium Spectra: Mass, Decays, and Transitions

Halil Mutuk

Physics Department, Faculty of Arts and Sciences, Ondokuz Mayis University, 55139 Samsun, Turkey

Correspondence should be addressed to Halil Mutuk; halilmutuk@gmail.com

Received 20 August 2018; Revised 18 October 2018; Accepted 30 October 2018; Published 25 November 2018

Guest Editor: Xian-Wei Kang

In this paper we revisited phenomenological potentials. We studied S-wave heavy quarkonium spectra by two potential models. The first one is power potential and the second one is logarithmic potential. We calculated spin averaged masses, hyperfine splittings, Regge trajectories of pseudoscalar and vector mesons, decay constants, leptonic decay widths, two-photon and two-gluon decay widths, and some allowed M1 transitions. We studied ground and 4 radially excited S-wave charmonium and bottomonium states via solving nonrelativistic Schrödinger equation. Although the potentials which were studied in this paper are not directly QCD motivated potential, obtained results agree well with experimental data and other theoretical studies.

1. Introduction

Heavy quarkonium is the bound state of $b\bar{b}$ and $c\bar{c}$ and one of the most important playgrounds for our understanding of the strong interactions of quarks and gluons. Quantum chromodynamics (QCD) is thought to be the *true* theory of these strong interactions. QCD is a nonabelian local gauge field theory with the symmetry group $SU(3)$. In principle, one should be able to calculate hadronic properties such as mass spectrum and transitions by using QCD principles. But QCD does not readily supply us these hadronic properties. This challenge can be attributed to the several features that are not present in other local gauge field theories.

Foremost, being a nonabelian gauge theory, gluons which are gauge bosons, have color charge and interact among themselves. Unlike from quantum electrodynamics (QED), where a photon does not interact with other photon, in QCD one must consider interactions among gluons. This nonabelian nature of the theory makes some calculations complicated, for example, loops in propagators.

There are three other important features of QCD: *asymptotic freedom*, *confinement,* and *dynamical breaking of chiral symmetry*. Asymptotic freedom says that strong interaction coupling constant, α_s, is a function of momentum transfer. When the momentum transfer in a quark-quark collision increases (at short distances), the coupling constant becomes weaker whereas it becomes larger when momentum transfer decreases (at large distances). The idea behind confinement is that, there are no free quarks outside of a hadron; i.e., color charged particles (quarks and gluons) cannot be isolated out of hadrons. Flux tube model gives a reasonable explanation of confinement. When the distance between quark-antiquark (or quarks) pair increases, the gluon field between a pair of color charges forms a flux tube (or string) between them resulting a potential energy which depends linearly on the distance, $V(r) =\sim \sigma r$ where σ is the string constant. As distance increases between quarks, the potential energy can create new quark-antiquark pairs in colorless forms instead of a free quark. Up to now, nobody has been able to prove that confinement from QCD. Lattice QCD calculations simulate this confinement well and give a value for the string tension [1]. The last feature of QCD is the dynamical breaking of chiral symmetry. The QCD Lagrangian with N quark flavor has an exact chiral $SU(N) \times SU(N)$ symmetry but breaks down to $SU(N)$ symmetry because of the nonvanishing expectation value of QCD vacuum [2, 3]. The Goldstone bosons corresponding to this symmetry breaking are the pseudoscalar mesons.

The present aspects of the QCD caused other approaches to deal with these challenges. QCD sum rules, Lattice QCD,

and potential models (quark models) are examples of these approaches. These approaches are nonperturbative since the strong interaction coupling constant, which should be the perturbation parameter of QCD is of the order one in low energies, hence the truncation of the perturbative expansion cannot be carried out. Since perturbation theory is not applicable, a nonperturbative approach has to be used to study systems that involve strong interactions. QCD sum rules and lattice QCD are based on QCD itself whereas in potential models, one assumes an interquark potential and solves a Schrödinger-like equation. The advantage of potential model is that, excited states can be studied in the framework of potential models whereas in QCD sum rules and lattice QCD, only the ground state or in some exceptional cases excited states can be studied.

After the discovery of charmonium ($c\overline{c}$) states, potential models have played a key role in understanding of heavy quarkonium spectroscopy [4, 5]. These potentials were in type of Coulomb plus linear confining potential with spin dependent interactions. The discovery of bottomonium ($b\overline{b}$) states were well described by the potential model picture which was used in the charmonium case. Heavy quarkonium spectroscopy was studied since that era with fruitful works [6–18]. A general review about potential models can be found in [19, 20] and references therein.

In the potential models, many features such as mass spectra and decay properties of heavy quarkonium could be described by an interquark potential in two-body Schrödinger equation. Interquark potentials are obtained both from phenomenology and theory. In the phenomenological method, it is assumed that a potential exist with some parameters to be determined by fits to the data. In the theory side, one can use perturbative QCD to determine the potential form at short distances and use lattice QCD at long distances [19]. These potentials can be classified as QCD motivated potentials [21–25] and phenomenological potentials [26–31]. The most commonly used phenomenological potentials are power-law potentials, for example [26] and logarithmic potentials, for example [30]. The detailed properties of these type potentials are studied extensively in [29]. All the potentials which are mentioned here have almost similar behaviour in the range of $0.1\ \text{fm} \leq r \leq 1\ \text{fm}$ which is characteristic region of charmonium and bottomonium systems [32, 33]. Outside the range, the behaviour of potentials differ. Up to now, no one was able to obtain a potential which is compatible at the whole range of distances by using QCD principles.

The potential model calculations have been quite successful in describing the hadron spectrum. Most of the phenomenological potentials must satisfy the following conditions:

$$\frac{dV}{dr} > 0, \qquad \frac{d^2V}{dr^2} \leq 0. \tag{1}$$

It means that static potential is a monotone nondecreasing and concave function of r which is a general property of gauge theories [34].

The great success of quarkonium phenomenology was somehow cracked at 2003 after the observation of $X(3872)$ [35]. The properties of this exotic particle are not compatible with the conventional quark model, the reason why it is named *exotic*. For example in [36], the authors studied $X(3872)$ near threshold zero in the $D^0\overline{D}^{*0}$ S-wave. There are other exotic states, XYZ, and the exotic particle zoo is growing. In this paper we will present some exotic states in the framework of quark model.

Energy spectra of heavy quarkonium are a rich source of the information on the nature of interquark forces and decay mechanisms. The prediction of mass spectrum in accordance with the experimental data does not verify the validity of a model for explaining hadronic interactions. Different potentials can produce reliable spectra with the experimental data. Thus other physical properties such as decay constants, leptonic decay widths, radiative decay widths, etc. need to be calculated.

A specific form of the QCD potential in the whole range of distances is not known. Therefore one needs to use potential models. In this work we revisited a power-law potential [26] and a logarithmic potential [30] to study S-wave heavy quarkonium. These potentials satisfy Eqn. (1), i.e. having nonsingular behaviour for $r \longrightarrow 0$. For our purposes, it must be mentioned that power-law and logarithmic potentials have nice scaling properties when used with a nonrelativistic Schrödinger equation [19]. We generated S-wave charmonium and bottomonium mass spectrum with the decays and M1 transitions. At Section 2 we give out theoretical model. In Sections 3 and 4, we generate S-wave heavy quarkonium spectrum, decays and transitions. In Section 5 we discuss our results and in Section 6 we conclude our results.

2. Formulation of the Model

When quark model was proposed, many authors treated baryons in detail with the harmonic oscillator quark model by using harmonic oscillator wave functions [37–39]. Mesons comparing to baryons are simpler objects since they are composites of two quarks. The reason for using harmonic oscillator wave function is that they form a complete set for a confining potential [40].

In order to obtain mass spectra, we solved Schrödinger equation by variational method. The variational method by using harmonic oscillator wave function gave successful results for heavy and light meson spectrum [15, 41, 42]. The procedure for this method is calculating expectation value of the Hamiltonian via the trial wave function:

$$E = \frac{\langle \Psi | H | \Psi \rangle}{\langle \Psi | \Psi \rangle}. \tag{2}$$

The mass of the meson is found by adding two times the mass of quark to the eigenenergy

$$M = 2m_q + E. \tag{3}$$

The Hamiltonian we consider is

$$H = M + \frac{p^2}{2\mu} + V(r) \tag{4}$$

Table 1: Spin-averaged mass spectrum of charmonium (in MeV).

State	Power	Logarithmic	[15]	[12]
1S	3067	3067	3067	3117
2S	3701	3655	3667	3684
3S	4054	3980	4121	4078
4S	4306	4204	4513	4407
5S	4504	4376	4866	

where $M = m_q + m_{\overline{q}}$, p is the relative momentum, μ is the reduced mass, and $V(r)$ is the potential between quarks. The spectrum can be obtained via solving Schrödinger equation

$$H\left|\Psi_n\right\rangle = E_n\left|\Psi_n\right\rangle \tag{5}$$

with the harmonic oscillator wave function defined as

$$\Psi_{nlm}(r,\theta,\phi) = R_{nl}(r)\,Y_{lm}(\theta,\phi). \tag{6}$$

Here R_{nl} is the radial wave function given as

$$R_{nl} = N_{nl} r^l e^{-\nu r^2} L^{l+1/2}_{(n-l)/2}\left(2\nu r^2\right) \tag{7}$$

with the associated Laguerre polynomials $L^{l+1/2}_{(n-l)/2}$ and the normalization constant

$$N_{nl} = \sqrt{\sqrt{\frac{2\nu^3}{\pi}}\frac{2\left((n-l)/2\right)!\nu^l}{\left((n+l)/2+1\right)!!}}. \tag{8}$$

$Y_{lm}(\theta,\phi)$ is the well-known spherical harmonics.

Armed with these, the expectation value of the given Hamiltonian can be calculated. In the variational method, one chooses a trial wave function depending on one or more parameters and then finds the values of these parameters by minimizing the expectation value of the Hamiltonian. It is a good tool for finding ground state energies but as well as energies of excited states. The condition for obtaining excited states energies is that the trial wave function should be orthogonal to all the energy eigenfunctions corresponding to states having a lower energy than the energy level considered. In (7), ν is treated as a variational parameter and it is determined for each state by minimizing the expectation value of the Hamiltonian.

In the following sections we study power-law and logarithmic potentials in order to obtain full spectrum.

3. Mass Spectra of Power-Law and Logarithmic Potentials

Power-law potential is given by [26]

$$V(r) = -8.064\ \text{GeV} + 6.898\ \text{GeV}\ r^{0.1}. \tag{9}$$

They showed that upsilon and charmonium spectra can be fitted with that potential. The small power of r refers to a situation in which the spacing of energy levels is independent of the quark masses. This situation is also valid for the purely logarithmic potential [30]

$$V(r) = -0.6635\ \text{GeV} + 0.733\ \text{GeV}\ \ln\left(r \times 1\ \text{GeV}\right). \tag{10}$$

At first step we obtained spin averaged mass spectrum for $c\overline{c}$ and $b\overline{b}$ systems, respectively. The constituent quark masses are $m_c = 1.8$ GeV and $m_b = 5.174$ GeV for power-law potential and $m_c = 1.5$ GeV and $m_b = 4.906$ GeV for logarithmic potential. Table 1 shows the charmonium spectrum and Table 2 shows the bottomonium spectrum.

Since the interquark potential does not contain the spin dependent part, (2) gives the spin averaged mass for the corresponding states. The calculated masses agree well with the available experimental data and with the values obtained from other theoretical studies. A general potential usually includes spin-spin interaction, spin-orbit interaction, and tensor force terms. To obtain whole picture, it is necessary to consider spin dependent terms within the potential. For $l \geq 1$, there are spin-orbit and tensor force terms which contribute to the fine structure. For equal mass m, the spin-orbit interaction is given by

$$V_{SO} = 2\frac{\alpha_s}{m_q^2 r^3}\left(3\left(\mathbf{S_1}+\mathbf{S_2}\right)\cdot\mathbf{L}\right) \tag{11}$$

and is responsible for the P wave splittings. Again for equal mass m, the tensor potential is given by

$$V_T = \frac{4}{3}\frac{\alpha_s}{m_q^2 r^3}\left(\frac{3\left(\mathbf{S_1}\cdot\mathbf{r}\right)\left(\mathbf{S_2}\cdot\mathbf{r}\right)}{r^2} - \mathbf{S_1}\cdot\mathbf{S_2}\right). \tag{12}$$

For $l = 0$, there is spin-spin term which we will consider in the present work. In the model of the spin averaged mass spectra discussion, all the spin dependent effects are ignored and hence it fails to take into account the splittings due to spin. For example, such splitting exist between the $\eta_c(1S)$ and J/ψ mesons by $\Delta m \simeq 110$ MeV. These mesons occupy the $l = 0$ level. The $c\overline{c}$ in the $\eta_c(1S)$ have $s = 0$, while in the J/ψ, $s = 1$. As a result of this, the mass difference should be related to spin dependent interaction.

3.1. Spin-Spin Interaction. Mass splitting is closely connected with the Lorentz-structure of the quark potential [45]. The origin of the spin-spin interaction term lies in the one-gluon exchange term which is related to $1/r$. Spin is proportional of the magnetic moment of a particle. Magnetic moments generate short range fields $\sim 1/r^3$. In the case of heavy quarkonium systems which are nonrelativistic, wave functions of two particles overlap in a significant amount. This means that particles are very close to each other. So spin-spin

Table 2: Spin-averaged mass spectrum of Bottomonium (in MeV).

State	Power	Logarithmic	[15]	[12]
1S	9473	9444	9443	9523
2S	10049	10033	9729	10035
3S	10384	10357	10312	10373
4S	10624	10581	10593	
5S	10813	10753	10840	
6S	10986	10964	11065	

Table 3: Charmonium mass spectrum (in MeV). In [18] LP denotes linear potential and SP denotes screened potential.

State	Exp. [43]	Power	Logarithmic	[13]	[11]	[18] LP	[18] SP
$\eta_c(1S)$	2984	2980	2954	2979	2982	2983	2984
$\eta_c(2S)$	3639	3624	3555	3623	3630	3635	3637
$\eta_c(3S)$		3983	3887	3991	4043	4048	4004
$\eta_c(4S)$		4240	4117	4250	4384	4388	4264
$\eta_c(5S)$		4441	4294	4446		4690	4459
J/ψ	3097	3096	3104	3097	3090	3097	3097
$\psi(2S)$	3686	3727	3689	3673	3672	3679	3679
$\psi(3S)$	4040	4078	4011	4022	4072	4078	4030
$\psi(4S)$		4328	4233	4273	4406	4412	4281
$\psi(5S)$		4525	4403	4463		4711	4472

interactions play a significant role in the dynamics. The *spin-spin* interaction term of two particles can be written as

$$V_{SS}(r) = \frac{32\pi\alpha_s}{9m_q m_{\overline{q}}} \mathbf{S_q} \cdot \mathbf{S_{\overline{q}}} \delta(\mathbf{r}). \tag{13}$$

This term can explain s wave splittings and has no contribution to $l \neq 0$ states. Putting this term into Schrödinger equation we get

$$E_{HF} = \frac{32\pi\alpha_s}{9m_q m_{\overline{q}}} \int d^3 r \Psi^{\star}(\mathbf{r}) \boldsymbol{\Psi}(\mathbf{r}) \delta(\mathbf{r}) \left\langle \mathbf{S_q} \cdot \mathbf{S_{\overline{q}}} \right\rangle. \tag{14}$$

Implementing Dirac-delta function property

$$\int f(x) \delta(x) dx = f(0), \tag{15}$$

we obtain

$$E_{HF} = \frac{32\pi\alpha_s}{9m_q m_{\overline{q}}} |\Psi(0)|^2 \left\langle \mathbf{S_q} \cdot \mathbf{S_{\overline{q}}} \right\rangle. \tag{16}$$

The matrix element of spin products can be obtained via

$$\mathbf{S}_1 \cdot \mathbf{S}_2 = \frac{1}{2}\left(\mathbf{S}^2 - \mathbf{S}_1^2 - \mathbf{S}_2^2\right) = \frac{1}{2}\left(S(S+1) - \frac{3}{2}\right) \tag{17}$$

so that

$$\left\langle \mathbf{S_q} \cdot \mathbf{S_{\overline{q}}} \right\rangle = \begin{cases} \frac{1}{4}, & \text{for } \overrightarrow{S} = 1 \\ -\frac{3}{4}, & \text{for } \overrightarrow{S} = 0. \end{cases} \tag{18}$$

Therefore we obtain hyperfine splittings energy as

$$E_{HF} = \begin{cases} \frac{8\pi\alpha_s}{9m_q m_{\overline{q}}} |\Psi(0)|^2, & \text{for } \overrightarrow{S} = 1 \\ -\frac{8\pi\alpha_s}{3m_q m_{\overline{q}}} |\Psi(0)|^2, & \text{for } \overrightarrow{S} = 0. \end{cases} \tag{19}$$

Here $\Psi(0)$ is the wave function at the origin and can be obtained by the following relation:

$$|\Psi(0)|^2 = \frac{\mu}{2\pi\hbar} \left\langle \frac{dV(r)}{dr} \right\rangle. \tag{20}$$

Expectation value is obtained by the wave function given in (6). S-wave charmonium and bottomonium masses can be seen in Tables 3 and 4. In this calculation, α_s is taken to be 0.37 for charmonium and 0.26 for bottomonium [15].

The mass differences are shown in Tables 5 and 6 for charmonium and bottomonium, respectively.

As can be seen from Tables 3, 4, 5, and 6 our results are compatible with both experimental and theoretical results.

The Regge trajectories for pseudoscalar and vector mesons are shown in Figures 1 and 2 for charmonium and in Figures 3 and 4 for bottomonium.

As can be seen from figures, Regge trajectories show nonlinear behaviour.

4. Dynamical Properties

4.1. Decay Constants. Leptonic decay constants give information about short distance structure of hadrons. In the experiments this regime is testable since the momentum transfer is very large. The pseudoscalar (f_p) and the vector

Table 4: Bottomonium mass spectrum (in MeV).

State	Exp. [43]	Power	Logarithmic	[14]	[18]	[44]	[16]
$\eta_b(1S)$	9399	9452	9420	9389	9390	9402	9455
$\eta_b(2S)$	9999	10030	10011	9987	9990	9976	9990
$\eta_b(3S)$		10367	10338	10330	10326	10336	10330
$\eta_b(4S)$		10608	10562	10595	10584	10623	
$\eta_b(5S)$		10798	10735	10817	10800	10869	
$\eta_b(6S)$		11005	10990	11011	10988	11097	
$\Upsilon(1S)$	9460	9480	9452	9460	9460	9465	9502
$\Upsilon(2S)$	10023	10055	10040	10016	10015	10003	10015
$\Upsilon(3S)$	10355	10393	10364	10351	10343	10354	10349
$\Upsilon(4S)$	10579	10629	10588	10611	10597	10635	10607
$\Upsilon(5S)$	10865	10818	10759	10831	10811	10878	10818
$\Upsilon(6S)$	11019	11019	11006	11023	10997	11102	10995

Table 5: Mass differences of S-wave charmonium states (in MeV).

State	Exp. [43]	Power	Logarithmic	[13]	[11]	[18] LP	[18] SP
J/ψ-$\eta_c(1S)$	113	116	150	118	108	114	113
$\psi(2S)$-$\eta_c(2S)$	47	103	134	50	42	44	42
$\psi(3S)$-$\eta_c(3S)$		95	124	31	29	30	26
$\psi(4S)$-$\eta_c(4S)$		88	116	23	22	24	17
$\psi(5S)$ - $\eta_c(5S)$		84	109	17		21	13

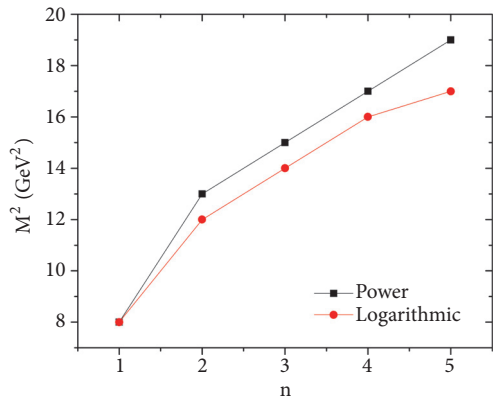

Figure 1: Regge trajectories of pseudoscalar charmonium in (n, M^2) plane. The polynomial fit is $M^2 = -0.397857\ n^2 + 5.04014\ n + 4.356$ (GeV^2) for power potential and $M^2 = -0.382143\ n^2 + 4.65786\ n + 4.55$ (GeV^2) for logarithmic potential.

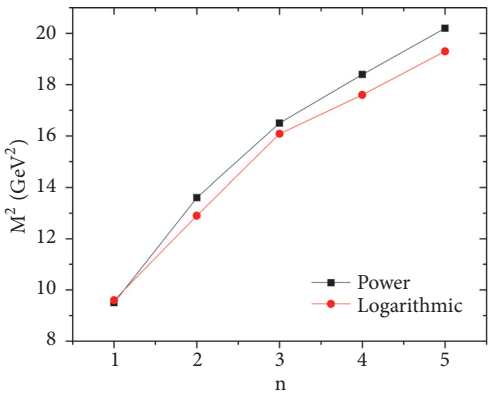

Figure 2: Regge trajectories of vector charmonium in (n, M^2) plane. The polynomial fit is $M^2 = -0.405\ n^2 + 5.091\ n + 4.986$ (GeV^2) for power potential and $M^2 = -0.403571\ n^2 + 4.80643\ n + 5.316$ (GeV^2) for logarithmic potential.

(f_v) decay constants are defined, respectively, through the matrix elements [12]

$$p^\mu f_p = i \left\langle 0 \left| \overline{\Psi} \gamma^\mu \gamma^5 \Psi \right| p \right\rangle \tag{21}$$

and

$$m_v f_v \epsilon^\mu = \left\langle 0 \left| \overline{\Psi} \gamma^\mu \Psi \right| v \right\rangle . \tag{22}$$

In the first relation, p^μ is meson momentum and $|p\rangle$ is pseudoscalar meson state. In the second relation, m_v is mass, ϵ^μ is the polarization vector, and $|v\rangle$ is the state vector of meson.

The matrix elements can be calculated by quark model wave function in the momentum space. The result is

$$f_p = \sqrt{\frac{3}{m_p}} \int \frac{d^3k}{(2\pi)^3} \sqrt{1 + \frac{m_q}{E_k}} \sqrt{1 + \frac{m_{\overline{q}}}{E_{\overline{k}}}} \left(1 - \frac{k^2}{\left(E_k + m_q\right)\left(E_{\overline{k}} + m_{\overline{q}}\right)} \right) \phi\left(\vec{k}\right) \tag{23}$$

Table 6: Mass differences of S-wave bottomonium states (in MeV).

State	Exp. [43]	Power	Log	[14]	[18]	[44]	[16]
$\Upsilon(1S)$-$\eta_b(1S)$	61	28	32	71	70	63	47
$\Upsilon(2S)$-$\eta_b(2S)$	24	25	29	29	25	27	25
$\Upsilon(3S)$-$\eta_b(3S)$		26	26	21	17	18	19
$\Upsilon(4S)$-$\eta_b(4S)$		21	26	16	13	12	
$\Upsilon(5S)$-$\eta_b(5S)$		20	24	14	11	9	
$\Upsilon(6S)$-$\eta_b(6S)$	14	16	12	9			

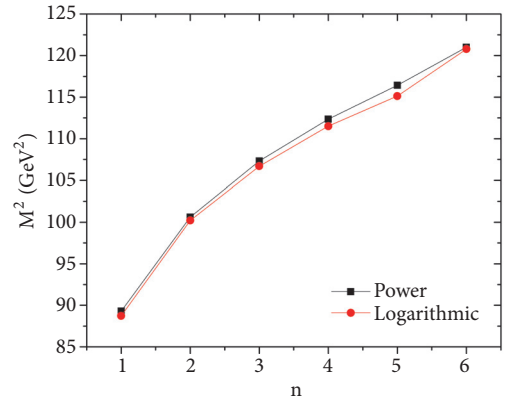

Figure 3: Regge trajectories of pseudoscalar bottomonium in (n, M^2) plane. The polynomial fit is $M^2 = -0.79\ \mathrm{n}^2 + 11.5586\ \mathrm{n} + 79.36\ (\mathrm{GeV}^2)$ for power potential and $M^2 = -0.636071\ \mathrm{n}^2 + 10.3054\ \mathrm{n} + 80.92\ (\mathrm{GeV}^2)$ for logarithmic potential.

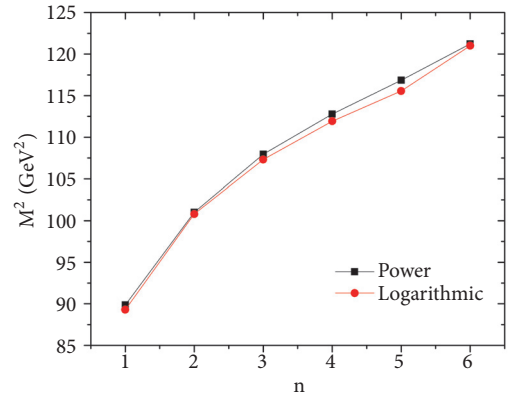

Figure 4: Regge trajectories of vector bottomonium in (n, M^2) plane. The polynomial fit is $M^2 = -0.809286\ \mathrm{n}^2 + 11.6401\ \mathrm{n} + 79.812\ (\mathrm{GeV}^2)$ for power potential and $M^2 = -0.7475\ \mathrm{n}^2 + 11.1579\ \mathrm{n} + 79.936\ (\mathrm{GeV}^2)$ for logarithmic potential.

for pseudoscalar meson and

$$f_v = \sqrt{\frac{3}{m_v}} \int \frac{d^3k}{(2\pi)^3} \sqrt{1 + \frac{m_q}{E_k}} \sqrt{1 + \frac{m_{\overline{q}}}{E_{\overline{k}}}} \left(1 + \frac{k^2}{3\left(E_k + m_q\right)\left(E_{\overline{k}} + m_{\overline{q}}\right)}\right) \phi\left(\vec{k}\right) \tag{24}$$

for the vector meson [12].

In the nonrelativistic limit, these two equations take a simple form which is known to be Van Royen and Weisskopf relation [46] for the meson decay constants

$$f_{p/v}^2 = \frac{12\left|\Psi_{p/v}(0)\right|^2}{m_{p/v}}. \tag{25}$$

The first-order correction which is also known as QCD correction factor is given by

$$\overline{f}_{p/v}^2 = \frac{12\left|\Psi_{p/v}(0)\right|^2}{m_{p/v}} C^2(\alpha_s) \tag{26}$$

where $C(\alpha_s)$ is given by [47]

$$C(\alpha_s) = 1 - \frac{\alpha_s}{\pi}\left(\Delta_{p/v} - \frac{m_q - m_{\overline{q}}}{m_q + m_{\overline{q}}} \ln \frac{m_q}{m_{\overline{q}}}\right). \tag{27}$$

Here $\Delta_p = 2$ for pseudoscalar mesons and $\Delta_v = 8/3$ for vector mesons. Decay constants are given in Tables 7 and 8 for pseudoscalar and vector mesons, respectively.

4.2. Leptonic Decay Widths. Leptonic decay of a vector meson with $J^{PC} = 1^{--}$ quantum numbers can be pictured by the following annihilation via a virtual photon

$$V\left(q\overline{q}\right) \longrightarrow \gamma \longrightarrow e^+e^-. \tag{28}$$

This state is neutral and in principle can decay into a different lepton pair rather than electron-positron pair. The above amplitude can be calculated by the Van Royen and Weisskopf relation [46]

$$\Gamma\left(n^3\mathrm{S}_1 \longrightarrow e^+e^-\right) = \frac{16\pi\alpha^2 e_q^2 \left|\Psi(0)\right|^2}{m_n^2} \times \left(1 - \frac{16\alpha_s}{3\pi} + \cdots\right), \tag{29}$$

where $\alpha = 1/137$ is the fine structure constant, e_q is the quark charge, m_n is the mass of $n^3\mathrm{S}_1$ state, and $|\Psi_{p/v}(0)|$ is the wave function at the origin of initial state. The term in the parenthesis is the first-order QCD correction factor while $\cdots$ represents higher corrections. The obtained values for leptonic decay widths can be found in Tables 9 and 10 for charmonium and bottomonium, respectively.

Table 7: Pseudoscalar decay constants (in MeV).

State	Exp. [43]	Power f_p	Power $\overline{f_p}$	Logarithmic f_p	Logarithmic $\overline{f_p}$	[15] f_p	[15] $\overline{f_p}$	[12]
$\eta_c(1S)$	335 ± 75	543	415	578	442	471	360	402
$\eta_c(2S)$		473	362	497	380	374	286	240
$\eta_c(3S)$		330	252	442	338	332	254	193
$\eta_c(4S)$		325	248	412	315	312	239	
$\eta_c(5S)$		253	193	387	304			
$\eta_b(1S)$		517	431	585	488	834	694	599
$\eta_b(2S)$		479	400	535	447	567	472	411
$\eta_b(3S)$		345	288	504	421	508	422	354
$\eta_b(4S)$		313	261	482	402	481	401	
$\eta_b(5S)$		283	236	465	388			
$\eta_b(6S)$		208	186	434	374			

Table 8: Vector decay constants (in MeV).

State	Exp. [43]	Power f_v	Power $\overline{f_v}$	Logarithmic f_v	Logarithmic $\overline{f_v}$	[15] f_p	[15] $\overline{f_p}$	[12]
J/ψ	335 ± 75	529	363	563	386	462	317	393
$\psi(2S)$	279 ± 8	463	318	487	334	369	253	293
$\psi(3S)$	174 ± 18	324	222	436	299	329	226	258
$\psi(4S)$		319	219	406	279	310	212	
$\psi(5S)$		248	170	382	262	290	199	
$\Upsilon(1S)$	708 ± 8	516	402	584	455	831	645	665
$\Upsilon(2S)$	482 ± 10	482	373	535	416	566	439	475
$\Upsilon(3S)$	346 ± 50	350	269	504	393	507	393	418
$\Upsilon(4S)$	325 ± 60	316	243	482	375	481	373	388
$\Upsilon(5S)$	369 ± 93	285	222	464	362	458	356	367
$\Upsilon(6S)$		241	203	442	354	439	341	

Table 9: Charmonium leptonic decay widths (in keV). The widths calculated with and without QCD corrections are denoted by $\Gamma_{l^+l^-}$ and $\Gamma^0_{l^+l^-}$.

	Power		Logarithmic		[13]		[15]		Exp. [43]
State	$\Gamma^0_{l^+l^-}$	$\Gamma_{l^+l^-}$	$\Gamma^0_{l^+l^-}$	$\Gamma_{l^+l^-}$	$\Gamma^0_{l^+l^-}$	$\Gamma_{l^+l^-}$	$\Gamma^0_{l^+l^-}$	$\Gamma_{l^+l^-}$	
J/ψ	3.435	1.277	3.154	1.173	11.8	6.60	6.847	2.536	$5.55 \pm 0.14 \pm 0.02$
$\psi(2S)$	2.880	1.071	2.362	0.878	4.29	2.40	3.666	1.358	2.33 ± 0.07
$\psi(3S)$	2.153	0.800	1.888	0.702	2.53	1.42	2.597	0.962	0.86 ± 0.07
$\psi(4S)$	1.839	0.684	1.642	0.610	1.73	0.97	2.101	0.778	0.58 ± 0.07
$\psi(5S)$	1.590	0.591	1.551	0.576	1.25	0.70	1.710	0.633	

Table 10: Bottomonium leptonic decay widths (in keV). The widths calculated with and without QCD corrections are denoted by $\Gamma_{l^+l^-}$ and $\Gamma^0_{l^+l^-}$.

	Power		Logarithmic		[25]		[15]		Exp. [43]
State	$\Gamma^0_{l^+l^-}$	$\Gamma_{l^+l^-}$	$\Gamma^0_{l^+l^-}$	$\Gamma_{l^+l^-}$	$\Gamma^0_{l^+l^-}$	$\Gamma_{l^+l^-}$	$\Gamma^0_{l^+l^-}$	$\Gamma_{l^+l^-}$	
$\Upsilon(1S)$	0.817	0.456	0.847	0.473	2.31	1.60	1.809	0.998	1.340 ± 0.018
$\Upsilon(2S)$	0.686	0.383	0.709	0.396	0.92	0.64	0.797	0.439	0.612 ± 0.011
$\Upsilon(3S)$	0.610	0.340	0.630	0.352	0.64	0.44	0.618	0.341	0.443 ± 0.008
$\Upsilon(4S)$	0.557	0.311	0.576	0.322	0.51	0.35	0.541	0.298	0.272 ± 0.029
$\Upsilon(5S)$	0.526	0.294	0.535	0.299	0.42	0.29	0.481	0.265	0.31 ± 0.07
$\Upsilon(6S)$	0.492	0.278	0.501	0.282	0.31	0.22	0.432	0.238	0.130 ± 0.030

4.3. Two-Photon Decay Width. $^1S_0$ states with $J^{PC} = 0^{-+}$ quantum number of charmonium and bottomonium can decay into two photons. In the nonrelativistic limit, the decay width for $^1S_0$ state can be written as [48]

$$\Gamma\left(^1S_0 \longrightarrow \gamma\gamma\right) = \frac{12\pi\alpha^2 e_q^4 |\Psi(0)|^2}{m_q^2} \times \left(1 - \frac{3.4\alpha_s}{\pi}\right). \quad (30)$$

The term in the parenthesis is the first-order QCD radiative correction. The results are listed in Table 11.

4.4. Two-Gluon Decay Width. Two-gluon decay width is given by [48]

$$\Gamma\left(^1S_0 \longrightarrow gg\right) = \frac{8\pi\alpha_s^2 |\Psi(0)|^2}{3m_q^2} \times \begin{cases} (1 + 4.8\alpha_s\pi) & \text{for } \eta_c \\ (1 + 4.4\alpha_s\pi) & \text{for } \eta_b. \end{cases} \quad (31)$$

The terms in the parenthesis refer to QCD corrections. The obtained results are given in Table 12.

4.5. M1 Transitions. M1 (magnetic dipole transition) decay widths can give more information about spin-singlet states. Moreover M1 transition rates show the validity of theory against experiment [11]. Magnetic transitions conserve both parity and orbital angular momentum of the initial and final states but in the M1 transitions the spin of the state changes. M1 width between two S-wave states is given by [51]

$$\Gamma\left(n^3S_1 \longrightarrow n'^1S_0 + \gamma\right) = \frac{4\alpha e_q^2 E_\gamma^3}{3m_q^2}\left(2J_f + 1\right)\left|\left\langle f\left|j_0\left(\frac{kr}{2}\right)\right|i\right\rangle\right|^2, \quad (32)$$

where $E_\gamma = (M_i^2 - M_f^2)/2M_i$ is the photon energy and $j_0(x)$ is the zeroth-order spherical Bessel function. In the case of small E_γ, spherical Bessel function $j_0(kr/2)$ tends to 1, $j_0(kr/2) \longrightarrow 1$. Thus transitions between the same principal quantum numbers, $n' = n$, are favored and usually known to be *allowed*. In the other case, when $n' \neq n$ the overlap integral between initial and final state is 0 and generally designated as *forbidden* transitions. The obtained transition rates for the allowed ones of S-wave charmonium and bottomonium states are given in Tables 13 and 14, respectively.

5. Results and Discussion

In the present paper we studied S-wave heavy quarkonium spectra with two phenomenological potentials. We have computed spin averaged masses, hyperfine splittings, Regge trajectories for pseudoscalar and vector mesons, decay constants, leptonic decay widths, two-photon and gluon decay widths, and allowed M1 partial widths of S-wave heavy quarkonium states.

In general, most of the quark model potentials tend to be similar, having a Coulomb term and a linear term. For example, in [11] they used standard color Coulomb plus linear scalar form, and also included a Gaussian smeared contact hyperfine interaction in the zeroth-order potential. In [13], the authors used a nonrelativistic potential model with screening effect. In [18] nonrelativistic linear potential and screened potential, in [14, 16, 44] a modified of nonrelativistic potential models and in [15] Hulthen potential are used. Potential models give reliable results with the appropriate parameters in the model. Therefore, the shape of the potential at the limits $r \longrightarrow 0$ and $r \longrightarrow \infty$ have similar behaviours.

Spin averaged mass spectra give idea about the formulation of model since the results are close to experimental values due to contributions from spin dependent interactions are small compared to contribution from potential part. If one ignores all spin dependent interactions, obtained results under this assumption are thought to be averages over related spin states for principal quantum number. Including hyperfine interaction, we obtained the mass spectra for pseudoscalar and vector mesons. The obtained spectra for both charmonium and bottomonium are in good agreement with the experimentally observed spectra and other theoretical studies.

Both power and logarithmic potentials produced approximately same mass differences and are in agreement with experiment for the lowest state in charmonium sector. But for the highest states, the shift is not compatible with the references. The reason for this should be the behaviour of linear part of the potential. In the case of bottomonium sector, mass differences of both power and logarithmic potentials are in accord with the given studies except the lowest state.

The fundamental point in the Regge trajectories is that they can predict masses of unobserved states. For the hadrons constituting of light quarks, the Regge trajectories are approximately linear but for the heavy quarkonium case Regge trajectories can be nonlinear. In the present work, we found that all Regge trajectories show nonlinear properties.

The decay constants are calculated for pseudoscalar and vector mesons by equating their field theoretical definition with the analogous quark model potential definition. This is valid in the nonrelativistic and weak binding limits where quark model state vectors form good representations of the Lorentz group [52, 53]. For pseudoscalar mesons, the corrected value of power and logarithmic potentials are a few MeV above than the available experimental data. For the rest of the pseudoscalar mesons, obtained results are compatible with other studies. In the case of vector mesons, logarithmic potential gave higher values than power potential. In the Υ meson, when the radially states are excited, both two potential gave similar results within the error of experimental value. Computations of the vector decay constant beyond the weak binding limit can be important in the quark potential model frame and need more elaboration [12].

Obtained leptonic decay widths are comparable with the experimental values and other theoretical studies. The QCD corrected factors are more close to experimental values for power and logarithmic potential and this can be referred as the importance of the QCD correction factor in calculating

Table 11: Two-photon decay widths (in keV). The widths calculated with and without QCD corrections are denoted by $\Gamma_{\gamma\gamma}$ and $\Gamma^0_{\gamma\gamma}$.

	Power		Logarithmic		[15]		[8]	[12]	Exp. [43]
State	$\Gamma^0_{\gamma\gamma}$	$\Gamma_{\gamma\gamma}$	$\Gamma^0_{\gamma\gamma}$	$\Gamma_{\gamma\gamma}$	$\Gamma^0_{\gamma\gamma}$	$\Gamma_{\gamma\gamma}$	$\Gamma_{\gamma\gamma}$	$\Gamma_{\gamma\gamma}$	
$\eta_c(1S)$	1.10	0.664	1.450	0.869	11.17	6.668	3.69	7.18	$7.2 \pm 0.7 \pm 0.2$
$\eta_c(2S)$	0.987	0.592	1.291	0.774	8.48	5.08	1.4	1.71	
$\eta_c(3S)$	0.907	0.543	1.184	0.710	7.57	4.53	0.930	1.21	
$\eta_c(4S)$	0.847	0.508	1.105	0.662			0.720		
$\eta_c(5S)$	0.801	0.480	1.044	0.620					
$\eta_b(1S)$	0.277	0.199	0.277	0.199	0.58	0.42	0.214	0.45	
$\eta_b(2S)$	0.212	0.153	0.246	0.177	0.29	0.20	0.121	0.11	
$\eta_b(3S)$	0.195	0.142	0.226	0.162	0.24	0.17	0.09	0.063	
$\eta_b(4S)$	0.188	0.136	0.211	0.151			0.07		
$\eta_b(5S)$	0.176	0.129	0.199	0.143					
$\eta_b(6S)$	0.164	0.116	0.182	0.134					

Table 12: Two-gluon decay widths (in MeV). The widths calculated with and without QCD corrections are denoted by Γ_{gg} and Γ^0_{gg}.

	Power		Logarithmic		[15]		[49]	Exp. [43]
State	Γ^0_{gg}	Γ_{gg}	Γ^0_{gg}	Γ_{gg}	Γ^0_{gg}	Γ_{gg}	Γ^0_{gg}	Γ_{gg}
$\eta_c(1S)$	32.04	50.15	41.93	32.44	50.82	66.68	15.70	26.7 ± 3.0
$\eta_c(2S)$	28.55	44.70	37.32	24.64	38.61	5.08	8.10	14 ± 7
$\eta_c(3S)$	26.22	41.04	34.23	53.59	21.99			
$\eta_c(4S)$	24.50	38.35	31.96	50.03				
$\eta_c(5S)$	23.15	36.24	30.18	47.24				
$\eta_b(1S)$	5.50	7.50	12.82	17.49	13.72	18.80	11.49	
$\eta_b(2S)$	4.90	6.69	11.41	15.56	6.73	9.22	5.16	
$\eta_b(3S)$	4.50	6.14	10.46	14.28	5.58	7.64	3.80	
$\eta_b(4S)$	4.20	5.74	9.77	13.33				
$\eta_b(5S)$	3.97	5.42	9.22	12.58				
$\eta_b(6S)$	3.62	5.18	8.68	10.86				

Table 13: Radiative M1 decay widths of charmonium. In [18] LP stands for linear potential and SP stands for screened potential.

Initial	Final	Power		Logarithmic		[15]	[18]		Exp. [43]
		E_γ (MeV)	Γ (keV)	E_γ (MeV)	Γ (keV)	Γ (keV)	Γ_{LP} (keV)	Γ_{SP} (keV)	Γ (keV)
J/ψ	$\eta_c(1S)$	114.9	1.96	113.8	2.83	3.28	2.39	2.44	1.13 ± 0.35
$\psi(2S)$	$\eta_c(2S)$	111.5	1.39	101.5	2.01	1.45	0.19	0.19	
$\psi(3S)$	$\eta_c(3S)$	93.8	1.10	93.8	1.59		0.051	0.088	
$\psi(4S)$	$\eta_c(4S)$	87.1	0.88	87.1	1.27				
$\psi(5S)$	$\eta_c(5S)$	83.2	0.74	83.2	1.10				

Table 14: Radiative M1 decay widths of bottomonium.

Initial	Final	Power		Logarithmic		[10]	[44]	[16]	Exp. [43]
		E_γ (MeV)	Γ (eV)	E_γ (MeV)	Γ (eV)	Γ (eV)	Γ (eV)	Γ (eV)	Γ (eV)
$\Upsilon(1S)$	$\eta_b(1S)$	27.9	0.88	31.9	1.46	5.8	10	9.34	
$\Upsilon(2S)$	$\eta_b(2S)$	24.9	0.62	28.9	1.09	1.4	0.59	0.58	
$\Upsilon(3S)$	$\eta_b(3S)$	25.9	0.54	25.9	0.78	0.8	0.25	0.66	
$\Upsilon(4S)$	$\eta_b(4S)$	20.9	0.37	20.9	0.41				
$\Upsilon(5S)$	$\eta_b(5S)$	19.9	0.32	19.9	0.35				
$\Upsilon(6S)$	$\eta_b(6S)$	14.3	0.29	14.4	0.27				

Table 15: Exotic states. Experimental data are taken from [43] unless stated. The units for mass and strong decays are in MeV and two-photon decay is in keV.

	Mass			Strong decay			Two-photon decay		
	Power	Logarithmic	Experiment	Power	Logarithmic	Experiment	Power	Logarithmic	Experiment
$X(3940)$			$3942^{+7}_{-6} \pm 6$			$37^{+26}_{-15} \pm 8$			
$\eta_c(3S)$	3983	3887		41.04	53.59		0.543	0.710	
$X(4160)$			4191 ± 5			70 ± 10			0.48 ± 0.22 [50]
$\eta_c(4S)$	4240	4117		38.35	50.03		0.508	0.612	
$\psi(4415)$			4421 ± 4			62 ± 20			0.58 ± 0.07
$\eta_c(5S)$	4441	4297		36.24	47.24		0.480	0.620	

the decay constants and other short range phenomena using potential models.

$^1S_0$ levels of charmonium and bottomonium states can decay into two photons or gluons. Especially two- photon decays of these levels are important for understanding the accuracy of theoretical models. Obtained results are smaller than the nonrelativistic widths including the one-loop QCD correction factor. For example, results of power and logarithmic potentials in $\eta_c(1S)$ are not in accord with experimental data. The reason of these differences can be due to the static potential between quarks that we used in the solution of two-body Schrödinger equation. For higher states, power and logarithmic potentials results are comparable with other studies. Two-photon decays are complicated processes such as pseudoscalar meson decay to two photons is governed by an intermediate vector meson followed by a meson dominance transition to a photon [12]. These schematic diagrams must be added to calculations to obtain a whole picture. For two-gluon decay widths, two phenomenological potentials gave comparable results with the available experimental data. Notice that in some cases QCD corrected factor is in accord with the experimental data whereas in some cases it is not. The reason for this can be that, there are significant radiative corrections from three-gluon decays so computing only two-gluon decay width could not explain the mechanism in all details.

Finally M1 transitions are calculated. The M1 radiative decay rates are very sensitive to relativistic effects. Even for allowed transitions relativistic and nonrelativistic results differ significantly. An important example is the decay of $J/\psi \longrightarrow \eta_c\gamma$. The nonrelativistic predictions for its rate are more than two times larger than the experimental data [10]. In the charmonium sector, the available experimental data for $J/\psi \longrightarrow \eta_c(1S)$ is comparable with the power potential result, while logarithmic potential result is 1 eV higher. In the bottomonium sector, there is no experimental data available on M1 transitions. Since photon energies and transition rates are very small, the detection of these transitions is an objection. And this can be a reason why no spin-singlet S-wave levels $\eta_b(n^1S_0)$ have been observed yet [10]. The obtained values for M1 transitions are comparable with the references.

Some states in the charmonium and bottomonium sector show properties different from the conventional quarkonium state. Some examples are $X(3940)$, $X(4160)$, and $\psi(4415)$. For $X(3940)$, there is not much available experimental data and more is needed. Wang et al. studied two-body open charm OZI-allowed strong decays of $X(3940)$ and $X(4160)$ considered as $\eta_c(3S)$ and $\eta_c(4S)$, respectively, by the improved Bethe-Salpeter method combined with the $^3P_0$ [54]. They calculated strong decay width of $X(3940)$ as $\Gamma = (33.5^{+18.4}_{-15.3})$ MeV and $X(4160)$ as $\Gamma = (69.9^{+22.4}_{-21.1})$ MeV where the experimental values are $\Gamma = (37^{+26}_{-15} \pm 8)$ MeV for $X(3940)$ and $\Gamma = (70 \pm 10)$ MeV for $X(4160)$ [43]. They concluded that $\eta_c(3S)$ is a good candidate of $X(3940)$ and $\eta_c(4S)$ is a not good candidate of $X(4160)$ due to larger decay width of $\Gamma(D\overline{D}^*)/\Gamma(D^*\overline{D}^*)$ comparing to experimental data. We give our results comparing to these exotic states in Table 15.

Looking at Table 15, we can deduce that, according to our model and results, we can assign $X(3940)$ as $\eta_c(3S)$, $X(4160)$ as $\eta_c(4S)$, and $\psi(4415)$ as $\eta_c(5S)$. To be more accurate, more data is needed to corroborate whether these states are conventional quarkonium or not.

6. Conclusions

Quark potential models have been very successful to study on various properties of mesons. The short distance behaviour of interquark potential appears to be similar where QCD perturbation theory can be applied where at large distance the potential is linear in r where nonperturbative methods are need to be used. The improvements on the potentials can be made and spin-spin, spin-orbit type interactions can be added to model to arrive high accuracy. The potential model approach is a valuable task, which has given to us many insights into the nature of both heavy and light quarkonium physics. Using a relativistic approach together with a model in which $B\overline{B}$ and $D\overline{D}$ thresholds are taken into account, detailed analysis can be made on various aspects of heavy quarkonium.

Data Availability

No data were used to support this study.

Conflicts of Interest

The author declares that they have no conflicts of interest.

References

[1] T. Kawanai and S. Sasaki, "Charmonium potential from full lattice QCD," *Physical Review D: Particles, Fields, Gravitation and Cosmology*, vol. 85, no. 9, 2012.

[2] A. Le Yaouanc, L. Oliver, O. Pène, and J. C. Raynal, "Spontaneous breaking of chiral symmetry for confining potentials," *Physical Review D: Particles, Fields, Gravitation and Cosmology*, vol. 29, no. 6, pp. 1233–1257, 1984.

[3] S. Bolognesi, K. Konishi, M. Shifman, and D. Phys. Rev, "Patterns of symmetry breaking in chiral QCD," *Physical Review D, Covering Particles, Fields, Gravitation, and Cosmology*, vol. 97, no. 9, Article ID 094007, 2018.

[4] T. Appelquist and H. D. Politzer, " Heavy Quarks and ," *Physical Review Letters*, vol. 34, no. 1, pp. 43–45, 1975.

[5] A. De Rújula and S. L. Glashow, "Is bound charm found?" *Physical Review Letters*, vol. 34, no. 1, pp. 46–49, 1975.

[6] E. Eichten, K. Gottfried, T. Kinoshita, K. D. Lane, and T. M. Yan, "Interplay of confinement and decay in the spectrum of charmonium," *Physical Review Letters*, vol. 36, p. 500, 1976.

[7] D. P. Stanley and D. Robson, "Nonperturbative potential model for light and heavy quark-antiquark systems," *Physical Review D: Particles, Fields, Gravitation and Cosmology*, vol. 21, no. 11, pp. 3180–3196, 1980.

[8] S. Godfrey and N. Isgur, "Mesons in a relativized quark model with chromodynamics," *Physical Review D: Particles, Fields, Gravitation and Cosmology*, vol. 32, no. 1, pp. 189–231, 1985.

[9] L. P. Fulcher, "Matrix representation of the nonlocal kinetic energy operator, the spinless Salpeter equation and the Cornell potential," *Physical Review D*, vol. 50, p. 447, 1994.

[10] D. Ebert, R. N. Faustov, and V. O. Galkin, " Properties of heavy quarkonia and ," *Physical Review D: Particles, Fields, Gravitation and Cosmology*, vol. 67, no. 1, 2003.

[11] T. Barnes, S. Godfrey, and E. S. Swanson, "Higher charmonia," *Physical Review D: Particles, Fields, Gravitation and Cosmology*, vol. 72, article 054026, 2005.

[12] O. Lakhina and E. S. Swanson, "Dynamic properties of charmonium," *Physical Review D*, vol. 74, 2006.

[13] B. Q. Li and K. T. Chao, "Higher charmonia and X, Y, Z states with screened potential," *Physical Review D: Particles, Fields, Gravitation and Cosmology*, vol. 79, Article ID 013011, 2009.

[14] B. Q. Li and K. T. Chao, "Bottomonium Spectrum with Screened Potential," *Communications in Theoretical Physics*, vol. 52, pp. 653–661, 2009.

[15] K. B. V. K. Bhaghyesh and A. P. Monteiro, "Heavy quarkonium spectra and its decays in a nonrelativistic model with Hulthen potential," *Journal of Physics G: Nuclear and Particle Physics*, vol. 38, Article ID 085001, 2011.

[16] J. Segovia, P. G. Ortega, D. R. Entem, and F. Fernandez, "Bottomonium spectrum revisited," *Physical Review D*, vol. 93, 2016.

[17] S. Godfrey, K. Moats, and E. S. Swanson, "B and B_s meson spectroscopy," *Physical Review D: Particles, Fields, Gravitation and Cosmology*, vol. 94, no. 5, 2016.

[18] W.-J. Deng, H. Liu, L.-C. Gui, and X.-H. Zhong, "Spectrum and electromagnetic transitions of bottomonium," *Physical Review D: Particles, Fields, Gravitation and Cosmology*, vol. 95, Article ID 074002, 2017.

[19] D. B. Lichtenberg, "Excited quark production at Hadron colliders," *International Journal of Modern Physics A*, vol. 2, no. 6, pp. 1669–1705, 1987.

[20] N. Brambilla, *Quarkonium Working Group*, CERN Yellow Report, 2005, arXiv:hep-ph/0412158.

[21] E. Eichten, K. Gottfried, T. Kinoshita, J. Kogut, K. D. Lane, and T.-M. Yan, "Spectrum of charmed quark-antiquark bound states," *Physical Review Letters*, vol. 34, no. 6, pp. 369–372, 1975.

[22] J. Richardson, "The heavy quark potential and the Υ, J/ψ systems," *Physics Letters B*, vol. 82B, p. 272, 1979.

[23] Y.-Q. Chen and Y.-P. Kuang, "Improved QCD-motivated heavy-quark potentials with explicit Λ_{MS} dependence," *Physical Review D*, vol. 46, p. 1165, 1992.

[24] Y.-Q. Chen and Y.-P. Kuang, "Erratum: "Improved QCD-motivated heavy-quark potentials with explicit Λ_{MS} dependence"," *Physical Review D: Particles, Fields, Gravitation and Cosmology*, vol. 47, p. 35, 1993.

[25] V. Khruschev, V. Savrin, and S. Semenov, "On the parameters of the QCD-motivated potential in the relativistic independent quark model," *Physics Letters B*, vol. 525, no. 3-4, pp. 283–288, 2002.

[26] A. Martin, "A simultaneous fit of bb, cc, ss (bcs Pairs) and cs spectra," *Physics Letters B*, vol. 100, p. 511, 1981.

[27] M. Machacek and Y. Tomozawa, "ψ Phenomenology and the nature of quark confinement," *Annals of Physics*, vol. 110, p. 407, 1978.

[28] G. Fogleman, D. B. Lichtenberg, and J. G. Wills, "Heavy-meson spectra calculated with a one-parameter potential," *Lettere al Nuovo Cimento*, vol. 26, p. 369, 1979.

[29] C. Quigg and J. L. Rosner, "Quantum mechanics with applications to quarkonium," *Physics Reports*, vol. 56, no. 4, pp. 167–235, 1979.

[30] C. Quigg and J. L. Rosner, "Quarkonium level spacings," *Physics Letters B*, vol. 71B, pp. 153–157, 1977.

[31] S. Xiaotong and L. Hefen, "A new phenomenological potential for heavy quarkonium," *Zeitschrift für Physik C Particles and Fields*, vol. 34, no. 2, pp. 223–231, 1987.

[32] C. Quigg, H. B. Thacker, and J. L. Rosner, "Constructive evidence for flavor independence of the quark-antiquark potential," *Physical Review D: Particles, Fields, Gravitation and Cosmology*, vol. 21, Article ID 3393, p. 234, 1980.

[33] W. Buchmüller, Y. Jack Ng, and S.-H. H. Tye, "Hyperfine splittings in heavy-quark systems," *Physical Review D: Particles, Fields, Gravitation and Cosmology*, vol. 24, no. 12, pp. 3312–3314, 1981.

[34] C. Bachas, "Concavity of the quarkonium potential," *Physical Review D: Particles, Fields, Gravitation and Cosmology*, vol. 33, no. 9, pp. 2723–2725, 1986.

[35] S. K. Choi, "Belle collaboration," *Physical Review Letters*, vol. 91, Article ID 262001, 2003.

[36] X.-W. Kang and J. A. Oller, "Different pole structures in line shapes of the X(3872)," *The European Physical Journal C*, vol. 77, no. 6, 2017.

[37] R. R. Horgan, "The construction and classification of wavefunctions for the harmonic oscillator model of three quarks," *Journal of Physics G: Nuclear Physics*, vol. 2, p. 625, 1976.

[38] N. Isgur and G. Karl, "P-wave baryons in the quark model," *Physical Review D: Particles, Fields, Gravitation and Cosmology*, vol. 18, no. 11, pp. 4187–4205, 1978.

[39] A. W. Hendry, "Decays of high spin Δ^* and N^* resonances in the quark model," *Annals of Physics*, vol. 140, no. 65, 1982.

[40] A. W. Hendry and D. B. Lichtenberg, "Properties of hadrons in the quark model," *Fortschritte der Physik/Progress of Physics banner*, vol. 33, no. 3, pp. 139–231, 1985.

[41] K. B. V. Kumar, B. Hanumaiah, and S. Pepin, "Meson spectrum in a relativistic harmonic model with instanton-induced interaction," *The European Physical Journal A - Hadrons and Nuclei*, vol. 19, no. 9, p. 247, 2004.

[42] K. B. V. Kumar, M. Y.-L. Bhavyashri, and A. P. Monteiro, "P-wave meson spectrum in a relativistic model with instanton induced interaction," *International Journal of Modern Physics A*, vol. 24, 2009.

[43] M. Tanabashi, "Particle Data Group," *Physical Review D: Particles, Fields, Gravitation and Cosmology*, vol. 98, Article ID 030001, 2018.

[44] S. Godfrey and K. Moats, " Erratum: ," *Physical Review D: Particles, Fields, Gravitation and Cosmology*, vol. 92, no. 11, 2015.

[45] V. Lengyel, Y. Fekete, I. Haysak, and A. Shpenik, "Calculation of hyperfine splitting in mesons using configuration interaction approach," *The European Physical Journal C*, vol. 21, no. 2, pp. 355–359, 2001.

[46] R. Van Royen and V. F. Weisskopf, "Protsyessy raspada adronov i modyel cyrillic small soft sign kvarkov," *Il Nuovo Cimento A*, vol. 50, no. 3, pp. 617–645, 1967.

[47] E. Braaten and S. Fleming, "QCD radiative corrections to the leptonic decay rate of the B_c meson," *Physical Review D*, vol. 52, p. 181, 1995.

[48] W. Kwong, P. B. Mackenzie, R. Rosenfeld, and J. L. Rosner, "Quarkonium annihilation rates," *Physical Review D: Particles, Fields, Gravitation and Cosmology*, vol. 37, no. 11, pp. 3210–3215, 1988.

[49] J. T. Laverty, S. F. Radford, and W. W. Repko, "\ga\ga and g g decay rates for equal mass heavy quarkonia," *High Energy Physics - Phenomenology*, 2009, arXiv:hep-ph/0901.3917v3.

[50] M. Ablikim, J. Z. Bai, Y. Ban, X. Cai, H. F. Chen, and H. S. Chen, "Determination of the $\psi(3770)$, $\psi(4040)$, $\psi(4160)$ and $\psi(4415)$ resonance parameters," *Physics Letters B*, vol. 660, no. 3, pp. 315–319, 2008.

[51] E. Eichten, K. Gottfried, T. Kinoshita, K. D. Lane, and T. -. Yan, "Charmonium: The model," *Physical Review D: Particles, Fields, Gravitation and Cosmology*, vol. 17, no. 11, pp. 3090–3117, 1978.

[52] C. Hayne and N. Isgur, "Beyond the wave function at the origin: Some momentum-dependent effects in the nonrelativistic quark model," *Physical Review D: Particles, Fields, Gravitation and Cosmology*, vol. 25, no. 7, pp. 1944–1950, 1982.

[53] N. Isgur, D. Scora, B. Grinstein, and M. B. Wise, "Semileptonic *B* and *D* decays in the quark model," *Physical Review D: Particles, Fields, Gravitation and Cosmology*, vol. 39, no. 3, pp. 799–818, 1989.

[54] Z.-H. Wang, Y. Zhang, L.-B. Jiang, T.-H. Wang, Y. Jiang, and G.-L. Wang, "The strong decays of X(3940) and X(4160)," *European Physical Journal C*, vol. 77, no. 1, article 43, 2017.

Hindawi
Advances in High Energy Physics
Volume 2018, Article ID 7627308, 11 pages
https://doi.org/10.1155/2018/7627308

Research Article

Analysis of CP Violation in $D^0 \longrightarrow K^+K^-\pi^0$

Hang Zhou,[1] Bo Zheng,[1,2] and Zhen-Hua Zhang[1]

[1]*School of Nuclear Science and Technology, University of South China, Hengyang, Hunan 421001, China*
[2]*Helmholtz Institute Mainz, Johann-Joachim-Becher-Weg 45, D-55099 Mainz, Germany*

Correspondence should be addressed to Bo Zheng; zhengbo_usc@163.com and Zhen-Hua Zhang; zhangzh@usc.edu.cn

Received 21 August 2018; Accepted 3 October 2018; Published 22 November 2018

Guest Editor: Tao Luo

We study the CP violation induced by the interference between two intermediate resonances $K^*(892)^+$ and $K^*(892)^-$ in the phase space of singly-Cabibbo-suppressed decay $D^0 \longrightarrow K^+K^-\pi^0$. We adopt the factorization-assisted topological approach in dealing with the decay amplitudes of $D^0 \longrightarrow K^\pm K^*(892)^\mp$. The CP asymmetries of two-body decays are predicted to be very tiny, which are $(-1.27 \pm 0.25) \times 10^{-5}$ and $(3.86 \pm 0.26) \times 10^{-5}$, respectively, for $D^0 \longrightarrow K^+K^*(892)^-$ and $D^0 \longrightarrow K^-K^*(892)^+$, while the differential CP asymmetry of $D^0 \longrightarrow K^+K^-\pi^0$ is enhanced because of the interference between the two intermediate resonances, which can reach as large as 3×10^{-4}. For some NPs which have considerable impacts on the chromomagnetic dipole operator O_{8g}, the global CP asymmetries of $D^0 \longrightarrow K^+K^*(892)^-$ and $D^0 \longrightarrow K^-K^*(892)^+$ can be then increased to $(0.56\pm0.08)\times10^{-3}$ and $(-0.50\pm0.04)\times10^{-3}$, respectively. The regional CP asymmetry in the overlapped region of the phase space can be as large as $(1.3 \pm 0.3) \times 10^{-3}$.

1. Introduction

Charge-Parity (CP) violation, which was first discovered in K meson system in 1964 [1], is one of the most important phenomena in particle physics. In the Standard Model (SM), CP violation originates from the weak phase in the Cabibbo-Kobayashi-Maskawa (CKM) matrix [2, 3] and the unitary phases which usually arise from strong interactions. One reason for the smallness of CP violation is that the unitary phase is usually small. Nevertheless, CP violation can be enhanced in three-body decays of heavy hadrons, when the corresponding decay amplitudes are dominated by overlapped intermediate resonances in certain regions of phase space. Owing to the overlapping, a regional CP asymmetry can be generated by a relative strong phase between amplitudes corresponding to different resonances. This relative strong phase has nonperturbative origin. As a result, the regional CP asymmetry can be larger than the global one. In fact, such kind of enhanced CP violation has been observed in several three-body decay channels of B meson [4–7], which was followed by a number of theoretical works [8–19].

The study of CP violation in singly-Cabibbo-suppressed (SCS) D meson decays provides an ideal test of the SM and exploration of New Physics (NP) [20–23]. In the SM, CP violation is predicted to be very small in charm system. Experimental researches have shown that there is no significant CP violation so far in charmed hadron decays [24–33]. CP asymmetry in SCS D meson decay can be as small as

$$A_{CP} \sim \frac{\left|V_{cb}^* V_{ub}\right|}{\left|V_{cs}^* V_{us}\right|} \frac{\alpha_s}{\pi} \sim 10^{-4}, \tag{1}$$

or even less, due to the suppression of the penguin diagrams by the CKM matrix as well as the smallness of Wilson coefficients in penguin amplitudes. The SCS decays are sensitive to new contributions to the $\Delta C = 1$ QCD penguin and chromomagnetic dipole operators, while such contributions can affect neither the Cabibbo-favored (CF) ($c \longrightarrow s\bar{d}u$) nor the doubly-Cabibbo-suppressed (DCS) ($c \longrightarrow d\bar{s}u$) decays [34]. Besides, the decays of charmed mesons offer a unique opportunity to probe CP violation in the up-type quark sector.

Several factorization approaches have been wildly used in nonleptonic B decays. In the naive factorization approach [35, 36], the hadronic matrix elements were expressed as a product of a heavy to light transition form factor and a decay constant. Based on Heavy Quark Effect Theory, it is shown

in the QCD factorization approach that the corrections to the hadronic matrix elements can be expressed in terms of short-distance coefficients and meson light-cone distribution amplitudes [37, 38]. Alternative factorization approach based on QCD factorization is often applied in study of quasi two-body hadronic B decays [19, 39, 40], where they introduced unitary meson-meson form factors, from the perspective of unitarity, for the final state interactions. Other QCD-inspired approaches, such as the perturbative approach (pQCD) [41] and the soft-collinear effective theory (SCET) [42], are also wildly used in B meson decays.

However, for D meson decays, such QCD-inspired factorization approaches may not be reliable since the charm quark mass, which is just above 1 GeV, is not heavy enough for the heavy quark expansion [43, 44]. For this reason, several model-independent approaches for the charm meson decay amplitudes have been proposed, such as the flavor topological diagram approach based on the flavor $SU(3)$ symmetry [44–47] and the factorization-assisted topological-amplitude (FAT) approach with the inclusion of flavor $SU(3)$ breaking effect [48, 49]. One motivation of these aforementioned approaches is to identify as complete as possible the dominant sources of nonperturbative dynamics in the hadronic matrix elements.

In this paper, we study the CP violation of SCS D meson decay $D^0 \longrightarrow K^+K^-\pi^0$ in the FAT approach. Our attention will be mainly focused on the region of the phase space where two intermediate resonances, $K^*(892)^+$ and $K^*(892)^-$, are overlapped. Before proceeding, it will be helpful to point out that direct CP asymmetry is hard to be isolated for decay process with CP-eigen-final-state. When the final state of the decay process is CP eigenstate, the time integrated CP violation for $D^0 \longrightarrow f$, which is defined as

$$a_f \equiv \frac{\int_0^\infty \Gamma\left(D^0 \longrightarrow f\right) dt - \int_0^\infty \Gamma\left(\overline{D}^0 \longrightarrow f\right) dt}{\int_0^\infty \Gamma\left(D^0 \longrightarrow f\right) dt + \int_0^\infty \Gamma\left(\overline{D}^0 \longrightarrow f\right) dt}, \tag{2}$$

can be expressed as [34]

$$a_f = a_f^d + a_f^m + a_f^i, \tag{3}$$

where a_f^d, a_f^m, and a_f^i are the CP asymmetries in decay, in mixing, and in the interference of decay and mixing, respectively. As is shown in [34, 50, 51], the indirect CP violation $a^{\text{ind}} \equiv a^m + a^i$ is universal and channel-independent for two-body CP-eigenstate. This conclusion is easy to be generalized to decay processes with three-body CP-eigenstate in the final state, such as $D^0 \longrightarrow K^+K^-\pi^0$. In view of the universality of the indirect CP asymmetry, we will only consider the direct CP violations of the decay $D^0 \longrightarrow K^+K^-\pi^0$ throughout this paper.

The remainder of this paper is organized as follows. In Section 2, we present the decay amplitudes for various decay channels, where the decay amplitudes of $D^0 \longrightarrow K^\pm K^*(892)^\mp$ are formulated via the FAT approaches. In Section 3, we study the CP asymmetries of $D^0 \longrightarrow K^\pm K^*(892)^\mp$ and the CP asymmetry of $D^0 \longrightarrow K^+K^-\pi^0$ induced by the interference between different resonances in the phase space. Discussions and conclusions are given in Section 4. We list some useful formulas and input parameters in the Appendix.

2. Decay Amplitude for $D^0 \longrightarrow K^+K^-\pi^0$

In the overlapped region of the intermediate resonances $K^*(892)^+$ and $K^*(892)^-$ in the phase space, the decay process $D^0 \longrightarrow K^+K^-\pi^0$ is dominated by two cascade decays, $D^0 \longrightarrow K^+K^*(892)^- \longrightarrow K^+K^-\pi^0$ and $D^0 \longrightarrow K^-K^*(892)^+ \longrightarrow K^-K^+\pi^0$, respectively. Consequently, the decay amplitude of $D^0 \longrightarrow K^+K^-\pi^0$ can be expressed as

$$\mathcal{M}_{D^0 \longrightarrow K^+K^-\pi^0} = \mathcal{M}_{K^{*+}} + e^{i\delta}\mathcal{M}_{K^{*-}} \tag{4}$$

in the overlapped region, where $\mathcal{M}_{K^{*+}}$ and $\mathcal{M}_{K^{*-}}$ are the amplitudes for the two cascade decays and δ is the relative strong phase. Note that nonresonance contributions have been neglected in (4).

The decay amplitude for the cascade decay $D^0 \longrightarrow K^+K^*(892)^- \longrightarrow K^+K^-\pi^0$ can be expressed as

$$\mathcal{M}_{K^{*-}} = \frac{\sum_\lambda \mathcal{M}^\lambda_{K^{*-} \longrightarrow K^-\pi^0} \cdot \mathcal{M}^\lambda_{D^0 \longrightarrow K^{*-}K^+}}{s_{\pi^0K^-} - m^2_{K^{*-}} + i m_{K^{*-}}\Gamma_{K^{*-}}}, \tag{5}$$

where $\mathcal{M}^\lambda_{K^{*-} \longrightarrow K^-\pi^0}$ and $\mathcal{M}^\lambda_{D^0 \longrightarrow K^+K^{*-}}$ represent the amplitudes corresponding to the strong decay $K^{*-} \longrightarrow K^-\pi^0$ and weak decay $D^0 \longrightarrow K^+K^{*-}$, respectively, λ is the helicity index of K^{*-}, $s_{\pi^0K^-}$ is the invariant mass square of π^0K^- system, and $m_{K^{*-}}$ and $\Gamma_{K^{*-}}$ are the mass and width of $K^*(892)^-$, respectively. The decay amplitude for the cascade decay, $D^0 \longrightarrow K^-K^*(892)^+ \longrightarrow K^-K^+\pi^0$, is the same as (5) except replacing the subscripts K^{*-} and $K^\pm$ with K^{*+} and $K^\mp$, respectively.

For the strong decays $K^*(892)^\pm \longrightarrow \pi^0K^\pm$, one can express the decay amplitudes as

$$\mathcal{M}_{K^{*\pm} \longrightarrow \pi^0K^\pm} = g_{K^{*\pm}K^\pm\pi^0}\left(p_{\pi^0} - p_{K^\pm}\right) \cdot \varepsilon_{K^{*\pm}}\left(p, \lambda\right), \tag{6}$$

where p_{π^0} and $p_{K^\pm}$ represent the momentum for π^0 and $K^\pm$ mesons, respectively, and $g_{K^{*\pm}K^\pm\pi^0}$ is the effective coupling constant for the strong interaction, which can be extracted from the experimental data via

$$g^2_{K^{*\pm}K^\pm\pi^0} = \frac{6\pi m^2_{K^{*\pm}}\Gamma_{K^{*\pm} \longrightarrow K^\pm\pi^0}}{\lambda^3_{K^{*\pm}}}, \tag{7}$$

with

$$\lambda_{K^{*\pm}} = \frac{1}{2m_{K^{*\pm}}} \cdot \sqrt{\left[m^2_{K^{*\pm}} - \left(m_{\pi^0} + m_{K^\pm}\right)^2\right] \cdot \left[m^2_{K^{*\pm}} - \left(m_{\pi^0} - m_{K^\pm}\right)^2\right]}, \tag{8}$$

and $\Gamma_{K^{*\pm} \longrightarrow K^\pm\pi^0} = \text{Br}(K^{*\pm} \longrightarrow K^\pm\pi^0) \cdot \Gamma_{K^{*\pm}}$. The isospin symmetry of the strong interaction implies that $\Gamma_{K^{*\pm} \longrightarrow K^\pm\pi^0} \simeq (1/3)\Gamma_{K^{*\pm}}$.

The decay amplitudes for the weak decays, $D^0 \longrightarrow K^+K^*(892)^-$ and $D^0 \longrightarrow K^-K^*(892)^+$, will be handled with

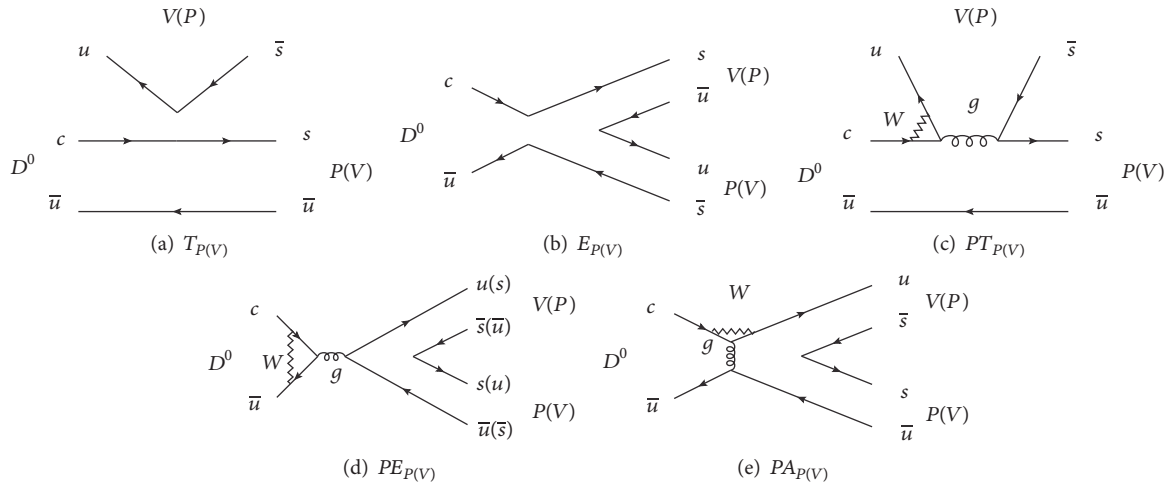

Figure 1: The relevant topological diagrams for $D \longrightarrow PV$ with (a) the color-favored tree amplitude $T_{P(V)}$, (b) the W-exchange amplitude $E_{P(V)}$, (c) the color-favored penguin amplitude $PT_{P(V)}$, (d) the gluon-annihilation penguin amplitude $PE_{P(V)}$, and (e) the gluon-exchange penguin amplitude $PA_{P(V)}$.

the aforementioned FAT approach [48, 49]. The relevant topological tree and penguin diagrams for $D \longrightarrow PV$ are displayed in Figure 1, where P and V denote a light pseudoscalar and vector meson (representing $K^{\pm}$ and $K^{*\pm}$ in this paper), respectively.

The two tree diagrams in first line of Figure 1 represent the color-favored tree diagram for $D \longrightarrow P(V)$ transition and the W-exchange diagram with the pseudoscalar (vector) meson containing the antiquark from the weak vertex, respectively. The amplitudes of these two diagrams will be, respectively, denoted as $T_{P(V)}$ and $E_{P(V)}$.

According to these topological structures, the amplitudes of the color-favored tree diagrams $T_{P(V)}$, which are dominated by the factorizable contributions, can be parameterized as

$$T_P = \frac{G_F}{\sqrt{2}}\lambda_s a_2(\mu) f_V m_V F_1^{D\longrightarrow P}\left(m_V^2\right) 2\left(\varepsilon^* \cdot p_D\right), \quad (9)$$

and

$$T_V = \frac{G_F}{\sqrt{2}}\lambda_s a_2(\mu) f_P m_V A_0^{D\longrightarrow V}\left(m_P^2\right) 2\left(\varepsilon^* \cdot p_D\right), \quad (10)$$

respectively, where G_F is the Fermi constant, $\lambda_s = V_{us}V_{cs}^*$, with V_{us} and V_{cs} being the CKM matrix elements, $a_2(\mu) = c_2(\mu) + c_1(\mu)/N_c$, with $c_1(\mu)$ and $c_2(\mu)$ being the scale-dependent Wilson coefficients, and the number of color $N_c = 3$, $f_{V(P)}$ and $m_{V(P)}$ are the decay constant and mass of the vector (pseudoscalar) meson, respectively, $F_1^{D\longrightarrow P}$ and $A_0^{D\longrightarrow V}$ are the form factors for the transitions $D \longrightarrow P$ and $D \longrightarrow V$, respectively, ε is the polarization vector of the vector meson, and p_D is the momentum of D meson. The scale μ of Wilson coefficients is set to energy release in individual decay channels [52, 53], which depends on masses of initial and final states and is defined as [48, 49]

$$\mu = \sqrt{\Lambda m_D\left(1 - r_P^2\right)\left(1 - r_V^2\right)}, \quad (11)$$

with the mass ratios $r_{V(P)} = m_{V(P)}/m_D$, where Λ represents the soft degrees of freedom in the D meson, which is a free parameter.

For the W-exchange amplitudes, since the factorizable contributions to these amplitudes are helicity-suppressed, only the nonfactorizable contributions need to be considered. Therefore, the W-exchange amplitudes are parameterized as

$$E_{P,V}^q = \frac{G_F}{\sqrt{2}}\lambda_s c_2(\mu)\chi_q^E e^{i\phi_q^E} f_D m_D \frac{f_P f_V}{f_\pi f_\rho}\left(\varepsilon^* \cdot p_D\right), \quad (12)$$

where m_D is the mass of D meson, f_D, f_π, and f_ρ are the decay constants of the D, π, and ρ mesons, respectively, and χ_q^E and ϕ_q^E characterize the strengths and the strong phases of the corresponding amplitudes, with $q = u, d, s$ representing the strongly produced q quark pair. The ratio of $f_P f_V$ over $f_\pi f_\rho$ indicates that the flavor $SU(3)$ breaking effects have been taken into account from the decay constants.

The penguin diagrams shown in the second line of Figure 1 represent the color-favored, the gluon-annihilation, and the gluon-exchange penguin diagrams, respectively, whose amplitudes will be denoted as $PT_{P(V)}$, $PE_{P(V)}$, and $PA_{P(V)}$, respectively.

Since a vector meson cannot be generated from the scalar or pseudoscalar operator, the amplitude PT_P does not include contributions from the penguin operator O_5 or O_6. Consequently, the color-favored penguin amplitudes PT_P and PT_V can be expressed as

$$PT_P = -\frac{G_F}{\sqrt{2}}\lambda_b a_4(\mu) f_V m_V F_1^{D\longrightarrow P}\left(m_V^2\right) 2\left(\varepsilon^* \cdot p_D\right), \quad (13)$$

and

$$PT_V = -\frac{G_F}{\sqrt{2}}\lambda_b\left[a_4(\mu) - r_\chi a_6(\mu)\right] f_P m_V A_0^{D\longrightarrow V}\left(m_P^2\right) \cdot 2\left(\varepsilon^* \cdot p_D\right), \quad (14)$$

respectively, where $\lambda_b = V_{ub}V_{cb}^*$ with V_{ub} and V_{cb}^* being the CKM matrix elements, $a_{4,6}(\mu) = c_{4,6}(\mu) + c_{3,5}(\mu)/N_c$, with $c_{3,4,5,6}$ being the Wilson coefficients, and r_χ is a chiral factor, which takes the form

$$r_\chi = \frac{2m_P^2}{\left(m_u + m_q\right)\left(m_q + m_c\right)}, \tag{15}$$

with $m_{u(c,q)}$ being the masses of $u(c,q)$ quark. Note that the quark-loop corrections and the chromomagnetic-penguin contribution are also absorbed into $c_{3,4,5,6}$ as shown in [49].

Similar to the amplitudes $E_{P,V}$, the amplitudes PE only include the nonfactorizable contributions as well. Therefore, the amplitudes $PE_{P,V}$, which are dominated by O_4 and O_6 [48], can be parameterized as

$$PE_{P,V}^q = -\frac{G_F}{\sqrt{2}}\lambda_b \left[c_4(\mu) - c_6(\mu)\right] \chi_q^E e^{i\phi_q^E} f_D m_D \cdot \frac{f_P f_V}{f_\pi f_\rho}\left(\varepsilon^* \cdot p_D\right). \tag{16}$$

For the amplitudes PA_P and PA_V, the helicity suppression does not apply to the matrix elements of $O_{5,6}$, so the factorizable contributions exist. In the pole resonance model [54], after applying the Fierz transformation and the factorization hypothesis, the amplitudes PA_P and PA_V can be expressed as

$$PA_P^q = -\frac{G_F}{\sqrt{2}}\lambda_b \left[(-2)\, a_6(\mu)\,(2g_S) \cdot \frac{1}{m_D^2 - m_{P^*}^2}\left(f_{P^*} m_{P^*}^0\right)\left(f_D \frac{m_D^2}{m_c}\right) + c_3(\mu) \cdot \chi_q^A e^{i\phi_q^A} f_D m_D \frac{f_P f_V}{f_\pi f_\rho}\right]\left(\varepsilon^* \cdot p_D\right), \tag{17}$$

and

$$PA_V^q = -\frac{G_F}{\sqrt{2}}\lambda_b \left[(-2)\, a_6(\mu)\,(-2g_S) \cdot \frac{1}{m_D^2 - m_{P^*}^2}\left(f_{P^*} m_{P^*}^0\right)\left(f_D \frac{m_D^2}{m_c}\right) + c_3(\mu) \cdot \chi_q^A e^{i\phi_q^A} f_D m_D \frac{f_P f_V}{f_\pi f_\rho}\right]\left(\varepsilon^* \cdot p_D\right), \tag{18}$$

respectively, where g_S is an effective strong coupling constant obtained from strong decays, e.g., $\rho \longrightarrow \pi\pi$, $K^* \longrightarrow K\pi$, and $\phi \longrightarrow KK$, and is set as $g_S = 4.5$ [54] in this work, m_{P^*} and f_{P^*} are the mass and decay constant of the pole resonant pseudoscalar meson P^*, respectively, and χ_q^A and ϕ_q^A are the strengths and the strong phases of the corresponding amplitudes.

From Figure 1, the decay amplitudes of $D^0 \longrightarrow K^+K^*(892)^-$ and $D^0 \longrightarrow K^-K^*(892)^+$ in the FAT approach can be easily written down

$$\mathcal{M}_{D^0\longrightarrow K^+K^{*-}}^{\lambda} = T_{K^{*-}} + E_{K^+}^u + PT_{K^{*-}} + PE_{K^{*-}}^s + PE_{K^+}^u + PA_{K^{*-}}^s, \tag{19}$$

and

$$\mathcal{M}_{D^0\longrightarrow K^-K^{*+}}^{\lambda} = T_{K^-} + E_{K^{*+}}^u + PT_{K^-} + PE_{K^-}^s + PE_{K^{*+}}^u + PA_{K^-}^s, \tag{20}$$

respectively, where λ is the helicity of the polarization vector $\varepsilon(p,\lambda)$. In the FAT approach, the fitted nonperturbative parameters, $\chi_{q,s}^E$, $\phi_{q,s}^E$, $\chi_{q,s}^A$, $\phi_{q,s}^A$, are assumed to be universal and can be determined by the data [49].

In Table 1, we list the magnitude of each topological amplitude for $D^0 \longrightarrow K^+K^*(892)^-$ and $D^0 \longrightarrow K^-K^*(892)^+$ by using the global fitted parameters for $D \longrightarrow PV$ in [49]. One can see from Table 1 that the penguin contributions are greatly suppressed. PT is dominant in the penguin contributions of $D^0 \longrightarrow K^-K^*(892)^+$, while PT is small in $D^0 \longrightarrow K^+K^*(892)^-$, which is even smaller than the amplitude PA. This difference is because of the chirally enhanced factor contained in (14) while not in (13). The very small PE do not receive the contributions from the quark-loop and chromomagnetic penguins, since these two contributions to c_4 and c_6 are canceled with each other in (16). Besides, the relations $PE_V^s = PE_P^s$, $PE_V^u = PE_P^u$, and $PE_V^s \neq PE_V^u$ can be read from Table 1; this is because that the isospin symmetry and the flavor $SU(3)$ breaking effect have been considered.

Since the form factors are inevitably model-dependent, we list in Table 2 the branching ratios of $D^0 \longrightarrow K^+K^*(892)^-$ and $D^0 \longrightarrow K^-K^*(892)^+$ predicted by the FAT approach, by various form factor models. The pole, dipole, and covariant light-front (CLF) models are adopted. The uncertainties in Table 2 mainly come from decay constants. The CLF model agrees well with the data for both decay channels, and other models are also consistent with the data. However, the model-dependence of form factor leads to large uncertainty of the branching fraction, as large as 20%. Because of the smallness of the Wilson coefficients and the CKM-suppression of the penguin amplitudes, the branching ratios are dominated by the tree amplitudes. Therefore, there is no much difference for the branching ratios whether we consider the penguin amplitudes or not.

3. CP Asymmetries for $D^0 \longrightarrow K^\pm K^*(892)^\mp$ and $D^0 \longrightarrow K^+K^-\pi^0$

The direct CP asymmetry for the two-body decay $D \longrightarrow PV$ is defined as

$$A_{CP}^{D\longrightarrow PV} = \frac{\left|\mathcal{M}_{D\longrightarrow PV}\right|^2 - \left|\mathcal{M}_{\overline{D}\longrightarrow \overline{PV}}\right|^2}{\left|\mathcal{M}_{D\longrightarrow PV}\right|^2 + \left|\mathcal{M}_{\overline{D}\longrightarrow \overline{PV}}\right|^2}, \tag{21}$$

where $\mathcal{M}_{\overline{D}\longrightarrow\overline{PV}}$ represents the decay amplitude of the CP conjugate process $\overline{D} \longrightarrow \overline{PV}$, such as $\overline{D}^0 \longrightarrow K^+K^*(892)^-$ or $\overline{D}^0 \longrightarrow K^-K^*(892)^+$. In the framework of FAT approach,

Table 1: The magnitude of tree and penguin contributions (in unit of 10^{-3}) corresponding to the topological amplitudes in (19) and (20). The factors "$(G_F/\sqrt{2})\lambda_s(\varepsilon^* \cdot p_D)$" and "$-(G_F/\sqrt{2})\lambda_b(\varepsilon^* \cdot p_D)$" are omitted in this table.

Decay modes	$T_{K^{*-}}$	$E^u_{K^+}$	$PT_{K^{*-}}$	$PE^s_{K^{*-}}$	$PE^u_{K^+}$	$PA^s_{K^{*-}}$
$D^0 \longrightarrow K^+K^*(892)^-$	0.23	−0.02 + 0.15i	3.83 + 4.32i	0.96 − 0.03i	0.13 − 0.81i	6.73 + 8.22i
	T_{K^-}	$E^u_{K^{*+}}$	PT_{K^-}	$PE^s_{K^-}$	$PE^u_{K^{*+}}$	$PA^s_{K^-}$
$D^0 \longrightarrow K^-K^*(892)^+$	0.44	−0.02 + 0.15i	−23.3 − 19.3i	0.96 − 0.03i	0.13 − 0.81i	−8.53 − 5.53i

Table 2: Branching ratios (in unit of 10^{-3}) of singly-Cabibbo-suppressed decays $D^0 \longrightarrow K^+K^*(892)^-$ and $D^0 \longrightarrow K^-K^*(892)^+$. Both experimental data [55–57] and theoretical predictions of FAT approach of the branching ratios are listed.

Form factors	$\mathrm{Br}(D^0 \longrightarrow K^+K^*(892)^-)$	$\mathrm{Br}(D^0 \longrightarrow K^-K^*(892)^+)$
Pole	1.57 ± 0.04	3.73 ± 0.17
Dipole	1.69 ± 0.04	4.02 ± 0.19
CLF	1.45 ± 0.04	4.44 ± 0.20
Exp.	1.56 ± 0.12	4.38 ± 0.21

we predict very small direct CP asymmetries of $D^0 \longrightarrow K^+K^*(892)^-$ and $D^0 \longrightarrow K^-K^*(892)^+$ presented in Table 3. The uncertainties induced by the model-dependence of form factor to the CP asymmetries of $D^0 \longrightarrow K^+K^*(892)^-$ and $D^0 \longrightarrow K^-K^*(892)^+$ are about 30% and 10%, respectively.

The differential CP asymmetry of the three-body decay $D^0 \longrightarrow K^+K^-\pi^0$, which is a function of the invariant mass of $s_{\pi^0K^+}$ and $s_{\pi^0K^-}$, is defined as

$$A_{CP}^{D^0\longrightarrow K^+K^-\pi^0}\left(s_{\pi^0K^+}, s_{\pi^0K^-}\right) = \frac{\left|\mathscr{M}_{D^0\longrightarrow K^+K^-\pi^0}\right|^2 - \left|\mathscr{M}_{\overline{D}^0\longrightarrow K^-K^+\pi^0}\right|^2}{\left|\mathscr{M}_{D^0\longrightarrow K^+K^-\pi^0}\right|^2 + \left|\mathscr{M}_{\overline{D}^0\longrightarrow K^-K^+\pi^0}\right|^2}, \quad (22)$$

where the invariant mass $s_{\pi^0K^\pm} = (p_{\pi^0} + p_{K^\pm})^2$. As can be seen from (4), the differential CP asymmetry $A_{CP}^{D^0\longrightarrow K^+K^-\pi^0}$ depends on the relative strong phase δ, which is impossible to be calculated theoretically because of its nonperturbative origin. Despite this, we can still acquire some information of this relative strong phase δ from data. By using a Dalitz plot technique [55, 58, 59], the phase difference δ^{exp} between D^0 decays to $K^+K^*(892)^-$ and $K^-K^*(892)^+$ can be extracted from data. One should notice that δ^{exp} is not the same as the strong phase δ defined in (4). The strong phase δ is the relative phase between the decay amplitudes of $D^0 \longrightarrow K^+K^*(892)^-$ and $D^0 \longrightarrow K^-K^*(892)^+$. On the other hand, the phase δ^{exp} is defined through

$$\mathscr{M}_{D^0\longrightarrow K^+K^-\pi^0} = \left(\left|\mathscr{M}_{K^{*+}}\right| + e^{i\delta^{\mathrm{exp}}}\left|\mathscr{M}_{K^{*-}}\right|\right)e^{i\delta_{K^{*+}}} \quad (23)$$

in the overlapped region of the phase space, where $\delta_{K^{*\pm}}$ is the phase of the amplitude $\mathscr{M}_{K^{*\pm}}$:

$$\mathscr{M}_{K^{*\pm}} = \left|\mathscr{M}_{K^{*\pm}}\right| e^{i\delta_{K^{*\pm}}}. \quad (24)$$

Therefore, neglecting the CKM suppressed penguin amplitudes, δ^{exp} and δ can be related by

$$\delta^{\mathrm{exp}} - \delta \approx \delta^{K^{*-}K^+} - \delta^{K^{*+}K^-}, \quad (25)$$

where $\delta^{K^{*\mp}K^\pm} = \arg(T_{K^{*\mp}} + E^u_{K^\pm})$ are the phases in tree-level amplitudes of $D^0 \longrightarrow K^\pm K^*(892)^\mp$ and are equivalent to $\delta_{K^{*\mp}}$ if the penguin amplitudes are neglected. With the relation of (25), and $\delta^{\mathrm{exp}} = -35.5^\circ \pm 4.1^\circ$ measured by the BABAR Collaboration [56], we have $\delta \approx -51.85^\circ \pm 4.1^\circ$.

In Figure 2, we present the differential CP asymmetry of $D^0 \longrightarrow K^+K^-\pi^0$ in the overlapped region of $K^*(892)^-$ and $K^*(892)^+$ in the phase space, with $\delta = -51.85^\circ$. Namely, we will focus on the region $m_{K^*} - 2\Gamma_{K^*} < \sqrt{s_{\pi^0K^-}}, \sqrt{s_{\pi^0K^+}} < m_{K^*} + 2\Gamma_{K^*}$ of the phase space. One can see from Figure 2 that the differential CP asymmetry of $D^0 \longrightarrow K^+K^-\pi^0$ can reach 3.0×10^{-4} in the overlapped region, which is about 10 times larger than the CP asymmetries of the corresponding two-body decay channels shown in Table 3.

The behavior of the differential CP asymmetry of $D^0 \longrightarrow K^+K^-\pi^0$ in Figure 2 motivates us to separate this region into four areas, area A ($m_{K^*} < \sqrt{s_{\pi^0K^-}} < m_{K^*} + 2\Gamma_{K^*}, m_{K^*} - 2\Gamma_{K^*} < \sqrt{s_{\pi^0K^+}} < m_{K^*}$), area B ($m_{K^*} < \sqrt{s_{\pi^0K^-}} < m_{K^*} + 2\Gamma_{K^*}, m_{K^*} < \sqrt{s_{\pi^0K^+}} < m_{K^*} + 2\Gamma_{K^*}$), area C ($m_{K^*} - 2\Gamma_{K^*} < \sqrt{s_{\pi^0K^-}} < m_{K^*}, m_{K^*} - 2\Gamma_{K^*} < \sqrt{s_{\pi^0K^+}} < m_{K^*}$), and area D ($m_{K^*} - 2\Gamma_{K^*} < \sqrt{s_{\pi^0K^-}} < m_{K^*}, m_{K^*} < \sqrt{s_{\pi^0K^+}} < m_{K^*} + 2\Gamma_{K^*}$). We further consider the observable of regional CP asymmetry in areas A, B, C, and D displayed in Table 4, which is defined by

$$A_{CP}^{\Omega} = \frac{\int_\Omega \left(\left|\mathscr{M}_{\mathrm{tot}}\right|^2 - \left|\overline{\mathscr{M}}_{\mathrm{tot}}\right|^2\right) \mathrm{d}s_{\pi^0K^-} s_{\pi^0K^+}}{\int_\Omega \left(\left|\mathscr{M}_{\mathrm{tot}}\right|^2 + \left|\overline{\mathscr{M}}_{\mathrm{tot}}\right|^2\right) \mathrm{d}s_{\pi^0K^-} s_{\pi^0K^+}}, \quad (26)$$

where Ω represents a certain region of the phase space.

Comparing with the CP asymmetries of two-body decays, the regional CP asymmetries, from Table 4, are less sensitive to the models we have used. We would like to use only the CLF model for the following discussion. The uncertainties in Table 4 come from decay constants as well as the relative phase δ^{exp}. In addition, if we focus on the right part of area A, that is, $m_{K^*} < \sqrt{s_{\pi^0K^-}} < m_{K^*} + 2\Gamma_{K^*}, m_{K^*} - \Gamma_{K^*} < \sqrt{s_{\pi^0K^+}} < m_{K^*}$, the regional CP violation will be $(1.09 \pm 0.16) \times 10^{-4}$.

The energy dependence of the propagator of the intermediate resonances can lead to a small correction to CP asymmetry. For example, if we replace the Breit-Wigner

Table 3: *CP* asymmetries (in unit of 10^{-5}) of $D^0 \longrightarrow K^+K^*(892)^-$ and $D^0 \longrightarrow K^-K^*(892)^+$ predicted by the FAT approach with pole, dipole, and CLF models adopted. The uncertainties in this table are mainly from decay constants.

Form factors	$A_{CP}(D^0 \longrightarrow K^+K^*(892)^-)$	$A_{CP}(D^0 \longrightarrow K^-K^*(892)^+)$
Pole	-1.45 ± 0.25	3.60 ± 0.23
Dipole	-1.63 ± 0.26	3.70 ± 0.24
CLF	-1.27 ± 0.25	3.86 ± 0.26

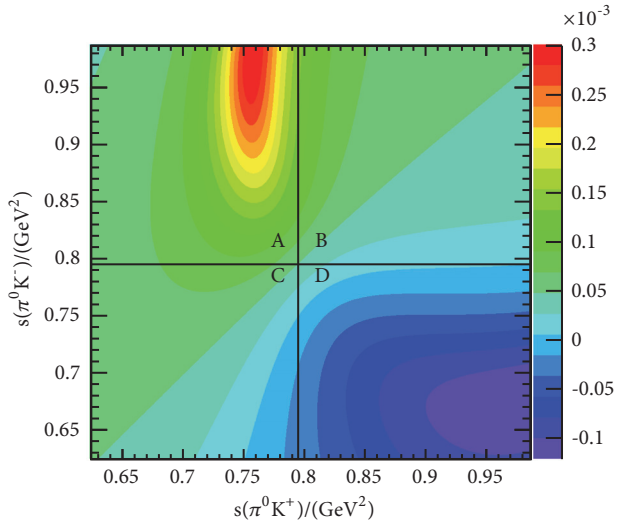

Figure 2: The differential *CP* asymmetry distribution of $D^0 \longrightarrow K^+K^-\pi^0$ in the overlapped region of $K^*(892)^-$ and $K^*(892)^+$ in the phase space.

propagator by the Flatté Parametrization [60], the correction to the regional *CP* asymmetry will be about 1%.

Since the *CP* asymmetry of $D^0 \longrightarrow K^+K^-\pi^0$ is extremely suppressed, it should be more sensitive to the NP. For example, some NPs have considerable impacts on the chromomagnetic dipole operator O_{8g} [34, 61–66]. Consequently, the *CP* violation in SCS decays may be further enhanced. In practice, the NP contributions can be absorbed into the corresponding effective Wilson coefficient c_{8g}^{eff} [67, 68]. For comparison, we first consider a relative small value of c_{8g}^{eff} (as in [48, 64]) lying within the range $(0, 1)$ and the global *CP* asymmetry of $D^0 \longrightarrow K^*(892)^{\pm}K^{\mp}$ are no larger than 5×10^{-5}. Moreover, if we follow [49] taking $c_{8g}^{\text{eff}} \approx 10$ (while $c_{8g}^{\text{eff}} = 10$, which is extracted from ΔA_{CP} measured by LHCb [69], is a quite large quantity even for the coefficients corresponding tree-level operators, however, such large contribution can be realized if some NPs effects are pulled in. For example, the up squark-gluino loops in supersymmetry (SUSY) can arise significant contributions to c_{8g}. More details about the squark-gluino loops and other models in SUSY can be found in [34, 62, 70–72]), the global *CP* asymmetries of $D^0 \longrightarrow K^+K^*(892)^-$ and $D^0 \longrightarrow K^-K^*(892)^+$ are then $(0.56\pm0.08)\times 10^{-3}$ and $(-0.50 \pm 0.04) \times 10^{-3}$, respectively.

We further display the *CP* asymmetry of $D^0 \longrightarrow K^+K^-\pi^0$ in the overlapped region of $K^*(892)^-$ and $K^*(892)^+$ in Figures 3(a) and 3(b) for $c_{8g}^{\text{eff}} = 1$ and $c_{8g}^{\text{eff}} = 10$, respectively. After taking the interference effect into account, the differential *CP* asymmetry of $D^0 \longrightarrow K^+K^-\pi^0$ can be increased as large as 5.5×10^{-4} and 2.8×10^{-3} for $c_{8g}^{\text{eff}} = 1$ and $c_{8g}^{\text{eff}} = 10$, respectively. The regional ones (in phase space of $\sqrt{0.74}$ GeV $< \sqrt{s_{\pi^0K^-}} < \sqrt{0.81}$ GeV, $\sqrt{0.84} < \sqrt{s_{\pi^0K^+}} < m_{K^*} + 2\Gamma_{K^*}$) can reach $(2.7\pm0.5)\times10^{-4}$ and $(1.3\pm0.3)\times10^{-3}$ for $c_{8g}^{\text{eff}} = 1$ and $c_{8g}^{\text{eff}} = 10$, respectively.

4. Discussion and Conclusion

In this work, we studied *CP* violations in $D^0 \longrightarrow K^*(892)^{\pm}K^{\mp} \longrightarrow K^+K^-\pi^0$ via the FAT approach. The *CP* violations in two-body decay processes $D^0 \longrightarrow K^+K^*(892)^-$ and $D^0 \longrightarrow K^-K^*(892)^+$ are very small, which are $(-1.27 \pm 0.25) \times 10^{-5}$ and $(3.86 \pm 0.26) \times 10^{-5}$, respectively. Our discussion shows that the *CP* violation can be enhanced by the interference effect in three-body decay $D^0 \longrightarrow K^+K^-\pi^0$. The differential *CP* asymmetry can reach 3.0×10^{-4} when the interference effect is taken into account, while the regional one can be as large as $(1.09 \pm 0.16) \times 10^{-4}$.

Besides, since the chromomagnetic dipole operator O_{8g} is sensitive to some NPs, the inclusion of this kind of NPs will lead to a much larger global *CP* asymmetries of $D^0 \longrightarrow K^+K^*(892)^-$ and $D^0 \longrightarrow K^-K^*(892)^+$, which are $(0.56 \pm 0.08) \times 10^{-3}$ and $(-0.50 \pm 0.04) \times 10^{-3}$, respectively, while the regional *CP* asymmetry of $D^0 \longrightarrow K^+K^-\pi^0$ can be also increased to $(1.3 \pm 0.3) \times 10^{-3}$ when considering the interference effect in the phase space. Since the $\mathcal{O}(10^{-3})$ of

Table 4: Three from factor models: the pole, dipole, and CLF models are used for the regional *CP* asymmetries (in unit of 10^{-4}) in the four areas, A, B, C, and D, of the phase space.

Form factors	A_{CP}^{A}	A_{CP}^{B}	A_{CP}^{C}	A_{CP}^{D}	A_{CP}^{All}
Pole	0.87 ± 0.11	0.42 ± 0.08	0.39 ± 0.07	−0.30 ± 0.08	0.33 ± 0.05
Dipole	0.87 ± 0.11	0.41 ± 0.08	0.38 ± 0.07	−0.30 ± 0.08	0.32 ± 0.05
CLF	0.84 ± 0.10	0.45 ± 0.08	0.42 ± 0.07	−0.25 ± 0.08	0.36 ± 0.06

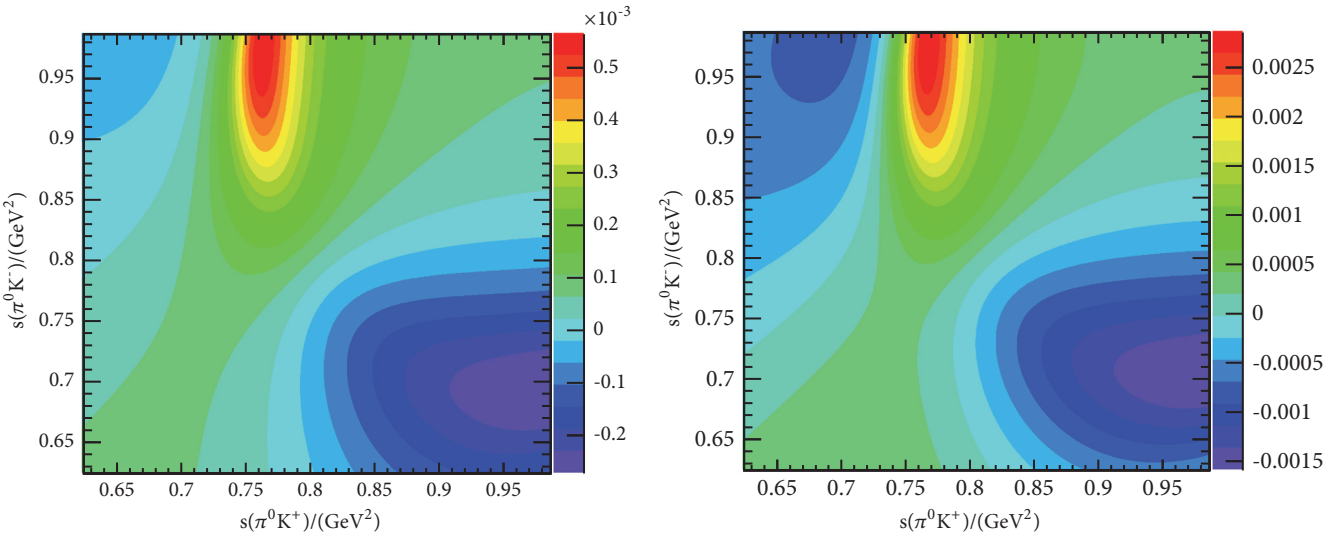

Figure 3: The differential *CP* asymmetry distribution of $D^0 \longrightarrow K^+K^-\pi^0$ for (a) $c_{8g}^{\text{eff}} = 1$ and (b) $c_{8g}^{\text{eff}} = 10$, in the overlapped region of $K^*(892)^-$ and $K^*(892)^+$ in the phase space.

CP asymmetry is attributed to the large c_{8g}^{eff}, which is almost impossible for the SM to generate such large contribution, it will indicate NP if such *CP* violation is observed. Here, we roughly estimate the number of $D^0\overline{D}^0$ needed for testing such kind of asymmetries, which is about $(1/Br)(1/A_{CP}^2) \sim 10^9$. This could be observed in the future experiments at Belle II [73, 74], while the current largest $D^0\overline{D}^0$ yields are about 10^8 at BABAR and Belle [75, 76] and 10^7 at BESIII [77].

Appendix

Some Useful Formulas and Input Parameters

(1) Effective Hamiltonian and Wilson Coefficients. The weak effective Hamiltonian for SCS *D* meson decays, based on the Operator Product Expansion (OPE) and Heavy Quark Effective Theory (HQET), can be expressed as [78]

$$\mathcal{H}_{\text{eff}} = \frac{G_F}{\sqrt{2}}\left[\sum_{q=d,s}\lambda_q\left(c_1O_1^q + c_2O_2^q\right) - \lambda_b\left(\sum_{i=3}^{6}c_iO_i + c_{8g}O_{8g}\right)\right] + h.c., \tag{A.1}$$

where G_F is the Fermi constant, $\lambda_q = V_{uq}V_{cq}^*$, c_i $(i = 1, \ldots, 6)$ is the Wilson coefficient, and O_1^q, O_2^q, O_i $(i = 1, \ldots, 6)$, and O_{8g} are four-fermion operators which are constructed from different combinations of quark fields. The four-fermion operators take the following form:

$$\begin{aligned}
O_1^q &= \overline{u}_\alpha\gamma_\mu\left(1-\gamma_5\right)q_\beta\overline{q}_\beta\gamma^\mu\left(1-\gamma_5\right)c_\alpha,\\
O_2^q &= \overline{u}\gamma_\mu\left(1-\gamma_5\right)q\overline{q}\gamma^\mu\left(1-\gamma_5\right)c,\\
O_3 &= \overline{u}\gamma_\mu\left(1-\gamma_5\right)c\sum_{q'}\overline{q}'\gamma^\mu\left(1-\gamma_5\right)q',\\
O_4 &= \overline{u}_\alpha\gamma_\mu\left(1-\gamma_5\right)c_\beta\sum_{q'}\overline{q}'_\beta\gamma^\mu\left(1-\gamma_5\right)q'_\alpha,\\
O_5 &= \overline{u}\gamma_\mu\left(1-\gamma_5\right)c\sum_{q'}\overline{q}'\gamma^\mu\left(1+\gamma_5\right)q',\\
O_6 &= \overline{u}_\alpha\gamma_\mu\left(1-\gamma_5\right)c_\beta\sum_{q'}\overline{q}'_\beta\gamma^\mu\left(1+\gamma_5\right)q'_\alpha,\\
O_{8g} &= -\frac{g_s}{8\pi^2}m_c\overline{u}\sigma_{\mu\nu}\left(1+\gamma_5\right)G^{\mu\nu}c,
\end{aligned} \tag{A.2}$$

where α and β are color indices and $q' = u, d, s$. Among all these operators, O_1^q and O_2^q are tree operators, $O_3 - O_6$ are QCD penguin operators, and O_{8g} is chromomagnetic dipole

operator. The electroweak penguin operators are neglected in practice. One should notice that SCS decays receive contributions from all aforementioned operators while only tree operators can contribute to CF decays and DCS decays.

The Wilson coefficients used in this paper are evaluated at $\mu = 1\text{GeV}$, which can be found in [48].

(2) CKM Matrix. We use the Wolfenstein parameterization for the CKM matrix elements, which up to order $\mathcal{O}(\lambda^8)$ read [79, 80]

$$\begin{aligned} V_{us} &= \lambda - \frac{1}{2}A^2\lambda^7\left(\rho^2+\eta^2\right), \\ V_{cs} &= 1 - \frac{1}{2}\lambda^2 - \frac{1}{8}\lambda^4\left(1+4A^2\right) \\ &\quad - \frac{1}{16}\lambda^6\left(1-4A^2+16A^2\left(\rho+i\eta\right)\right) \\ &\quad - \frac{1}{128}\lambda^8\left(5-8A^2+16A^4\right), \\ V_{ub} &= A\lambda^3\left(\rho-i\eta\right), \\ V_{cb} &= A\lambda^2 - \frac{1}{2}A^3\lambda^8\left(\rho^2+\eta^2\right), \end{aligned} \tag{A.3}$$

where A, ρ, η, and λ are the Wolfenstein parameters, which satisfy following relation:

$$\rho + i\eta = \frac{\sqrt{1-A^2\lambda^4}\left(\overline{\rho}+i\overline{\eta}\right)}{\sqrt{1-\lambda^2}\left[1-A^2\lambda^4\left(\overline{\rho}+i\overline{\eta}\right)\right]}. \tag{A.4}$$

Numerical values of Wolfenstein parameters which have been used in this work are as follows:

$$\begin{aligned} \lambda &= 0.22548^{+0.00068}_{-0.00034}, \\ A &= 0.810^{+0.018}_{-0.024}, \\ \overline{\rho} &= 0.145^{+0.013}_{-0.007}, \\ \overline{\eta} &= 0.343^{+0.011}_{-0.012}. \end{aligned} \tag{A.5}$$

(3) Decay Constants and Form Factors. In (17) and (18), the pole resonance model was employed for the matrix element $\langle PV|\overline{q}_1 q_2|0\rangle$ in the annihilation diagrams. By considering angular momentum conservation at weak vertex and all conservation laws are preserved at strong vertex, the matrix element $\langle PV|\overline{q}_1 q_2|0\rangle$ is therefore dominated by a pseudoscalar resonance [54],

$$\begin{aligned} \left\langle PV\left|\overline{q}_1 q_2\right|0\right\rangle &= \left\langle PV \mid P^*\right\rangle \left\langle P^*\left|\overline{q}_1 q_2\right|0\right\rangle \\ &= g_{P^*PV}\frac{m_{P^*}}{m_D^2 - m_{P^*}^2} f_{P^*}, \end{aligned} \tag{A.6}$$

where g_{P^*PV} is a strong coupling constant and m_{P^*} and f_{P^*} are the mass and decay constant of the pseudoscalar resonance P^*. Therefore, η and η' are the dominant resonances for the final states of $K^{*\pm}K^{\mp}$, which can be expressed as flavor mixing of η_q and η_s,

$$\begin{pmatrix} \eta \\ \eta' \end{pmatrix} = \begin{pmatrix} \cos\phi & -\sin\phi \\ \sin\phi & \cos\phi \end{pmatrix} \begin{pmatrix} \eta_q \\ \eta_s \end{pmatrix} \tag{A.7}$$

where ϕ is the mixing angle and η_q and η_s are defined by

$$\begin{aligned} \eta_q &= \frac{1}{\sqrt{2}}\left(u\overline{u} + d\overline{d}\right), \\ \eta_s &= s\overline{s}. \end{aligned} \tag{A.8}$$

The decay constants of η and η' are defined by

$$\begin{aligned} \left\langle 0\left|\overline{u}\gamma_\mu\gamma_5 u\right|\eta\left(p\right)\right\rangle &= if_\eta^u p_\mu, \\ \left\langle 0\left|\overline{u}\gamma_\mu\gamma_5 u\right|\eta'\left(p\right)\right\rangle &= if_{\eta'}^u p_\mu, \\ \left\langle 0\left|\overline{d}\gamma_\mu\gamma_5 d\right|\eta\left(p\right)\right\rangle &= if_\eta^d p_\mu, \\ \left\langle 0\left|\overline{d}\gamma_\mu\gamma_5 d\right|\eta'\left(p\right)\right\rangle &= if_{\eta'}^d p_\mu, \\ \left\langle 0\left|\overline{s}\gamma_\mu\gamma_5 s\right|\eta\left(p\right)\right\rangle &= if_\eta^s p_\mu, \\ \left\langle 0\left|\overline{s}\gamma_\mu\gamma_5 s\right|\eta'\left(p\right)\right\rangle &= if_{\eta'}^s p_\mu, \end{aligned} \tag{A.9}$$

where

$$\begin{aligned} f_\eta^u &= f_\eta^d = \frac{1}{\sqrt{2}} f_\eta^q, \\ f_{\eta'}^u &= f_{\eta'}^d = \frac{1}{\sqrt{2}} f_{\eta'}^q. \end{aligned} \tag{A.10}$$

According to [81, 82], the decay constants of η and η' can be expressed as

$$\begin{aligned} f_\eta^q &= f_q \cos\phi, \\ f_{\eta'}^q &= f_q \sin\phi, \\ f_\eta^s &= -f_s \sin\phi, \\ f_{\eta'}^s &= f_s \cos\phi, \end{aligned} \tag{A.11}$$

where $f_q = (1.07 \pm 0.02) f_\pi$ and $f_s = (1.34 \pm 0.02) f_\pi$ [81], and the mixing angle $\phi = (40.4 \pm 0.6)^\circ$ [83]. Other decay constants used in this paper are listed in Table 5.

The transition form factors $A_0^{D^0\to K^{*-}}$ and $F_1^{D^0\to K^-}$, based on the relativistic covariant light-front quark model [85], are expressed as a momentum-dependent, 3-parameter form (the parameters can be found in Table 6):

$$F\left(q^2\right) = \frac{F\left(0\right)}{1 - a\left(q^2/m_D^2\right) + b\left(q^2/m_D^2\right)^2}. \tag{A.12}$$

(4) Decay Rate. The decay width takes the form

$$\Gamma_{D\to KK^*} = \frac{\left|\mathbf{p}_1\right|^3}{8\pi m_{K^*}^2}\left|\frac{\mathscr{M}_{D\to KK^*}}{\varepsilon^*\cdot p_D}\right|^2, \tag{A.13}$$

Table 5: The meson decay constants used in this paper (MeV) [57, 84].

f_{K^*}	f_ρ	f_K	f_π	f_D
220(5)	216(3)	156(0.4)	130(1.7)	208(10)

Table 6: The parameters of $D \longrightarrow K^*, K$ transitions form factors in (A.12).

Form factor	$A_0^{D\longrightarrow K^*}$	$F_1^{D\longrightarrow K}$
$F(0)$	0.69	0.78
a	1.04	1.05
b	0.44	0.23

where $\mathbf{p}_1$ represents the center of mass (c.m.) 3-momentum of each meson in the final state and is given by

$$|\mathbf{p}_1| = \frac{\sqrt{\left[\left(m_D^2 - \left(m_{K^*} + m_K\right)^2\right)\left(m_D^2 - \left(m_{K^*} - m_K\right)^2\right)\right]}}{2m_D}. \quad \text{(A.14)}$$

$\mathscr{M}$ is the corresponding decay amplitude.

Data Availability

No data were used to support this study.

Conflicts of Interest

The authors declare that there are no conflicts of interest regarding the publication of this paper.

Acknowledgments

This work was partially supported by National Natural Science Foundation of China (Project Nos. 11447021, 11575077, and 11705081), National Natural Science Foundation of Hunan Province (Project No. 2016JJ3104), the Innovation Group of Nuclear and Particle Physics in USC, and the China Scholarship Council.

References

[1] J. H. Christenson, J. W. Cronin, V. L. Fitch, and R. Turlay, "Evidence for the 2π Decay of the $K_2{}^0$ Meson," *Physical Review Letters*, vol. 13, no. 4, pp. 138–140, 1964.

[2] M. Kobayashi and T. Maskawa, "*CP*-violation in the renormalizable theory of weak interaction," *Progress of Theoretical and Experimental Physics*, vol. 49, pp. 652–657, 1973.

[3] N. Cabibbo, "Unitary symmetry and leptonic decays," *Physical Review Letters*, vol. 10, no. 12, pp. 531–533, 1963.

[4] R. Aaij, LHCb Collaboration et al., "Measurement of *CP* Violation in the Phase Space of $B^\pm \longrightarrow K^\pm\pi^+\pi^-$ and $B^\pm \longrightarrow K^\pm K^+K^-$ Decays," *Physical Review Letters*, vol. 111, no. 2, Article ID 101801, 2017.

[5] R. Aaij, LHCb Collaboration et al., "Measurement of *CP* Violation in the Phase Space of $B^\pm \longrightarrow K^+K^-\pi^\pm$ and $B^\pm \longrightarrow \pi^+\pi^-\pi^\pm$ Decays," *Physical Review Letters*, vol. 112, no. 2, Article ID 011801, 2014.

[6] R. Aaij, LHCb Collaboration et al., "Measurements of *CP* violation in the three-body phase space of charmless $B^\pm$ decays," *Physical Review D*, vol. 90, Article ID 112004, 2014.

[7] J. H. A. Nogueira, S. Amato, A. Austregesilo et al., "Summary of the 2015 LHCb workshop on multi-body decays of D and B mesons," https://arxiv.org/abs/1605.03889.

[8] Z.-H. Zhang, X.-H. Guo, and Y.-D. Yang, "*CP* violation in $B^\pm \longrightarrow \pi^\pm\pi^+\pi^-$ in the region with low invariant mass of one $\pi^+\pi^-$ pair," *Physical Review D*, vol. 87, Article ID 076007, 2013.

[9] I. Bediaga, T. Frederico, and O. Lourenço, "*CP* violation and *CPT* invariance in $B^\pm$ decays with final state interactions," *Physical Review D*, vol. 89, Article ID 094013, 2014.

[10] H.-Y. Cheng and C.-K. Chua, "Branching fractions and direct *CP* violation in charmless three-body decays of *B* mesons," *Physical Review D*, vol. 88, Article ID 114014, 2013.

[11] Z.-H. Zhang, X.-H. Guo, and Y.-D. Yang, "CP violation induced by the interference of scalar and vector resonances in three-body decays of bottom mesons," https://arxiv.org/abs/1308.5242.

[12] B. Bhattacharya, M. Gronau, and J. L. Rosner, "CP asymmetries in three-body $B^\pm$ decays to charged pions and kaons," *Physics Letters B*, vol. 726, no. 1-3, pp. 337–343, 2013.

[13] D. Xu, G.-N. Li, and X.-G. He, "Large SU(3) Breaking Effects and CP Violation in B^+ Decays Into Three Charged Octet Pseudoscalar Mesons," *International Journal of Modern Physics A*, vol. 29, Article ID 1450011, 2014.

[14] W.-F. Wang, H.-C. Hu, H.-N. Li, and C.-D. Lü, "Direct *CP* asymmetries of three-body *B* decays in perturbative QCD," *Physical Review D*, vol. 89, Article ID 074031, 2014.

[15] Z.-H. Zhang, C. Wang, and X.-H. Guo, "Possible large *CP* violation in three-body decays of heavy baryon," *Physics Letters B*, vol. 751, pp. 430–433, 2015.

[16] C. Wang, Z.-H. Zhang, Z.-Y. Wang, and X.-H. Guo, "Localized direct CP violation in $B^\pm \longrightarrow \rho^0(\omega)\pi^\pm \longrightarrow \pi^+\pi^-\pi^\pm$," *The European Physical Journal C*, vol. 75, p. 536, 2015.

[17] J. H. A. Nogueira, I. Bediaga, A. B. R. Cavalcante, T. Frederico, and O. Lourenço, "*CP* violation: Dalitz interference, *CPT*, and final state interactions," *Physical Review D*, vol. 92, Article ID 054010, 2015.

[18] J. Dedonder, A. Furman, R. Kamiński, L. Leśniak, and B. Loiseau, "S-, P- and D-wave $\pi\pi$ final state interactions and CP violation in $B^\pm \longrightarrow \pi^\pm\pi^\mp\pi^\pm$ decays," *Acta Physica Polonica B*, vol. 42, no. 9, Article ID 2013, 2011.

[19] B. El-Bennich, A. Furman, R. Kamiński, L. Leśniak, and B. Loiseau, "Interference between $f_0(980)$ and $\rho(770)^0$ resonances in $B \longrightarrow \pi^+\pi^-K$ decays," *Physical Review D*, vol. 74, Article ID 114009, 2006.

[20] I. Bigi and A. Sanda, "On $D^0\overline{D}^0$ mixing and *CP* violation," *Physics Letters B*, vol. 171, no. 2-3, pp. 320–324, 1986.

[21] G. Blaylock, A. Seiden, and Y. Nir, "The role of CP violation in $D^0\overline{D}^0$ mixing," *Physics Letters B*, vol. 335, no. 3, pp. 555–560, 1995.

[22] S. Bergmann, Y. Grossman, Z. Ligeti, Y. Nir, and A. A. Petrov, "Lessons from CLEO and FOCUS measurements of D^0-$\overline{D}^0$ mixing parameters," *Physics Letters B*, vol. 486, no. 3-4, pp. 418–425, 2000.

[23] U. Nierste and S. Schacht, "Neutral D⟶KK* decays as discovery channels for charm *CP* violation," *Physical Review Letters*, vol. 119, Article ID 251801, 2017.

[24] G. Bonvicini, CLEO Collaboration et al., "Search for CP violation in $D^0 \longrightarrow K^o_S\pi^0$, $D^0 \longrightarrow \pi^0\pi^0$ and $D^0 \longrightarrow K^o_S K^o_S$ decays," *Physical Review D*, vol. 63, Article ID 071101, 2001.

[25] J. M. Link, "Search for *CP* Violation in the decays $D^+ \longrightarrow K_S\pi^+$ and $D^+ \longrightarrow K_S K^+$," *Physical Review Letters*, vol. 88, Article ID 041602, 2002.

[26] T. Aaltonen, CDF Collaboration et al., "Measurement of *CP*-violating asymmetries in $D^0 \longrightarrow \pi^+\pi^-$ and $D^0 \longrightarrow K^+K^-$ decays at CDF," *Physical Review D*, vol. 85, Article ID 012009, 2012.

[27] R. Cenci, "Mixing and CP Violation in Charm Decays at BABAR," in *Proceedings of the 7th International Workshop on the CKM Unitarity Triangle (CKM 2012)*, Cincinnati, Ohio, USA, 2012.

[28] J. P. Lees, BABAR Collaboration et al., "Search for *CP* violation in the decays $D^\pm \longrightarrow K^o_S K^\pm$, $D^\pm_s \longrightarrow K^o_S K^\pm$, and $D^\pm_s \longrightarrow K^o_S\pi^\pm$," *Physical Review D*, vol. 87, Article ID 052012, 2013.

[29] M. Starič, A. Abdesselam, I. Adachi et al., "Measurement of D^0-$\overline{D}^0$ mixing and search for *CP* violation in $D^0 \longrightarrow K^+K^-, \pi^+\pi^-$ decays with the full Belle data set," *Physics Letter B*, vol. 753, pp. 412–418, 2016.

[30] R. Aaij, R. Aaij, B. Adeva et al., "Measurement of *CP* asymmetries in $D^\pm \longrightarrow \eta\prime\pi^\pm$ and $D^\pm_s \longrightarrow \eta\prime\pi^\pm$ decays," *Physics Letters B*, vol. 771, pp. 21–30, 2017.

[31] R. Aaij, LHCb Collaboration et al., "Measurements of charm mixing and *CP* violation using $D^0 \longrightarrow K^\pm\pi^\mp$ decays," *Physical Review D*, vol. 95, Article ID 052004, 2017.

[32] LHCb Collaboration, "Search for *CP* violation in the phase space of $D^0 \longrightarrow \pi^+\pi^-\pi^+\pi^-$ decays," *Physics Letters B*, vol. 769, pp. 345–356, 2017.

[33] V. Bhardwaj, "Latest Charm Mixing and CP results from B-factories," in *Proceedings of the 9th International Workshop on the CKM Unitarity Triangle (CKM2016)*, vol. 139, Mumbai, India, 2017.

[34] Y. Grossman, A. L. Kagan, Y. Nir et al., "New physics and CP violation in singly Cabibbo suppressed Ddecays," *Physical Review D*, vol. 75, Article ID 036008, 2007.

[35] J. D. Bjorken, "Topics in B-physics," *Nuclear Physics B (Proceedings Supplements)*, vol. 11, no. C, pp. 325–341, 1989.

[36] M. J. Dugan and B. Grinstein, "QCD basis for factorization in decays of heavy mesons," *Physics Letters B*, vol. 255, no. 4, pp. 583–588, 1991.

[37] M. Beneke, G. Buchalla, M. Neubert, and C. T. Sachrajda, "QCD factorization for $B \longrightarrow \pi\pi$ decays: strong phases and CP violation in the heavy quark limit," *Physical Review Letters*, vol. 83, no. 10, pp. 1914–1917, 1999.

[38] M. Beneke and M. Neubert, "QCD factorization for B⟶PP and B⟶PV decays," *Nuclear Physics B*, vol. 675, no. 1-2, pp. 333–415, 2003.

[39] D. R. Boito, J. Dedonder, B. El-Bennich, O. Leitner, and B. Loiseau, "Scalar resonances in a unitary," *Physical Review D*, vol. 96, Article ID 113003, 2017.

[40] A. Furmana, R. Kamińskia, L. Leśniaka, and B. Loiseaub, "Long-distance effects and final state interactions in $B \longrightarrow \pi\pi K$ and $B \longrightarrow K\overline{K}K$ decays," *Physics Letters B*, vol. 622, pp. 207–217, 2005.

[41] Y.-Y. Keum, H.-N. Li, A. I. Sanda et al., "Penguin enhancement and $\overrightarrow{B}K\pi$ decays in perturbative QCD," *Physical Review D*, vol. 63, Article ID 054008, 2001.

[42] C. W. Bauer, D. Pirjol, I. Z. Rothstein, and I. W. Stewart, "B⟶M_1M_2: Factorization, charming penguins, strong phases, and polarization," *Physical Review D*, vol. 70, Article ID 054015, 2004.

[43] B. Loiseau, "Theory overview on amplitude analyses with charm decays," in *Proceedings of the 8th International Workshop on Charm Physics (Charm 2016)*, Bologna, Italy, 2017.

[44] H.-Y. Cheng and C.-W. Chiang, "Direct CP violation in two-body hadronic charmed meson decays," *Physical Review D*, vol. 85, no. 3, Article ID 034036, 2012, Erratum: [Physical Review D, vol. 85, Article ID 079903, 2012].

[45] L.-L. Chau, "Quark mixing in weak interactions," *Physics Reports*, vol. 95, no. 1, pp. 1–94, 1983.

[46] B. Bhattacharya, M. Gronau, and J. L. Rosner, "Publisher's Note:," *Physical Review D*, vol. 85, Article ID 054014, 2012.

[47] H.-Y. Cheng, C.-W. Chiang, and A.-L. Kuo, "Global analysis of two-body D⟶VP decays within the framework of flavor symmetry," *Physical Review D*, vol. 93, Article ID 114010, 2016.

[48] H.-N. Li, C.-D. Lu, F.-S. Yu et al., "Branching ratios and direct CP asymmetries in D⟶PP decays," *Physical Review D*, vol. 86, Article ID 036012, 2012.

[49] Q. Qin, H.-N. Li, C.-D. Lü, and F.-S. Yu, "Branching ratios and direct CP asymmetries in D⟶PV decays," *Physical Review D*, vol. 89, Article ID 054006, 2014.

[50] B. Aubert (BABAR Collaboration) et al., "Limits on $D^0 - \overline{D}^0$ Mixing and CP Violation from the Ratio of Lifetimes for Decay to $K^-\pi^+$, K^-K^+, and $\pi^-\pi^+$," *Physical Review Letters*, vol. 91, Article ID 121801, 2003.

[51] K. Abe (Belle Collaboration) et al., "Measurement of the $D^0\overline{D}^0$ lifetime difference using $D^0 \longrightarrow K\pi/KK$ decays," in *Proceedings of the 21st International Symposium on Lepton and Photon Interactions at High Energies*, pp. 11–16, Batavia, ILL, USA, 2003, https://arxiv.org/abs/hep-ex/0308034.

[52] Y.-Y. Keum, H.-N. Li, and A. I. Sandac, "Fat penguins and imaginary penguins in perturbative QCD," *Physics Letters B*, vol. 504, pp. 6–14, 2001.

[53] C.-D. Lü, K. Ukai, and M.-Z. Yang, "Branching ratio and CP violation of B⟶ $\pi\pi$ decays in the perturbative QCD approach," *Physical Review D*, vol. 63, Article ID 074009, 2001.

[54] F.-S. Yu, X.-X. Wang, and C.-D. Lü, "Nonleptonic two-body decays of charmed mesons," *Physical Review D*, vol. 84, Article ID 074019, 2011.

[55] C. Cawlfield (CLEO Collaboration) et al., "Measurement of interfering $K^{*+}K^-$and $K^{*-}K^+$amplitudes in the decay $D^0 \longrightarrow K^+K^-\pi^0$," *Physical Review D*, vol. 74, Article ID 031108, 2006.

[56] B. Aubert, L. L. Zhang, S. Chen et al., "Amplitude analysis of the decay $D^0 \longrightarrow K^-K^+\pi^0$," *Physical Review D*, vol. 76, Article ID 011102, 2007.

[57] C. Patrignani, K. Agashe, G. Aielli et al., "Review of Particle Physics," *Chinese Physics C*, vol. 40, no. 10, Article ID 100001, 2016.

[58] J. L. Rosner and D. A. Suprun, "Measuring the relative strong phase in $D^0 \longrightarrow K^{*+}K^-$and $D^0 \longrightarrow K^{*-}K^+$ decays," *Physical Review D*, vol. 68, Article ID 054010, 2003.

[59] I. Bediaga, I. I. Bigi, A. Gomes, G. Guerrer, J. Miranda, and A. C. dos Reis, "On a CP anisotropy measurement in the Dalitz plot," *Physical Review D*, vol. 80, no. 9, Article ID 096006, 2009.

[60] S. M. Flatte, "Coupled-channel analysis of the $\pi\eta$ and $K\overline{K}$ systems near $K\overline{K}$ threshold," *Physics Letters B*, vol. 63, no. 2, pp. 224–227, 1976.

[61] M. Golden and B. Grinstein, "Enhanced CP violations in hadronic charm decays," *Physics Letters B*, vol. 222, no. 3-4, pp. 501–506, 1989.

[62] G. F. Giudice, G. Isidori, and P. Paradisi, "Direct CP violation in charm and flavor mixing beyond the SM," *Journal of High Energy Physics*, vol. 1204, Article ID 060, 2012.

[63] M. Gronau, "New physics in singly Cabibbo-suppressed D decays," *Physics Letters B*, vol. 738, pp. 136–139, 2014.

[64] J. Brod, A. L. Kagan, and J. Zupan, "Size of direct CP violation in singly Cabibbo-suppressed D decays," *Physical Review D*, vol. 86, Article ID 014023, 2012.

[65] Y. Grossman, A. L. Kagan, and J. Zupan, "Testing for new physics in singly Cabibbo suppressed D decays," *Physical Review D*, vol. 85, Article ID 114036, 2012.

[66] G. Isidori, J. F. Kamenik, Z. Ligetie, and G. Perez, "Implications of the LHCb evidence for charm CP violation," *Physics Letters B*, vol. 711, no. 1, pp. 46–51, 2012.

[67] M. Beneke, G. Buchalla, M. Neubert, and C. T. Sachrajda, "QCD factorization in $B\longrightarrow \pi K$, $\pi\pi$ decays and extraction of Wolfenstein parameters," *Nuclear Physics B*, vol. 606, no. 1-2, pp. 245–321, 2001.

[68] H.-n. Li, S. Mishima, and A. I. Sanda, "Resolution to the $B\longrightarrow \pi K$ puzzle," *Physical Review D*, vol. 72, Article ID 114005, 2005.

[69] R. Aaij (LHCb Collaboration) et al., "Evidence for CP violation in time-integrated $D^0 \longrightarrow h^-h^+$ decay rates," *Physical Review Letters*, vol. 108, Article ID 111602, 2012.

[70] F. Gabbiani, E. Gabrielli, A. Masiero, and L. Silvestrini, "A complete analysis of FCNC and CP constraints in general SUSY extensions of the standard model," *Nuclear Physics B*, vol. 477, no. 2, pp. 321–352, 1996.

[71] E. Gabrielli, A. Masiero, and L. Silvestrini, "Flavour changing neutral currents and CP violating processes in generalized supersymmetric theories," *Physics Letters B*, vol. 374, no. 1-3, pp. 80–86, 1996.

[72] J. S. Hagelin, S. Kelley, and T. Tanaka, "Supersymmetric flavor-changing neutral currents: exact amplitudes and phenomenological analysis," *Nuclear Physics B*, vol. 415, no. 2, pp. 293–331, 1994.

[73] G. De Pietro, "Charm physics prospects at Belle II," in *Proceedings of the European Physical Society Conference on High Energy Physics (EPS-HEP2017)*, vol. 314, Venice, Italy, 2017.

[74] T. Abe, I. Adachi, K. Adamczyk et al., "Belle II Technical Design Report," https://arxiv.org/abs/1011.0352.

[75] J. P. Lees, V. Poireau, V. Tisserand et al., "Measurement of the $D^0 \longrightarrow \pi^- e^+ \nu_e$ differential decay branching fraction as a function of q^2 and study of form factor parametrizations," *Physical Review D*, vol. 91, Article ID 052022, 2015.

[76] N. K. Nisar, G. B. Mohanty, K. Trabelsi et al., "Search for the rare decay $D^0 \longrightarrow \gamma\gamma$ at Belle," *Physical Review D*, vol. 93, Article ID 051102, 2016.

[77] M. Ablikim (BESIII Collaboration) et al., "Search for $D^0 \longrightarrow \gamma\gamma$ and improved measurement of the branching fraction for $D^0 \longrightarrow \pi^0\pi^0$," *Physicla Review D*, vol. 91, no. 11, Article ID 112015, 2015.

[78] G. Buchalla, A. J. Buras, and M. E. Lautenbacher, "Weak decays beyond leading logarithms," *Reviews of Modern Physics*, vol. 68, no. 4, pp. 1125–1244, 1996.

[79] A. J. Buras, M. E. Lautenbacher, and G. Ostermaier, "Waiting for the top quark mass, $K^+ \longrightarrow \pi^+\nu\overline{\nu}$, $B_s^0 - \overline{B}_s^0$ mixing, and *CP* asymmetries in *B* decays," *Physical Review D*, vol. 50, Article ID 3433, 1994.

[80] J. Charles, A. Höcker, and H. Lacker, "*CP* violation and the CKM matrix: assessing the impact of the asymmetric *B* factories," *The European Physical Journal C*, vol. 41, no. 1, pp. 1–131, 2005.

[81] T. Feldmann, P. Kroll, and B. Stech, "Mixing and decay constants of pseudoscalar mesons," *Physical Review D*, vol. 58, Article ID 114006, 1998.

[82] T. Feldmann, P. Kroll, and B. Stech, "Mixing and decay constants of pseudoscalar mesons: the sequel," *Physics Letters B*, vol. 449, no. 3-4, pp. 339–346, 1999.

[83] F. Ambrosino, A. Antonelli, and M. Antonelli, "A global fit to determine the pseudoscalar mixing angle and the gluonium content of the η' meson," *Journal of High Energy Physics*, vol. 907, Article ID 105, 2009.

[84] P. Ball, G. W. Jones, and R. Zwicky, "$B\longrightarrow V\gamma$ beyond QCD factorization," *Physical Review D*, vol. 75, Article ID 054004, 2007.

[85] H.-Y. Cheng, C.-K. Chua, and C.-W. Hwang, "Covariant light-front approach for s-wave and p-wave mesons: Its application to decay constants and form factors," *Physical Review D*, vol. 69, Article ID 074025, 2004.

Hindawi
Advances in High Energy Physics
Volume 2018, Article ID 5428734, 7 pages
https://doi.org/10.1155/2018/5428734

Research Article

Study on the Resonant Parameters of Y (4220) and Y (4390)

Jielei Zhang, Limin Yuan, and Rumin Wang

College of Physics and Electronic Engineering, Xinyang Normal University, Xinyang 464000, China

Correspondence should be addressed to Jielei Zhang; zhangjielei@ihep.ac.cn

Received 31 July 2018; Revised 7 October 2018; Accepted 30 October 2018; Published 18 November 2018

Guest Editor: Tao Luo

Many vector charmonium-like states have been reported recently in the cross sections of $e^+e^- \longrightarrow \omega\chi_{c0}$, $\pi^+\pi^- h_c$, $\pi^+\pi^- J/\psi$, $\pi^+\pi^-\psi(3686)$, and $\pi^+ D^0 D^{*-} + c.c.$ To better understand the nature of these states, a combined fit is performed to these cross sections by using three resonances $Y(4220)$, $Y(4390)$, and $Y(4660)$. The resonant parameters for the three resonances are obtained. We emphasize that two resonances $Y(4220)$ and $Y(4390)$ are sufficient to explain these cross sections below 4.6 GeV. The lower limits of $Y(4220)$ and $Y(4390)$'s leptonic decay widths are also determined to be $(36.4 \pm 2.0 \pm 4.2)$ and $(123.8 \pm 6.5 \pm 9.0)$ eV.

In the last decade, charmonium physics has gained renewed strong interest from both the theoretical and the experimental side, due to the observation of a series of charmonium-like states, such as the $X(3872)$ [1], the $Y(4260)$ [2], and the $Y(4360)$ [3]. These states do not fit in the conventional level system of charmonium states and are good candidates for exotic states not encompassed by the naive quark model [4]. Moreover, many charged charmonium-like states or their neutral partners [5] were observed, which might indicate the presence of new dynamics in this energy region.

$Y(4260)$ is the first charmonium-like state, which was observed in the process $e^+e^- \longrightarrow \pi^+\pi^- J/\psi$ by the *BABAR* experiment using an initial-state-radiation (ISR) technique [2]. This observation was immediately confirmed by the CLEO [6] and Belle experiments [7] in the same process. Being produced in e^+e^- annihilation, the Y state has quantum numbers $J^{PC} = 1^{--}$. $Y(4360)$ is the second Y state, which was observed in the $e^+e^- \longrightarrow \gamma_{\mathrm{ISR}} Y(4360) \longrightarrow \gamma_{\mathrm{ISR}}\pi^+\pi^-\psi(3686)$ by *BABAR* [3] and subsequently confirmed by Belle experiment [8]. Belle also observed another structure, $Y(4660)$, in the $\pi^+\pi^-\psi(3686)$ [8]. The observation of these Y states has stimulated substantial theoretical discussions on their nature [4].

Recently, with higher statistic data, the $e^+e^- \longrightarrow \pi^+\pi^- J/\psi$ cross section was measured by BESIII experiment more precisely [9]. The fine structure was observed for $Y(4260)$ in $e^+e^- \longrightarrow \pi^+\pi^- J/\psi$. The $Y(4260)$ structure is a combination of two resonances: the lower one is $Y(4220)$ and the higher is $Y(4320)$. Using the results for $e^+e^- \longrightarrow \pi^+\pi^-\psi(3686)$ from Belle [10], *BABAR* [11], and BESIII experiments [12], the authors of [13] also observed the fine structure for $Y(4360)$ in $e^+e^- \longrightarrow \pi^+\pi^-\psi(3686)$, inferring that the $Y(4360)$ structure is also a combination of two resonances: the lower one is $Y(4220)$ and the higher is $Y(4360)$. The $Y(4220)$ state also is observed in the processes $e^+e^- \longrightarrow \omega\chi_{c0}$ [14, 15], $\pi^+\pi^- h_c$ [16], and $\pi^+ D^0 D^{*-} + c.c.$ [17] by BESIII experiment. In the $e^+e^- \longrightarrow \pi^+\pi^- h_c$ and $\pi^+ D^0 D^{*-} + c.c.$, besides the $Y(4220)$, another Y state $Y(4390)$ is observed [16, 17]. The parameters for $Y(4220)$, $Y(4320)$, $Y(4360)$, and $Y(4390)$ states in different processes are listed in Table 1. In addition, the authors of [18] have performed a combine fit to the cross sections of $e^+e^- \longrightarrow \omega\chi_{c0}$, $\pi^+\pi^- h_c$, $\pi^+\pi^- J/\psi$, and $\pi^+ D^0 D^{*-} + c.c.$ to obtain the resonant parameters for $Y(4220)$, $Y(4320)$, and $Y(4390)$ states.

These states challenge the understanding of charmonium spectroscopy as well as QCD calculations [4, 19, 20]. According to potential models, there are five vector charmonium states between the $1D$ state $\psi(3770)$ and 4.7 GeV/c^2, namely, the $3S$, $2D$, $4S$, $3D$, and $5S$ states [4]. Besides the three well-established structures observed in the inclusive hadronic cross section [21], i.e., $\psi(4040)$, $\psi(4160)$, and $\psi(4415)$, five Y states, i.e., $Y(4220)$, $Y(4320)$, $Y(4360)$, $Y(4390)$, and $Y(4660)$, have been observed. These newly observed Y states exceed the number of vector charmonium states predicted by potential

Table 1: The parameters for $Y(4220)$ ($\omega\chi_{c0}$, $\pi^+\pi^- h_c$, $\pi^+\pi^- J/\psi$, $\pi^+\pi^-\psi(3686)$ and $\pi^+ D^0 D^{*-}$ + *c.c.*), $Y(4320)$ ($\pi^+\pi^- J/\psi$), $Y(4360)$ ($\pi^+\pi^-\psi(3686)$), and $Y(4390)$ ($\pi^+\pi^- h_c$ and $\pi^+ D^0 D^{*-}$ + *c.c.*) states in different processes. The first uncertainties are statistical, and the second systematic.

	$Y(4220)$		$Y(4320)/Y(4360)/Y(4390)$	
	M (MeV/c^2)	Γ (MeV)	M (MeV/c^2)	Γ (MeV)
$\omega\chi_{c0}$ [15]	$4226 \pm 8 \pm 6$	$39 \pm 12 \pm 2$		
$\pi^+\pi^- h_c$ [16]	$4218.4^{+5.5}_{-4.5} \pm 0.9$	$66.0^{+12.3}_{-8.3} \pm 0.4$	$4391.5^{+6.3}_{-6.8} \pm 1.0$	$139.5^{+16.2}_{-20.6} \pm 0.6$
$\pi^+\pi^- J/\psi$ [9]	$4222.0 \pm 3.1 \pm 1.4$	$44.1 \pm 4.3 \pm 2.0$	$4320.0 \pm 10.4 \pm 7.0$	$101.4^{+25.3}_{-19.7} \pm 10.2$
$\pi^+\pi^-\psi(3686)$ [13]	$4209.1 \pm 6.8 \pm 7.0$	$76.6 \pm 14.2 \pm 2.4$	$4383.7 \pm 2.9 \pm 6.2$	$94.2 \pm 7.3 \pm 2.0$
$\pi^+ D^0 D^{*-}$ + *c.c.* [17]	$4224.8 \pm 5.6 \pm 4.0$	$72.3 \pm 9.1 \pm 0.9$	$4400.1 \pm 9.3 \pm 2.1$	$181.7 \pm 16.9 \pm 7.4$

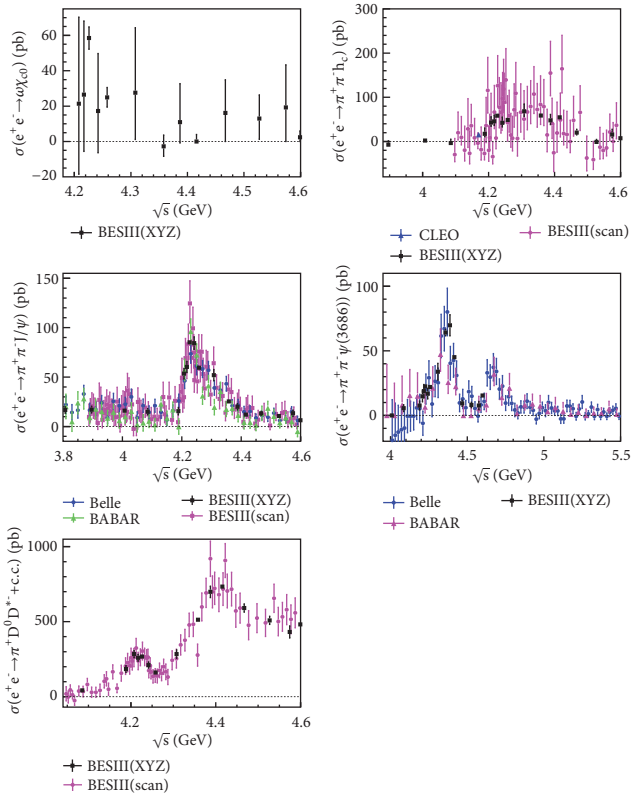

Figure 1: Cross sections of $e^+e^- \longrightarrow \omega\chi_{c0}$, $\pi^+\pi^- h_c$, $\pi^+\pi^- J/\psi$, $\pi^+\pi^-\psi(3686)$, and $\pi^+ D^0 D^{*-}$ + *c.c.* measured by Belle, *BABAR*, CLEO, and BESIII experiments.

models in this energy region. They are thus good candidates for exotic states, such as hybrid states, tetraquark states, and molecule states [5].

Figure 1 shows the cross sections of $e^+e^- \longrightarrow \omega\chi_{c0}$ [14, 15], $\pi^+\pi^- h_c$ [16, 22], $\pi^+\pi^- J/\psi$ [9, 23, 24], $\pi^+\pi^-\psi(3686)$ [10–12], and $\pi^+ D^0 D^{*-}$ + *c.c.* [17] measured by Belle, *BABAR*, CLEO, and BESIII experiments. For data from BESIII, "XYZ" data sample refers to the energy points with integrated luminosity larger than 40 pb^{-1} and "scan" data sample refers to the energy points with integrated luminosity smaller than 20 pb^{-1}. In this paper, we perform a combined fit to these cross sections.

These vector charmonium-like states in the fit are assumed to be resonances. We parameterize the cross section with the coherent sum of a few amplitudes, either resonance represented by a Breit-Wigner (BW) function or nonresonant production term parameterized with a phase space function or an exponential function. The BW function used in this article is [18]

$$BW\left(\sqrt{s}\right) = \frac{\sqrt{12\pi\Gamma_{e^+e^-}\mathscr{B}_f\Gamma}}{s - M^2 + iM\Gamma}\sqrt{\frac{PS\left(\sqrt{s}\right)}{PS\left(M\right)}}, \tag{1}$$

where M and Γ are the mass and total width of the resonance, respectively; $\Gamma_{e^+e^-}$ is the partial width to e^+e^-, $\mathscr{B}_f$ is the branching fraction of the resonance decays into final state f, and $PS(\sqrt{s})$ is the phase space factor that increases smoothly from the mass threshold with the $\sqrt{s}$ [21]. In the fit, $\Gamma_{e^+e^-}$ and $\mathscr{B}_f$ can not be obtained separately; we can only extract the product $\Gamma_{e^+e^-}\mathscr{B}_f$.

Ref. [18] has performed a combine fit to the cross sections of $e^+e^- \longrightarrow \omega\chi_{c0}$, $\pi^+\pi^- h_c$, $\pi^+\pi^- J/\psi$, and $\pi^+ D^0 D^{*-}$ + *c.c.*, while the cross section of $e^+e^- \longrightarrow \pi^+\pi^-\psi(3686)$ is not included. In Ref. [18], the resonances $Y(4320)$ and $Y(4390)$ are regarded as different states in the fit, while, from Table 1, we notice that the parameters for $Y(4320)$, $Y(4360)$, and $Y(4390)$ are relatively close. Although there are some differences in the obtained mass and width in different channels, there are only a few data points with small errors around 4.4 GeV. It is not reasonable that there are three states in such a close position. In addition, the analysis in [25] also indicates that the charmonium-like states $Y(4360)$ in the $\pi^+\pi^-\psi(3686)$ and $Y(4320)$ in the $\pi^+\pi^- J/\psi$ should be the same state. Therefore, we consider $Y(4320)$, $Y(4360)$, and $Y(4390)$ as the same state, which has been suggested in [26]. The same state is marked as "$Y(4390)$" in this paper. A least χ^2 fit method is used to perform a combined fit to the five cross sections using three resonances $Y(4220)$, $Y(4390)$, and $Y(4660)$, assuming the two resonances $Y(4220)$ and $Y(4390)$ are the same two states in these processes. The fit functions are

$$\sigma_{\omega\chi_{c0}}\left(\sqrt{s}\right) = \left|BW_1\left(\sqrt{s}\right)\right|^2, \tag{2}$$

$$\sigma_{\pi^+\pi^- h_c}\left(\sqrt{s}\right) = \left|BW_1\left(\sqrt{s}\right) + BW_2\left(\sqrt{s}\right)e^{i\phi_1}\right|^2, \tag{3}$$

$$\sigma_{\pi^+\pi^- J/\psi}\left(\sqrt{s}\right) = \left|c_1\sqrt{\exp\left(\sqrt{s}\right)} + BW_1\left(\sqrt{s}\right)e^{i\phi_2} + BW_2\left(\sqrt{s}\right)e^{i\phi_3}\right|^2, \tag{4}$$

$$\sigma_{\pi^+\pi^-\psi(3686)}\left(\sqrt{s}\right) = \left|BW_1\left(\sqrt{s}\right) + BW_2\left(\sqrt{s}\right)e^{i\phi_4} + BW_3\left(\sqrt{s}\right)e^{i\phi_5}\right|^2, \quad (5)$$

$$\sigma_{\pi^+D^0D^{*-}+c.c.}\left(\sqrt{s}\right) = \left|c_2\sqrt{PS\left(\sqrt{s}\right)} + BW_1\left(\sqrt{s}\right)e^{i\phi_6} + BW_2\left(\sqrt{s}\right)e^{i\phi_7}\right|^2, \quad (6)$$

where BW_1, BW_2, and BW_3 denote the resonances $Y(4220)$, $Y(4390)$, and $Y(4660)$, respectively; $PS(\sqrt{s})$ is the phase space factor; $\exp(\sqrt{s}) = e^{-p_0(\sqrt{s}-M_{th})}PS(\sqrt{s})$ is an exponential function, where p_0 is free parameter, $M_{th} = 2m_\pi + m_{J/\psi}$ is the mass threshold of the $\pi^+\pi^-J/\psi$ system; ϕ_1, ϕ_2, ϕ_3, ϕ_4, ϕ_5, ϕ_6, and ϕ_7 are relative phases; c_1 and c_2 are amplitudes of exponential function term and phase space term.

We fit to the cross sections of $e^+e^- \longrightarrow \omega\chi_{c0}$, $\pi^+\pi^-h_c$, $\pi^+\pi^-J/\psi$, $\pi^+\pi^-\psi(3686)$, and $\pi^+D^0D^{*-} + c.c.$ simultaneously. The fits for $e^+e^- \longrightarrow \omega\chi_{c0}$, $\pi^+\pi^-h_c$, $\pi^+\pi^-J/\psi$, $\pi^+\pi^-\psi(3686)$, and $\pi^+D^0D^{*-} + c.c.$ are found to have one solution, two solutions, four solutions, four solutions, and four solutions with the same minimum values of χ^2, respectively. The masses and widths of the resonances are identical, but the $\Gamma_{e^+e^-}\mathscr{B}_f$ vary with the different solutions for each process.

Figure 2 shows the fit results with a goodness of the fit being $\chi^2/ndf = 460/474 = 0.97$, corresponding to a confidence level of 67%. The good fit indicates that the assumption that the two resonances $Y(4220)$ and $Y(4390)$ are same two states in these processes is reasonable. From fit results, we can get $M_{Y(4220)} = (4216.5 \pm 1.4)$ MeV/c^2, $\Gamma_{Y(4220)} = (61.1 \pm 2.3)$ MeV; $M_{Y(4390)} = (4383.5 \pm 1.9)$ MeV/c^2, $\Gamma_{Y(4390)} = (114.5 \pm 5.4)$ MeV; $M_{Y(4660)} = (4623.4 \pm 10.5)$ MeV/c^2, $\Gamma_{Y(4660)} = (106.1 \pm 16.2)$ MeV. The all obtained resonant parameters from fit are listed in Table 2.

From the fit results, the obtained parameters of $Y(4660)$ are quite different from Belle's results [10]. There are two main reasons. One is that the interference between $Y(4390)$ and $Y(4660)$ has large influence on $Y(4660)$'s parameters. We can see the obtained combined $Y(4390)$'s parameters are very different from the $Y(4360)$'s parameters from Belle's results; it will lead to the fact that $Y(4660)$'s parameters are also different. Another is that the data point at 4.6 GeV from BESIII has very small error, so the fitted $Y(4660)$'s BW curve is influenced greatly by this data point. From Figure 2, we can see that, in order to cover the data point, the $Y(4660)$'s BW curve has to have some deviations from Belle data points around 4.66 GeV.

The systematic uncertainties on the resonant parameters in the combined fit to the cross sections of $e^+e^- \longrightarrow \omega\chi_{c0}$, $\pi^+\pi^-h_c$, $\pi^+\pi^-J/\psi$, $\pi^+\pi^-\psi(3686)$, and $\pi^+D^0D^{*-} + c.c.$ are mainly from the uncertainties of the center-of-mass energy determination, parametrization of the BW function, background shape, and the cross section measurements.

Since the uncertainty of the beam energy is about 0.8 MeV at BESIII, so the uncertainty of the resonant parameters caused by the beam energy is estimated by varying $\sqrt{s}$ within 0.8 MeV for BESIII data. Instead of using a constant total width, we assume an energy dependent width to estimate the uncertainty due to parametrization of BW function. To model the $e^+e^- \longrightarrow \pi^+\pi^-J/\psi$ cross section near 4 GeV, a BW function is used to replace the exponential function, and the differences of the fit results in the two methods are taken as the uncertainty from background shape. The uncertainty of the cross section measurements will affect the resonant parameters in fit, we vary the cross sections within the systematic uncertainty, and the differences in the final results are taken as the uncertainty. By assuming all these sources of systematic uncertainties are independent, we add them in quadrature. The systematic uncertainty from the parametrization of the BW function for the parameters mass and width is dominant, while the systematic uncertainty from the cross section measurements for the parameter $\Gamma_{e^+e^-}\mathscr{B}_f$ is dominant.

The leptonic decay width for a vector state is an important quantity for discriminating various theoretical models [27–29]. By considering the isospin symmetric modes of the measured channels, we can estimate the lower limits on the leptonic partial width of the $Y(4220)$ and $Y(4390)$ decays. For an isospin-zero charmonium-like state, we expect

$$\begin{aligned}
&\mathscr{B}\left(Y \longrightarrow \pi\pi h_c\right) = \frac{3}{2} \times \mathscr{B}\left(Y \longrightarrow \pi^+\pi^- h_c\right),\\
&\mathscr{B}\left(Y \longrightarrow \frac{\pi\pi J}{\psi}\right) = \frac{3}{2} \times \mathscr{B}\left(Y \longrightarrow \frac{\pi^+\pi^- J}{\psi}\right),\\
&\mathscr{B}\left(Y \longrightarrow \pi\pi\psi\left(3686\right)\right)\\
&\quad = \frac{3}{2} \times \mathscr{B}\left(Y \longrightarrow \pi^+\pi^-\psi\left(3686\right)\right),\\
&\mathscr{B}\left(Y \longrightarrow \pi D\overline{D}^*\right) = 3 \times \mathscr{B}\left(Y \longrightarrow \pi^+D^0D^{*-} + c.c.\right),
\end{aligned} \quad (7)$$

so we have

$$\begin{aligned}
\Gamma_{e^+e^-}^{Y(4220)} &= \sum_f \mathscr{B}\left(Y\left(4220\right) \longrightarrow f\right) \times \Gamma_{e^+e^-}^{Y(4220)}\\
&= \mathscr{B}\left(Y\left(4220\right) \longrightarrow \omega\chi_{c0}\right) \times \Gamma_{e^+e^-}^{Y(4220)}\\
&\quad + \mathscr{B}\left(Y\left(4220\right) \longrightarrow \pi\pi h_c\right) \times \Gamma_{e^+e^-}^{Y(4220)}\\
&\quad + \mathscr{B}\left(Y\left(4220\right) \longrightarrow \frac{\pi\pi J}{\psi}\right) \times \Gamma_{e^+e^-}^{Y(4220)}\\
&\quad + \mathscr{B}\left(Y\left(4220\right) \longrightarrow \pi\pi\psi\left(3686\right)\right) \times \Gamma_{e^+e^-}^{Y(4220)}\\
&\quad + \mathscr{B}\left(Y\left(4220\right) \longrightarrow \pi D\overline{D}^*\right) \times \Gamma_{e^+e^-}^{Y(4220)} + \cdots
\end{aligned} \quad (8)$$

and

$$\begin{aligned}
\Gamma_{e^+e^-}^{Y(4390)} &= \sum_f \mathscr{B}\left(Y\left(4390\right) \longrightarrow f\right) \times \Gamma_{e^+e^-}^{Y(4390)}\\
&= \mathscr{B}\left(Y\left(4390\right) \longrightarrow \pi\pi h_c\right) \times \Gamma_{e^+e^-}^{Y(4390)}\\
&\quad + \mathscr{B}\left(Y\left(4390\right) \longrightarrow \frac{\pi\pi J}{\psi}\right) \times \Gamma_{e^+e^-}^{Y(4390)}
\end{aligned}$$

Table 2: The fitted parameters from the combined fit to the cross sections of $e^+e^- \longrightarrow \omega\chi_{c0}, \pi^+\pi^- h_c, \pi^+\pi^- J/\psi, \pi^+\pi^-\psi(3686)$, and $\pi^+ D^0 D^{*-} + c.c.$ The first uncertainties are statistical, and the second systematic.

(a)

Parameter	$Y(4220)$	$Y(4390)$	$Y(4660)$
M (MeV/c^2)	$4216.5 \pm 1.4 \pm 3.2$	$4383.5 \pm 1.9 \pm 6.0$	$4623.4 \pm 10.5 \pm 16.1$
Γ (MeV)	$61.1 \pm 2.3 \pm 3.1$	$114.5 \pm 5.4 \pm 9.9$	$106.1 \pm 16.2 \pm 17.5$

(b)

Parameter	SolutionI	SolutionII	SolutionIII	SolutionIV
$\Gamma_{e^+e^-}^{Y(4220)} \mathscr{B}(Y(4220) \longrightarrow \omega\chi_{c0})$ (eV)	$3.5 \pm 0.4 \pm 0.5$			
$\Gamma_{e^+e^-}^{Y(4220)} \mathscr{B}(Y(4220) \longrightarrow \pi^+\pi^- h_c)$ (eV)	$6.5 \pm 0.5 \pm 1.1$	$3.1 \pm 0.2 \pm 0.8$		
$\Gamma_{e^+e^-}^{Y(4390)} \mathscr{B}(Y(4390) \longrightarrow \pi^+\pi^- h_c)$ (eV)	$15.1 \pm 1.0 \pm 2.8$	$7.5 \pm 0.6 \pm 1.8$		
$\Gamma_{e^+e^-}^{Y(4220)} \mathscr{B}(Y(4220) \longrightarrow \pi^+\pi^- J/\psi)$ (eV)	$10.5 \pm 0.5 \pm 1.7$	$12.3 \pm 0.7 \pm 2.1$	$3.7 \pm 0.3 \pm 0.6$	$3.1 \pm 0.3 \pm 0.6$
$\Gamma_{e^+e^-}^{Y(4390)} \mathscr{B}(Y(4390) \longrightarrow \pi^+\pi^- J/\psi)$ (eV)	$0.3 \pm 0.1 \pm 0.1$	$12.1 \pm 0.7 \pm 3.2$	$10.4 \pm 0.6 \pm 2.3$	$0.3 \pm 0.1 \pm 0.1$
$\Gamma_{e^+e^-}^{Y(4220)} \mathscr{B}(Y(4220) \longrightarrow \pi^+\pi^-\psi(3686))$ (eV)	$1.6 \pm 0.3 \pm 0.3$	$1.5 \pm 0.3 \pm 0.3$	$1.6 \pm 0.3 \pm 0.3$	$1.5 \pm 0.3 \pm 0.3$
$\Gamma_{e^+e^-}^{Y(4390)} \mathscr{B}(Y(4390) \longrightarrow \pi^+\pi^-\psi(3686))$ (eV)	$13.4 \pm 1.1 \pm 1.4$	$9.9 \pm 1.0 \pm 1.2$	$13.4 \pm 1.1 \pm 1.4$	$9.9 \pm 1.0 \pm 1.2$
$\Gamma_{e^+e^-}^{Y(4660)} \mathscr{B}(Y(4660) \longrightarrow \pi^+\pi^-\psi(3686))$ (eV)	$8.8 \pm 1.2 \pm 1.4$	$3.0 \pm 0.5 \pm 0.6$	$8.8 \pm 1.2 \pm 1.4$	$3.0 \pm 0.5 \pm 0.6$
$\Gamma_{e^+e^-}^{Y(4220)} \mathscr{B}(Y(4220) \longrightarrow \pi^+ D^0 D^{*-} + c.c.)$ (eV)	$39.0 \pm 2.5 \pm 3.1$	$7.1 \pm 0.6 \pm 1.3$	$57.5 \pm 3.0 \pm 6.1$	$10.5 \pm 1.1 \pm 2.7$
$\Gamma_{e^+e^-}^{Y(4390)} \mathscr{B}(Y(4390) \longrightarrow \pi^+ D^0 D^{*-} + c.c.)$ (eV)	$55.4 \pm 5.7 \pm 7.8$	$32.4 \pm 2.1 \pm 2.8$	$313.6 \pm 13.9 \pm 26.4$	$183.1 \pm 11.2 \pm 19.3$

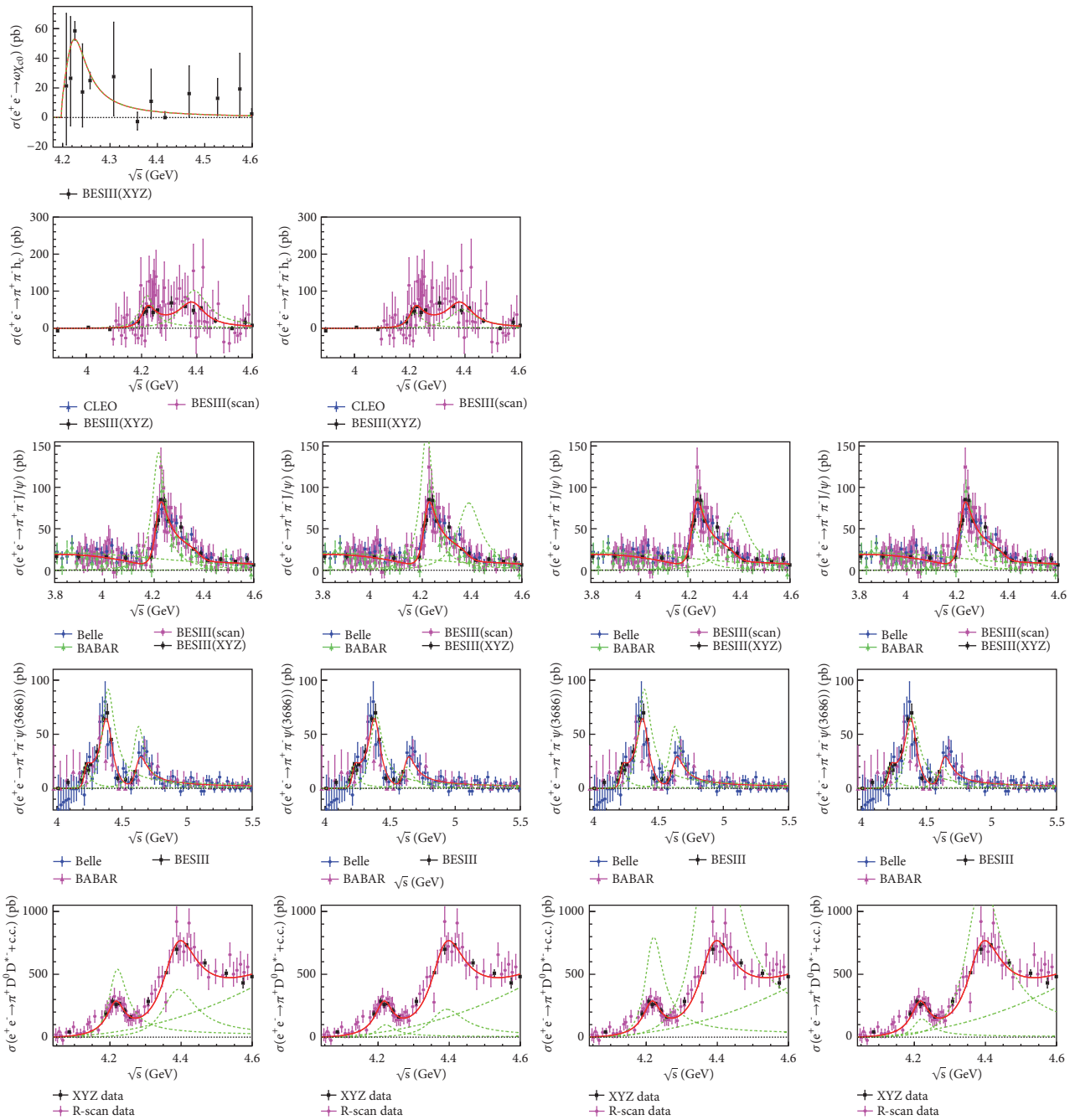

FIGURE 2: The results of the combined fit to the cross sections of $e^+e^- \longrightarrow \omega\chi_{c0}$, $\pi^+\pi^- h_c$, $\pi^+\pi^- J/\psi$, $\pi^+\pi^-\psi(3686)$, and $\pi^+ D^0 D^{*-} + c.c.$ (from the top to the bottom row). The solid red curves show the best fits, and the dashed green ones are individual components.

$$+ \mathscr{B}\left(Y(4390) \longrightarrow \pi\pi\psi(3686)\right) \times \Gamma_{e^+e^-}^{Y(4390)}$$
$$+ \mathscr{B}\left(Y(4390) \longrightarrow \pi D\overline{D}^{*}\right) \times \Gamma_{e^+e^-}^{Y(4390)} + \cdots \tag{9}$$

By inserting the numbers from Table 2, considering the solutions with the smallest $\mathscr{B}(Y(4220) \longrightarrow f) \times \Gamma_{e^+e^-}^{Y(4220)}$ and $\mathscr{B}(Y(4390) \longrightarrow f) \times \Gamma_{e^+e^-}^{Y(4390)}$, we obtain

$$\begin{aligned}\Gamma_{e^+e^-}^{Y(4220)} &= (3.5 \pm 0.4 \pm 0.5) + \frac{3}{2} \times (3.1 \pm 0.2 \pm 0.8) \\ &+ \frac{3}{2} \times (3.1 \pm 0.3 \pm 0.6) + \frac{3}{2} \\ &\times (1.5 \pm 0.3 \pm 0.3) + 3 \times (7.1 \pm 0.6 \pm 1.3) \\ &+ \cdots \text{ eV} = (36.4 \pm 2.0 \pm 4.2) + \cdots \text{ eV} \\ &> (36.4 \pm 2.0 \pm 4.2) \text{ eV},\end{aligned} \tag{10}$$

and

$$\begin{aligned}\Gamma_{e^+e^-}^{Y(4390)} &= \frac{3}{2}\times(7.5\pm0.6\pm1.8)+\frac{3}{2}\times(0.3\pm0.1\pm0.1)\\ &\quad+\frac{3}{2}\times(9.9\pm1.0\pm1.2)+3\\ &\quad\times(32.4\pm2.1\pm2.8)+\cdots\ \text{eV}\\ &=(123.8\pm6.5\pm9.0)+\cdots\ \text{eV}\\ &>(123.8\pm6.5\pm9.0)\ \text{eV},\end{aligned}\tag{11}$$

where the first uncertainties are statistical, and the second systematic.

On the other hand, if we take the results with the largest $\mathcal{B}(Y(4220)\longrightarrow f)\times\Gamma_{e^+e^-}^{Y(4220)}$ and $\mathcal{B}(Y(4390)\longrightarrow f)\times\Gamma_{e^+e^-}^{Y(4390)}$ in Table 2, we obtain $\Gamma_{e^+e^-}^{Y(4220)}=(206.6\pm9.1\pm18.7)+\cdots$ and $\Gamma_{e^+e^-}^{Y(4390)}=(1001.7\pm41.8\pm79.5)+\cdots$ eV. This means that the leptonic partial widths of $Y(4220)$ and $Y(4390)$ can be as large as 200 and 1000 eV or even higher based on current information, because maybe there are some other decay channels for $Y(4220)$ and $Y(4390)$ that we have not observed.

In summary, a combined fit is performed to the cross sections of $e^+e^-\longrightarrow\omega\chi_{c0}$, $\pi^+\pi^-h_c$, $\pi^+\pi^-J/\psi$, $\pi^+\pi^-\psi(3686)$, and $\pi^+D^0D^{*-}+c.c.$ by using three resonances $Y(4220)$, $Y(4390)$, and $Y(4660)$. The parameters are determined to be $M_{Y(4220)}=(4216.5\pm1.4\pm3.2)\ \text{MeV}/c^2$, $\Gamma_{Y(4220)}=(61.1\pm2.3\pm3.1)$ MeV; $M_{Y(4390)}=(4383.5\pm1.9\pm6.0)\ \text{MeV}/c^2$, $\Gamma_{Y(4390)}=(114.5\pm5.4\pm9.9)$ MeV; $M_{Y(4660)}=(4623.4\pm10.5\pm16.1)\ \text{MeV}/c^2$, $\Gamma_{Y(4660)}=(106.1\pm16.2\pm17.5)$ MeV, where the first uncertainties are statistical and the second systematic. We emphasize that two resonances $Y(4220)$ and $Y(4390)$ are sufficient to explain these cross sections below 4.6 GeV. The resonances $Y(4320)$, $Y(4360)$, and $Y(4390)$ should be one state. The lower limits of $Y(4220)$ and $Y(4390)$'s leptonic decay widths are also determined to be $(36.4\pm2.0\pm4.2)$ and $(123.8\pm6.5\pm9.0)$ eV. These results will be useful in understanding the nature of charmonium-like states in this energy region. Higher precision measurements around this energy region are desired, and this can be achieved in BESIII and BelleII experiments in the further.

Data Availability

All the data used in this work are from Ref. [9–12, 14–17, 22–24].

Conflicts of Interest

The authors declare that they have no conflicts of interest.

Acknowledgments

This work is supported by the Foundation of Henan Educational Committee (No. 19A140015), Nanhu Scholars Program for Young Scholars of Xinyang Normal University, and Open Research Program of Large Research Infrastructures (2017), Chinese Academy of Sciences.

References

[1] S.-K. Choi et al., "Observation of a Narrow Charmoniumlike State in Exclusive $B^{\pm}\longrightarrow K^{\pm}\pi^+\pi^-J/\psi$ Decays," *Physical Review Letters*, vol. 91, Article ID 262001, 2003.

[2] B. Aubert, R. Barate, and D. Boutigny, "Observation of a Broad Structure in the $\pi^+\pi^-J/\psi$ Mass Spectrum around 4.26 GeV/c^2," *Physical Review Letters*, vol. 95, Article ID 142001, 2005.

[3] B. Abelev et al., "vidence of a Broad Structure at an Invariant Mass of 4.32 GeV/c^2 in the Reaction $e^+e^-\longrightarrow\pi+\pi^-\psi(2^S)$ Measured at BABAR," *Physical Review Letters*, vol. 98, no. 19, Article ID 212001, 2007.

[4] N. Brambilla, "Heavy quarkonium: progress, puzzles, and opportunities," *The European Physical Journal C*, vol. 71, Article ID 1534, 2011.

[5] H.-X. Chen, W. Chen, and X. Liu, "The hidden-charm pentaquark and tetraquark states," *Physics Reports*, vol. 639, pp. 1–121, 2016.

[6] S. Nojiri and S. D. Odintsov, "Confirmation of the *Y(4260)* resonance production in initial state radiation," *Physical Review D*, vol. 74, Article ID 091104, 2006.

[7] C. Z. Yuan, "Measurement of the $e^+e^-\longrightarrow\pi^+\pi^-J/\psi$ Cross Section Via Initial-State Radiation at Belle," *Physical Review Letters*, vol. 99, Article ID 182004, 2007.

[8] T. Aoyama, M. Hayakawa, T. Kinoshita, and M. Nio, "Observation of Two Resonant Structures in $e^+e^-\longrightarrow\pi^+\pi^-\psi(2S)$ via Initial-State Radiation at Belle," *Physical Review Letters*, vol. 99, Article ID 142002, 2007.

[9] M. Ablikim et al., "Precise Measurement of the $e^+e^-\longrightarrow\pi^+\pi^-J/\psi$ Cross Section at Center-of-Mass Energies from 3.77 to 4.60 GeV," *Physical Review Letters*, vol. 118, Article ID 092001, 2017.

[10] X. L. Wang et al., "Measurement of $e^+e^-\longrightarrow\pi^+\pi^-\psi(2S)$ via initial state radiation at Belle," *Physical Review D*, vol. 91, Article ID 112007, 2015.

[11] J. P. Lees, "Study of the reaction $e^+e^-\longrightarrow\psi(2S)\pi^+\pi^-$ via initial-state radiation at *BaBar*," *Physical Review D*, vol. 89, Article ID 111103, 2014.

[12] M. Ablikim et al., "BESIII Collaboration," *Physical Review D: Particles, Fields, Gravitation and Cosmology*, vol. 96, Article ID 032004, 2017.

[13] J. Zhang and J. Zhang, "Revisiting the $e^+e^-\longrightarrow\pi^+\pi^-\psi(3686)$ line shape," *Physical Review D*, vol. 96, Article ID 054008, 2017.

[14] M. Ablikim, "Study of $e^+e^-\longrightarrow\omega\chi_{cJ}$ at Center of Mass Energies from 4.21 to 4.42 GeV," *Physical Review Letters*, vol. 114, Article ID 092003, 2015.

[15] M. Ablikim et al., "Observation of $e^+e_-\longrightarrow\omega\chi_{c1,2}$ near $\sqrt{s}$=4.42 and 4.6 GeV," *Physical Review D*, vol. 93, Article ID 011102, 2016.

[16] M. Ablikim et al., "Evidence of Two Resonant Structures in $e^+e^-\longrightarrow\pi^+\pi^-h_c$," *Physical Review Letters*, vol. 118, Article ID 092002, 2017.

[17] C. Yuan, "The BESIII Collaboration," in *10th workshop of the France China Particle Physics Laboratory*, Tsinghua University, Beijing, China, 2017, http://indico.ihep.ac.cn/event/6651/timetable/#20170329.detailed.

[18] X. Y. Gao, C. P. Shen, and C. Z. Yuan, "Particles, Fields, Gravitation and Cosmology," *Physical Review D*, vol. 95, Article ID 092007, 2017.

[19] R. A. Briceno, "Issues and Opportunities in Exotic Hadrons," *Chinese Physics C*, vol. 40, Article ID 042001, 2016.

[20] M. N. Anwar, Y. Lu, and B. S. Zou, "Modeling charmonium-η decays of $J^{PC}=1^{--}$ higher charmonia," *Physical Review D*, vol. 95, Article ID 114031, 2017.

[21] C. Patrignani, "Particle Data Group," *Chinese Physics C*, vol. 40, Article ID 100001, 2016.

[22] T. K. Pedlar, "Observation of the $h_c(1P)$ Using e^+e^- Collisions above the *DD* Threshold," *Physical Review Letters*, vol. 107, Article ID 041803, 2011.

[23] Z. Q. Liu et al., "Study of $e^+e- \longrightarrow \pi^+\pi^- J/\psi$ and Observation of a Charged Charmoniumlike State at Belle," *Physical Review Letters*, vol. 110, Article ID 252002, 2013.

[24] Q.-G. Huang, Y.-S. Piao, and S.-Y. Zhou, "Study of the reaction $e^+e^- \longrightarrow J/psi\pi^+\pi^-$ via initial-state radiation at BaBar," *Physical Review D*, vol. 86, Article ID 051102, 2016.

[25] J. Zhang and L. Yuan, "Combined fit to the $e^+e^- \longrightarrow \pi^+\pi^- J/\psi$ and $e^+e^- \longrightarrow \pi^+\pi^-\psi(3686)$ line shape," *The European Physical Journal C*, vol. 77, p. 727, 2017.

[26] J. Soto, "Heavy Quarkonium Hybrids," *Nuclear and Particle Physics Proceedings*, vol. 87, pp. 294–296, 2018.

[27] Y. Chen, W. F. Chiu, and M. Gong, "Exotic vector charmonium and its leptonic decay width," *Chinese Physics C*, vol. 40, no. 8, Article ID 081002, 2016.

[28] A. V. Astashenok and S. D. Odintsov, "Production of Y(4260) as a hadronic molecule state DD_1+c.c. in e^+e^- annihilations," *Physical Review D: Particles, Fields, Gravitation and Cosmology*, vol. 94, no. 6, Article ID 063008, 2016.

[29] L. Y. Dai, M. Shi, G. Y. Tang, and H. Q. Zheng, "Nature of X(4260)," *Physical Review D*, vol. 92, Article ID 014020, 2015.

Hindawi
Advances in High Energy Physics
Volume 2018, Article ID 8095653, 8 pages
https://doi.org/10.1155/2018/8095653

Research Article

Mass Spectra and Decay Constants of Heavy-Light Mesons: A Case Study of QCD Sum Rules and Quark Model

Halil Mutuk

Physics Department, Ondokuz Mayis University, 55139 Samsun, Turkey

Correspondence should be addressed to Halil Mutuk; halilmutuk@gmail.com

Received 25 July 2018; Revised 27 August 2018; Accepted 5 September 2018; Published 25 September 2018

Guest Editor: Xian-Wei Kang

We visited mass spectra and decay constants of pseudoscalar and vector heavy-light mesons (B, B_s, D, and D_S) in the framework of QCD sum rule and quark model. The harmonic oscillator wave function was used in quark model while a simple interpolating current was used in QCD sum rule calculation. We obtained good results in accordance with the available experimental data and theoretical studies.

1. Introduction

The ultimate objective of particle physics is to investigate and examine the structure and the origin of matter. For this purpose many theoretical and experimental endeavors are made, and a resulting model was theorized, which we call the Standard Model of particle physics. Quark model which was proposed by Gell-Mann and Zweig in 1964 [1] is a part of the Standard Model, and interprets hadrons fairly compatible with the experimental data. According to the quark model, mesons are made of quark-antiquark pairs ($q\overline{q}$) and baryons are made of three quarks qqq or antiquarks $\overline{q}\,\overline{q}\,\overline{q}$. These quarks interact with each other via emitting and/or absorbing gluons. The resulting theory which explains these interactions is the Quantum Chromodynamics (QCD).

The interaction of quarks is described by QCD, which is part of the Standard Model of particle physics. QCD is thought to be the *true* theory of strong interactions. QCD is a SU(3) gauge theory describing the interactions of six quarks which transform under the fundamental representation of SU(3) group via the exchange of gluons that transform under the adjoint representation. Although it has been more than 50 years that QCD has been proposed, a solution has been evaded. Contrary to electroweak theory, where it is possible to obtain precise results using perturbation theory, the order of precision obtained in QCD has been lower by orders of magnitude. The main reason for this is that the coupling constant (which should be the perturbation parameter) of QCD is of the order one in low energies; hence the truncation of the perturbative expansion cannot be carried out. However, it is an important subject to study the spectrum of particles predicted by QCD.

Since perturbation theory is not applicable, a nonperturbative approach has to be used to study systems that involve strong interactions. Some of the nonperturbative approaches to strongly interacting systems are the QCD sum rules, quark models, and lattice QCD. The advantage of QCD sum rules and lattice QCD is that they are based on QCD itself, whereas, in quark models, one assumes a potential energy between the quarks and solves a Schrödinger-like equation. The advantage of quark models, on the other hand, is that it allows one to study also the excited states, whereas, in QCD sum rules and lattice QCD, only the ground state or in some exceptional cases the first excited state can be studied.

In quark models one assumes a potential interaction among quarks which makes model as a nonrelativistic approach. Therefore, the systems that are best suited for study in quark models are the heavy quark system which contain c or b quarks. The bare masses of u, d, and s quarks are 2 MeV, 4 MeV, and 96 MeV, respectively [2]. At a first look, quark model seems rather difficult to apply to light quarks. Capstick et al. presented reasonable explanations to link quark models including a minimal amount of relativity to the basics of QCD [3]. Although the pole masses of u, d and s quarks are

very low and hence they are relativistic, in constituent quark models, instead of treating the physical u, d, and s quarks, one treats the so-called constituent quarks, which are nothing else than quarks dressed by gluons and other sea quarks inside the hadron. The masses of constituent quarks are around 300 MeV and hence they can also be treated in nonrelativistic quark models. Such an approach has been applied to light quark systems with a surprising success [4–6], leading to that model so-called Constituent Quark Model (CQM), which, based on the Gell Mann-Zweig idea, explains meson and baryon bound systems.

A different situation is for heavy-light quark systems ($Q\overline{q}$). For example an electron is more relativistic in the hydrogen atom (p, e^-) than in the positronium atom (e^+e^-) [7]. Positronium can be taken as a naive model for quarkonium. The binding energy of the positronium is half of the hydrogen atom and is small compared to the electron mass. For this reason the positronium bound state can be described by nonrelativistic quantum mechanics. But the decay of the positronium resonance is a purely relativistic phenomenon. Nevertheless, we can attempt to apply the quark model to heavy-light mesons. The outcome of this attempt is not directly using of Heavy Quark Symmetry (HQS), but one aspect of it. Mesons are two particle systems and the reduced mass is dominated by the light quark mass, $1/\mu = 1/m + 1/M \simeq 1/M$ if $M \gg m$. The spectra for ($c\overline{q}$) and ($b\overline{q}$) should be very similar under this assumption [7]. Indeed reasonable spectroscopy of D and B mesons can be obtained. There is a rich literature for the spectrum and dynamics of the heavy-light mesons, for example [8–25]. In [26], they studied semileptonic D and D_s decays based on the predictions of the relevant form factors from the covariant light-front quark model. In [27], the authors studied the Cabibbo-Kobayashi-Maskawa matrix element $|V_{ub}|$ which is not determined up to now in inclusive or exclusive B decays.

Light quark physics is a key topic to understand the nature of QCD. They can be thought of a probe of the strong interactions by means of nonperturbative effects [28]. Heavy-light meson systems ($Q\overline{q}$) is also central to enlighten the nature of QCD and strong interactions. Heavy-light meson spectroscopy has been the subject of both theoretical and experimental studies since the 2000s. Especially in the charm sector, new excited states were observed in D and D_s mesons [28–32].

An important feature of B meson physics is that it is sensitive to New Physics (NP) Beyond the Standard Model (BSM) via rare decays. Furthermore hadronic decay channels of B mesons might have more systematic uncertainties due to the model indetermination, compared to the lepton/photon decay channels. Thus studying $B \longrightarrow lepton/photon$ decays present a play field for the search of NP. Besides that, B factory experiments BaBar and Belle were built to test the description of quark mixing in the Standard Model. The first theoretical description of quark mixing was proposed by Cabibo in 1963 [33]. One year later in 1964, Christenson et al. discovered CP violation in neutral kaon decays with a tiny friction [34]. This phenomenon is referred to as conclusion that matter and antimatter might behave differently. Kobayashi and Maskawa generalized Cabibbo's idea by adjusting new quarks to the model [35]. In the framework of Standard Model, CP violation can be accommodated by introducing a complex phase in the 3×3 unitary Cabibo-Kobayashi-Maskawa (CKM) matrix. Indeed this phase can be measured in experiments. The cost of adding a parameter is to use a third generation of quarks. CP violation also occurs in B decays. The B factories were built to test for this purpose. B factories gave a substantial contribution to particle physics such as first observation of CP violation apart from the kaon, measurements of CKM matrix elements, measurements of purely leptonic B meson decays, and searches for new physics.

In this work, we obtained mass spectrum and decay constants of the D and B mesons via QCD Sum Rule and a Quark Model potential. We also predicted decay constant for the B_s meson where there are no specific experimental data. Harmonic oscillator wave function is used in the quark model and a sufficiently trivial interpolating current is used in QCD Sum Rule calculations. We studied ground states since they are accessible in the framework of QCD Sum Rules.

2. QCD Sum Rule Formalism

In perturbation theory we assume that the eigenvalues and eigenfunctions can be expanded in a power series as follows:

$$\begin{aligned} E_n &= E_n^0 + \lambda E_n^1 + \lambda^2 E_n^2 + \cdots \\ |n\rangle &= \left|n^0\right\rangle + \lambda \left|n^1\right\rangle + \lambda^2 \left|n^2\right\rangle + \cdots, \end{aligned} \tag{1}$$

where n is the principal quantum number and λ is a parameter. These series are in principle divergent, but they are asymptotic. This means that when the perturbation parameter is small, the first two or three terms are convergent so that the rest of the series can be ignored. In the case of QCD, due to the largeness of the parameter in lower energies, such a truncation, cannot be performed. The nonperturbative aspect of QCD makes it almost impossible to study bound states in terms of perturbation theory. For this reason, there is a need of nonperturbative methods to overwhelm this situation and study bound states. Among others such as Effective Field Theory and Lattice QCD, QCD Sum Rule is maybe the most popular nonperturbative method.

QCD Sum Rule is first formulated by Shifman, Vansthein, and Zakharov for mesons in [36] and generalized to baryons by Iofe in [37]. The basic idea of the this formalism is to study bound state phenomena in QCD from the asymptotic freedom side, *i.e.*, to start evaluation of correlation function at short distances, where quark-gluon dynamics are perturbative and move to larger distances where hadronization occurs, including nonperturbative effects and using some approximate procedure to get information on hadronic properties [38].

To obtain physical observables from QCD sum rules, a correlator of two hadronic currents which is defined as follows

$$\Pi = i \int d^4x e^{ipx} \left\langle 0 \left| \mathcal{T}\, j(x)\, j^{\dagger}(0) \right| 0 \right\rangle, \tag{2}$$

is studied. Here p is momentum and $j(x)$ is a current composed of quarks and gluon fields with the hadron's

quantum numbers. When this operator is applied to vacuum, it can create the hadron that we study. Equation (2) is known as correlation function. The fundamental assumption of the QCD sum rules is that there is a region of p where correlation function can be equivalently described at both quark and hadron sector. The former is known as QCD or OPE (Operator Product Expansion) side, and the latter is known as the phenomenological side. Matching these two sides of the sum rule, one can obtain information about hadron properties [38].

For $p^2 > 0$, resolution of identity operator of hadron states can be written between the operators. This results in correlation function as follows:

$$\Pi = \sum_h \langle 0 | j | h(p) \rangle \frac{1}{p^2 - m_h^2} \langle h(p) | j^\dagger | 0 \rangle + \text{higher states}. \tag{3}$$

It can be seen from (3) the poles in the correlation function, which indicates the presence of hadrons, created by operator $j(x)$.

For $-p^2 \gg \Lambda^2_{\text{QCD}} (p^2 < 0)$, major contribution to the correlation function will come from the $x \sim 0$ region [39]. In this case the product of two operators can be written in terms of OPE:

$$\mathcal{T}\, j(x)\, j^\dagger(0) = \sum_d C_d(x)\, O_d. \tag{4}$$

Here $C_d(x)$ are the coefficients, which can be calculated by the perturbation theory, and $O_d's$ are the operators with the mass dimension d. If Fourier transformation applies to (4), correlation function can be written as follows:

$$\Pi = \sum_d C_d^f(p) \frac{\langle O_d \rangle}{p^d}, \tag{5}$$

where $\langle O_d \rangle$ are the vacuum condensates that cannot be calculated by perturbation theory except $d = 0$. $d = 0$ corresponds to unitary operator and can be calculated via perturbation theory. Other operators can be written as $\langle \overline{q}q \rangle$ ($d = 3$); $m_q \langle \overline{q}q \rangle$ ($d = 4$), $\langle G_{\mu\nu} G^{\mu\nu} \rangle$ ($d = 4$), $\langle \overline{q} g \sigma G q \rangle$ ($d = 5$). For $d = 1$ and $d = 2$ there exists no operator. As a result of this, the expansion converges quickly although it is an infinite summation.

In order to get sum rules we must equate (3) and (5). But these two expressions are obtained in different regions of p. By using spectral density representation of correlation function, this matching can be made:

$$\Pi(p^2) = \int_0^\infty \frac{\rho(s)}{s - p^2} + \text{polynomials of } p^2. \tag{6}$$

Spectral density $\rho(s)$ can be acquired from (3). Inserting $\rho(s)$ into (6), an expression of correlation function can be obtained from (3) for $p^2 < 0$ region. If we denote $\rho^{phen}(s)$ as spectral density from (3) and $\rho^{QCD}(s)$ from (5), we get

$$\int_0^\infty ds \frac{\rho^{phen}(s)}{s - p^2} + \text{polynomials} = \int_0^\infty ds \frac{\rho^{QCD}(s)}{s - p^2} + \text{polynomials}. \tag{7}$$

In order to extract physical properties from this expression, one must eliminate the polynomial terms, for example, by using derivatives. In principle, no one knows the polynomial degree and how many polynomials are. The correct procedure is then to use the Borel transformation, which contains infinite derivative:

$$\mathcal{B}^2_M \left[\Pi(q^2) \right] = \lim_{-q^2, n \to \infty, -q^2/n = M^2} \frac{-(q^2)^{n+1}}{n!} \left(\frac{d}{dq^2} \right)^n \Pi(q^2). \tag{8}$$

Here M^2 is defined as the Borel parameter [36]. This transformation effectively removes the polynomials and makes

$$\frac{1}{s - p^2} \longrightarrow e^{-s/M^2}. \tag{9}$$

Then,

$$\sum_h \left| \langle 0 | j | h(p) \rangle \right|^2 e^{-m_h^2/M^2} + \text{higher states} = \int_0^\infty \rho^{QCD}(s)\, e^{-s/M^2}, \tag{10}$$

which resembles QCD parameters and hadronic properties. This equation still shows presence of unknown parameters. The $e^{-m_h^2/M^2}$ factor makes the contribution of small masses dominant. To parameterize contributions of higher states, quark-hadron duality approximation is used. According to quark-hadron duality, for $s > s_0$, $\rho^{phen}(s) \simeq \rho^{QCD}(s)$. $\rho^{phen}(s)$ has contribution of higher states and heavier hadrons when $s > s_0$. s_0 is called as continuum threshold and is related mass of the hadron that is studied in sum rules. So, we can write (10) as follows:

$$\left| \langle 0 | j | m_h(p) \rangle \right|^2 e^{-m_h^2/M^2} = \int_0^{s_0} \rho^{QCD}(s)\, e^{-s/M^2}. \tag{11}$$

In this equation m_h is the hadron of the smallest mass which can be created by j.

Physical properties extracted from the sum rules must be independent of Borel parameter, (M^2). Here we assume that there exist a range of M^2, called Borel window, in which two sides have a good overlap and information on the lowest state can be extracted. Minimum and maximum values of Borel window can be extracted in a way that QCD side convergence gives the minimum value, and the condition that pole contribution should be bigger than the continuum contribution gives the maximum value of Borel window [38].

2.1. Mass Sum Rule. The mass sum rule can be obtained by matching QCD and phenomenological sides of correlation function [36, 38, 39]. Here we will give the following formula:

$$m^2 = \frac{\int_{s_{min}}^{s_0} ds e^{-s/M^2} s\rho^{QCD}(s)}{\int_{s_{min}}^{s_0} ds e^{-s/M^2} \rho^{QCD}(s)}. \quad (12)$$

2.2. Decay Constant. The decay constant can be obtained from the formula [40] as follows:

$$f_{m_h}^2 = e^{m_h/M^2} \frac{1}{m_h^2} \int_{s_{min}}^{s_0} ds e^{-s/M^2} \rho^{QCD}(s), \quad (13)$$

where m_h is the hadron mass extracted from sum rules.

3. Quark Model

Also known as potential model or quark potential model, quark model considers one or more interacting particles under a given potential. In the early 60s quarks were modelled and experimental evidences were found subsequently. This approach provided a reliable basis to study and investigate particle physics and gave compatible results with the experiments.

The most important part of the quark model is the potential. After the November revolution of particle physics in 1974, the year in which charmonium states were observed, new models were proposed to calculate spectrum and radiative transitions [41–43]. The so-called Cornell potential, proposed in [42], reads as

$$V(r) = -\frac{a}{r} + br + c, \quad (14)$$

where a, b, and c are some parameters to extract from fit to the experimental data. This potential is still used with some modifications to account, for example, for hyperfine splittings in the energy levels. The other potentials such as power law potential [44], logarithmic potential [45], Richardson potential [46], Buchmüller-Tye potential [47], and Song-Lin potential [48] were used to fit quarkonium spectra and gave good results in agreement with experiments. These were phenomenological spin-independent potentials and not directly QCD motivated. The interquark potential was not derived from first principles of QCD in the early quarkonium phenomenology. This means, in terms of QCD, that potential is universal (flavour independent) and since quarks are colorless particles, it was reasonable to assume the universality as valid, despite the fact that gluons couple to color charge. These spin-independent potential models performed good but not complete explanation of the energy level splittings. If we want to accommodate these splittings in the theory, we have to take care, *i.e.*, of *spin-spin* and *spin-orbit* interactions in the model. Reference [49] reports an example of a QCD-motivated, spin- and velocity-dependent potential. These potentials deliver reliable results.

Table 1: Mass spectra of heavy-light mesons in MeV. QM denotes quark model and SR denotes sum rule calculations. The parameters are $\kappa = 0.471$, $a = 0.192\ GeV^2$, $m_c = 1.320\ GeV$, $m_b = 4.740\ GeV$ [52], $\langle\overline{q}q\rangle = 0.241\ GeV^3$, $m_u = m_d = 0.340\ GeV$, and $m_s = 0.600\ GeV$.

Meson	Exp. [2]	QM	SR	[9]	[14]
D^0/D^+	1869.3 ± 0.4	1859	1972 ± 94	1870.82	1854.7
D_s^+	1968.2 ± 0.4	2056	2118 ± 75	1966.62	1974.5
B^+/B^0	5279.0 ± 0.5	5260	5259 ± 109	5273.50	5277.2
B_s^0	5367.7 ± 1.8	5442	5488 ± 76	5365.99	5384.8

4. Elaboration of the Problem

4.1. QCD Sum Rules. In QCD sum rules, the choice of the $j(x)$ current is important, since it creates hadrons from vacuum. We used the following current:

$$j(x) = i\overline{Q}_a(x)\gamma_5 q_a(x), \quad (15)$$

where Q is heavy quark, q is light quark, a is the color index, and γ_5 is the Dirac matrix. We take care of $m_q \longrightarrow 0$ limit. In the limit of $m_q \longrightarrow 0$, there appears a flavor symmetry between b and c quarks. By this symmetry it is possible to extract information about c and b sector with the same current. b and c quarks are heavy quarks so that it cannot be expected to be in the vacuum by themselves. So it is possible to ignore such condensate terms like $\langle\alpha_s(GG/\pi)\rangle$ and $\langle\overline{q}g_s\sigma Gq\rangle$. By introducing the current term into (2), one can obtain the following spectral density:

$$\begin{aligned} F\left(s_0, M^2\right) = & -\langle q\overline{q}\rangle e^{-m_Q^2/M^2} m_Q \\ & + 6e^{-s_0/M^2} e^{-s_u/M^2} (u_1 - u_2) \\ & \times \left[e^{-s_0/M^2} M^2 \left(m_Q^2 + s(u) + M^2\right)\right. \\ & \left. - e^{-s_u/M^2} \left(m_Q^4 + M^2\left(s_0 + M^2\right)\right)\right] \end{aligned} \quad (16)$$

where $\langle q\overline{q}\rangle$ is the condensate, and u_1 and u_2 are solutions of $s(u) = m_Q^2/(1-u) + m_q^2/u = s_0$.

The mass sum rule can be obtained by taking derivative with respect to $1/M^2$ and dividing the result by (16):

$$m_h^2 = M^4 \frac{1}{F\left(s_0, M^2\right)} \frac{dF\left(s_0, M^2\right)}{dM^2}. \quad (17)$$

The decay constant sum rule can be obtained as follows:

$$f_{m_h}^2 = e^{m_h^2/M^2} \frac{1}{m_h^2} F\left(s_0, M^2\right). \quad (18)$$

The mass values and decays constants for heavy-light mesons are presented in Tables 1 and 2 and Figures 1–8.

4.2. Quark Model. Energy eigenvalues can be obtained by solving the Schrödinger equation in the quark model. The Schrödinger equation reads as follows:

$$H\left|\Psi_n\right\rangle = E_n\left|\Psi_n\right\rangle, \quad (19)$$

Table 2: Pseudoscalar and vector decay constants of heavy-light mesons in MeV. QM denotes quark model and SR denotes sum rule calculations.

Meson	Exp.	QM	SR	[9]	[16]	[53]
D^0/D^+	206 ± 8.9	199	210.25 ± 11.60	205.14	206.2 ± 7.3 ± 5.1	207.53
D_s^+	249	253	245.70 ± 7.46	241.84	245.3 ± 15.7 ± 4.5	262.56
B^+/B^0	204 ± 31	209	223.45 ± 12.4	201.09	193.4 ± 12.3 ± 4.3	208.13
B_s^0		275	277.22 ± 11	292.04	232.5 ± 18.6 ± 2.4	262.39

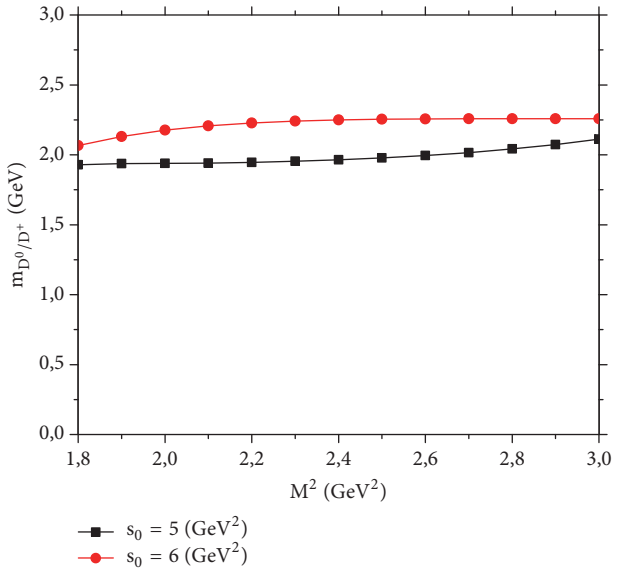

Figure 1: Borel parameter dependence of the D^0/D^+ masses.

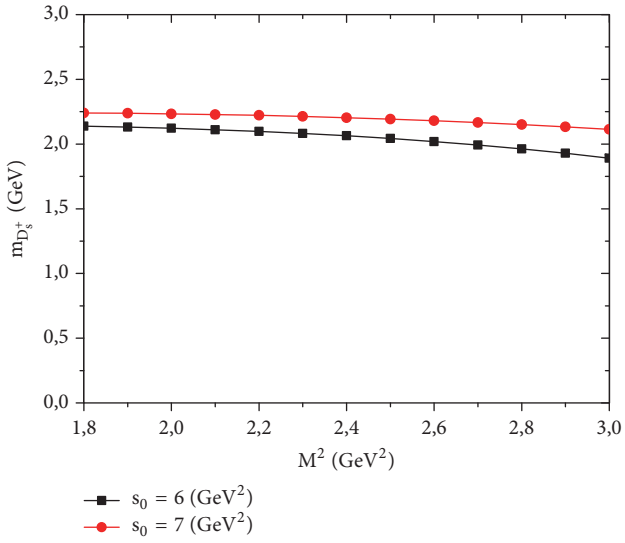

Figure 2: Borel parameter dependence of the D_s^+ mass.

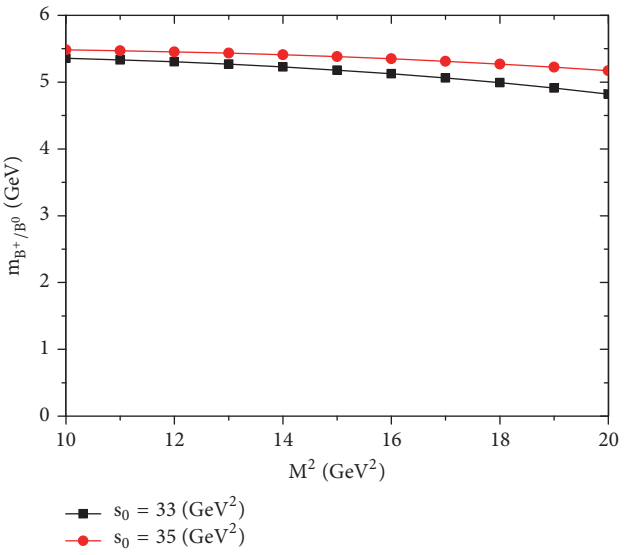

Figure 3: Borel parameter dependence of the B^+/B^0 masses.

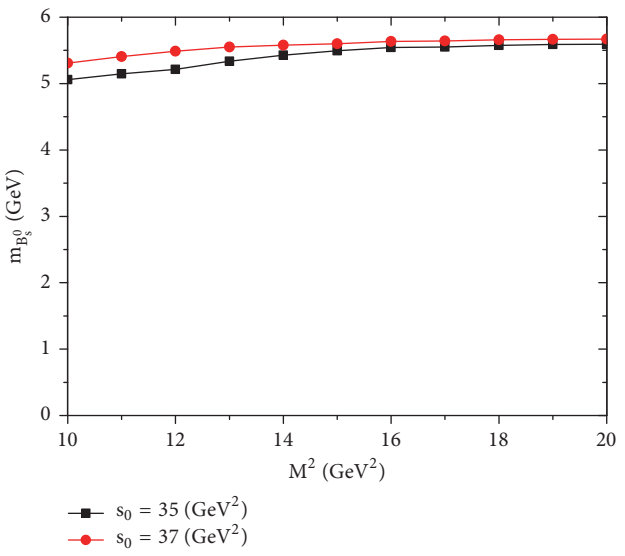

Figure 4: Borel parameter dependence of the B_s^0 mass.

where n denotes the principal quantum number. We can separate the wave function into radial R_{nl} and angular parts $Y_{lm}(\theta, \phi)$ as follows:

$$\Psi_{nlm}(r, \theta, \phi) = R_{nl}(r) Y_{lm}(\theta, \phi). \quad (20)$$

R_{nl} is the radial wave function given as follows:

$$R_{nl} = N_{nl} r^l e^{-\nu r^2} L_{(n-l)/2}^{l+1/2}\left(2\nu r^2\right), \quad (21)$$

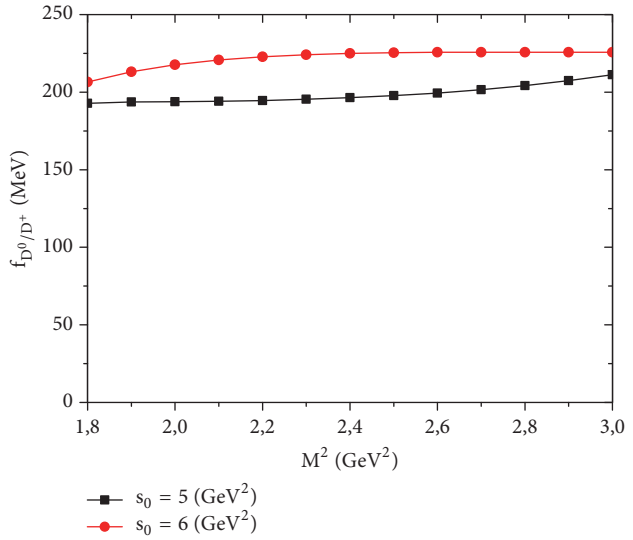

FIGURE 5: Borel parameter dependence of the D^0/D^+ decay constants.

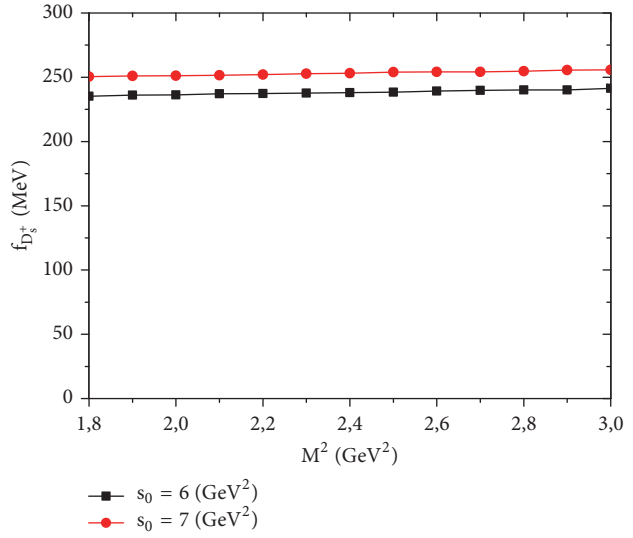

FIGURE 6: Borel parameter dependence of the D_s^+ decay constant.

with the associated Laguerre polynomials $L_{(n-l)/2}^{l+1/2}$ and the normalization constant:

$$N_{nl} = \sqrt{\sqrt{\frac{2\nu^3}{\pi}} \frac{2\left((n-l)/2\right)!\nu^l}{\left((n+l)/2+1\right)!!}}. \tag{22}$$

With the wave function in hand one can obtain masses as well as decay constants for heavy and light mesons. The mass spectra can be obtained by solving (19). For the decay constants we employ the following formulas:

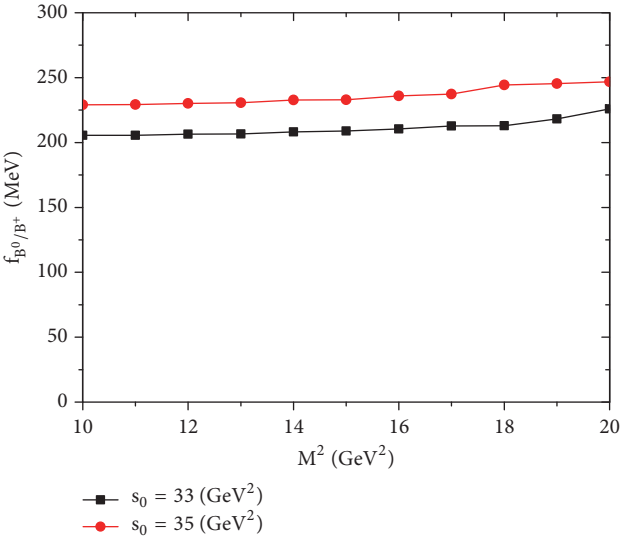

FIGURE 7: Borel parameter dependence of the B^+/B^0 decay constants.

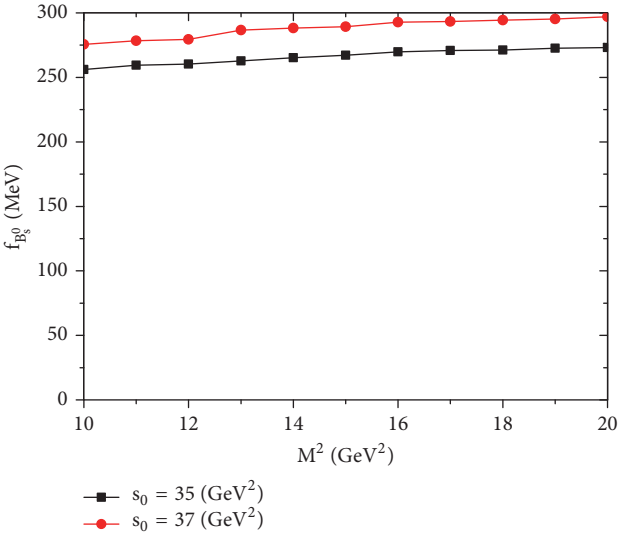

FIGURE 8: Borel parameter dependence of the B_s^0 decay constant.

The results are as follows:

$$f_p = \sqrt{\frac{3}{m_p}} \times \int \frac{d^3k}{(2\pi)^3} \sqrt{1+\frac{m_q}{E_k}} \times \sqrt{1+\frac{m_{\overline{q}}}{E_{\overline{k}}}} \times \left(1 - \frac{k^2}{\left(E_k + m_q\right)\left(E_{\overline{k}} + m_{\overline{q}}\right)}\right) \phi\left(\vec{k}\right), \tag{23}$$

for pseudoscalar mesons and

$$f_v = \sqrt{\frac{3}{m_v}} \times \int \frac{d^3k}{(2\pi)^3} \sqrt{1+\frac{m_q}{E_k}} \times \sqrt{1+\frac{m_{\overline{q}}}{E_{\overline{k}}}} \times \left(1 + \frac{k^2}{3\left(E_k + m_q\right)\left(E_{\overline{k}} + m_{\overline{q}}\right)}\right) \phi\left(\vec{k}\right), \tag{24}$$

for the vector mesons [50].

In the nonrelativistic limit, these two equations take a simple form, which is known to be Van Royen and Weisskopf relation [51]. For the meson decay constants,

$$f_{p/v}^2 = \frac{12\left|\Psi_{p/v}(0)\right|^2}{m_{p/v}}. \quad (25)$$

Here $m_{p/v}$ denotes the pseudoscalar and vector mass of the related meson.

The results are shown in Tables 1 and 2.

5. Summary and Conclusions

In this paper, we calculated mass spectra and decay constants of pseudoscalar and vector heavy-light mesons (B, B_s, D, and D_S) in the framework of QCD sum rule and quark model. Obtained results for masses of B and D mesons are in good agreement with the available experimental data. In the mass spectra, the extrapolation via quark model gave close results to experimental data compared to the QCD sum rule consideration. The QCD sum rules approach gives reasonable but not very good-matching results compared to the experimental values, because of the adopted approximation when evaluating the current, whereas the higher dimension of that operator could improve the estimates. Other potentials and further studies should be taken into consideration for a better understanding.

The heavy-light mesons under study in this paper are well established indeed, and any prediction or reproduction of mass spectrum does not directly guarantee the validity of the model, but shows a possible path to follow for a further investigation. Therefore other physical observables such as decay constants should be experimentally investigated to give more inputs to the theory. For example the only precise value of decay constant is known for D mesons, and systematics are evaluated. The other mesons in this study need more experimental data. For B_s there is no available experimental data. We predicted for the first time decay constant value for B_s in this manner.

Decay constants give information about short distance structure of hadrons. The obtained results for decay constants are in agreement with the other studies and available data. We did not consider in this work relativistic corrections.

In QCD Sum Rule calculations, physical observables must be independent of the Borel parameter. In Figures 1–8 the smoothness of the graphs is compatible with existing data. It is worthy to note that in Figures 1 and 5 the 'slope' of the two curves of D^0/D^+ is not in the same range. The reason for that could be the smallness of the Borel parameter and continuum threshold energy, since correlation function receives main contribution at $s \neq M^2$. On the other hand, the smallness of Borel parameter can blow up the corrections to the perturbative part of the correlation function.

In summary, we obtained good results in accordance with the available data and theoretical studies. As mentioned before, other potential models and interpolating currents can be used to study mass spectra and decay constants. Heavy-light systems in view of the quark model are important to study hadronic interactions. In particular, Heavy Quark Spin Symmetry can play an essential role in heavy-light systems. The higher dimensions of the operators in interpolating currents would deliver more accurate results.

Data Availability

The data used to support the findings of this study are available from the corresponding author upon request.

Conflicts of Interest

The author declares that there are no conflicts of interest.

References

[1] M. Gell-Mann, "A schematic model of baryons and mesons," *Physics Letters*, vol. 8, no. 3, pp. 214-215, 1964.

[2] C. Patrignani et al., "Review of Particle Physics," *Chinese Physics C*, vol. 40, article 100001, 2016.

[3] S. Capstick, S. Godfrey, N. Isgur, and J. Paton, "Taking the "naive" and "non-relativistic" out of the quark potential model," *Physics Letters B*, vol. 175, no. 4, pp. 457–461, 1986.

[4] S. Gasiorowicz and J. L. Rosner, "Hadron spectra and quarks," *American Journal of Physics*, vol. 49, no. 10, pp. 954–984, 1981.

[5] B. Juliá-Díaz and D. O. Riska, "Baryon magnetic moments in relativistic quark models," *Nuclear Physics A*, vol. 739, no. 1-2, pp. 69–88, 2004.

[6] K. B. Vijaya Kumar, B. Hanumaiah, and S. Pepin, "Meson spectrum in a relativistic harmonic model with instanton-induced interaction," *The European Physical Journal A*, vol. 19, no. 2, pp. 247–250, 2004.

[7] J.-M. Richard, "An Introduction to Quark Model," 2012, https://arxiv.org/abs/1205.4326.

[8] D. Ebert, R. N. Faustov, and V. O. Galkin, "Radiative M1-decays of heavy–light mesons in the relativistic quark model," *Physics Letters B*, vol. 537, no. 3-4, pp. 241–248, 2002.

[9] K. K. Pathak, D. K. Choudhury, and N. S. Bordoloi, "Leptonic decay of Heavy-light Mesons in a QCD Potential," *International Journal of Modern Physics A*, vol. 28, no. 02, p. 1350010, 2013.

[10] D. Ebert, R. N. Faustov, and V. O. Galkin, "Decay constants of heavy-light mesons in the relativistic quark model," *Modern Physics Letters A*, vol. 17, no. 13, pp. 803–807, 2002.

[11] T. A. Lähde, C. J. Nyfält, and D. O. Riska, "Spectra and M1 decay widths of heavy-light mesons," *Nuclear Physics A*, vol. 674, no. 1-2, pp. 141–167, 2000.

[12] D. U. Matrasulov, F. C. Khanna, and H. Yusupov, "Spectra of heavy-light mesons," *Journal of Physics G: Nuclear and Particle Physics*, vol. 29, no. 3, pp. 475–483, 2003.

[13] B. L. G. Bakker, "Spectrum and decay donstants of heavy-light mesons," *Few-Body Systems*, vol. 44, pp. 91–93, 2008.

[14] B. H. Yazarloo and H. Mehraban, "Mass spectrum and decay properties of heavy-light mesons: D, D_s, B and B_s mesons," *The European Physical Journal Plus*, vol. 132, no. 2, p. 80, 2017.

[15] J. B. Liu and M. Z. Yang, "Heavy-light mesons in a relativistic model," *Chinese Physics C*, vol. 40, no. 7, p. 073101, 2016.

[16] W. Lucha, D. Melikhov, and S. Simula, "Decay constants of heavy pseudoscalar mesons from QCD sum rules," *Journal of Physics G: Nuclear and Particle Physics*, vol. 38, no. 10, Article ID 105002, 2011.

[17] J. Liu and C. Lü, "Spectra of heavy–light mesons in a relativistic model," *The European Physical Journal C*, vol. 77, no. 5, p. 312, 2017.

[18] T. Lesiak, "B Meson Spectroscopy," *Acta Physica Polonica*, vol. 29, pp. 3379–3386, 1998.

[19] H. A. Alhendi, T. M. Aliev, and M. Savcı, "Strong decay constants of heavy tensor mesons in light cone QCD sum rules," *Journal of High Energy Physics*, vol. 2016, no. 4, 2016.

[20] Z. Wang, "Analysis of the masses and decay constants of the heavy-light mesons with QCD sum rules," *The European Physical Journal C*, vol. 75, no. 9, p. 427, 2015.

[21] A. K. Rai, R. H. Parmar, and P. C. Vinodkumar, "Masses and decay constants of heavy-light flavour mesons in a variational scheme," *Journal of Physics G: Nuclear and Particle Physics*, vol. 28, no. 8, pp. 2275–2282, 2002.

[22] T. Huang and C. Luo, "Decay constants of heavy-light mesons in heavy quark effective theory," *Physical Review D: Particles, Fields, Gravitation and Cosmology*, vol. 53, no. 9, pp. 5042–5050, 1996.

[23] A. Duncan, E. Eichten, J. M. Flynn, B. R. Hill, and H. Thacker, "Masses and decay constants of heavy-light mesons using the multistate smearing technique," *Nuclear Physics B (Proceedings Supplements)*, vol. 34, no. C, pp. 445–452, 1994.

[24] P. Gelhausen, A. Khodjamirian, A. A. Pivovarov, and D. Rosenthal, "Erratum: Decay constants of heavy-light vector mesons from QCD sum rules (Phys. Rev. D (2013) 88 (014015))," *Physical Review D: Particles, Fields, Gravitation and Cosmology*, vol. 91, no. 9, 2015.

[25] S. Narison, "Decay Constants of Heavy-Light Mesons from QCD," *Nuclear and Particle Physics Proceedings*, vol. 270-272, pp. 143–153, 2016.

[26] H.-y. Cheng and X.-W. Kang, "Branching fractions of semileptonic D and Ds decays from the covariant light-front quark model," *European Physical Journal C*, vol. 77, no. 9, p. 587, 2017.

[27] X. Kang, B. Kubis, C. Hanhart, and U. Meissner, "Bl4 decays and the extraction of —Vub—," *Physical Review D*, vol. 89, no. 5, Article ID 053015, 2014.

[28] N. Brambilla, S. Eidelman, P. Foka et al., "QCD and strongly coupled gauge theories: challenges and perspectives," *The European Physical Journal C*, vol. 74, no. 10, 2014.

[29] B. Aubert, R. Barate, M. Bona et al., "Observation of a New Ds Meson Decaying to DK at a Mass of 2.86GeV/c2," *Physical Review Letters*, vol. 97, Article ID 222001, 2006.

[30] J. Brodzicka, H. Palka, I. Adachi et al., "Observation of a New D_{sJ} Meson in $B^+ \longrightarrow D^0 D^0 K^+$ Decays," *Physical Review Letters*, vol. 100, Article ID 092001, 2008.

[31] R. Aaij, B. Adeva, M. Adinolfi et al., "Dalitz plot analysis of $B_s^0 \longrightarrow D^0 K^- \pi^+$ decays," *Physical Review*, vol. 90, Article ID 072003, 2014.

[32] R. Aaij, B. Adeva, M. Adinolfi et al., "Observation of Overlapping Spin-1 and Spin-3 D0K- Resonances at Mass 2.86GeV/c2," *Physical Review Letters*, vol. 113, Article ID 162001, 2014.

[33] N. Cabibbo, "Unitary symmetry and leptonic decays," *Physical Review Letters*, vol. 10, no. 12, pp. 531–533, 1963.

[34] J. H. Christenson, J. W. Cronin, V. L. Fitch, and R. Turlay, "Evidence for the 2π Decay of the K02 Meson," *Physical Review Letters*, vol. 13, no. 4, pp. 138–140, 1964.

[35] M. Kobayashi and T. Maskawa, "CP violation in the renormalizable theory of weak interaction," *Progress of Theoretical and Experimental Physics*, vol. 49, pp. 652–657, 1973.

[36] M. A. Shifman, A. I. Vainshtein, and V. I. Zakharov, "QCD and resonance physics applications," *Nuclear Physics B*, vol. 147, no. 5, pp. 448–518, 1979.

[37] B. L. Ioffe, "Calculation of baryon masses in quantum chromodynamics," *Nuclear Physics B*, vol. 188, no. 2, pp. 317–341, 1981.

[38] M. Nielsen, F. S. Navarra, and S. H. Lee, "New charmonium states in QCD sum rules: a concise review," *Physics Reports*, vol. 497, no. 2-3, pp. 41–83, 2010.

[39] P. Colangelo and A. Khodjamirian, "QCD sum rules, a modern perspective," in *at The Frontier of Particle Physics*, M. Shifman, Ed., vol. 3, pp. 1495–1576, 2001.

[40] H. Sundu, "The Mass and Current-Meson Coupling Constant of the Exotic X(3872) State from QCD Sum Rules," *Süleyman Demirel University Journal of Natural and Applied Sciences*, vol. 20, no. 3, p. 448, 2016.

[41] A. De Rújula and S. L. Glashow, "Is bound charm found?" *Physical Review Letters*, vol. 34, no. 1, pp. 46–49, 1975.

[42] E. Eichten, K. Gottfried, T. Kinoshita, J. Kogut, K. D. Lane, and T.-M. Yan, "Spectrum of charmed quark-antiquark bound states," *Physical Review Letters*, vol. 34, no. 6, pp. 369–372, 1975.

[43] T. Appelquist, A. De Rújula, H. D. Politzer, and S. L. Glashow, "Spectroscopy of the new mesons," *Physical Review Letters*, vol. 34, no. 6, pp. 365–369, 1975.

[44] A. Martin, "A fit of upsilon and charmonium spectra," *Physics Letters B*, vol. 93, no. 3, pp. 338–342, 1980.

[45] C. Quigg and J. L. Rosner, "Quarkonium level spacings," *Physics Letters B*, vol. 71, no. 1, pp. 153–157, 1977.

[46] J. L. Richardson, "The heavy quark potential and the Υ, J/ψ systems," *Physics Letters B*, vol. 82, no. 2, pp. 272–274, 1979.

[47] W. Buchmüller and S.-H. H. Tye, "Quarkonia and quantum chromodynamics," *Physical Review D: Particles, Fields, Gravitation and Cosmology*, vol. 24, no. 1, pp. 132–156, 1981.

[48] S. Xiaotong and L. Hefen, "A new phenomenological potential for heavy quarkonium," *Zeitschrift für Physik C Particles and Fields*, vol. 34, no. 2, pp. 223–231, 1987.

[49] E. Eichten and F. Feinberg, "Spin-dependent forces in quantum chromodynamics," *Physical Review D: Particles, Fields, Gravitation and Cosmology*, vol. 23, no. 11, pp. 2724–2744, 1981.

[50] O. Lakhina and E. S. Swanson, "Dynamic properties of charmonium," *Physical Review D: Particles, Fields, Gravitation and Cosmology*, vol. 74, no. 1, 2006.

[51] R. Van Royen and V. F. Weisskopf, "Protsyessy raspada adronov i modyelcyrillic small soft sign kvarkov," *Il Nuovo Cimento A*, vol. 50, no. 3, pp. 617–645, 1967.

[52] S. Jacobs, M. G. Olsson, and C. Suchyta, "Comparing the Schrödinger and spinless Salpeter equations for heavy-quark bound states," *Physical Review D: Particles, Fields, Gravitation and Cosmology*, vol. 33, no. 11, pp. 3338–3348, 1996.

[53] S. Nam, "Extended nonlocal chiral-quark model for the D- and B- meson weak-decay constants," *Physical Review D*, vol. 85, no. 3, Article ID 034019, 2012.